MOLTEN SALTS AND THEIR VAPOURS

A Thermodynamic Study of Some High Temperature Halides and Sulphates

By

RAYMOND GEORGE ANTHONY, B.Sc. (Hons.),

New South Wales

Submitted in fulfilment of the requirements for the degree of

Doctor of Philosophy

UNIVERSITY OF TASMANIA

HOBART

December, 1970.

Thesis.
Ph.D.

This thesis contains no material which has been accepted for the award of any other degree or diploma in any University, nor, to the best of my knowledge and belief, does it contain any copy or paraphrase of material previously published or written by another person, except where due reference is made in the text of the thesis.

R. G. Anthony

Chemistry Department — R.G. Anthony

University of Tasmania — December, 1970.

ABSTRACT

Reciprocal sulphate-halide liquid salt mixtures have been investigated using transpiration vapour pressure measurements. Mass spectrometric methods have also been used to investigate the binary halide mixtures in the vapour phase. Where possible the applicability of theory to the prediction of the thermodynamic properties of these systems has been studied.

An activity study of the liquid reciprocal salt system:

$$ZnCl_2 + Na_2SO_4 = ZnSO_4 + 2\ NaCl$$

has been carried out. Behaviour in this system is quite complex; the best fit to the data is made with the Conformal Ionic Solution Theory which contains terms involving (1) the free energy change for the above exchange reaction (2) binary type interaction terms and (3) ternary excess terms. This theory has also been found to fit some lead sulphate-alkali halide mixtures.

Vapour phase mixtures $PbBr_2$-MBr, $ZnCl_2$-MCl, (M = Na, K, Rb, Cs) were found to contain complex species of the type MAX_3. Possible structures of these species were estimated with the aid of Extended Hückel, Molecular Orbital calculations. Conclusions concerning the formation of vapour phase complexes are drawn from available information.

ACKNOWLEDGEMENTS

The author would like to acknowledge the supervision and guidance of Professor H. Bloom throughout the course of this work. Advice given by Professor B.J. Welch and Dr. L.A. Dunn on the vapour pressure studies and by Dr. B.V. O'Grady on the mass spectrometry work is also acknowledged. Thanks are due to Professor J.D. Morrison for assistance with Molecular Orbital calculations and for supplying a copy of the program. Helpful communications with Dr. M. Blander are acknowledged. The invaluable assistance of Mr. J. Marshall in maintaining the mass spectrometer was very much appreciated. The author would like to express his thanks to Professor H. Bloom, Dr. L.A. Dunn, and Dr. B.V. O'Grady for their criticisms of the manuscript. This work was made possible by a research scholarship from Mimets Development Pty. Ltd., and by financial assistance from the Australian Research Grants Committee.

TABLE OF CONTENTS

SYMBOLS USED IN THIS THESIS

Chapter 1.

T_o : constant used in Angell's transport equation, related to glass transition temperature.

Chapter 2.

z : valency of an ion

e : electronic charge

u : pair potential between two ions

r : interionic distance

d : characteristic parameter length; sum of anion, cation radii

K : microscopic dielectric constant

P : pressure

V : volume

π : reduced pressure

τ : reduced temperature

θ : reduced volume

ΔG_m : Gibb's free energy of mixing

ΔA_m : Helmholtz free energy of mixing

ΔH_m : Enthalpy of mixing

ΔE_m : internal energy of mixing

ΔS_m : entropy of mixing

ΔG_m^E, ΔS_m^E : excess over the ideal of that thermodynamic quantity upon mixing

$\Delta \bar{G}_{AB}$, $\Delta \bar{H}_{AB}$ etc : partial molar thermodynamic quantity of component AB

$\Delta \bar{G}_{AB}^E$, $\Delta \bar{S}_{AB}^E$ etc : excess partial molar value thermodynamic quantity of component AB

a : thermodynamic activity

γ : activity coefficient

n_i : moles of salt i

N_i : mole fraction of salt i

X_j : ion fraction of ion j

X_j' : equivalent ion fraction of ion j

x_j : total ion fraction (Haase model) of ion j

f_i : Haase activity coefficient of salt i

[A] : one equivalent of ion/salt A

R : gas constant

b : regular solution interaction parameter

δ' : distance parameter $\frac{d_1 - d_2}{d_1 + d_2}$

δ : R.K.K. distance parameter $\frac{d_1 - d_2}{d_1 d_2}$

λ : heat of mixing interaction parameter, $\Delta H_m / N_1 N_2$

F : entropy of mixing parameter

Z : coordination number

ξ : coupling parameter

U : energy

R.M.K : theory of Reiss, Mayer and Katz

R.K.K : theory of Reiss, Katz and Kleppa

D.R. : theory of Davis and Rice

F.F.G. : equation derived by Flood, Førland and Grjotheim

C.I.S. : Conformal Ionic Solution Theory

λ_{∞} : heat of mixing interaction parameter at infinite dilution of a divalent species

$\Delta G^{o}_{(mole)}$: free energy change per mole of total salt for a metathetical reaction

$\Delta G^{o}_{(equiv)}$: free energy change per equivalent of salt for metathetical reaction

Y : Quasi-chemical non-randomness parameter

Av : Avogadro's number

Λ : C.I.S. ternary excess parameter

T_c : upper consolute temperature

T(m) : melting point of pure component

T(f) : fusion point of a mixture

ΔH_{fus} : enthalpy of fusion

M : alkali metal

X : halogen

ΔH_D : enthalpy of dimerization

ΔS_D : entropy of dimerization

I^+ : ion current

k : constant relating partial pressures to I^+T.

K_p : equilibrium constant

K_r : ratio of values of I^+T, proportional to K_p.

ΔH_f : enthalpy of formation

ΔH_{vap} : enthalpy of vaporisation

Chapter 3

P^o : vapour pressure of a pure salt

M_i : molecular weight of salt i

P_n : vapour pressure of an n-mer

N_g : moles of gas transpired

P_{corr} : corrected atmospheric pressure

P_W : saturation vapour pressure of water

K_D : dimerization equilibrium constant

$V_0 \cos\omega t$: RF voltage

V_1 : DC voltage

r_0 : 1/2 distance between opposite quadrupoles

α, β : parameters involved in quadrupole mass filter operation

Chapter 4

ΔH_o : heat of vaporisation at $0(^oK)$

I : constant

Σ : $\Delta H_o + I$

X' : equivalent ion fraction

X : ion fraction

$[AB]$: 1 equivalent of salt AB

n'_A : equivalents of ion A

n_A : moles of ion A

$\Delta G^E_{(equiv)}$: excess free energy of mixing per equivalent of salt

$\Delta G^E_{(mole)}$: excess free energy of mixing per mole of salt

N_{AB} : mole fraction of salt AB

δ : size parameter $\frac{d_1 - d_2}{d_1 d_2}$

$\Delta G^{E}_{(A-M)SO_4(equiv)}$: excess free energy of mixing per equivalent in the ASO_4-M_2SO_4 binary

F.F.G. (S.S.) : Flood, Førland and Grjotheim Solid Solution Model

F.F.G. : Flood, Førland and Grjotheim Regular Solution Model

F.F.G. + Forland : Model of Førland incorporating four binary terms and the F.F.G. Regular Solution Equation

Z : average coordination number

λ_{12} : Interaction Parameter for the binary mixture of salts, e.g. (AD) and 2 (BD), such that $\Delta G^{E}_{(A-B)D(equiv)} = \lambda_{12} X'_A X'_B$

Q : an arbitrary total number of equivalents of all salts

b,b' : constants in the Bloom and Welch equation

Y : Quasi-chemical non randomness parameter

δ_r : reciprocal size parameter

$= (d_1-d_4)(d_1-d_3)(d_1+d_2)/d_1d_2d_3d_4$

Chapter 5

A : divalent metal species, Pb, Zn, Cd

M : alkali metal species

X : halogen

ψ_K : Kth molecular orbital

ϕ_j : jth atomic orbital

a_{ij}	:	eigen vector of jth atomic orbital in ith molecular orbital
H	:	Hamiltonian operator
E	:	energy
S	:	overlap integral
K	:	constant in Ballhausen, Gray equation
q	:	charge on an ion
E.H.	:	Extended Hückel
M.O.	:	Molecular Orbital

LIST OF FIGURES

1. INTRODUCTION

1.1. Objects of This Work

1.1.1. Introduction

In recent years an increasing amount of research has been carried out on molten salts, largely because of their applications to metallurgy, power industries and space research.[1,2,3,4] Simultaneously a need for research on vapours above molten salts and their mixtures has become apparent.[5] In the field of extractive metallurgy, main interest has been in the development of new processes, e.g. in uranium[6] and titanium production,[7] and in the optimisation of existing processes. In this regard the aluminium industry has given considerable impetus to molten salt technology.[8] Often the interest in fused salts is indirect; increasing corrosion problems as greater production rates necessitate higher process temperatures in the production of steel[9] are a typical example. Mass spectrometic investigations of salt vapours have revealed possible vaporisation processes, e.g. aluminium purification at high temperatures by vapour transport:[10]

$$2Al + AlCl_3 = 3AlCl$$

$$3AlCl = AlCl_3 + 2Al$$

In the last ten years considerable advances have been made in the thermodynamics of molten salts and salt vapours.[11,12,13,14,15] For simple systems, i.e. univalent or at least charge symmetrical,

reasonable predictions of thermodynamic properties may be made with little or no further experimental work. This thesis takes an example of a complex metallurgical process involving both fused salt and vaporisation equilibria and attempts to determine whether thermodynamic properties involved are adequately predicted by modern theory.

1.1.2. Salt Roasting Reactions

One process which has been known for some time but with little understanding of its physical chemistry is "salt roasting".[16] In this process, valuable metals are volatilised, usually from low grade sulphide ores or pyrite cinders, by mixing with an inexpensive chloride and heating in air. Alternatively a lower temperature leaching process is sometimes used. The overall reaction scheme, when sodium chloride is used, is of the type:

$$AS + 2NaCl + 2O_2 = ACl_2 + Na_2SO_4$$

where AS is the metal sulphide. That sodium sulphate is a major product of this reaction has been well established by Gerlach and Pawlek,[17] and others;[18] studies carried out in the course of this work further confirm this finding. What is not fully understood is the mechanism by which this process takes place. Gerlach and Pawlek have proposed the following reaction scheme for zinc sulphide:

$$2ZnS(s) + 3O_2(g) = 2ZnO(s) + 2SO_2(g)$$

$$O_2(g) + SO_2(g) + 2NaCl(s) = Na_2SO_4(s) + Cl_2(g)$$

$$2Cl_2(g) + 2ZnO(s) = 2ZnCl_2(g) + O_2(g)$$

Alternatively a second pathway has been proposed by Bloom,[19] involving firstly oxidation to the sulphate (or another oxidation product with significant solubility in molten sodium chloride):

$$ZnS(s) + 2O_2(g) = ZnSO_4(s)$$

In the second stage zinc sulphate dissolves in molten sodium chloride and undergoes an exchange reaction to form $ZnCl_2$:

$$ZnSO_4(1) + 2NaCl(1) = Na_2SO_4(1) + ZnCl_2(1),(g)$$

It is likely that either or both of these reaction mechanisms are operative depending upon conditions. The first reaction would require that the amount of liquid phase present be small so as not to hinder the series of heterogeneous reactions. The second reaction scheme requires a large amount of a liquid phase to allow a fast rate for the exchange reactions; moreover, either the sulphate formed should be thermally stable, or the rate of decomposition to oxide should be slow. Both reaction mechanisms are thermodynamically feasible from 600°C - 1000°C.

It is beyond the scope of this thesis to determine which of these reaction schemes predominates at proposed operating conditions. Such a study would require a very extensive study of the thermodynamics and kinetics of both reactions. Rather, the aim of the thesis is to investigate the liquid and vapour equilibria involved in the exchange step in the second mechanism. This involves charge unsymmetrical reciprocal mixtures of the type 2-2 in 1-1 and 2-1 in 1-2. Besides forming a severe test of modern thermodynamic theories, study of such a

system would significantly add to the fundamental understanding of salt roasting. Bloom and Welch,[20,21] some years ago, carried out a thermodynamic study of the system

$$PbCl_2(l) + Na_2SO_4(l) = PbSO_4(l) + 2NaCl(l)$$

at different compositions. The properties of the systems were very largely determined by the energy of the exchange step; other types of interactions between ions in the melt were not very great and relatively simple equations were found to fit the system. For this study the somewhat similar system

$$ZnCl_2(l) + Na_2SO_4(l) = ZnSO_4(l) + 2NaCl(l)$$

was chosen. Here, binary type interactions predominate over those of the exchange reaction to a large degree. The purpose is to determine the applicability of more advanced theories in predicting the effect of the binary type interactions and to compare the two systems. Moreover, the effect of temperature as well as composition on activities has been determined. For further comparison, activities have been determined in the system K_2SO_4 - $PbCl_2$.

Mass spectrometic studies have been carried out firstly to understand the vapour phase equilibria of this type of process. The presence of complexes of the type $NaZnCl_3$ in the vapour during salt roasting would be of great importance in a commercial process as far as further process stages are concerned. This study also served as a second check on the assumed vapour composition used to calculate activities in the liquid phase

study. Of further importance is the adaptation of commercial quadrupole mass spectrometers to salt vapour studies. Most mass spectrometic studies have been carried out with magnetic or time-of-flight instruments. Commercial quadrupole types, being less costly, are likely to find much use in high temperature laboratories where a knowledge of the vapour phase is one of many equilibria necessary for an understanding of a whole process.

In order to develop the technique, binary salt systems were chosen for which trends predicted large amounts of complex formation in the vapour phase. Examples of cation mixtures: lead bromide-alkali bromides and an anion mixture: cadmium chloride, cadmium bromide were chosen for quantitative studies. With the zinc chloride-alkali chloride systems investigated, only small amounts of complex vapour species were observed. The closely related systems of cadmium chloride-alkali chlorides were similarly found to exhibit relatively little complexing in the vapour phase.

Qualitative comparison is made between trends observed in the systems studied and those set up in other systems. To assist in this comparison, the most likely structures of vapour phase complexes were determined using Extended Hückel Molecular Orbital calculations.

1.2. Introduction to Fused Salts and Salt Vapours

As members of the general class of liquids, molten salts have two distinctive features: firstly, they consist of particles electrostatically charged, at least to some extent; secondly, they exist at temperatures high enough for thermal energy to be able to counteract strongly binding coulombic forces.[22]

Many of the properties of molten salts, density, surface tension, viscosity, refractive index, are of the same order of magnitude as most liquids.[23] The distinctions mentioned above, however, usually lead to electrical conductivities and melting points which are greater than those of most liquids. Their transport properties, which will not receive much attention in this thesis, are usually of the following order of magnitude for a fully ionised salt:[24]

equivalent conductance	: 100 - 200 $ohm^{-1}cm^2equiv^{-1}$
viscosity	: ca 1 centipoise
self diffusion coefficient	: ca 5 x 10^{-5} cm^2sec^{-1}

The Nernst-Einstein and Stokes-Einstein relationships are approximately obeyed; the Walden product ($\Lambda\ \eta$) is usually greater than the theoretical value.

Because they are liquids, the properties of fused salts are difficult to predict since they have neither the structural regularity of ideal solids nor the random behaviour of ideal gases. Most recent theories emphasise the similarity between molten and solid, rather than gaseous, salts. X-ray and neutron

diffraction studies[25] indicate that, although the long range order of the solid is largely lost upon melting, the short range order is largely preserved. Hence, there are distinct positions for cations and anions in a molten salt. Furthermore, upon melting volume increases of the order of 20% are observed for the alkali halides, whereas cation-anion distances are shortened and the coordination numbers of the ions are usually reduced. The "Quasi Lattice", "Hole" and "Significant Structures"[23] models are each based upon an assumed type of disordering of the solid in the formation of the liquid.

A new approach has been developed by Angell,[26] based upon the liquid free volume model of Cohen and Turnbull.[27] There is assumed to exist a temperature T_0, related to the glass transition temperature, below which transport stops. Transport equations are of the form: $A \exp(B/T-T_0)$, where A,B,T_0 are constants. This model may have particular application to zinc systems where glasses sometimes are formed.

Since the work of Miller and Kusch[28] on the molecular weights of alkali halide vapours, and with an increasing number of mass spectrometric studies,[29] it has become apparent that high temperature vapours usually do not consist only of monomer molecules. In the case of oxide vapours, for example, both gaseous association and dissociation may occur. For example,[30] lead oxide vapour consists of PbO, Pb_2O_2, Pb_3O_3 and Pb_4O_4; cadmium oxide however vaporises as follows:

$$CdO(s) = Cd(g) + \tfrac{1}{2}O_2(g)$$

Vapours above molten salts frequently contain polymeric species; for example

$$2NaCl(g) = (NaCl)_2(g)$$

Vapour phase complexing above salt mixtures is common[31] e.g.:

$$NaCl(g) + PbCl_2(g) = NaPbCl_3(g)$$

The stability of complexes in the vapour is found to be very dependent upon relative sizes of species taking part; broad trends have been observed between the stability of vapour phase complexes and the thermodynamic properties of corresponding liquid salt mixtures.

2. THEORETICAL REVIEW

2.1. Thermodynamics of fused salts

2.1.1. Pure Salts

In attempting to produce an adequate theory to account for the properties of fused salts, the thermodynamic approach has proved to be among the most useful.[11,13,15] The relatively simple structures of ionic liquids, such as the alkali halides, lend themselves to a theoretical approach. The first assumption is that they may be regarded as charged spheres. Secondly, it is assumed that short range order exists such that cations are normally surrounded by anions and vice versa for the anions. Such order results from the large energy, of the order of 200 kcal/mole for NaCl,[22] necessary to remove say a cation from a position surrounded by anions to one surrounded by cations. A third assumption normally made is that the total energy of the system is the sum of the energies of all pair interactions. While this is a poor assumption in molecular liquids, it has proved to be a good first approximation for molten salts.

Considering the equilibrium properties of pure fused salts, the most advanced fundamental approach has been made by Stillinger.[22] The following equation is given for the pair potential (u) between two ions i, j of charge z_i, z_j, of polarisability α_i, α_j, as a function of interionic distance r:

$$u_{ij}(r) = A_{ij} \exp(-B_{ij}r) + \frac{z_i z_j e^2}{r} - \frac{(z_i e)^2 \alpha_j + (z_j e)^2 \alpha_i}{2r^4} - \frac{C_{ij}}{r^6} \qquad (11\text{-}1)$$

The terms on the right-hand side represent, in order:

(1) short range repulsive potential

(2) charge-charge interaction

(3) charge-dipole interaction

(4) dipole-dipole interaction

The coefficient C is approximated by the London formula for the dispersion energy

$$C_{ij} = 3/2\ \alpha_i\alpha_j\ I_iI_j/(I_i + I_j) \qquad (11\text{-}2)$$

where I_i is the ionization potential of the ion. Higher order terms include such terms as dipole-quadrupole interactions. Of the above terms, (1), (2), and (4) are taken to be additive; the polarisation interaction term (3) is not. Additional problems arise when partly covalently bonded salts such as BeF_2 or $ZnCl_2$ are studied. Although these rigorous theories are able to predict some of the properties of molten salts with reasonable accuracy, particularly surface tensions, they have not been developed sufficiently to provide a basis for thermodynamic studies, especially of mixtures. A number of approximate theories, based upon assumed structural properties of melts, has been developed to evaluate a partition function. These theories have been reviewed by Bloom and Bockris.[23]

Of greater usefulness has been the statistical mechanical approach of Reiss, Mayer and Katz (R.M.K.)[32] based upon the method of corresponding states. The ideal ionic melt considered by these authors is assumed to have the following properties:

(a) long range coulomb forces create a locally ordered structure wherein cations are surrounded by anions and vice versa.

(b) because of this local structure and coulomb repulsions, short range interactions between ions of like sign are neglected.

(c) the pair potential u_{ij} between ions i and j is given by: (1) unlike sign

$$u_{ij} = \infty \qquad r_{ij} \leq d$$
$$u_{ij} = -(ze)^2/Kr_{ij} \qquad r_{ij} > d \qquad (11\text{-}3)$$

(2) like sign

$$u_{ij} = (ze)^2/r_{ij} \qquad r_{ij} \geq 0 \qquad (11\text{-}4)$$

where $|ze|$ is the charge on the ions i and j,

K is the dielectric constant,

r_{ij} is the distance between ions i and j.

Each salt is fully characterised by the single parameter length d; this has been set equal to sums of ionic radii of the anion and cation. For a charge symmetrical salt the following equations are given for the reduced pressure, the reduced temperature and reduced volume:

$$\pi = Kd^4P/z^2$$
$$\tau = dKT/z^2$$
$$\phi = V/\tau^3 \qquad (11\text{-}5)$$

Assuming the dielectric constant K = 1, Reiss et al are able to make good predictions of melting points, vapour pressure and surface tensions for 1:1 salts such as the alkali halides. Extensions of this model to mixtures have had the greatest importance.

2.1.2. Solutions of Fused Salts

Studies of solutions of fused salts have justly attracted a wide interest. Mixtures have a theoretical and applied value of their own as well as shedding light on the properties of the pure components: the nature of interactions between dissimilar species in a mixture is more easily determined experimentally than those between similar species in a pure salt. Theoretical interpretation however is often made more difficult.

Of all thermodynamic properties, free energy has the widest applications; the measurement or ability to predict activities of the components of a solution is therefore of first importance.

2.1.3. Simple Models of Fused Salt Solutions

(A) Temkin

Temkin's definition of activities in fused salts was a great advance in this field.[33] In a large number of cases this simple theory predicts relatively good values for activities. This model considers the strong coulombic forces and assumes that two interlocking quasi-lattices exist in a melt. The cations mix randomly in one lattice and the anions mix similarly in the other. Ion fractions for cations and anions are defined, e.g. for a mixture containing salts A_rB_s:

$$X_A = \frac{n_A}{\sum_i n_{\text{cations}}} \quad ; \quad X_B = \frac{n_B}{\sum_j n_{\text{anions}}} \qquad (11\text{-}6)$$

X_A, X_B are the cationic and anionic ion fractions respectively, n_i, n_j are the numbers of moles of i^+ and j^- ions. The activity

of $A_r B_s$ is defined:

$$a = (X_A)^r (X_B)^s \tag{11-7}$$

The following thermodynamic relationships hold for ideal mixing of salts AB and CD:

$$\begin{aligned} \Delta H_m &= 0 \\ \Delta S_m &= -R(n_A \ln X_A + n_B \ln X_B + n_C \ln X_C + n_D \ln X_D) \\ \Delta G_m &= RT(n_A \ln X_A + n_B \ln X_B + n_C \ln X_C + n_D \ln X_D) \end{aligned} \tag{11-8}$$

Partial molar quantities of AB are:

$$\begin{aligned} \Delta\overline{H}_{AB} &= 0 \\ \Delta\overline{S}_{AB} &= -R \ln X_A X_B \\ \Delta\overline{G}_{AB} &= RT \ln X_A X_B \end{aligned} \tag{11-9}$$

Generally, Temkin's definition has been accepted for an ideal ionic melt. Consequently, excess thermodynamic quantities may be defined. The activity coefficient is given by:

$$\gamma_{AB} = \frac{a_B}{X_A X_B} \tag{11-10}$$

Excess partial molar free energies are given as:

$$\Delta\overline{G}^E = RT \ln \gamma_{AB} \tag{11-11}$$

(B) Haase "total ion fraction" method

Recently, Haase[34] has proposed a different definition of ideal activity. Whereas Temkin's equation is based upon Raoult's law, Haase's is based upon Henry's; the standard state is the infinitely dilute solution. Other than complete dissociation into ions, no assumption is made as to the structure of the melt. The chemical potential of any ion j is

given:

$$\mu_j = u_{oj} + RT \ln x_j \qquad (11\text{-}12)$$

μ_{oj} = chemical potential of (hypothetical) pure liquid ion j

x_j is a "total ion fraction", the number of j ions divided by the total number of ions.

Haase has derived expressions for the ideal activity of components in a binary mixture as functions of total ion fractions of constituent ions. In practice, activities calculated from either Haase's of Temkin's equations agree quite closely. With mixtures of the same charge type, calculated activities are the same. As yet, Haase has restricted his definition to binaries and has not treated ternary systems.

(C) Flood, Førland and Grjotheim Solid Solution Model

Temkin's model does not take into account the charge of an ion in its quasi-lattice. Flood et al[35] have reasoned from analogy with solid solutions that the positioning of a doubly charged ion into a lattice of singly charged ions will create a vacancy. For a charge unsymmetrical system such as $A_cC_a + B_dD_b$ made up of A^{a+} C^{c-}, B^{b+} D^{d-}, equivalent ion fractions have been defined:

$$X'_A = \frac{an_A}{an_A + bn_B} \quad ; \quad X'_C = \frac{cn_C}{cn_C + dn_D}$$

and: $$a_{AC} = (X'_A)^c \, (X'_C)^a \qquad (11\text{-}13)$$

The notion of equivalents introduced with this theory will be used later in this thesis.

[A] = 1 gram equivalent of ion A^+

[B] = 1 gram equivalent of ion B^+

[A][C] = [AC] = 1 gram equivalent of salt A_cC_a

n'_A = number of equivalents of A

= nA/a

$$X'_A = \frac{n'_A}{n'_A + n'_B} \quad ; \quad X'_C = \frac{n'_C}{n'_C + n'_D} \qquad (11\text{-}14)$$

(D) Entropy Models

Førland[36,37] has examined the problem of entropy of mixing in charge unsymmetrical systems. He has presented four approaches, differing in the assumed degree of pairing between B^{2+} and a vacancy and also A^+ with A^+. He has concluded that in most cases best results are obtained if the effect of added vacancies is neglected; the number of vacancies added upon mixing is apparently small compared with the number already present in the pure molten salts.

2.1.4. Thermodynamic Studies of Binary Fused Salts

(A) Theory of Regular Solutions

Temkin's model assumes both zero heat of mixing and random mixing. In practice, it is found that a significant enthalpy change usually occurs upon mixing fused salts,[11] which partly explains why activities differ from their ideal values. The second assumption appears to be valid as a first approximation in a large number of cases.[38] Lumsden[15] has given many examples in binary systems where activities are predicted quite

accurately, if the enthalpic effect is taken into account.

The simplest and most used equation for estimating the enthalpic effect is the regular solution method, first developed by Hildebrand;[39] its application to fused salt mixtures has been discussed by Lumsden.[40] In a mixture of n_A moles of AC and n_B moles of BC, it is assumed that random cation mixing occurs and that the heat of mixing is given by:

$$\Delta H_m = b\, n_A n_B/(n_A + n_B) \qquad (11\text{-}15)$$

and $\Delta\bar{H}_{AC} = b\, n_B^2/(n_A + n_B)^2$; $\Delta\bar{H}_{BC} = b\, n_A^2/(n_A + n_B)^2$.

where b is a constant. Activity coefficients are given by:

$$\ln \gamma_{AC} = b\, N_{BC}^2/RT; \quad \ln \gamma_{BC} = b\, N_{AC}^2/RT \qquad (11\text{-}16)$$

where N_{BC}, N_{AC} are mole fractions.

(B) Excess Entropies of Mixing

When large interactions occur between ions in solution, deviations from randomness are likely to occur. Lumsden[40] has used the formula:

$$\Delta S^E = \frac{F n_X n_Y}{n_X + n_Y} \qquad (11\text{-}17)$$

to express such changes, where F is a constant.

(C) Heats of Mixing

The most important set of data on the heats of mixing of fused salts is that of Kleppa and coworkers.[11] Cationic mixtures of the alkali nitrates were found to undergo exothermic mixing.[41] Heats of mixing were found to be relatively temperature independent and could be expressed[42] as

$$\Delta H_m = N(1-N)(a + bN + cN(1-N)) \qquad (11\text{-}18)$$

where N is the mole fraction of the salt with the smaller cation. The value of an interaction parameter $\lambda = \Delta H_m/N_1N_2$ at 0.5 mole fraction, largely specified the system; the asymmetry and non-linearity constants b and c were usually small compared with a. A linear relationship was found:

$$\Delta H_m/N_1N_2 = -U\delta'^2 = -140\delta'^2 \qquad (11\text{-}19)$$

where δ' is a size parameter

$$\delta' = \frac{d_1 - d_2}{d_1 + d_2} \qquad (11\text{-}20)$$

where d_1 and d_2 are the sums of cation-anion radii of the pure fused salts; U has about the magnitude of the lattice energy of the alkali nitrates.

First attempts to rationalise exothermic mixing were those of Førland[36,14] and Blander.[43] Førland considered an arrangement of three hard sphere ions. After mixing, rearrangements of the type shown in figure 2-1, lead to a change in repulsion energy given approximately by

$$E = \frac{-2e^2}{d_1 + d_2}\left(\frac{d_1 - d_2}{d_1 + d_2}\right)^2 \qquad (11\text{-}21)$$

e = electronic charge

This form of equation is quite similar to the empirical one.

Blander[43] has extended the calculation to an infinite linear assembly of ions. His calculation of the exothermic effect is only about 0.4 times that of Førland. This model correctly predicts an energetic asymmetry, such that the larger

FIGURE 2-1

FØRLAND MODEL FOR HEATS OF MIXING AC+ BC

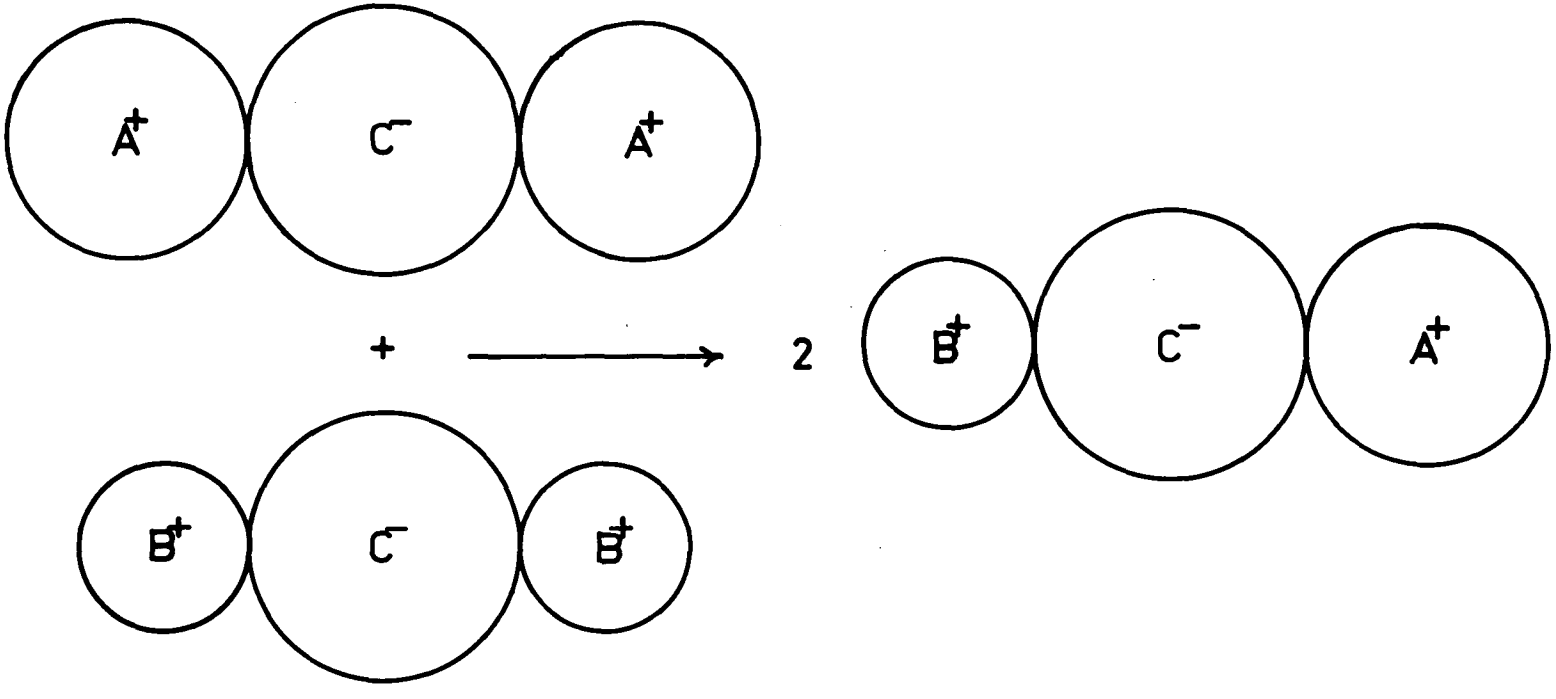

ion has the more exothermic heat of solution at infinite dilution.

Lumsden has taken a different approach, assuming that the exothermic mixing arises from polarisation of the anions by the cations.[44] He has obtained an equation where the change in polarisation energy is of the same form as the observed heat of mixing.

Kleppa[42] was able to fit his results for alkali nitrates to Guggenheim's quasi-chemical theory;[45,46] this would further infer that these heats of mixing are primarily caused by cations' preference for unlike cations as next nearest neighbours.

Measurements of volumes of mixing in the alkali nitrates[47,48] indicate positive deviations from ideality, obeying the approximate equation

$$\Delta V^E = N_1 N_2 \, V'(\delta')^4 \qquad (11\text{-}22)$$

where $V' = 22{,}000 \text{ cm}^3/\text{mole}$.

This behaviour is different from non electrolyte solutions where excess thermodynmaic functions usually have the same sign.

2.1.5. Statistical Mechanical Theories of Binary Solutions

(A) The Theory of Reiss, Katz and Kleppa (R.K.K.)

Rigorous mathematical justification of the empirical equation used by Kleppa has been made by Reiss, Katz and Kleppa[49] using the methods of conformal ionic solution theory. It is an

extension of the earlier derivation of Reiss, Mayer and Katz.[32] The pair potential between ions of opposite charge has been generalised for a monovalent salt to the form

$$u(r) = (1/d)f(r/d) \qquad (11\text{-}23)$$

otherwise the same ideal ionic melt is assumed. The following equation is derived for the heat of mixing:

$$\Delta H_m = N_1 N_2 \Omega (T,P)\delta^2 \qquad (11\text{-}24)$$

where $\delta = \dfrac{d_2 - d_1}{d_1 d_2}$

and Ω (T,P) is a function of temperature and pressure only. It is noticed that the derived interaction parameter is somewhat similar to the earlier empirical one δ' (11-20). In practice use of either parameter yields results equally consistent with experiment.

Blander[50] has extended the derivation to third and fourth order terms of perturbation theory and derived the same form of equation found experimentally:

$$\Delta H_m = N_1 N_2 (a + bN_1 + cN_1 N_2) \qquad (11\text{-}25)$$

He has related the constants a, b, c to power expressions in δ.

Recently Davis and McDonald[51] have developed the R.K.K. theory for measuring at constant temperature and pressure. Explicit but complicated formulae for heats and volumes of mixing are derived, and a successful order of magnitude prediction of the heat of mixing of NaCl and KCl is made. Volumes of mixing of binary alkali nitrates are also examined.

The R.K.K., Davis-McDonald theories do not take into account any changes of polarization upon mixing. With mixtures containing polarisable cations, Ag^{51} or Tl^{52} in the systems $AgNO_3$-MNO_3, $TlNO_3$-MNO_3, (M = alkali metal), both exothermic and endothermic mixing were observed. Kleppa et al reasoned that non-ionic contributions to the lattice energy in pure salts resulted in an endothermic contribution to the heats of mixing. Blander[54] has calculated the change in Van der Waals energy on mixing and could account for most of the positive deviations in heats of mixing from values calculated from equations fitting the alkali nitrates. It would seem, however, that there is some partial covalent bonding in these pure silver and thallium salts, giving rise to an endothermic mixing component.

(B) The Davis, Rice (D.R.) Theory

These authors have considered the effect of dispersion interactions in the R.K.K. derivation. Their generalised form of the pair potential is written:

$$u(r) = (1/d)f(r/d) + \xi\, V(r) \qquad (11\text{-}26)$$

where $\xi\, V(r)$ accounts for dispersion interactions and ξ represents a coupling parameter. The heat of mixing is given by:

$$\Delta H_m = N_1 N_2 (U_o + U_1\, \delta_{12} + U_2\, \delta^2_{12}) \qquad (11\text{-}27)$$

where the coefficients U_o, U_1, U_2 are complicated functions of δ.

Heats of mixing of the alkali halides[56] follow the D.R. type expression:

$$\Delta H_m\ (0.5) - N_1N_2U_o = - U_2N_1N_2\delta^2 \qquad (11\text{-}28)$$

where the term on the left is the "corrected heat of mixing" at 0.5 mole fraction. Hersh et al[56] also fitted heats of mixing in AgX - MX system to the D.R. equation. However, an apparently large dispersion interaction contribution is probably partly due to some covalent bonding in the pure salts.

2.1.6. Alkali Halides

Despite experimental difficulties, comprehensive data is now available for the thermodynamic properties of cationic mixtures of the alkali halides. Usually deviations from regular solution behaviour are not very great; these occur, as would be expected, with cations of very different size, e.g. NaF-CsF. Lumsden[57] and Janz[58] have critically reviewed and tabulated available data, and Kleppa and coworkers have very recently determined heats of mixing in binary alkali fluorides[59] and iodides.[60] Regular solution interaction parameters (b) vary from slightly positive (K-Cs)Cl : 0.2 kcal to quite negative (Li-Cs)Br : -5.2 kcal. Melnichak and Kleppa[60] have investigated the effect of the anion and cation mixing: for equivalent values of δ, the fluorides have less negative, while iodides have more negative corrected enthalpies of mixing than the alkali chlorides or bromides. As the iodide ion is the largest and most polarisable, these findings are in accord with Lumsden's[44] view that increased anion polarisation upon mixing contributes towards exothermic mixing.

2.1.7. Anion Mixtures of Molten Salts

Anion mixtures have received less attention than cation mixtures: in general heats of mixing are much smaller in magnitude for anion mixtures and frequently endothermic mixing is observed.[61] As yet theoretical evaluation is not far advanced. In alkali nitrate - alkali chloride[62] mixtures, positive enthalpies of mixing are observed which decrease with increasing radius ratio of the alkali chloride.

It has been suggested that the positive deviations result from anion-anion next nearest neighbour core repulsions. With mixtures of large non-spherical anions,[63] e.g. (CrO_4^{2-}, ClO_4^-, SO_4^{2-}) with alkali nitrates, heats of mixing were found to be quite small and either positive or slightly exothermic.

2.1.8. Charge Unsymmetrical Cation Mixtures

(A) Davis Theory

Charge unsymmetrical mixtures have received a great deal of attention by a large number of workers; nevertheless the theoretical understanding is less advanced than for more simple salts.

Davis[64] has recently extended the R.K.K. theory to the case of mixtures of the type $(P^+ - Q^{z+})X^-$. The assumed pair potential between anions takes the form:

$$u(r) = e^2Kr \qquad r \geq 0 \qquad (11\text{-}29)$$

The pair potential between cations and between an anion and a cation are, respectively:

$$
\begin{aligned}
z^2u(r) &= z^2e^2/Kr && r \geq 0 \\
u(r) &= +\infty && r \leq d \\
zu(r) &= -ze^2/Kr && r > d
\end{aligned}
\qquad (11\text{-}30)
$$

where z is the valence of the ion.

A complicated equation is derived for the heats of mixing; to a first approximation the following equation may be derived for the interaction parameter at infinite dilution of the divalent species:[13]

$$\lim_{X_2 \to 0} \frac{\Delta H_m}{X_1 X_2} = \lambda_\infty = A + B\delta \qquad (11\text{-}31)$$

where X_2 is the ion fraction of the divalent cation. A and B are unevaluated integrals containing temperature and pressure dependence. The same form of equation applies for free energy of mixing except that A and B are different.

This form of equation has been shown to be valid for heats of mixing: Kleppa and coworkers have found linear relationships between λ_∞ and δ within sets of systems:

alkaline earth nitrates	-	MNO_3[64]
$PbCl_2$	-	MCl[65]
$MgCl_2$	-	MCl[66]
BeF_2	-	MF (M ≠ Na, Cs)[67]
$NiCl_2$	-	MCl[68]

(M = Na, K, Rb, Cs; Li is often an exception)

At finite concentrations heats of mixing are quite complex. Davis[69] has since extended the derivation to the general case

where salt 1 = $C_{z_A}^{z_1+} A_{z_1}^{z_A-}$, salt 2 = $C_{z_A}^{z_2+} A_{z_2}^{z_A-}$.

(B) Association in Fused Salts

Mixtures of univalent salts do not deviate greatly from ideal behaviour in most of their transport or thermodynamic properties. However, in mixtures of the type AX_2 - MX, large deviations from ideality frequently occur at specific stoichiometric ratios. The structural changes causing this behaviour have constituted a major point of controversy in fused salt chemistry. Many workers[70,23] have considered that complex ions of the type $PbCl_3^-$ [71] result from interactions:

$$CsCl + PbCl_2 = CsPbCl_3$$

The presence of compounds of the same stoichiometry in solid mixtures and also vapour phase complexes in mixed vapours has considerably strengthened their argument.

The alternative view[72,73,13,15] is that such behaviour is brought about by preferred packing on the cation sublattice in the melt: in the simplest case, cations prefer unlike cations as next nearest neighbours, where others claim a 1:1 complex ion is formed. In this thesis, the term "complex ion formation" will be used to describe this behaviour. The fact that there exists an alternate point of view should however be kept in mind.

Heats of mixing of $MgCl_2$-MCl mixtures are typical examples of this behaviour. Plots of $\lambda = \Delta H_m/N(1-N)$ become more negative as N_{MgCl_2} increases to a sharp minimum at $N_{MgCl_2} = 0.33$.

The magnitude of the minimum energy becomes more negative from Li to Cs. Kleppa has postulated the formation of $MgCl_4^{2-}$ complex ions to account for this behaviour. Similar results have been found in the comparable $PbCl_2$-MCl,[67] $NiCl_2$-MCl[68] systems with minima at $N_{PbCl_2} = 0.75$, $N_{NiCl_2} = 0.33$.

(C) Thermodynamic properties of ACl_2-MCl Mixtures (A = Pb, Cd, Zn, Mg).

A large number of activity measurements have been carried out on these systems chiefly by Lantratov and Alabyshev[74] and Bloom and coworkers.[75] Activities are generally very much less than ideal especially at high concentrations of alkali halides, and complex ion formation has been proposed to explain this phenomenon. Negative deviations from ideality increase as the size of the divalent ion decreases in the series[76] Pb^{2+} (1.2 Å), Cd^{2+} (0.97 Å), Zn^{2+} (0.74 Å), Mg^{2+} (0.65 Å). This effect has been attributed to increasing stability of the partly covalent bonded complex ion as the polarising power of the divalent ion is increased. In any one series, negative deviations similarly increase as the size of the alkali ion increases, from Li^+ (0.6 Å), Na^+ (0.95 Å), K^+ (1.33 Å), Rb (1.47 Å), Cs (1.67 Å). Replacement of the alkali metal by a divalent ion, e.g. K^+ by Ba^{2+} considerably reduces the negative effect. The alkali ion has been postulated to have a disruptive effect on the complex ion so that complex ion stability decreases with smaller-charge density on the alkali ion; replacement by a divalent cation of

the same size obviously increases charge density and further destabilises the complex ion.

Lantratov et al have found with some $PbBr_2$-MBr[77,78] mixtures that replacement of chlorine by bromine atoms brings about greater deviations from ideality. Presumably, a greater degree of covalent Pb-X bonding is achieved with the larger, more polarisable anion.

Volumes of mixing[74] deviate from ideality in a similar manner to heats of mixing and activities, except that the sign of the change is different. Where large negative deviations in activities occur, volumes of mixings are quite positive; where only small activity deviations occur, volumes of mixing are sometimes slightly negative.

Where stable complex ions are formed, the work of McCarty and Kleppa on $PbCl_2$-MCl mixtures[64] would indicate that positive partial molar entropies of mixing occur, increasing with complex ion stability. This behaviour is different from that of non electrolytes where excess thermodynamic quantities normally have the same sign.

2.1.9. Zinc Chloride and its Mixtures

(A) Properties of Pure Zinc Chloride

Molten zinc chloride has rather special properties and has attracted a great deal of attention. Electrical conductance and viscosity (κ = 1.99 x 10^{-3} $ohm^{-1}cm^{-1}$, η = 44.7 poise at 320°C) are much different from simple molten salts. On the basis of

large temperature dependent activation energies for electrical conductance and viscous flow and the Raman work of Bues,[80] Mackenzie and Murphy[79] have proposed a network structure for zinc chloride at temperatures near the freezing point. As temperature is increased, the network gradually breaks up:

$$3\ \text{-}(ZnCl_2)\text{-} = 2Zn^{2+} + ZnCl_6^{4-}$$

Entropies of activation for electrical conductance and viscous flow were +30 e.u. near the freezing point; this value is much greater than that for the alkali halides and is similar to that found in associated liquids. Crook[81] has also concluded from electrical conductance and viscosity measurements near the freezing point that molten zinc chloride consists of a three dimensional network of polymers, complex cations and simple anions.

Gruber and Litovitz[82] have made an ultrasonic and shear viscosity study on molten zinc chloride. They concluded that the network structure is completely destroyed at temperatures of 20°C above the melting point. Bockris, Richards and Nanis[83] and others find remnants of polymer beyond 100°C of the melting point.[86,87,88]

A large number of workers have studied the Raman spectra of zinc chloride and its mixtures. Bues[80] studied both the crystalline and molten states and found the 233 cm^{-1} band, which he assigned to a polymer structure of $\text{-}(ZnCl_6)\text{-}$ groups. However, Brehler[84] has more recently shown that chlorine atoms are

tetrahedrally coordinated about the zinc atom in crystalline zinc chlorine; the tetrahedra are linked together by sharing corners to form a three dimensional network. Upon the addition of KCl, Bues found bands which he assigned to $ZnCl_4^{2-}$ and $ZnCl_3^-$ complex ions. Bredig and Van Artsdalen[85] have since questioned the existence of $ZnCl_3^-$ on theoretical grounds and from cryoscopic studies of $ZnCl_2$ in $NaNO_3$.

Irish and Young[86] found an intense band at 230 cm^{-1} in molten zinc chloride spectra, which they assigned to polymeric species made up of $ZnCl_4^{2-}$ units; other, weaker bands were assigned to discrete molecules $ZnCl_2$ and $ZnCl_n^{2-n}$, which tended to ionize with increasing temperature.

Moyer, Evans and Lo[87] studied the KCl-$ZnCl_2$ system and found polymeric zinc chloride still dominant at 500°C. The KCl depolymerises the structure successively with increasing concentration:

$$(ZnCl_2)_n + Cl^- = (ZnCl_2)_{n-m} + (ZnCl_2)_m\,Cl^-$$
$$(ZnCl_2)_m Cl^- + Cl^- = ZnCl_4^{2-} + (ZnCl_2)_{m-1} \qquad (11\text{-}32)$$

Ellis[88] has studied the $ZnCl_2$-MCl (M = Li, K, Rb, Cs) systems and found bands which corresponded to the polymer, and also $ZnCl_4^{2-}$, $ZnCl_3^-$, $ZnCl_2$ and other minor species. Increase of temperature breaks down the polymer while increasing MCl concentration causes splitting off of peripheral units.

Wilmshurst,[89] on the other hand, has disagreed with the inference of complex ion formation; he considers his infrared

spectra to arise from lattice type interactions of simple ions. A review of the vibrational spectra of $ZnCl_2$ and other halides has been given by Janz.[90]

(B) Thermodynamic Properties of $ZnCl_2$-MCl Mixtures

Lantratov and Alabyshev reasoned that the low activities in the $ZnCl_2$-MCl system were caused by $ZnCl_4^{2-}$ formation, on the basis of Na_2ZnCl_4, K_2ZnCl_4 formation in the appropriate solid state mixtures.[74] Bloom et al[91] also found large negative deviations from ideality in $ZnCl_2$-NaCl which could not, however, be quantitatively explained as the formation of a single complex ion. Thermodynamic properties of $ZnCl_2$-MCl mixtures all deviate further from ideality as M increases in size from Li to Cs: activities,[74,91,92,93,94] heats of mixing,[95] volumes of mixing.[96,97] Usually the deviations from ideality become less pronounced with increasing temperature. Weeks[97] for example has found that the effect of Na^+ and Cs^+ upon volumes of mixing is not very much different at 600°C, while Cs^+ has a much greater effect at 400°C.

(C) Transport Properties $ZnCl_2$-MCl Mixtures

Weeks[97] has carried out a systematic study of electrical conductance (M = Li, Na, K, Cs) and viscosity (M = Na) of these mixtures. Addition of MCl to pure $ZnCl_2$ initially brings about a very marked reduction in specific conductance activation energies; the effect becomes less pronounced as MCl concentration increases up to about 0.5 mole fraction. Beyond this point, little further reduction of activation energies with increasing MCl concentration

occurs. For $ZnCl_2$-KCl at 400°C, for example, E_κ fell from 21 kcal/mole in pure $ZnCl_2$ to about 5 kcal/mole at 0.5 mole fraction. This effect became less pronounced as temperatures increased from 300°C to 600°C. Viscosity activation energies followed the same trend. Weeks interpreted these results firstly as a breaking down of a $ZnCl_2$ network structure followed by complex ion formation at higher MCl concentrations.

2.1.10. Molten Sulphates

Molten sulphates have not received the attention given to molten nitrates or carbonates. Nitrates are low melting and therefore relatively easy to work with; carbonates have considerable importance as electrolytes for high temperature fuel cells. Sulphate melts are generally high melting and have as yet little practical importance apart from their deleterious effects on boiler tubes in power stations burning sulphur-containing fossil fuels.[98] There has been, however, a recent interest in their electro-chemical properties. Burrows and Hills[99] and also Gul'din and Buzhinskaya[100] have recently investigated electrode processes in fused alkali sulphates. Other work has been directed towards electrowinning metals from sulphate containing melts.[101]

Zarzycki[102] has carried out X-ray study on some molten alkali sulphates, which indicate that the species in solution are M^+ and SO_4^{2-}. Free rotation of the anion is more likely to occur for potassium rather than lithium sulphate owing to preferred positioning of the potassium on the corner of the sulphate

tetrahedron. Walrafen[103] has studied the Raman spectra of molten Li_2SO_4 and Na_2SO_4 and found no evidence for any other associated species besides SO_4^{2-}.

A few thermodynamic measurements have been made on fused sulphates, the bulk comprising phase diagram studies.[58] Lumsden[104] has used these studies to classify some alkali halide-alkali sulphate binaries and also Li_2SO_4-K_2SO_4. Øye[105] has investigated the Li_2SO_4-Ag_2SO_4 system in both solid and liquid states using concentration cells. Very recently Holm[106] has measured heats of mixing in the Li_2SO_4-Na_2SO_4 system by high temperature calorimetry. These are expressed:

$$\Delta H_m = N(1-N)\ (-1388-2390N + 1683N^2) \qquad (11\text{-}33)$$

where N = mole fraction of Li_2SO_4.

The energetic asymmetry displayed in this system is remarkable and may be caused by a preferred cation orientation suggested by Zarzycki.[102]

2.1.11. Reciprocal Salt Solutions

(A) Introduction

A reciprocal salt mixture[1,12,13,14] contains at least two different cations and two different anions. In a mixture of four ions A^+, B^+, C^-, D^-, there are three degrees of freedom: four components and one restriction, electroneutrality. For a mixture made from two salts AC and BD, where in all phases $n_A = n_C$ and $n_B = n_D$, the ternary system reduces to a quasi-binary. A ternary mixture of arbitrary composition: X_A, X_B, X_C, X_D, can be made by

mixing any three of the four components.

The thermodynamic properties of reciprocal salt mixtures differ from those of simple binaries in that a metathetical equilibrium is set up:

$$AC + BD = AD + BC$$

If the Temkin model[33] is to apply, then the free energy and enthalpy change for the metathetical reaction should be zero and the behaviour of the binaries AC-BC, AD-BD, AC-AD, BC-BD should all be ideal. If the free energy change ΔG^{o} for the metathetical reaction is positive, then components AC, BD will tend to have greater than ideal activities; if ΔG^{o} is negative, then AC, BD will tend to have smaller than ideal activities. If ΔG^{o} is large (greater than about 15 kcal/mole), liquid-liquid immiscibility[107,58] may occur in some regions of the ternary phase diagram.

Among reciprocal mixtures of the alkali halides, the stable pair are the small cation-small anion, large anion-large anion combinations. Positive deviations from ideal behaviour increase in the order:

$$NaF - KCl < LiF - KCl < LiF - CsCl < LiF - CsBr.$$

Interactions in reciprocal systems are usually greater in magnitude than those in binary systems, because the former are mostly between nearest neighbour cations and anions.[12]

(B) Flood, Førland and Grjotheim Regular Solution Model (F.F.G.)

The authors[108] have proposed a method of predicting activities

in a ternary system from tabulated data for the pure salts and easily measured ion exchange equilibria in binary mixtures (including reciprocal quasi-binaries). They assumed regular solution behaviour and used the equations:

$$a_{AB} = X_A X_B \gamma_{AB}$$
$$\gamma_{AB} = \gamma'_{AB} \cdot \exp\left(\Delta G^{o}_{\cdot} X_C X_D / RT\right) \qquad (11\text{-}34)$$

where γ'_{AB} accounts for deviations from ideality not brought about by the exchange equilibria. Using a thermodynamic cycle, an equation is derived for the activity coefficient involving mixed ion activity coefficients, obtainable from ion exchange measurements.

In most cases it is assumed that binary interaction terms are negligible and only the metathetical equilibria are considered. The resultant equation may be used in mixtures of n components, of any charge type:

$$RT \ln a_{M_1X_1} = RT \ln (X_{M_1} X_{X_2}) + X'_{M_2} \cdot X'_{X_2} \Delta G^{o}_{M_2X_2} + X'_{M_3} X'_{X_3} \Delta G^{o}_{M_3X_3} + \ldots \qquad (11\text{-}35)$$

$\Delta G^{o}_{M_iX_i}$ are exchange free energies for the reactions:

$$M_1X_1 + M_iX_i = M_1X_i + M_iX_1$$

No binary measurements are necessary.

The F.F.G. equation predicts that the upper consolute temperature, T_C, below which a ternary separates into two layers is given by:

$$T_C = \Delta G^{o}/4R \qquad (11\text{-}36)$$

at $X_A = X_B = X_C = X_D = 0.5$

An example of this approach, of understanding a complicated ternary system by resolution into simple binary systems is Blander's calculation of solubility products and enthalpies of solution.[109]

(C) Grjotheim's Equilibrium Method

Grjotheim's equilibrium method[110,111] is similar to the F.F.G. treatment, utilizing ion exchange equilibria for the prediction of activities in ternary systems. Four equations are derived to determine the four unknowns, the activity coefficients of the four components. Briefly, the first equation involves the metathetical equilibrium, for example:

$$-\ln \gamma^2_{NaCl} - \ln \gamma_{CaO} + \ln \gamma_{CaCl_2} + \ln \gamma_{CaCl_2} = -\Delta G^o/RT, \quad (11\text{-}37)$$

the second, the Gibbs-Duhem equation applied to the ternary system:

$$2(X'_{Na^+} - X'_{O^{2-}})\, d \ln \gamma_{NaCl} + X'_{Ca^+}\, d \ln \gamma_{CaCl_2} + X'_{O^{2-}}\, d \ln \gamma_{Na_2O} = 0. \quad (11\text{-}38)$$

The third and fourth equations are based upon (1) anion exchange equilibria:

$$2X'_{Na^+}\, NaCl(1) + X'_{Ca^{2+}}\, CaCl_2(1) + \tfrac{1}{2}O_2(g) = Cl_2(g) + X'_{Na^+}\, Na_2O(1) + X'_{Ca^{2+}}\, CaO(1) \quad (11\text{-}39)$$

and (2) cation exchange equilibria:

$$2X'_{Cl^-}\, NaCl(1) + X'_{O^{2-}}\, Na_2O(1) + Ca(g) = 2Na(g) + X'_{Cl^-}\, CaCl_2(1) + X'_{O^{2-}}\, CaO(1) \quad (11\text{-}40)$$

It is possible to calculate activities if either anion or cation exchange equilibria are known over the concentration range of the ternary system and, respectively, the corresponding cation or anion exchange for the binary systems. The derivation has been extended to the general case where any number of components of any charge type may be present.

(D) Quasi-lattice Models

Quasi-lattice models proposed by Blander[12,13] and Førland[14] differ from earlier regular solution models in that non-random mixing is taken into account. A restriction upon these models is that they do not treat the long range forces which are present in binary mixtures and therefore apply only to dilute solutions.

The methods are based upon the quasi-lattice theory of Guggenheim.[45] Both authors' derivations are similar. Førland's will be given greater emphasis here, in that the final form is more applicable to later work.

Førland considers that in a random mixture of A^+, B^+, C^-, D^-, the probability that a particular cation site and a particular anion site are occupied by an A^+ and a C^- ion is $X_A X_C$; the number of A-C nearest neighbour pairs is $ZAvX_AX_C$ where Z is an effective coordination number, Av is Avogadro's number. In a non-random mixture, a parameter Y is introduced such that the number of A-C pairs is $ZAv(X_AX_C+Y)$. The energy of the reaction of the ion pairs

$$A^+ - D^- + B^+ - C^- = A^+ - C^- + B^+ - D^-$$ is given as

$\frac{\omega}{Z}$, where $Av\ \omega = \Delta E^o$. (11-41)

Neglecting interactions beyond next neighbours:

$$\frac{(X_A X_C + Y)(X_B X_D + Y)}{(X_A X_D - Y)(X_B X_C - Y)} = e^{-Av\omega/ZRT} \qquad (11\text{-}42)$$

When this equation is solved for Y, a logarithmic expansion results if $Av\omega$ is smaller than ZRT. Neglecting second and higher order terms, then the excess energy, excess free energy and excess entropy of mixing are given by:

$$\Delta E^E = -X_A X_B X_C X_D \Delta E^o/ZRT$$
$$\Delta G^E = -\frac{1}{2} X_A X_B X_C X_D (\Delta E^o)^2/ZRT$$
$$\Delta S^E = \frac{1}{2} X_A X_B X_C X_D (\Delta E^o)^2/ZRT^2 \qquad (11\text{-}43)$$

In molten salts, the pressure-volume work is usually quite small and $\Delta E^o = \Delta H^o$. The partial molar free energy of one component, AC, is given

$$\Delta \bar{G}_{AC} = -\frac{1}{2} X_B X_C (X_A + X_C - 3X_A X_C)(\Delta E^o)^2/ZRT \qquad (11\text{-}44)$$

In the symmetric approximation, Blander has considered the case where ΔE^o is greater than ZRT and solved the quadratic equation for Y. Activity coefficients are given as functions of Y. Where exchange energies are high,[112] association is likely to occur:

$$mA^+ + nC^- = A_m C_n^{(m-n)+} \qquad (11\text{-}45)$$

In the symmetric approximation, the energy of attachment of either an A^+ or X^- to any complex aggregate is the same, independent of the type or number of ions previously attached. The asymmetric approximation is somewhat more reasonable: the energy of successive attachments of C^- to an AC_{n+1}^{n-} grouping is the same

but not necessarily equal to the interaction energy between A^+ and C^-. Solutions however must be so dilute that no two A^+ ions are adjacent. Blander[12,113] has used his equations for activity coefficients to derive association constants for species in dilute solution.

(E) Conformal Ionic Solution Theory (C.I.S.)

Førland[36] suggested a modification to the simple F.F.G. equations. Four linearly additive binary terms were added, which expressed deviations from ideality in the four binary mixtures which could be made up of the ions in a ternary reciprocal salt. This form has since been derived in a more rigorous fashion by Blander et al.[114] His equation involves the first term of the F.F.G. theory, four linearly additive binary terms introduced by Førland and the fifth, a ternary excess mixing term. In the derivation, four monovalent ions are assumed, but it is equally applicable to any charge symmetrical system.

The mathematical derivation[114] is based upon the methods of Reiss, Katz and Kleppa. The following equation results for the excess Helmholtz free energy for a mixture made from the salts BC, AD, BD; (AB is also present in the ternary):

$$\Delta A^E_m = X_A X_C \, \Delta A^\circ + X_C \, \Delta A^E_{12} + X_D \, \Delta A^E_{34} + X_A \, \Delta A^E_{13}$$

$$+ X_B \, \Delta A^E_{24} + X_A \, X_B \, X_C \, X_D \, \Lambda + \ldots \qquad (11\text{-}46)$$

For molten salts ΔA^E_m may be set equal to ΔG^E_m; ΔG°,(ΔA°) is again the free energy change per mole for the exchange reaction. The terms ΔA^E_{12} refer to excess free energies of mixing in binary

mixtures of salts (1) and (2). Here, AD = salt (1), BD = (2), AC = (3), BC = (4). These binary mixtures are assumed to follow the regular solution equation, so that:

$$\Delta G^{E}_{12} = X_A X_B \lambda_{12}$$

$$\Delta G^{E}_{13} = X_C X_D \lambda_{13} \quad \text{etc.} \qquad (11\text{-}47)$$

where λ_{ij} are the regular solution interaction parameters for the mixture of salts (i) and (j); X_A, X_B etc. are the ion fractions of ions A, B in the ternary system. The final term in the C.I.S. equation corresponds to a correction for non-random mixing. This is the only term which is characteristic of the ternary system rather than binaries or pure salts. Λ is a function of complicated unevaluated integrals. By analogy with the equation for ΔG^{E}_{m} resulting from the quasi-lattice model, Blander gives an equation for Λ:

$$\Lambda = -(\Delta G^{o})^2/2ZRT \qquad (11\text{-}48)$$

where Z is the nearest neighbour coordination number.

Combining these binary equations with the C.I.S. equation[115] and differentiating with respect to the number of moles of one component, say BD, for an arbitrary total number of moles n, γ_{BD} may be evaluated:

$$RT \ln \gamma_{ED} = \frac{\partial n\Delta G^E_m}{\partial n_{BD}} = \frac{\partial n\Delta G^E_m}{\partial n_B} + \frac{\partial n\Delta G^E_m}{\partial n_D}$$

$$= X_A X_C \Delta G^o + X_A X_C(X_C - X_D)\lambda_{13}$$

$$+ X_C(X_A X_D + X_B X_C)\lambda_{24} + X_A(X_A X_D + X_B X_C)\lambda_{12}$$

$$+ X_A X_C(X_A - X_B)\lambda_{34} + X_A X_C(X_A X_D + X_B X_C - X_B X_D)\Lambda \qquad (11\text{-}49)$$

The upper consolute temperature for $X_A = X_B = X_C = X_D = 0.5$ is given approximately by:

$$T_C = \frac{\Delta G^o}{5.5R} + \frac{\lambda_{12} + \lambda_{24} + \lambda_{13} + \lambda_{34}}{11R} \qquad (11\text{-}50)$$

General systems have been investigated using these methods such as LiF-KCl.[116] A particularly useful application is a prediction of the topological features of simple reciprocal fused salt phase diagrams.[117]

2.2. Thermodynamics and Structural Properties of Salt Vapours

2.2.1. Theoretical Review

(A) Introduction

Interest[119] in the thermodynamic properties of salt vapours arises firstly from a theoretical and practical importance of their own and secondly because a knowledge of salt vapour composition is necessary for determining activities in liquid salt mixtures by vapour pressure methods. Moreover, experimental investigations on salt vapours can be used to develop theories of general ionic interactions if structural knowledge is known.

Methods of investigating salts vapours have been reviewed in chapters in two recent books;[119,5] therefore only a list need be given here.

mass spectrometry

infrared spectroscopy (including matrix isolation)

electron diffraction

electric deflection in an inhomogeneous field

absolute and relative vapour pressures

molecular beam analysis

microwave spectroscopy

Apart from a tendency to polymerise and form complexes at low pressures (< 150 mm) most salt vapours seem to obey the ideal gas laws. In many cases, heat capacities are approximately predicted by the classical kinetic theory of gases.[120]

(B) Alkali Halides

The simplest type of salt vapours are the alkali halides - these have been most widely studied and the presence of dimers and in some cases higher polymers has been well established.[5,121,122,123]

Vapour species have been shown to consist essentially of aggregates of ions held by electrostatic attraction. Vaporisation may be considered as a further extension of the structural changes occurring upon melting: the anion-cation distance is shortened and the coordination number (C.N.) is decreased. A comparison of interionic M-X distances is given below for solid, liquid,[25] dimer[125] and monomer vapour[5,119,124] species for the alkali chlorides.

Compound	Solid		Liquid		Dimer	Monomer
	C.N.	M-X (Å)	C.N.	M-X (Å)	C.N.	M-X (Å)	M-X (Å)
LiCl	6	2.66	4.0	2.47	2	2.33	2.02
NaCl	6	2.95	4.7	2.80	2	2.62	2.36
KCl	6	3.26	3.7	3.1	2	2.82	2.67
RbCl	6	3.41	4.2	3.30	2	3.06	2.79
CsCl	6	3.57	4.6	3.53	2	3.18	2.91

Distances in the solid and liquid states are taken from Levy and Danford[25] and are derived from first peaks of radial distributions. Apart from LiCl, M-X distances in the dimers are best estimates given by Bauer and Porter.[119] Dimers of the alkali halides have been shown to have a rhombohedral structure, although an isomeric

form of $(LiF)_2$ is known which has $D_{\infty h}$ symmetry.[126,127]

Cubicciotti and coworkers have found that thallium I halide vapours have similar properties to the alkali halides in that polymers as well as monomer species are formed. The dimer is the most important polymer. However, results indicate that $(TlX)_2$ species have a linear structure and possibly a Tl - Tl bond.[128,129]

Blander has proposed a dimensional theory to predict the degree of dimerization in alkali halide vapours.[132] The derivation is analogous to the R.M.K.[32] and R.K.K.[49] treatments of ionic liquids. The degree of dimer formation is found to be related to the cation to anion lengths, d, in the pure salts.

Recent interest has centered upon binary mixtures of alkali halides where "mixed dimers" may form:

$$(AX)_2 + (BX)_2 = 2ABX_2 \qquad (11\text{-}51)$$

Schoonmaker et al[130] have studied the fluorides, Milne and Kline[131] some of the chlorides. According to Blander, the equilibrium constant (K) for the formation of "mixed dimers" is related to the size parameters of AX and BX (d,d'):

$$\log(K/4) = m\left(\frac{1}{d} - \frac{1}{d'}\right) \qquad (11\text{-}52)$$

where m is a function only of temperature and of the properties of a reference salt. The predicted linear relationship has been observed in mixed alkali fluorides; it does not strictly apply with chloride or bromide mixtures. Van der Waals and higher order polarisation interactions are probably significant in these mixtures.[126]

A short review will now be given of halide vapours in groups II (with emphasis on the B subgroup) and group IV, with a mention of these in group III.

(C) Group IIA Halide Vapours

Dimer species are frequently formed with group II halides when the cation to anion radius ratio is less than 0.4.[134,135] The degree of dimerization is not as great as with the alkali halides. Complexes are formed with the alkali halides,[122] the most predominant of which is MAX_3, for example:

$$MgCl_2(g) + KCl(g) = KMgCl_3(g) \qquad (11\text{-}53)$$

Schrier and Clark[136] performed vapour pressure measurements on binary liquid $MgCl_2$-KCl mixtures and observed asymmetry in the plot of P_{KMgCl_3} vs mole fraction $MgCl_2$. This behaviour was ascribed to the formation of a second complex KMg_2Cl_5 having a much lower partial pressure than the first complex. Usually, binary halide mixtures with both cation valencies greater than one do not interact to form complexes unless both pure dimers are present.[126]

Electric deflection[137] and matrix isolated infrared[138] methods have been used to investigate geometries of some of the dihalides: all beryllium halides are linear while all other group IIA fluorides are bent.[139] Hildenbrand,[140] and also Zmbov,[141] have recently investigated dissociation energies in these halides.

(D) Group IIB Halide Vapours

Solid, liquid and vapour phases of group IIB halides have received considerable attention. Brehler's tetrahedral model[84] for solid zinc chloride and the results of Raman studies[80,86-90] on the liquid have already been presented.

A number of workers have studied the vibrational spectra of zinc halides. Klemperer[142] investigated the infrared spectra of the chlorides and bromides; antisymmetric stretching frequencies ν_3 were measured in emission in the gas phase. These results correspond to a linear geometry with $D_{\infty h}$ symmetry. Klemperer[143] and coworkers also determined their absorption spectra; in addition to the antisymmetric stretching frequencies found earlier, broad absorption bands were found for zinc chloride and zinc bromide. For cadmium halides no further absorption bands were found beside the stretching ν_3. The force constants derived from these frequencies differed from the bending force constants calculated from an ionic model by a factor of ten. It has been determined since that the new absorption bands in fact did not result from bending vibrations of the monomer but rather from vibrations of a dimer species. Infrared absorption spectra of matrix isolated zinc halides from 800 to 35 cm^{-1} by Loewenschuss et al[144] yielded four absorption regions for all the zinc halides. The highest energy region is structured and represents the antisymmetric stretching frequency ν_3. The second and third absorption regions are due to polymeric

species. The lowest absorption frequency was assigned as the bending vibration ν_2. The bending force constants calculated from this data agreed fairly well with those calculated earlier for the ionic model.[143]

Cubicciotti and Eding[145] have determined heat capacities of zinc chloride and zinc bromide to 700°C. Third law entropies for these molecules in the gas phase were calculated from the vibrational frequencies[144] which compared very favourably with those derived by statistical mechanics from the thermochemical measurements. As entropies calculated from thermochemical measurements are very sensitive to the bond angle of the zinc chloride monomer, a linear molecule seems most likely. As further evidence, Büchler et al[146,137] have carried out electric deflection studies and found no deflection in any of the group IIB halides studied: ZnF_2, CdF_2, HgF_2, $ZnCl_2$, $HgCl_2$, HgI_2. They concluded that all group IIB halides are linear. Electron diffraction studies[147] have further shown that group IIB halide monomers are linear.

The presence of dimer species in zinc chloride and zinc bromide vapour has been supported by use of relative and absolute vapour pressure methods and proved by mass spectrometry. Moss studied the chloride,[148] Keneshea and Cubicciotti[149a] the chloride and bromide, and Rice and Gregory[150] the chloride, bromide and iodide. Keneshea and Cubicciotti also carried out a mass spectrometry study in which in addition to monomer species,

$Zn_2X_3^+$ and weak ZnX_4^+ derived from $(ZnX_2)_2$, were found. They estimated that the amount of dimer in pure zinc chloride vapour varies from 14% at 412°C to 4% at 575°C. Heats and entropies of dimerization were found to be:

	$-\Delta H_D$ (kcal/mole)	$-\Delta S_D$ (cal/deg.mole)
$ZnCl_2$	40.1	48.6
$ZnBr_2$	30.5	37.3

Rice and Gregory reported much less dimer present: in the temperature range 500-600°C, the amount of dimer was less than 3%.

From vapour pressure studies on cadmium chloride vapour, Keneshea and Cubicciotti postulated the existence of a dimer.[149b] A mass spectrometric study up to 500°C yielded evidence for a very small amount of this dimer.

Loewenschuss et al[144] and Thompson and Carlson[151] have predicted a halogen bridged structure for ACl_2 dimers; see fig. 2-2. The bridge-bonding angle is likely to be 90°. Absorption bands attributed to $(ZnCl_2)_2$ can be accounted for with this structure.[144] Zinc halides differ from most salts that have polymeric vapour species in that while the heat of vaporisation of the monomer is greater than that of the dimer, the monomer is the predominant species at low temperatures (400°C). With magnesium halides the amount of dimer present increases with temperature.[149a]

Both Kerridge[152] and Corbett and Lynde[153] have postulated

FIGURE 2-2

DIMER STRUCTURES

1. $(MX)_2$

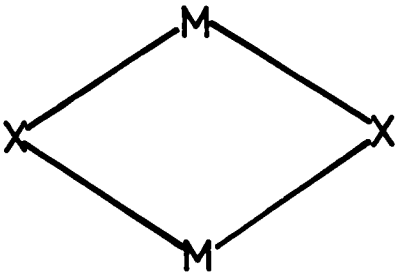

2. $(AlCl_3)_2$

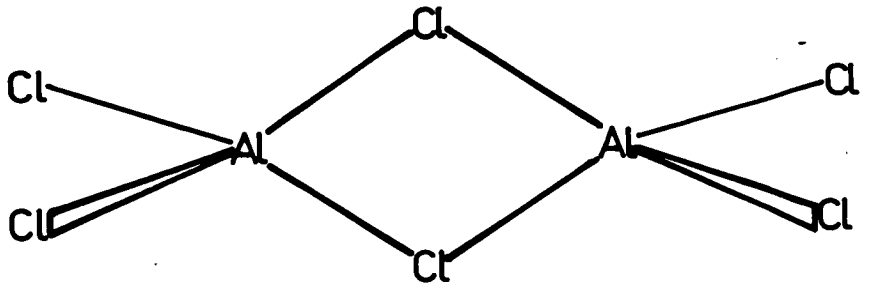

3. $(ZnCl_2)_2$

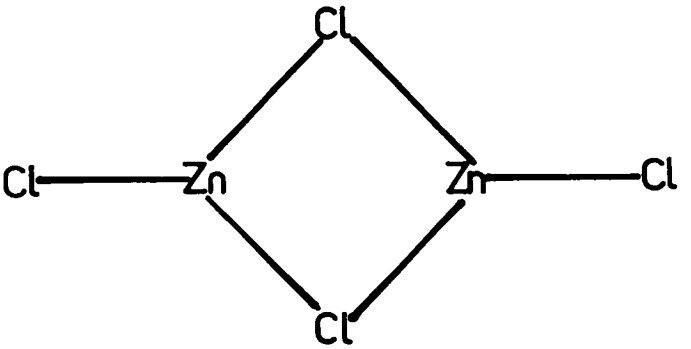

vapour species ZnX above mixtures of $Zn-ZnX_2$ (X = Cl,Br). Electronic and mass spectra indicate vapour phase reactions of the type

$$ZnCl_2(g) + Zn(g) = 2ZnX(g) \qquad (11\text{-}54)$$

in the temperature range 320-950°C.

Rice and Gregory[154] have examined vapour phase $ZnCl_2$-NaCl mixtures by vapour pressure methods. Evidence for complex formation was determined which they ascribed to the reaction:

$$ZnCl_2(g) + NaCl(g) = NaZnCl_3(g) \qquad (11\text{-}55)$$

Using transpiration methods, the amount of complex formed was found to be quite small, less than 1%. The calculated enthalpy change for the above reaction was -42 kcal/mole.

In a similar manner, Moss[148] investigated the gaseous $ZnCl_2$-KCl equilibria and suggested $KZnCl_3$ formation. Complex formation was also indicated in the $CdCl_2$-KCl system, which Moss ascribed to the reaction:

$$CdCl_2(g) + 2KCl(g) = K_2CdCl_4(g) \qquad (11\text{-}56)$$

That this is the major complex formed is unlikely in view of trends in other systems.[126] The vapour pressure work of Hastie[155] on $CdCl_2$-CsCl mixtures indicated $CsCdCl_3$ formation. Asymmetry in the amount of CsCl transpired as complex species was ascribed to formation of small concentrations of a higher complex $CsCd_2Cl_5$; this is analogous to the higher complex predicted for the $MgCl_2$-KCl system. Qualitative mass spectrometry of the systems $CdCl_2$-RbCl and $CdCl_2$-CsCl by Bloom and Hastie[31]

detected only the 1:1 species.

(E) Group III Halide Vapours

Aluminium halide systems have been the most widely studied. Only in AlF_3 does the monomer predominate in the vapour phase. Other aluminium halides are essentially dimeric having a halogen bridged structure;[119] see fig. 2-2. Vapour phase complexes of the type $NaAlF_4$[156] and $(NaAlF_4)_2$[157] have been shown to exist above their mixtures with alkali halides.

(F) Group IVA Halide Vapours

Only $SnCl_2$, $PbCl_2$ are easily studied as the divalent halides of Ge, Si and C show an increasing reactivity and tendency to disproportionate to tetravalent species.[158] $SnCl_2$ has been shown to form a dimer;[159] vapour pressure and mass spectrometric methods indicate that lead halide vapours are monomeric.[155,31] Electric deflection,[137] matrix isolation infrared,[138] and theoretical molecular orbital[155,160] studies all indicate a bent geometry for monomer molecules.

Vapour pressure studies above $SnCl_2$-MCl systems indicate complexing[159] reactions:

$$NaCl(g) + SnCl_2(g) = NaSnCl_3(g) \qquad (11\text{-}57)$$

Lead chloride-alkali chloride systems have been most extensively studied by vapour pressure,[155] vapour density and mass spectrometric techniques.[161] Large concentrations of complexes of the type $CsPbCl_3$ were found above the appropriate binary salt mixtures. There is no evidence for the formation of higher complexes.

2.2.2. Calculation of Thermodynamic Properties from Mass Spectrometric Data

The mass spectrometer may be used to derive the following quantities:[29]

(1) heats of vaporisation

(2) heat of formation of complex species

(3) equilibrium constants, free energies of complex formation

(4) partial pressures of high temperature species

With molecular flow conditions (see chapter 3), the partial pressure P of a species in the Knudsen cell is related to the observed ion current I^+ by the relationship:[162]

$$P = kI^+T \qquad (11\text{-}58)$$

where k is a constant, incorporating relative ionization cross sections and multiplier efficiency terms.

Considering the Clausius-Clapeyron equation for vapour liquid equilibrium

$$\ln P = -\frac{\Delta H_{vap}}{RT} + C \qquad (11\text{-}59)$$

heats of vaporisation may be determined from the slopes of linear plots of $\ln I^+T$ vs $\frac{1}{T}$.

Heats of formation of complex species may be determined by methods applying either the second or third law of thermodynamics.[29] The second law method requires measurement of ion currents over an adequate range of temperatures. For complex formation of the type:

$$NaBr(g) + PbBr(g) = NaPbBr_3(g)$$

an equilibrium ratio:

$$K_r = \frac{I^+T(NaPbBr_2^+)}{I^+T(Na^+).\ I^+T(PbBr^+)} \qquad (11\text{-}60)$$

where Na^+, $PbBr^+$, $NaPbBr_2^+$ are the observed ions, is directly proportional to the thermodynamic equilibrium constant K_P:

$$K_P = \frac{P_{NaPbBr_3}}{P_{NaBr}\ P_{PbBr_2}} \qquad (11\text{-}61)$$

From the Van't Hoff expression:

$$\ln K_P = -\frac{\Delta H_f}{RT} + C \qquad (11\text{-}62)$$

heats of formation of complexes (ΔH_f) may be found from slopes of $\ln K_r$ vs $\frac{1}{T}$. An equivalent method of obtaining the same result[161] is to utilize heats of vaporisation:

$$\Delta H_f = \Delta H_{vap}(NaPbBr_3) - \Delta H_{vap}(NaBr) - \Delta H_{vap}(PbBr_2) \qquad (11\text{-}63)$$

The first procedure is usually more applicable.

Third law methods require calculation of free energies of complex formation from equilibrium constant measurement and calculation of entropies of formation of each species from molecular constant data; alternatively estimates are used. Heats of formation are then derived from the equation

$$\Delta H_f = \Delta G_f + T\Delta S_f \qquad (11\text{-}64)$$

where ΔS_f is the entropy of formation of the complex.

Third law methods are usually more accurate if adequate data is available. Maximum accuracy to be expected then is ±2 kcal/mole.[126]

Methods of determining equilibrium constants and free energies of formation have been presented. Partial pressures of high temperature species may be determined by calibration of the Knudsen cell with a standard vaporising substance.[162]

3. EXPERIMENTAL

3.1. Materials Used

(A) Introduction

The following chemicals were used as starting materials:

Salt	Source	Purity
NaCl, KCl, KBr	Analar	>99.8%
NaBr	B.D.H.	>99%
RbCl, RbBr, CsCl, CsBr	Koch-Light	>99.5%
LiCl	May & Baker	99%
$ZnCl_2$	" " "	95%
$ZnSO_4 7H_2O$	" " "	99%
Na_2SO_4, K_2SO_4, $Pb(NO_3)_2$	Analar	99.5%
Zn metal	Electrolytic Zinc Co. Aust.	Ultrapure, (99.95%)
Cd metal	" " " "	"
$AgNO_3$	Matthey Garrett Pty. Ltd.	Chemically pure
Disodium ethylenediamine tetracetic acid	Analar	>99%

(B) Alkali Halides

These salts were dried for three hours at 400°C before use. Lithium chloride was dried for a longer period, about six hours.

(C) Sulphates

Na_2SO_4 and K_2SO_4 were dried in a similar manner to the alkali

halides. Anhydrous $ZnSO_4$ could not be obtained in the desired state of purity, therefore this salt was prepared by careful dehydration of the heptahydrate. About 150 g. $ZnSO_4$ was slightly heated to 30 - 40°C under a vacuum for 24 hours, during this time most of the water was removed. The salt was then crushed to a fine powder and again heated under a vacuum for 24 hours while the temperature was slowly increased to about 200°C. Final drying was achieved by heating to 450°C in a stream of dry argon. No sign of acid gases could be detected in this final stage. Analysis on the prepared product gave the following results:

	Actual	Theoretical
% Zn	40.40	40.50
% SO_4	59.40	59.50

The dried salt dissolved in water to give a solution neutral to phenolphthalein; melts containing $ZnSO_4$, when dissolved in water, sometimes left traces of undissolved material: the solution was still neutral. Hence it was concluded that negligible decomposition occurred during preparation and adequate drying had been achieved.

(D) Zinc Chloride

This salt proved to be the most difficult to prepare owing to its very hygroscopic nature. Upon heating, wet zinc chloride hydrolyses e.g.,

$$ZnCl_2 + H_2O = ZnOHCl + HCl$$

causing considerable changes in its properties. Therefore, zinc chloride was prepared only when needed; mixtures were made up as rapidly as possible and stored in a vacuum dessicator (molecular sieve type 5A being used as dessicant) before use within a few days.

Zinc chloride was purified by vacuum distillation, basically by the method given by Weeks.[97] About 100 g. impure zinc chloride were dried under vacuum at 200°C for several hours, this melted under an atmosphere of dry chlorine. Chlorine was then bubbled through the melt for 40 minutes before distillation.

The chlorine saturated melt was transferred to the silica apparatus shown in fig. 3-1; Weeks' design has been altered slightly to reduce bumping. The presence of chlorine in the melt would tend to prevent any formation of ZnCl reported by Kerridge.[152] Vacuum distillation at 600°C and 1 cm. pressure was used so that any moisture or chlorine present would be pumped away. The melt was maintained at this temperature by an air furnace and the receiver at 400°C by another furnace. The furnaces were fitted with windows to observe the distillation. An auxiliary nichrome wire heater around the side arm and glass wool insulation prevented premature condensation. Bumping during distillation was suppressed with a fine argon leak through a capillary tube; a thin platinum wire inserted through the capillary reduced the chance of blockage by solid particles.

FIGURE 3-1 $ZnCl_2$ DISTILLATION APPARATUS

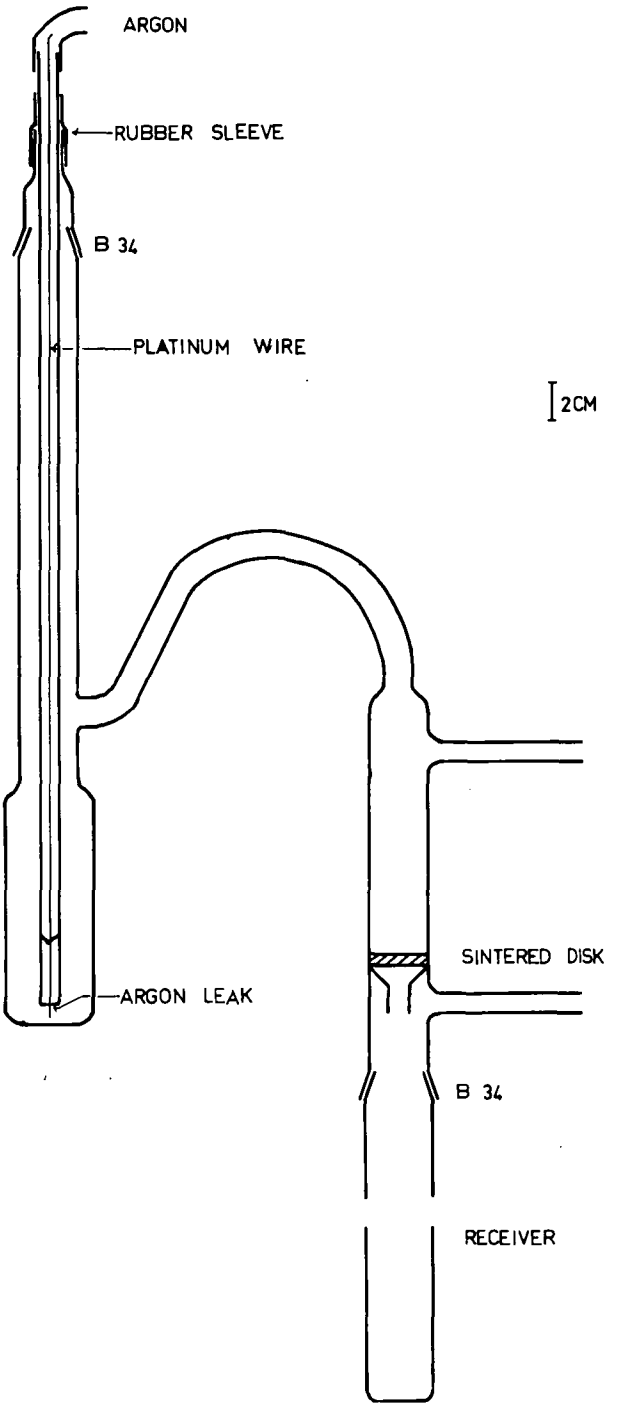

Side arms above and below the silica frit served either to evacuate the vessel, or to facilitate filtration of the collected melt, by applying pressure to the upper section. The clear distillate was collected in a Pyrex tube and sealed. Chemical analysis revealed that the product had a purity of better than 99.5%.

(E) Cadmium Halides

Cadmium halides were prepared by direct halogenation of pure molten cadmium metal with pure halogen gas. The method is outlined by Bloom et al[163] and has been shown to give a product of 99.5% purity.

(F) Lead Halides

Lead halides were precipitated from nitrate solutions using AR HCl or HBr solutions.[155] The product was recrystallised from boiling water to form fine needle-like crystals of better than 99.5% purity for $PbBr_2$ and 99.8% for $PbCl_2$.

(G) Sulphides

Sulphides were precipitated from $ZnCl_2$ or $Pb(NO_3)_2$ solutions with gaseous H_2S.

3.2 Experimental Methods of Studying Activities in Fused Salts.

3.2.1 Introduction

Reviews by Førland,[14] Blander,[12] and Janz[58] have very fully treated experimental methods of determining thermodynamic properties of fused salt mixtures. Therefore only the following list of general methods will be given here.

1. Heats of mixing
2. Activity measurements
    1. investigation of phase diagroms (cryoscopy)
    2. e.m.f. of galvanic cells - formation type
       - concentration type
    3. vapour pressure measurements:
       relative: transpiration, Knudsen effusion
       absolute: static, boiling point, torsion effusion
    4. heterogeneous equilibria.

3.2.2 Transpiration Techniques

In the investigation of reciprocal sulphate-chloride melts, a transpiration vapour pressure technique was used. With formation cells, Welch[21] has pointed out the possible reactions between electrode materials and species in the melt; moreover, achieving reversible anode reactions in sulphate melts could be troublesome. Of vapour pressure techniques, the transpiration method is best suited to handle a wide range of vapour pressures, as would be encountered in this study.

The transpiration technique has been described a number of times[164, 165] and only the essential details are given here. Basically, it is a non-absolute method so that vapour species transpired should be essentially monomeric or their molecular weights known. A sample of salt is placed in a furnace and a measured amount of an inert gas is passed over it. Salt vapour, saturating the inert gas, is swept into an exit tube where it condenses. The amount of salt vapour transpired is determined either by weighing or by chemical analysis. If vapour pressures are not too high (< 150 mm.), salt vapours have been found to behave ideally.[169] The salt vapour pressure P may be determined from the weight of salt collected m, if the molecular weight M is known:

$$P = \frac{m/M}{n_g + m/M} P_t \qquad (111\text{-}1)$$

n_g = moles of gas transpired, including other salt vapours.

P_t = pressure within furnace, mm. Hg.

For a mixture, if the vapour pressure measured is that of the monomer, then the activity of the salt under examination is given:

$$a = \frac{P}{P^o} \qquad (111\text{-}2)$$

P^o is the vapour pressure of the pure salt at the same temperature. Alternatively, if an n-mer vapour pressure has been determined then[165, 166]

$$a = \sqrt[n]{P_n/P^o_n} \qquad (111\text{-}3)$$

where P_n, P^o_n are the vapour pressures of the n-mer in the mixture and pure state respectively, of the considered salt.[165,166]

3.3. Experimental Procedures With Fused Salt Activity Studies

3.3.1 Preparation of Mixtures

While preparing mixtures greatest care was taken to minimise contact with air of the hygroscopic salts $ZnCl_2$ and $ZnSO_4$. To make up a mixture, a weighed amount of the less hygroscopic component was added to the other one, which was kept sealed in a cylindrical Pyrex container as much as possible. The mixture was then fused. In the activity studies it was desired to carry out four or five measurements at different temperatures, each one requiring three silica boats filled with salt mixtures of about the same composition. To facilitate filling, the fused mixture was first poured into a sealed spherical Pyrex flask (250 ml capacity) with a side arm for pouring. The boats were filled from this vessel in which mixing was facilitated and freezing during pouring eliminated.

Samples were also poured into tared silica dishes for analysis. Lead chloride mixtures were made up in the same way except that silica containers were used.

3.3.2. Temperature Control and Measurement

(A) Furnace

A Stanton Redcroft model 8104 internally Kanthal wound furnace was used to achieve the desired temperatures. Total length of the horizontal furnace was 24 inches. A constant temperature zone

± 0.5% was claimed for a length of 20 cm. Initially, a Stanton Redcroft "Eurotherm" PID/SCR Series Indicating Temperature Control Unit was used to maintain a constant temperature. Performance was at times less than satisfactory, fluctuations in temperature of the order of ± 0.5°C occurring. An earlier method used by Wong[164] was modified for use. The mains voltage was stabilised with a constant voltage regulator of 1.0 k V A rating. The furnace ran on a high current and low voltage; therefore a series combination of two 10A capacity variable auto transformers followed by a 240 V - 32 V step down transformer (750 watt rating) was used to control temperature. The first "variac" was usually set at about 200 V, the second maintained at 60 V. Fluctuations in furnace temperature were compensated for using the first "variac", which, being set at a higher voltage, permitted fine control to be achieved. In this way, furnace temperatures could be held constant to within 0.3°C for a period of hours.

(B) Temperature Measurement

Temperatures during transpirations were measured with a Pt-Pt (13% Rh) thermocouple using crushed ice -distilled water cold junctions. The wires were contained within capilliaries in an alumina insulator with a silica sheath outside. The e.m.f. was read on a Leeds and Northrup Co. Millivolt Potentiometer type 8686. The thermocouple was calibrated at the following thermometric points:[167]

(1) freezing point 99.95% Zn (419.5°C)

(2) freezing point 99.999% Al (660.1°C)

Deviations from the published e.m.f. temperature relationship were all within 0.2°C.

3.3.3. Transpiration Assembly

(A) Transpiration Tube

Earlier studies[164] indicated the need to restrict the volume of the transpiration tube to a minimum, in order to reduce changes of composition through loss of volatile salt. The assembly is shown in fig. 3-2. The transpiration tube was made from vitreous silica 30" long, 1" I.D., 1/8" thick, situated almost symmetrically within the horizontal furnace. Plugs of glass wool at the furnace ends improved temperature homogeneity. Argon entered the transpiration tube through one arm of a glass "T" piece - the other arm was connected to a dibutyl phthalate manometer, which measured the excess pressure within the transpiration tube caused by resistance to flow at the gas collection end. Use of dibutyl phthalate (May and Baker 99% pure, density 1.042 - 1.049 at 20°C) as manometer fluid allowed more accurate relative pressure measurement than mercury. The condenser tube was made from silica 20" x 5/16" O.D., the hot end was narrowed down to 1/16" I.D. to restrict inward diffusion of salt vapour. The condenser tube was placed nearer the top of the transpiration tube, collinear with the thermocouple to prevent accumulated salt flowing out of the orifice.

FIGURE 3-2

Transpiration Tube Assembly

Legend

A : Furnace 24" long

B : Silica transpiration tube, 30" long, 1" I.D., 1/8" thick

C : Condenser guard tube

D : Condenser tube 20" long x 5/16" O.D.

E : Thermocouple sheath

F : Argon inlet

G : Side arm to dibutyl phthalate manometer

H : Silica boats, 3" long, 0.4" wide, 0.6" deep

J : Rubber bungs

FIGURE 3-2
TRANSPIRATION TUBE ASSEMBLY

(not to scale)

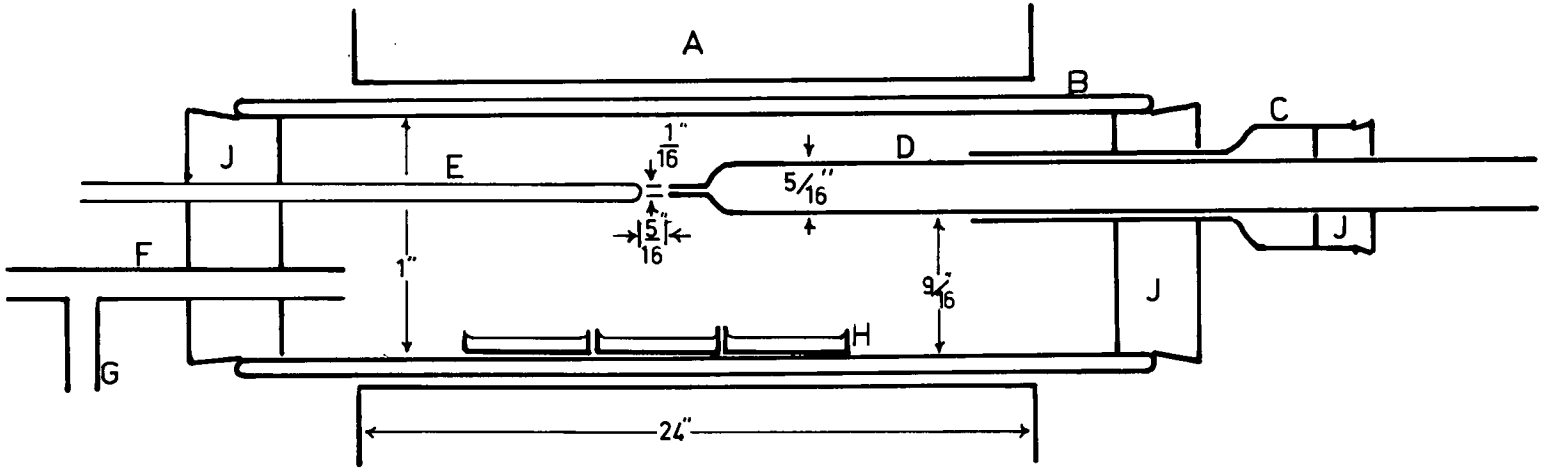

(B) Carrier Gas Driving System

The carrier gas driving system was an adaption of that already given by Wong.[164] The flow system is given in fig. 3-3. Argon from the cylinder was partially dried by passing through silica gel, then completely deoxygenated in a tower of copper metal finely dispersed on kieselguhr heated to 300°C. Last traces of moisture were removed in a tower of molecular sieve, type 5A. A capillary type gas flow meter, containing dibutyl phthalate, was preceded by a glass blow off containing the same liquid. Constant back pressure was achieved during a run by having a small flow out of this blow off.

A number of glass taps allowed argon to be passed through the furnace in either direction; transpired argon was collected by downward displacement of water in two or one litre volumetric flasks. A two-way tap permitted continuous argon collection. A capillary 2.5 cm. long, 1 mm. dia., at the end of the bubbling tube ensured an even flow rate into the flasks. A photograph of the assembled apparatus is shown in fig. 3-4.

3.3.4. Procedure During an Experiment

The furnace was allowed to achieve the desired stable temperature over several hours, preferably overnight. During this time air was flushed out of the transpiration tube with a continuous flow of argon (fig. 3-3); the condenser tube was not in position at this stage.

FIGURE 3-3

Carrier Gas Flow System

Legend

A : Fine control needle valve

B : Silica gel drying tower

C : Deoxygenation furnace; copper finely dispersed on kieselguhr at 300^{o}C

D : Molecular sieve (type 5A) drying tower

E : Blow off (dibutyl phthalate)

F : Capilliary flow meter (dibutyl phthalate)

G : Three way taps

H : One way tap

J : Two way tap

K : Blow off (dibutyl phthalate)

L : Manometer (dibutyl phthalate)

M : Transpiration furnace (arrow indicates direction of positive flow)

N : Capilliary bubbling tube (2.5 cm long, 1 mm dia.)

P : 2,000 ml volumetric flask

Arrow indicates direction of positive argon flow

FIGURE 3-3

CARRIER GAS FLOW SYSTEM

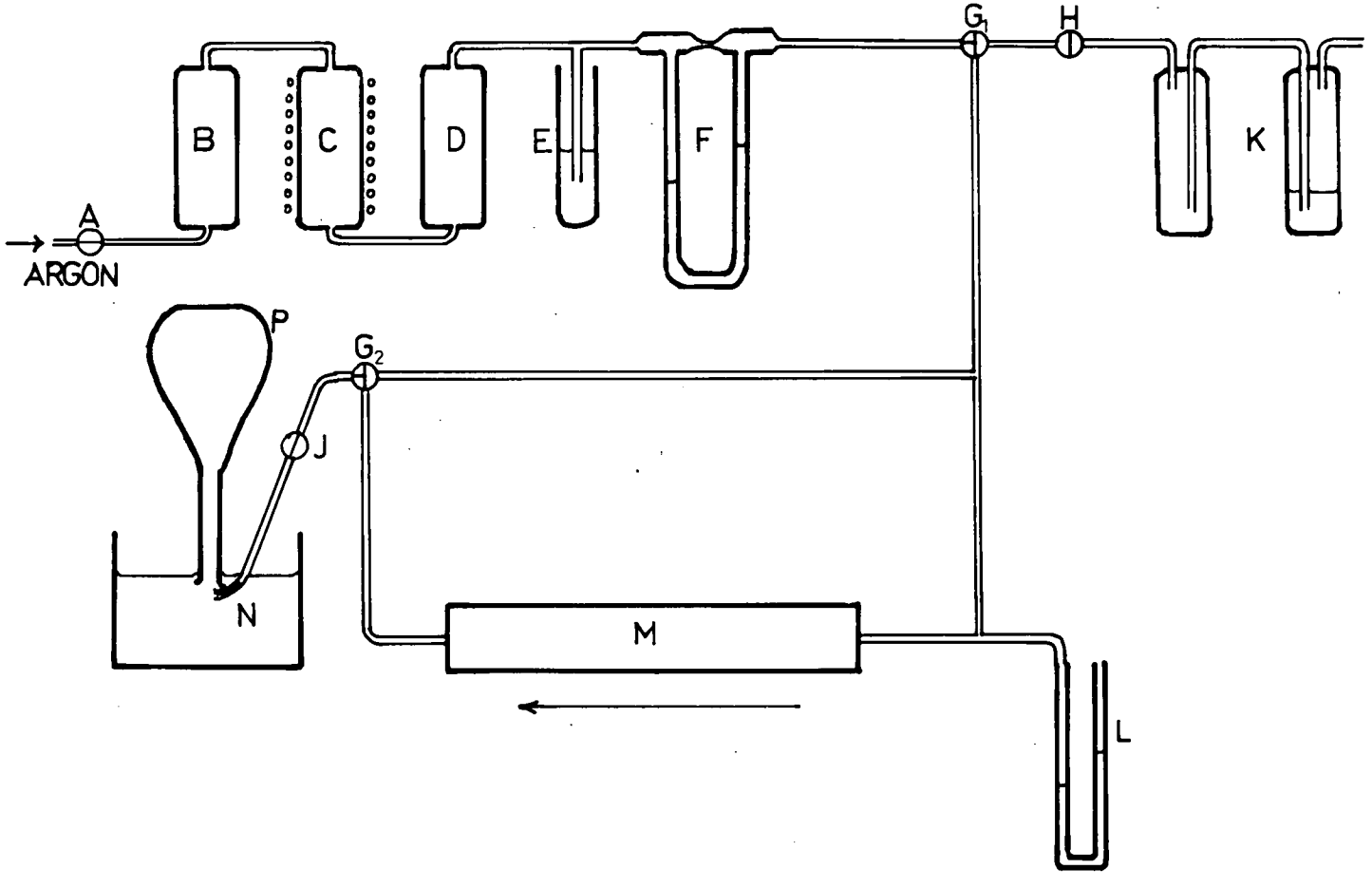

FIGURE 3-4

The Assembled Transpiration System

Legend

A : Line from argon cylinder

B : Purification Towers (silica gel, copper, molecular sieve)

C : Flow meter

D : Argon inlet and thermocouple

E : Potentiometer

F : Manometer (dibutyl phthalate)

G : Furnace temperature controls (mains stabiliser, "variacs", transformer)

H : Furnace

J : Transpiration Tube

K : Condenser tube and guard

L : 2,000 ml flasks for gas volume measurement

M : Constant volume tank (water)

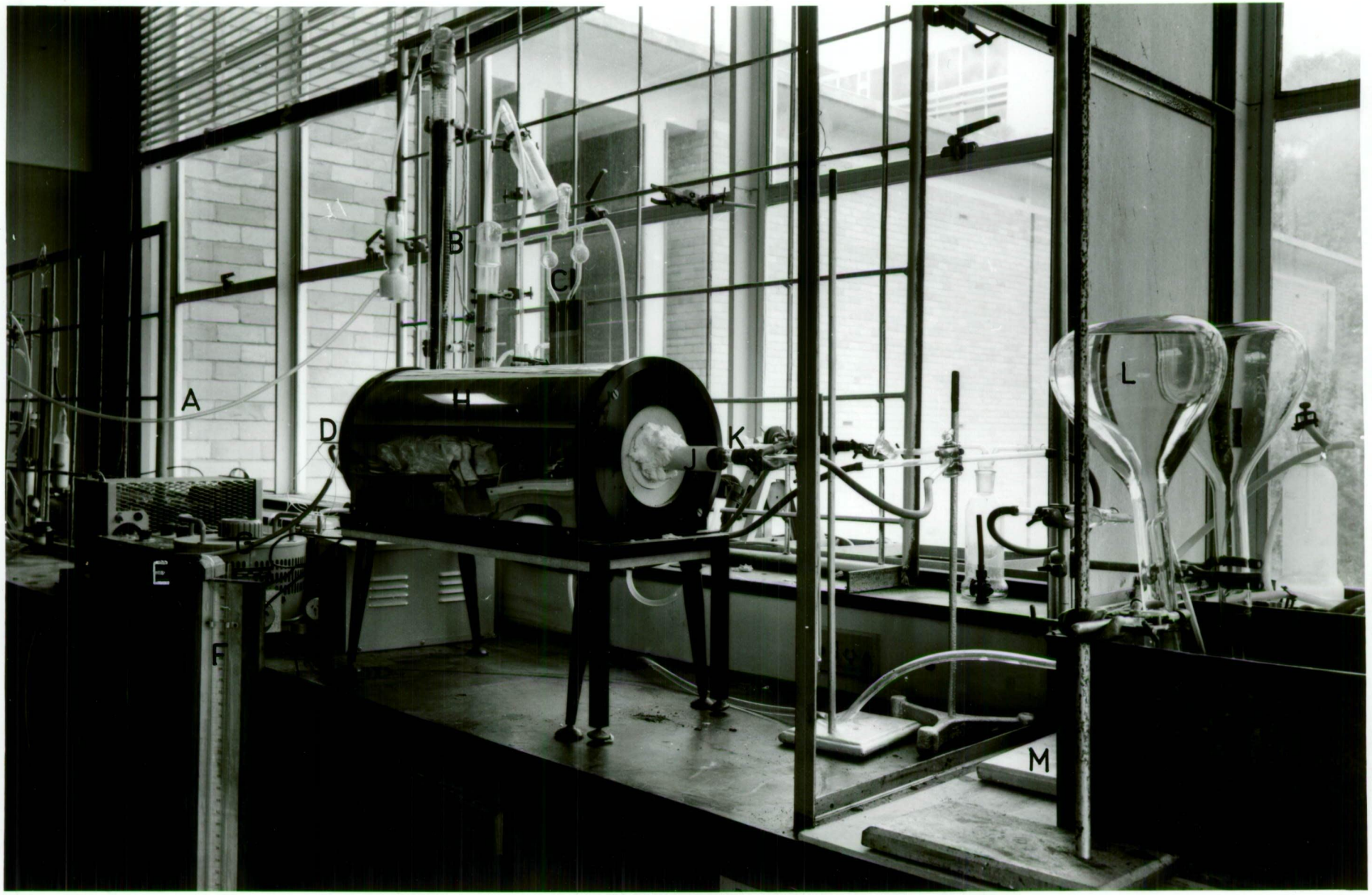
A
B
C
D
E
F
K
L
M

Before a run commenced, tests were made for any leaks by pressurising to 20 cm. excess of dibutyl phthalate, and isolating the system via the glass taps. If no significant drop in pressure occurred after 20 minutes, the procedure was continued. With a fast flow of argon in the positive direction, three silica boats, 3" long, 0.4" wide and 0.6" deep, three quarters full of salt mixture, were pushed into the transpiration tube with a marked silica rod, so that the boats were situated symmetrically about the hottest zone. The condenser guard was replaced, any air flushed out with argon and the flow direction reversed. The argon line was then connected to the predried condenser tube which was carefully inserted into position in the transpiration tube; an argon backflow of 10 ml/minute prevented diffusion of salt into the condenser tube until the actual transpiration began. The optimum position for the condenser tube was $\frac{5}{16}$ inch from the thermocouple tip and collinear with it. When no detectable drift in temperature was found for a period of 20 minutes, the transpiration was commenced by firstly reversing taps G_1 and G_2. Argon now simply passed straight through to blow off D; by turning off tap H, flow through the transpiration tube in the collection flasks commenced. At any time, the transpiration could be stopped without unduly upsetting the measurement by simply opening tap H. Temperatures were read every twenty minutes and fluctuations, less than $\pm$ 0.2°C, compensated for. Barometric pressure and relative dibutyl

phthalate manometer pressures were read every hour. When the required amount of argon had been transpired (typically sufficient to produce 2 x 10^{-3} moles of $ZnCl_2$ condensate) tap H was opened and the condenser tube removed. The outside was carefully washed free of salt, then the contents quantitatively washed into a 250 ml volumetric flask with distilled and deionized water. Soon after, the flasks were made up to volume and transferred to plastic bottles to minimise sodium uptake from the Pyrex glass. Silica boats were removed with a hooked silica rod and contents poured into tared silica dishes for analysis. To determine the volume of argon in the flasks, the water temperature was made equal to ambient air temperature (within 0.2°C) with addition of hot or cold water. The flasks were raised or lowered to equalise water levels and this level on each flask marked with a rubber band. If, after 15 minutes this level had not altered, the flask was removed, temperature and pressure noted. The difference between marked and calibrated levels was determined by addition of water from a burette.

Moles of argon passed n_g, were calculated from the volume of argon passed V, as follows:

$$n_g = \frac{(P_{corr} - P_W)V}{RT_W} \qquad (111\text{-}4)$$

P_{corr} = atmospheric pressure, corrected[168] for temperature (brass scale) and acceleration due to gravity.

P_W = vapour pressure of water at temperature T_W.

R = gas constant.

Transpired lead chloride was somewhat more difficult to dissolve than zinc chloride, contents were washed into a beaker with a solution of AR ammonium acetate AR - acetic acid, before addition to volumetric flask.

3.3.5. Preliminary Aspects

In order to ensure that correct conditions are maintained during transpiration, various checks are required. Merton and Bell[169] have discussed the limiting factors on the usefulness of the method.

(A) Diffusion

At high salt vapour pressures there is a tendency for diffusion of salt into the condenser tube. While thermal equilibrium is being achieved before the experiment, the effect will be reduced because of the backflow of argon. These effects were examined, by repeating the procedure without actually transpiring any gas, and determining the amount of salt entering the condenser. With pure $ZnCl_2$ at 590°C (about 75 mm. pressure), negligible diffusion occurred when a backflow of 5 ml/minute was used. With static tests on pure $ZnCl_2$, percentages of diffused salt were of the order of 0.2%; with $ZnCl_2$ mixtures somewhat larger values, about 0.4% were obtained. With $PbCl_2$-Na_2SO_4 mixtures, percentages of diffused salt were typically 0.2%. Amounts of diffused salt were subtracted from the total transpired.

(B) Temperature Homogeneity

As the thermocouple weld cannot be an intimate contact with the condenser tip, some temperature difference could occur. The effect was investigated by determining the temperature gradient within the transpiration tube. The thermocouple sheath was moved further into the furnace and temperatures measured at 1 cm. intervals as the insulator was removed; see fig. 3-5. The maximum temperature zone was found to be about 1.5 cm. off centre; the thermocouple tip and condenser tip were placed symmetrically about this point, $\frac{5}{16}$ inch apart, directly above the middle silica boat. The difference in temperature between the two was less than $0.1^{o}C$. The process was checked at a higher temperature for $PbCl_2$ mixtures.

(C) Saturation of Argon with Salt Vapour

Checks were made by measuring vapour pressures of salts of fixed temperature and variable flow rates, see fig. 3-5. For pure $ZnCl_2$, measurements at $554^{o}C$ indicated saturation at flow rates up to at least 60 ml/minute. In practice, flow rates between 30 and 40 ml/minute were used with pure zinc chloride. Smaller flow rates are needed with mixtures where surface depletion of the volatile salt may occur. Two independent checks were made, each using samples of the same composition.

FIGURE 3-5

STANDARDISATION OF APPARATUS

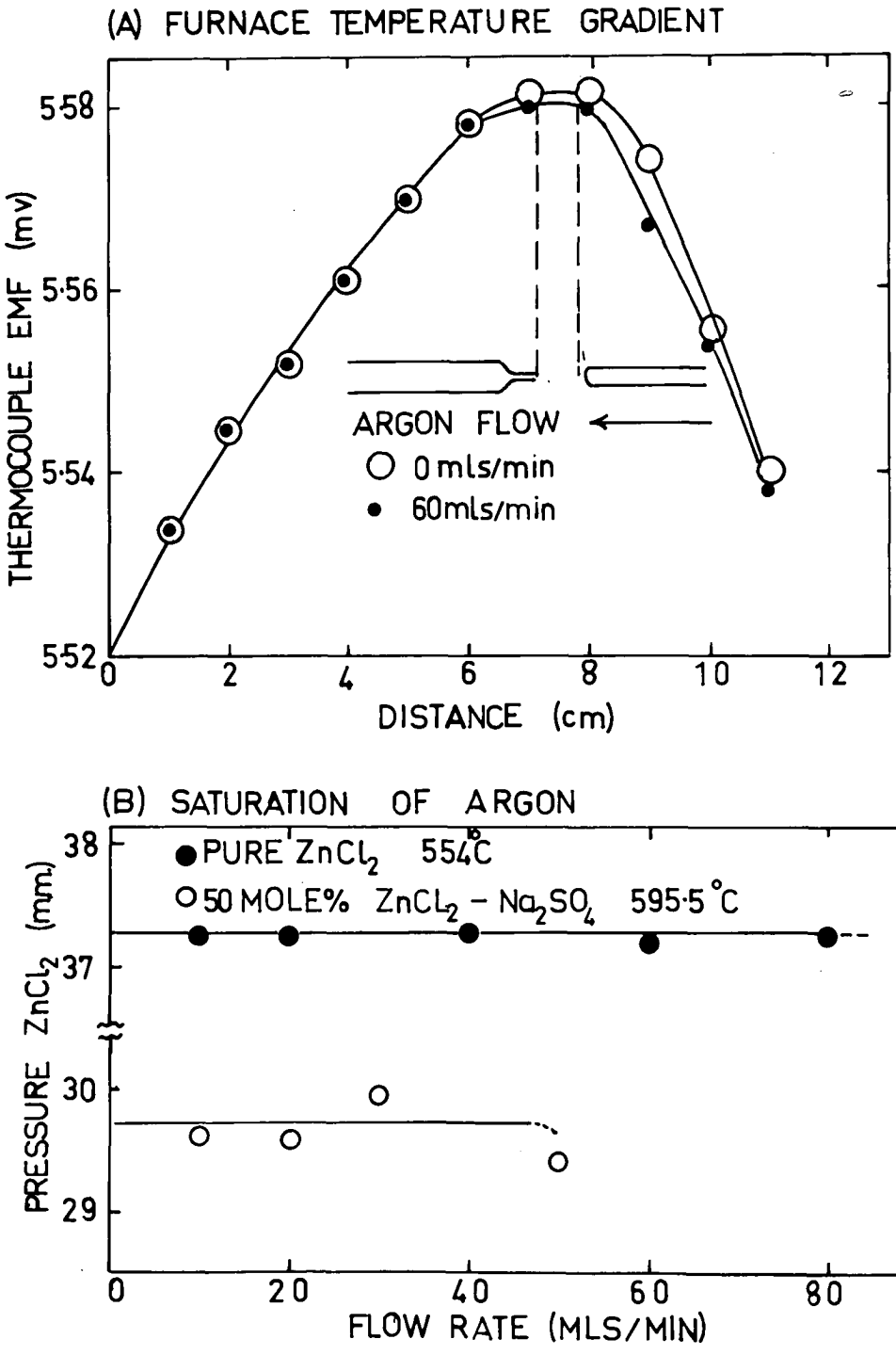

1. Approximately 50 mole % $ZnCl_2$-Na_2SO_4 at 595.5°C

Flow rate (ml/min)	V.P. $ZnCl_2$ (mm.)
10	29.62
20	29.57
30	30.11
40	29.40

2. 38 mole % $ZnCl_2$-Na_2SO_4 at 530.6°C

18 ml/min	0.339
26 ml/min	0.345

It was concluded that saturation was achieved for flow rates at least up to 20 ml/minute. Actually, flows between 15 and 20 ml/minute were used.

The higher temperature of $PbCl_2$ mixtures permitted greater flow rates to be used. Welch,[21] in similar systems found saturation prevailing with flow rates of up to 60 ml/minute. Again checks on a mixture were made:

Approximately 38 mole % $PbCl_2$-Na_2SO_4

35 ml/min	1.35
50 ml/min	1.32

Hence, saturation was being achieved at flow rates of 30-35 ml/minute which were used.

3.3.6. Chemical Analysis

Sampling

Analysis of boat contents after a run usually revealed that the first boat in line with the argon flow changed composition much more than the other two, where changes before and after a run were usually less than 0.5%, most of the transpired salt is removed from this front boat. Following the procedure of Barton,[170] Hastie,[155] and Keneshea and Cubicciotti[149a] the composition of the front boat was neglected; the arithmetic average of (1) the initial composition and compositions after the run of (2) boat two and (3) boat three was taken. General analytical procedures were based upon those given by Vogel.[171]

(A) Zinc and Lead

Zn^{2+} and Pb^{2+} were determined volumetrically with disodium ethylenediamine tetracetic acid. For Zn^{2+}, NH_4OH-NH_4Cl buffer and eriochrome black T indicator were used; for Pb^{2+}, hexamine buffer and xylenol orange indicator were used. With analysis of condensates, solutions of 0.01N were used, for boat analysis, 0.1N solutions were needed. In each case EDTA solutions were standardised against solutions of 99.997% Zn dissolved in excess of HCl. Reproducibility was better than 0.1%

(B) Chloride

Silver nitrate solutions were used with dichlorofluorescein as indicator; standardisation was made against AR NaCl. Some checks

were made on condensate analysis using 0.01N solutions; duplicates agreed to 0.1%. For boat compositions, $AgNO_3$ concentrations of 0.1N or 0.2N were needed. Some difficulty was encountered at these concentrations, owing to coagulation of AgCl precipitate; a back titration technique was used. Chloride solutions were diluted to 0.05N and 2 drops of a synthetic non-ionic detergent, nonylphenolnonaethoxyethanol added to prevent coagulation. An excess of 0.1N $AgNO_3$ was added and back titrated with 0.005N NaCl solution, until the suspension turned white, 0.2% reproducibility was obtained.

(C) Sulphate

Sulphate concentrations were determined gravimetrically by precipitation as $BaSO_4$ with solutions of AR $BaCl_2$. The precipitate was coagulated using agar-agar solutions, collected in porcelain filtering crucibles and heated at 650°C to constant weight.

(D) Potassium and Sodium

Small concentrations of K^+ and Na^+ ions in condensate solutions were analysed by atomic absorption spectrophotometry. A Techtron A.A.5 instrument was used. Calibration was made with dilute NaCl and KCl solutions and minor corrections made for slight interference from Zn^{2+} or Pb^{2+} present in relatively large concentrations.

3.3.7. Thermal Stability of Molten Sulphates

During vapour pressure experiments, no indication of

decomposition of molten sulphates was observed. Following drying, chemical analysis on $ZnSO_4$ showed that the correct stoichiometric proportions of Zn^{2+} and SO_4^{2-} were present. Samples of $ZnSO_4$-containing melts, when dissolved in water were neutral; chemical analysis for Zn^{2+}, SO_4^{2-} and Cl^- usually accounted for at least 99.8% of the sample weight. No acid gases were observed in the transpired argon effluent.

Ostroff and Sanderson[172] detected no sign of decomposition of solid $ZnSO_4$ at temperatures below 646°C, nor of solid $PbSO_4$ below 803°C. Published decomposition pressures of Stern and Weise[173] indicate that negligible decomposition of these sulphates should occur at the temperatures used. Alkali sulphates are able to be melted without decomposition.[174, 103].

3.3.8. Vapour composition

In this work, activities were calculated as relative transpiration vapour pressures which were based upon total moles of zinc chloride transpired. Dimerization and also complex formation in the vapour phase could slightly affect calculation of results. Fortunately, the effect of the one tends to offset the effect of the other. Previous workers, such as Wong[164] and Bloom et al[91] have simply ignored these effects on the basis of the small pressures of non-monomer vapours present.

(A) Complex formation

Mass spectrometric investigations described in this thesis indicate that probably only one vapour phase complex, $NaZnCl_3$, is present above $ZnCl_2$-NaCl mixtures; its relative partial pressure appeared to be quite small. Amounts of $ZnCl_2$ transpired as $NaZnCl_3$ would increase apparent activities. Na^+ analyses were carried out on condensate solutions, amounts present were quite small and varied somewhat with composition and temperature. Amounts of Na^+ transpired as NaCl species were calculated using Barton's[170] equation for NaCl vapour pressure, assuming melt activities of NaCl followed the Temkin equation. Actually, only a few percent of total Na^+ found would be transpired as NaCl species. Amounts of $ZnCl_2$ transported as $NaZnCl_3$ were calculated not to exceed 1% of the total $ZnCl_2$ transpired. These findings are in agreement with those of Rice and Gregory[154] who found only small $NaZnCl_3$ partial pressures above $ZnCl_2$-NaCl mixtures. Hence complex formation alone would render calculated activities a maximum of 1% too high.

(B) $ZnCl_2$ dimerization

Pure $ZnCl_2$ contains a small amount of dimer in its saturated vapour. Keneshea and Cubicciotti[149a] give figures of 14% at 412°C to 4% at 575°C for the percentage of dimer. The figures of Rice and Gregory[150] are a good deal lower, less than 3% at 500°C and

becoming smaller as temperatures increase. Measurements in this work were carried out between 500°C to 630°C. The effect of dimerization upon calculated activities will be greatest at 500°C.

It was noted earlier (111-3) that if n-mer pressures are compared, then thermodynamic activities are given by the equation:[166]

$$a = \sqrt[n]{\frac{P}{P^o}}$$

Assuming for the moment that the amount of dimer above the mixture is the same as that over pure $ZnCl_2$ at constant temperature, then n will lie between 1 and 2 and activities calculated on the assumption of n = 1 will be slightly low. This effect will be greatest at high $ZnCl_2$ activities; at low $ZnCl_2$ activities, dimer dissociation will tend to occur. With 90% $ZnCl_2$-Na_2SO_4, $a_{ZnCl_2} \approx 0.8$, $P^o_{ZnCl_2} = 10$ mm.; the amount of dimer present in pure saturated $ZnCl_2$ vapour at 500°C is probably less than 4%. The true activity is given by

$$a_{ZnCl_2} = \sqrt[1.04]{\frac{8}{10}}$$

$$= 0.807$$

Calculated activities would be about 0.8% too low. The experimental error in measuring activities is of the order of 2-3%. The small positive error due to $NaZnCl_3$ formation would cancel this small

negative error.

As activities of $ZnCl_2$ in mixtures decrease, the degree of dimerization in the vapour phase will also decrease. The dimerization equilibrium constant: $K_D = P_{dimer}/(P_{monomer})^2$ is a function only of temperature. In the very worst case where all dimer dissociates ($a_{ZnCl_2} < 0.01$) calculated activities could be up to 4% too low at 500°C on this basis. At higher temperatures there is less dimer and dissociation is not as significant. In practice the greatest error would be less than 4%; where a_{ZnCl_2} was low, a_{NaCl} was usually relatively high and percentages of $NaZnCl_3$ formed were about 1%. Therefore the true maximum error is 3%. For activities, such a figure is hardly greater than experimental error; adequate corrections have been made to calculated activities in those few cases where dissociation is significant. Partial molar enthalpies are also likely to be affected: if the amount of dimer present in pure $ZnCl_2$ were halved from 500°C to 600°C, at low activities partial molar enthalpies could be affected by 250 cals. Corrections have again been made where necessary.

(C) $PbCl_2$-K_2SO_4

Mass spectrometric and vapour pressure studies all indicate an absence of dimers in $PbCl_2$ vapours. Formation of $KPbCl_3$ is significant however. Analysis of condensates of $PbCl_2$-K_2SO_4 mixtures indicated that up to 9% of total $PbCl_2$ transpired was

present as $KPbCl_3$. Corrections for KCl species in the vapour, using Barton's KCl vapour pressures[170], were small. Amounts of $KPbCl_3$ found were subtracted from the total amount of $PbCl_2$ transpired.

(D) Conclusion

In the systems studied in this work, the effects of dimerization and complex formation are small and may be corrected for. Nevertheless it is apparent that attention to these effects is necessary when using the transpiration technique. In systems where large amounts of non-monomer species are present in the vapour, the transpiration technique would become inaccurate.

3.4. Experimental Mass Spectrometry

3.4.1. The Mass Spectrometer

The principal advantage of the mass spectrometer lies in its ability to scan a wide range of masses simultaneously. It consists of four components: sample source, ionizer, mass analyser and detector. Each of these will be briefly discussed in turn.

Any sample inlet system[175, 176] should allow pressures in the ionizer and analyser regions to be less than 10^{-5} mm. For thermodynamic studies, it is essential that the vapour entering the ionizer should be a representative sample and that equilibrium with the liquid phase should be attained. The Knudsen cell[177, 178] is widely used for this purpose. This consists of a closed inert heated container: vapour effuses through a small orifice in the form of a molecular beam at such a slow rate that vapour-liquid equilibrium is maintained within the cell; the molecular beam is ionized and mass analysed. The need to obtain Knudsen effusion places upper limits upon internal pressures and orifice dimensions.

The function of the ion source is to produce ions from species effusing from the Knudsen cell, and to accelerate them into the mass analyser. Of ionization methods, electron impact is by far the most widely used;[179] the need for a monoenergetic ion source has recently recreated interest in photoionization techniques.[180] With conventional ionizers, surface or chemical ionization modes may also

be partly taking place, complicating mass spectra.[179,181]

Usually, dissociation as well as simple ionization to positive ions occurs. Lead chloride for example is known to fragment as follows:[31]

$$\begin{aligned} e + PbCl_2 &\rightarrow PbCl_2^+ + 2e \\ e + PbCl_2 &\rightarrow PbCl^+ + Cl + 2e \\ e + PbCl_2 &\rightarrow Pb^+ + 2Cl + 2e \end{aligned} \qquad \text{(III-5)}$$

Dissociative ionization usually occurs in this manner for simple salts i.e. one electronegative atom is split off at a time. Many lithium salts however undergo different modes of dissociation.[119,126] Negative ions may be formed by electron capture:

$$e + PbCl_2 \rightarrow PbCl_2^- \qquad \text{(III-6)}$$

The appearance potential of an ion is the minimum energy required to produce the given ion from a given molecule. Increasingly fragmented ions from the one species have higher appearance potentials.[179,181]

Complications can occur if ionizer pressures become too high and ion molecule reactions are allowed to occur, for example:[29]

$$LiI^+ + LiI \rightarrow Li_2I^+ + I \qquad \text{(III-7)}$$

At normal operating temperatures, fragmentation patterns should be almost independent of temperature.[183] Therefore, ratios between ion currents of fragments derived from one common species should be

almost temperature independent.

Types of mass spectrometer used for high temperature studies are the magnetic, time of flight and recently the quadrupole type. A description of this last type will be presented here.

The quadrupole assembly is a true mass filter, details of which were first published by Paul et al in 1958.[184, 185] Commercial instruments have been available for only a few years. The mass filter is composed of four stainless steel cylindrical rods precisely located in a rectangular array. DC voltage $\pm V_1$ and superimposed RF voltage $\pm(V_0 \cos wt)$ are applied to the rods as shown in fig. 3-6, generating an electrostatic field.[186] The potential, ϕ of this electrostatic field is given approximately by

$$\phi = (V_1 + V_0 \cos wt)\ (x^2 - y^2)/r_0^2$$

where r_0 = (distance between rods) /2. (111-8)

The motion of a singly charged ion of mass m, when it enters the field, is given by

$$m\ddot{x} + (2e/r_0^2)(V_1 + V_0 \cos \omega t)\ x = 0 \qquad (111\text{-}9)$$

$$m\ddot{y} + (2e/r_0^2)(V_1 + V_0 \cos \omega t)\ y = 0 \qquad (111\text{-}10)$$

$$m\ddot{z} = 0 \qquad (111\text{-}11)$$

where x,y,z are the three dimensional coordinates. The filtering action of the rods results from motion described by (9) and (10).

FIGURE 3-6

MASS FILTER SYSTEM

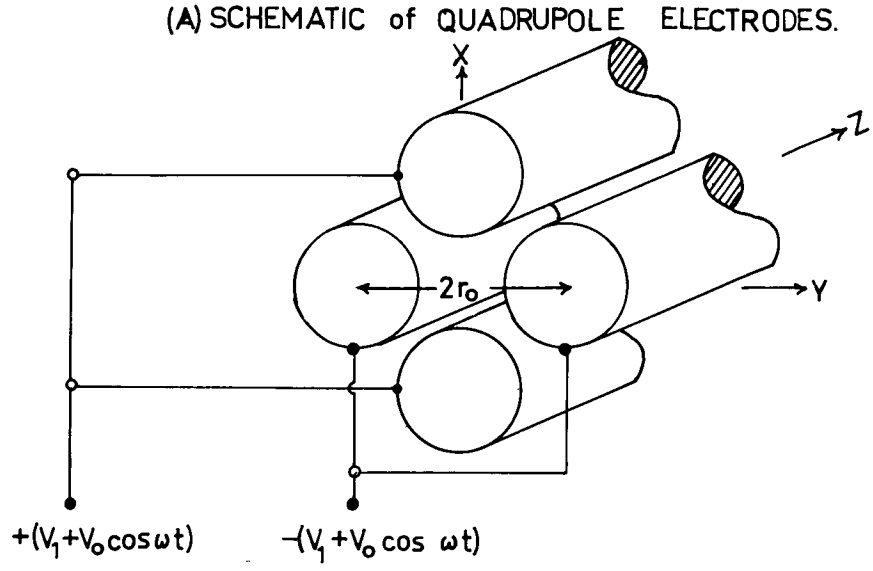

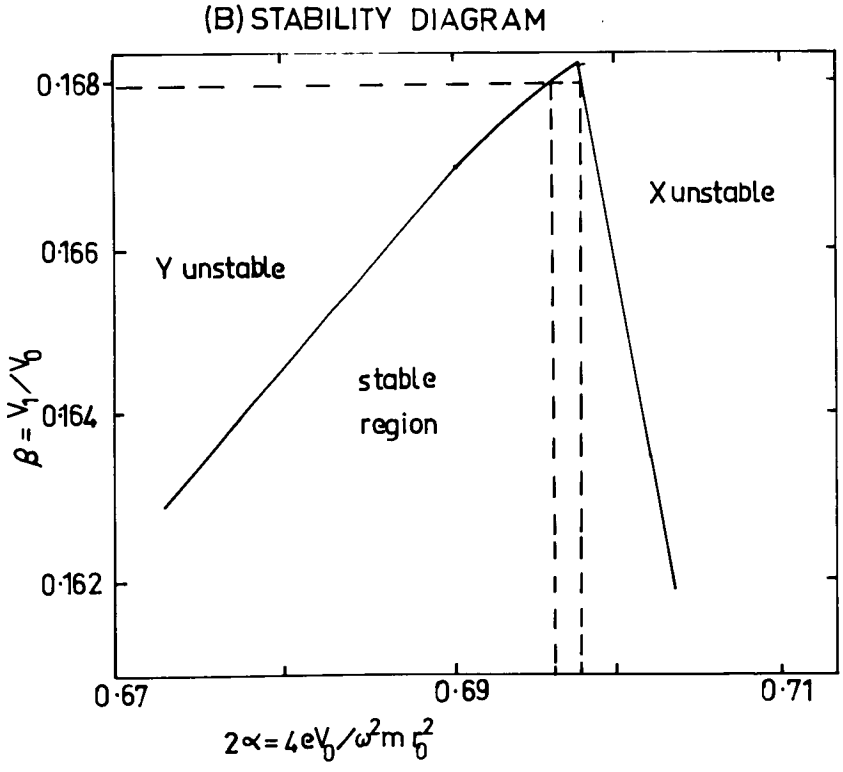

Under certain combinations the amplitude of trajectory increases without bound; the ion collides with one of the rods and is removed from the beam. To describe this filtering effect it is useful to define two parameters:

$$\alpha = (2e\ V_0)/(m\ V_0^2\ \omega^2)$$

$$\beta = V_1/V_0\ . \qquad \text{(111-12)}$$

The EAI stability diagram[186] is given in the fig. 3-6. For a given value of the parameter α, there exists a value for β which divides a region of stability from a region of instability. If the value of the parameter β is constant at a value of about 0.168, there is only a small range of values of α which will result in stable solutions. Physically this implies that only ions within a very small range of charge to mass ratios will be allowed to traverse the quadrupole structure. Ions having m/e beyond this range will have unstable trajectories and will be filtered out. Furthermore, if either V_0 or frequency ω are varied in such a manner that the ratio V_1/V_0 remains constant at about 0.168, the value of the transmitted charge to mass ratios will vary in a known manner. Assuming singly charged ions, the mass which reaches the detector is given by:

$$m = 0.136\ V_0/(R_0^2\ \omega^2) \qquad \text{(111-12)}$$

In practice, scanning a series of increasing masses is carried out

by increasing V_0, holding V_0/V_1 constant. Conditions for good sensitivity and good resolution properties are clearly opposed to one another; the art in quadrupole mass spectrometry is to achieve a suitable compromise.

The principal advantage of quadrupole instruments over other types of mass spectrometer is that higher sample pressures may be used, without corona discharge occurring. Ion inlet requirements to the quadrupoles are not critical; ions approaching at angles of up to 30° off the z axis are accepted by the field. Further advantages are that the mass scale is linear and that the resolving power is constant over this mass range. Quadrupole instruments do however have limited overall resolution properties compared with more expensive magnetic instruments.

Ion detectors are usually of the electron multiplier[187, 188] type with gains of about 10^6. Unfortunately, multipliers discriminate against ions of increasing mass number; this discrimination is approximately inversely proportional to the square root of the mass of the ion. Faraday cup methods are sometimes used for they do not discriminate.

3.4.2. Mass Spectrometry Assembly

(A) Quadrupole Mass Spectrometer

The E.A.I. Quad. 300[186] used in this study is composed of two units, the electronics console, containing the power supplies and

voltage controls, and the vacuum console composed of the vacuum system, sample inlet ports and quadrupole head. The quadrupole head is an assembly of ionizer: 1" dia. x 1/4" long, mass filter: (4 rods - 1/4" dia., 7 cm. long with $2r_0$ = 0.75 cm. - precisely aligned with ceramic spacers) and the electron multiplier. A photograph is given in fig. 3-7. High voltage cables connect this head to the controlling electronics console. On the vacuum console supplied, the sample inlets could not accommodate a Knudsen cell arrangement; therefore an independent vacuum system had to be set up for this work. The vacuum chamber was so constructed that the standard quadrupole head could be fitted via its 4" mounting flange.

For an understanding of the capability of the instrument, the most important details of the electronics subsystems are given. Essentially three independent power supplies are required.

The first, the RF/DC generator supplies and controls voltages applied to the mass filter. There are two RF voltages continuously variable from 0 to 2400 volts peak to peak and DC voltages variable from 0 to ±200 volts DC. The ratio of DC to RF supplied largely determines the sensitivity-resolution relationship. Maximum mass range is directly proportional to DC amplitude and is some inverse function of frequency. The unit is energised by mains rectified, regulated supplies of ±200 volts DC and 1200 volts DC. The RF is generated with variable oscillator circuits; selection of any one

FIGURE 3-7

E.A.I. Quad 300 "Head"

Legend

A : Ionizer

B : Quadrupole housing

C : Electron multiplier

D : Mounting flange, nominally 4"

E : Vacuum feedthroughs and copper leads

F : High voltage connectors (cables connect to electronics console)

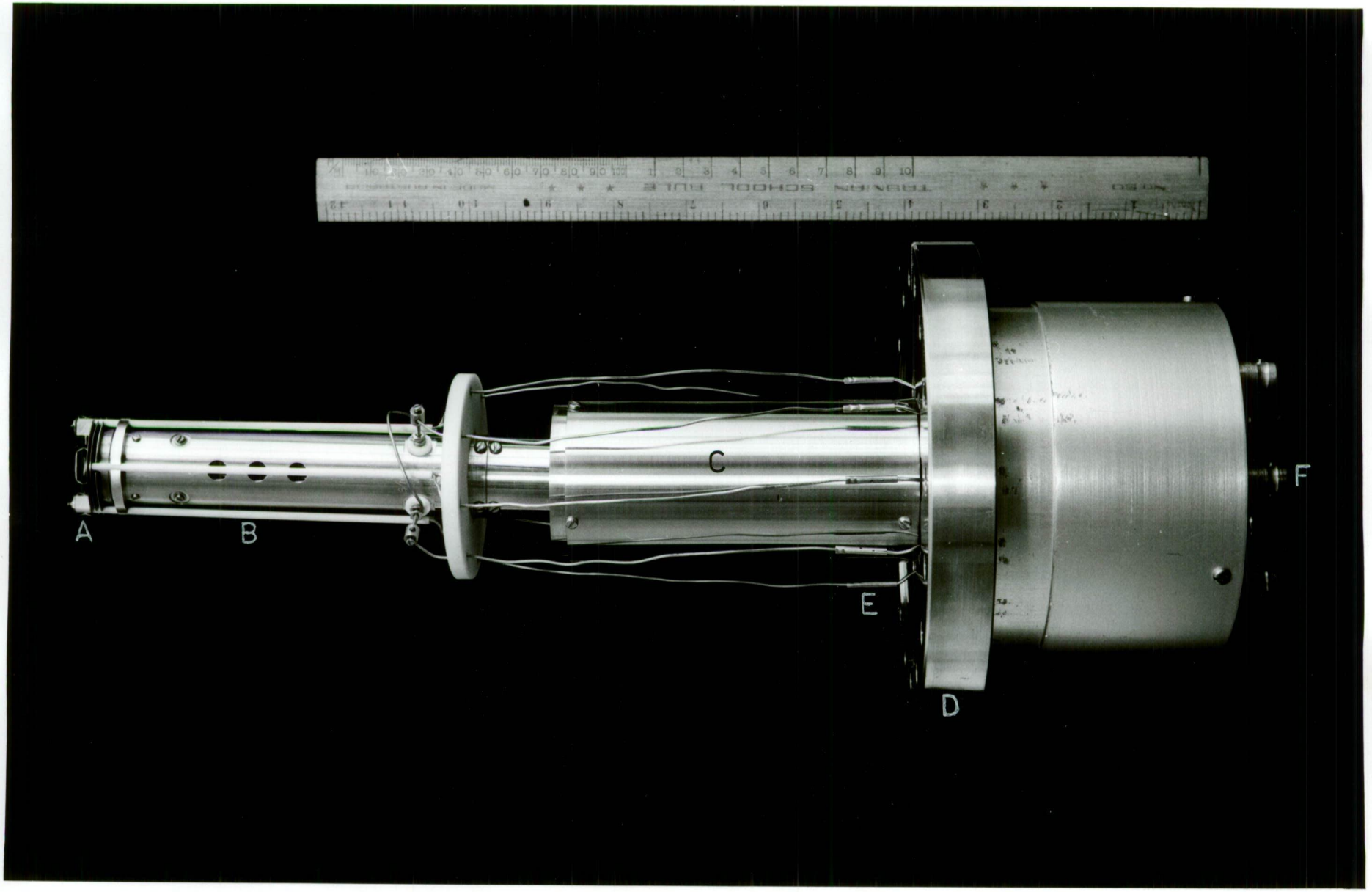
A
B
C
D
E
F

of three L-C "tank" circuits varies the frequency and gives a choice of three mass ranges. In this work the high mass range, 10-650 AMU with ω = 1.8 MHz, was employed. Feedback circuitry ensures a constant ratio of positive and negative DC to RF applied voltage. Automatic scanning of any desired mass range is brought about by a sweep which generates a linear sawtooth voltage, whose output precisely regulates the RF amplitude and hence the voltages applied to the rods.

The second supply applies the necessary potential to the electron multiplier, a Fluke High Voltage Power Supply model 405B is used. The electron multiplier supplied with the quadrupole head was an 18 stage "venetian blind" type with a gain of about 10^6 at 2.5kV.

The ionizer has its own regulated supply. Ionization is affected by electrons emitted from a hot rhenium coated tungsten filament, set at a negative potential (the electron energy) with respect to the ionization chamber; this chamber is in turn more positive than ground by the ion energy, which serves to repel positive ions into the quadrupole field.

The resolution-sensitivity relationship could easily be varied with RF/DC ratio controls and ion energy control. The resolution of lighter molecules was found to be more sensitive to the RF/DC ratio; heavier molecules were more affected by the ion energy. A small bias superimposed on the DC voltages could be

used to alter resolution at either end of the mass range; this control has a large effect on the relative heights of peaks in mass spectra. Correct adjustment was necessary for good resolution throughout the entire mass range.

A schematic diagram of the mass spectrometer assembly is given in fig. 3-8. A vacuum better than 10^{-6} mm. was obtained using a Speedivac oil diffusion pump, type E04 with an unbaffled pumping rate of 600 litres/second; Silicone 705 oil was used. This was backed by a Speedivac rotary vacuum pump, model ES35. To reduce backstreaming of oil vapour into the vacuum system, a Dynavac liquid nitrogen trap, type LNT4 was situated above the diffusion pump. The arrangement of three valves shown in the diagram allowed the system to be let up to atmosphere when required, then pumped down again, without interrupting the pumps. The top plate valve was a Dynavac type SV4; dry nitrogen could be admitted through a Dynavac NV1 needle valve in one of the ports off the plate valve. The other two valves were Dynavac types, a 3/4" diaphragm type and a solenoid type H.P. between the diffusion pump and backing pump. Pressures were measured with an Edwards ionization gauge, model 3B using gauge head type 1G 2HB, situated in a port of the plate valve. Solderless fittings were generally used to connect equipment.

(B) Knudsen Cell Arrangement

Hastie and Swingler[189] used an axial alignment of molecular

FIGURE 3-8

SCHEMATIC OF MASS SPECTROMETER ASSEMBLY

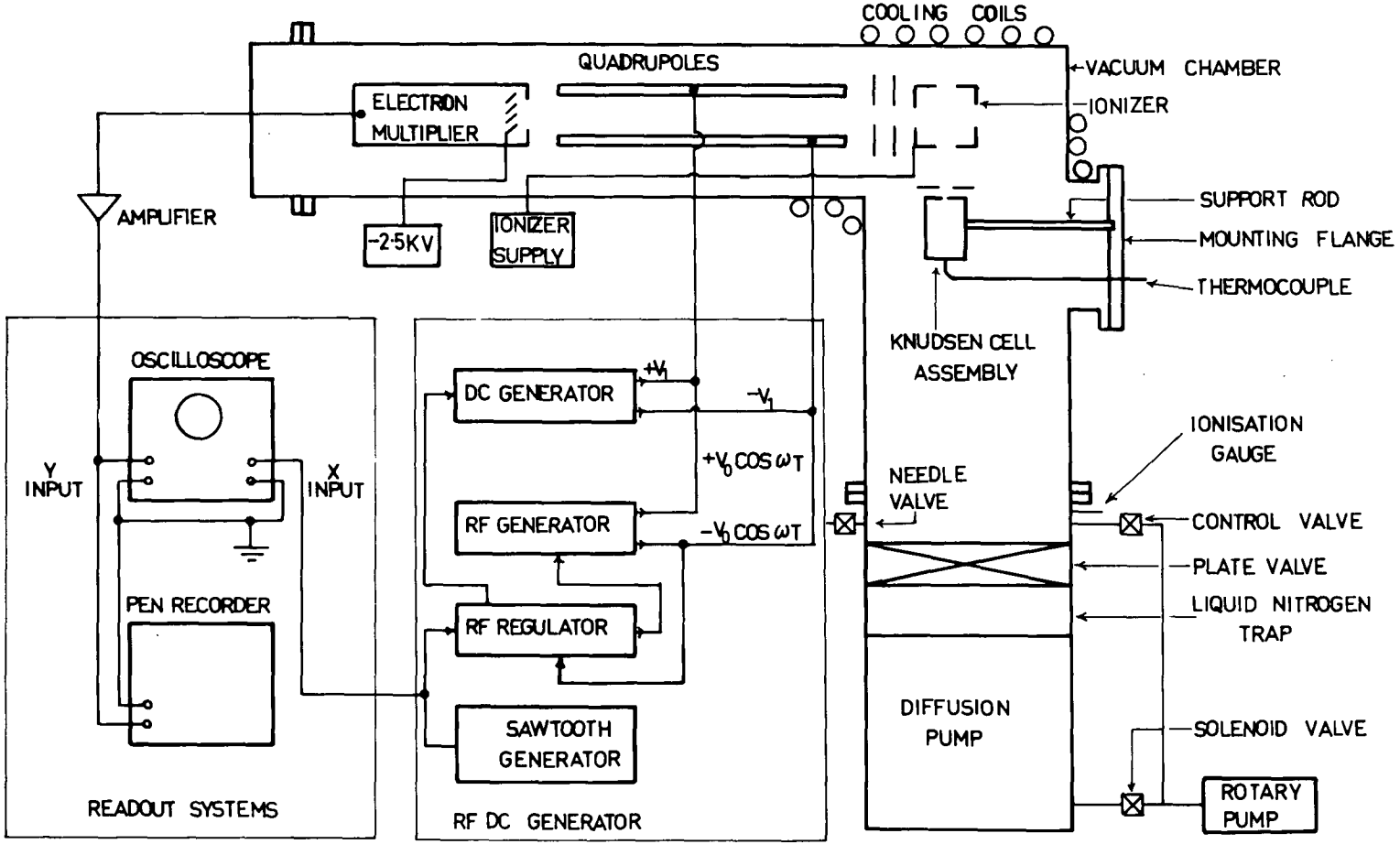

beam and quadrupole z axis; considerable contamination of rods and electron multiplier with unionized salt was reported. To reduce contamination, a cross beam arrangement was used in this study: the vertical molecular beam entered the open ionizer from underneath; the ion energy repelled positive ions into the quadrupole field, where the z axis was horizontal. Unionized salt condensed on the water cooled vacuum envelope. Although such an arrangement did indeed reduce contamination, especially of the electron multiplier, use of cross beam ionization was found to reduce senitivities by about an order of magnitude.

Fig. 3-9 illustrates the Knudsen cell assembly. Methods presented by Hastie and Swingler[189] were modified for use. The furnace arrangement was secured within the vacuum chamber with clamps screwed into the mounting flange. Considerable difficulty was at first encountered in achieving adequate temperature homogeneity over the cell. In the arrangement adopted, a silver Knudsen cell, 1" long x 1/2" O.D., was heated within an internally Kanthal wound boron nitride furnace 1½" long. Fired talc insulators served to position the cell in the centre of the furnace.

Knudsen flow conditions were obtained by use of nickel or molybdenum discs (0.05 - 0.1 mm. thick) sealed between the cap and body of the cell with a gold ring. Orifices were obtained by first indenting with a very fine needle, then filing the opposite side flat. Punching was then repeated, so that the needle just pierced

FIGURE 3-9

Knudsen Cell Assembly

Legend

A : Salt sample

B : Platinum liner

C : Silver Knudsen cell

D : Boron nitride furnace

E : Gold sealing ring

F : Replaceable nickel (or molybdenum) molecular beam defining disk

G : Furnace heating coil (Kanthal A 22B & S)

H : Fired talc insulators

J : Radiation shields, beam defining slits

K : Path of molecular beam

L : Stainless steel end supports

M : Groove for shutter in top support

N : Holes for support rods, (3 stainless steel rods, 1/8" thick screwed into position symmetrically about end supports; clamped to mounting flange by horizontal supports not shown)

O : Thermocouple with sheath

P : Adjustable screw for thermocouple support

Q : Radiation shield (clamped to horizontal support not shown)

FIGURE 3-9
KNUDSEN CELL ASSEMBLY

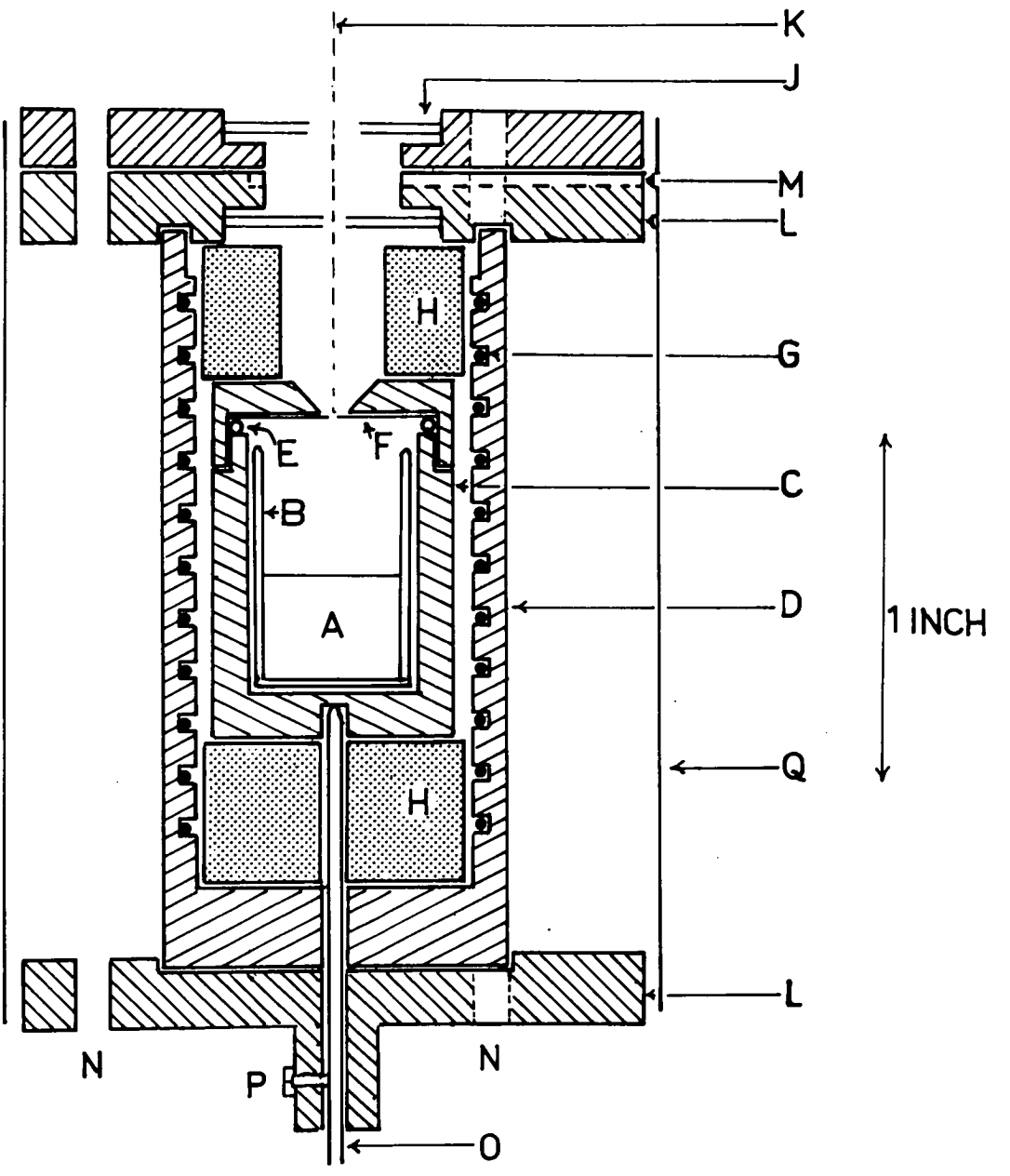

the metal; the back was again filed down and the hole rounded to produce a nearly knife-edged, circular orifice.

Using this technique orifices as small as 0.02 mm. diameter could be made. Small orifice diameters were preferred, so as to be able to work at higher temperatures. Following indentation and filing, actual orifice thicknesses were estimated at about 0.01-0.02 mm.; the number of collisions of molecules with orifice walls would be negligible.[190] Ratios of orifice area to salt surface area were smaller than 10^{-3}, so that vapour-liquid equilibrium would have existed[130b] (cooling coils on the vacuum jacket condensed unionised salt). Linear plots of log I^+T vs $\frac{1}{T}$ for pure salts and log K_r vs $\frac{1}{T}$ for mixtures would indicate that during quantitative runs, constant flow conditions were being maintained; moreover, the effects of any second order processes, such as ion-molecule collisions would have been negligible; this is expected at the low pressure ($< 10^{-6}$ mm.) prevailing in the ionizer.[31]

Thermal expansion of the nickel orifices over the range of temperatures used in quantitative runs would be about 0.1%;[191] expansion of molybdenum orifices would be less than half this value. Owing to its smallness, this factor may be neglected. Similarly, thermal expansion of the nickel collimating slits above the Knudsen cell would have a negligible effect.

An inconel sheathed $\frac{1}{16}$" dia., commercial, calibrated, chromel-alumel thermocouple was held in position with screws in a hole

at the base of the silver cell; the sheath was sealed through the flange with Araldite, as were the copper furnace leads. In this way the thermocouple was isolated from stray potentials while still measuring the correct temperature; the actual wires were not exposed to the high vacuum. Temperature was measured as described earlier. Attainment of correct values for heats of vaporisation of pure salts indicates that adequate temperature homogeneity had been achieved. The previous arrangement of series mains stabiliser and "variacs" were found suitable to control furnace temperatures to within $\cdot 0.5^{o}C$.

Slits above the cell served to condense any stray salt, thus collimating the molecular beam. Initially a shutter arrangement was used to permit shutting off of the molecular beam from the ionizer. This was manipulated from outside the vacuum system with a push rod. A vacuum seal through the flange was achieved with double sets of teflon rings; the region in between rings was pumped with an auxiliary rotary pump to 10^{-2} mm. The vacuum seal proved to be satisfactory but during some runs condensed salt tended to fall off while opening the shutter, blocking the Knudsen cell. Therefore, the shutter was only used during qualitative runs when only vapour composition was required.

(C) Read Out Systems

Currents from the electron multiplier, 10^{-6} to 10^{-12}A, were amplified with an E.S.A. Electrometer, model 75; variable gains from 10 to 10^{3} were possible. The output of the electrometer was

fed both to the y axis of a Tektronix model RM503 oscilloscope and to a Riken Denshi model SP-H twin channel strip chart recorder. A photograph of the assembled mass spectrometer is given in fig. 3-10.

3.4.3. Experimental Procedure

(A) Preparation of Mixtures

$ZnCl_2$ mixtures were made up in a closed Pyrex tube by adding an appropriate amount of alkali halide and melting. The melt was rapidly poured into a silica dish and finely ground in a dry box. Approximately 2-4g. were added to a small platinum crucible, which was in turn sealed within a silver cell by applying force to the lid. A new nickel disc and gold sealing ring were used each time. The platinum crucible was less than half full to allow space for vapour equilibrium.

$CdCl_2$ mixtures were made up in the same way; nickel orifices tended to be corroded by cadmium salts and molybdenum, which proved to be inert, was used. $PbBr_2$ mixtures were prepared by grinding together the components; silica internal crucibles were used to eliminate any attack by lead salts on platinum.

(B) Measurement

The silver cell was placed in the furnace and the thermocouple secured. The flange was mounted onto the vacuum chamber and the system evacuated slowly and pumped down for at least a day while the cell was heated to about 250°C. Powdered samples were used to prevent surface depletion of the solid during the experiment.

FIGURE 3-10

The Assembled Mass Spectrometer

Legend

A : E.A.I. Quad 300 electronics console (from top to bottom: RF/DC generator, cathode ray oscilloscope, ionizer controller, light beam recorder, electron multiplier power supply)

B : Rotary pump

C : Diffusion pump

D : Vacuum gauge controls

E : Plate valve

F : Vacuum chamber, with cooling coils

G : Furnace leads, thermocouple

H : Power supply for furnace

J : Amplifier

K : Pen recorder

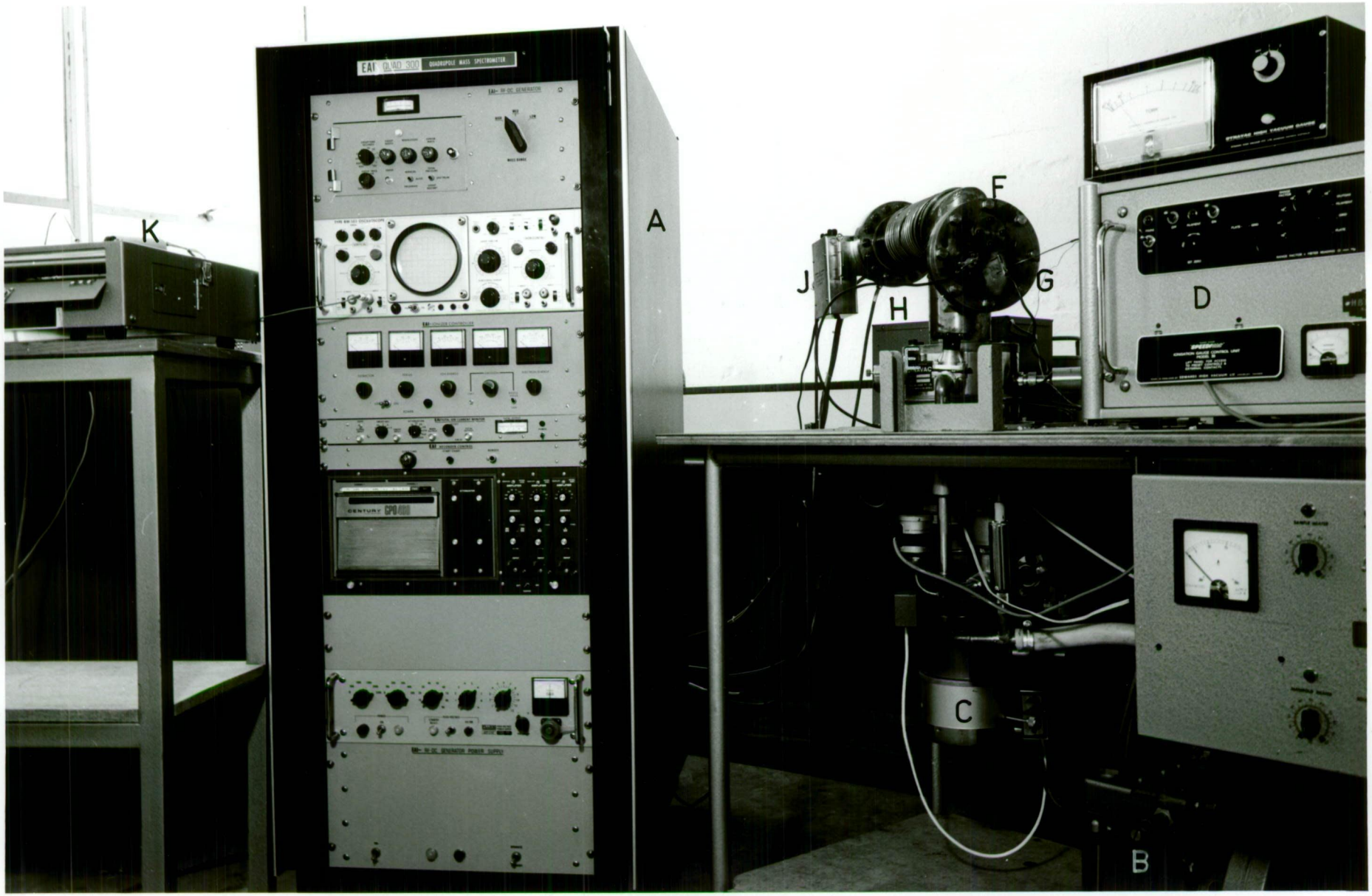
EAI QUAD 300 QUADRUPOLE MASS SPECTROMETER
CENTURY CPQ 400
A
B
C
D
F
G
H
J
K

When an adequate vacuum had been achieved ($< 10^{-6}$ mm.), the temperature of the furnace was increased until salt mass spectra were observed. Controls were adjusted to give maximum sensitivity while maintaining adequate resolution. Calibration of the mass scale was based upon peaks of $H_2O(18)$ and $N_2(28)$. The temperature was increased while mass spectra were examined for peaks corresponding to complex species.

In systems where reasonable intensities of complex species were found, ion currents as a function of temperature were measured. When equilibrium had been attained i.e. no change in temperature greater than $0.5^{o}C$ and no change in peak heights greater than 5% over a twenty minute period, mass spectra were recorded. The furnace temperature was raised in steps of 5-10 degrees and the procedure repeated. After a temperature range of about $80^{o}C$ had been covered, the furnace was cooled and some spectra recorded during cooling.

(C) Cleaning the Apparatus

A major feature of the Quad 300 is the ease with which various parts may be disassembled and cleaned. The ionizer was removed after each run and cleaned by washing in distilled water. If still not clean a solution of 10% formic acid, 10% H_2O_2 in water was used. The quadrupole rods themselves were cleaned after every few runs. The vacuum envelope was washed after each run. Silver Knudsen cells and platinum inserts were washed free of salt, then boiled in concentrated EDTA . solution to remove metal ions. Finally, they were rinsed then boiled in distilled water.

(D) Settings Used

During this work it was often required to separate ions of adjacent mass at the low end (HCl^+ 38, K^+ 39; Cs^+ 133, $ZnCl_2^+$ 134). At the high mass end, the ability to pick up complex species was most important and resolution was not critical. Usually, intermediate DC/AC resolution control settings were used so that the required separation was achieved at low mass end e.g. Pb^{206}, Pb^{207} peaks overlapped by no more than 15%. Use of fairly high ion energies, about 10 V, gave greater intensities at the high mass end while not affecting low masses as greatly. The tuning of RF/DC generator controls, particularly the bias superimposed on the DC was critical at all masses.

Relatively low ionizing electron energies of the order of 45 ev were used to achieve greater intensities of parent ions. Electron emission was normally set at 0.4 mA where no interaction was observed between electron emission and electron energy. Ion focus settings did not greatly affect mass spectra and 10 V was used. Ionizing controls were all stabilised and no fluctuation during a run was observed.

An applied potential of 2.25 kV was found to give an optimum signal to noise ratio with electron multiplier outputs. For recording signals of different intensities, gains on the electrometer were varied for recordings. In this work, no sign of detector saturation was observed.

Summary of conditions used

Ionizer:	electron emission:		45 ev
	electron energy	:	0.4 mA
	ion energy	:	10 V
	focus potential	:	10 V
detector potential		:	2.25 kV
scan time		:	300-600 seconds

(E) Performance

The Quad 300 was found to be satisfactory for detection of high temperature vapours with Knudsen cell pressures between 0.01-0.5 mm.Hg. Linearity in plots of log $I^{+}T$ against $^{1}/_{T}$ indicates that adequate electronics stability and a response proportional to ion currents was being achieved.

Unfortunately, equilibrium constants and appearance potentials of ions could not be determined. Ratio of peak heights at different masses was found to depend markedly upon the tuning given the instrument and to a lesser extent upon resolution and ion energy settings. As controls had to be optimised for sensitivity with each run, ratios between peaks of different masses also varied; equilibrium constants therefore could not be easily determined.

The open construction of the ionizer supplied prevented accurate measurement of appearance potentials as there were no safeguards against field penetration into the ionizing region.

4. RESULTS FOR FUSED SALT ACTIVITY STUDY

4.1. Preliminary Investigations

Some preliminary qualitative investigations on salt roasting reactions were first carried out. Both pure ZnS and a low grade ZnS, PbS ore (27% Zn, 10% Pb) were used.

Pure ZnS was added (10 wt %) to molten NaCl contained in a silica tube held in a furnace at 810°C. Air was bubbled through the melt for 1½ hours and samples of the melt and also of the solid residue on the bottom withdrawn at 15 minute intervals. Within 5 minutes of the addition, $ZnCl_2$ vapour was being evolved, condensing on the cooler parts of the apparatus. Acidic gases, most likely SO_2 and SO_3, were also evolved. At the conclusion of the experiment, some solid residue remained on the bottom of the silica container. Chemical analysis of melt samples dissolved in water revealed significant amounts of Zn^{2+} and SO_4^{2-}. Larger amounts of these were present in solutions of the residue. Powder X-ray studies, using a Philips Diffractometer (Cu $K\alpha_1$ radiation), indicated that one of the early samples of the solid contained mainly $ZnO.2ZnSO_4$ and ZnS. The ZnS peaks were not present in a sample taken some time after the first. No species apart from NaCl were positively identified in samples of the melt; others were likely to be present, but in too small a concentration to be identified by X-ray analysis.

Salt roasting studies on the low grade ore (50 wt % with NaCl) indicated that at temperatures between 850°C and 950°C

up to 75% of the Zn and 90% of the lead present could be volatilised as $ZnCl_2$ and $PbCl_2$. The presence of NaCl in the condensate indicated vapour complex formation was likely. $PbCl_2$ could be volatilised off at lower temperatures. The water soluble fraction of the solid residue was found to be composed essentially of Na_2SO_4.

The findings of these preliminary investigations are in agreement with those of Gerlach and Pawlek[17] and Donaldson and Kershner,[18] that $ZnCl_2$ and Na_2SO_4 are the major products of the salt roasting of ZnS. For this reaction, where there is a significant amount of a liquid phase, the Na-Zn-SO_4-Cl equilibria could possibly have a significant part in the reaction. Therefore an experimental investigation of this system seems worthwhile. Firstly it will aid in understanding the salt roasting reaction; secondly it is a good example for comparison of experimental results and theoretical predictions.

4.2. Vapour Pressure of Pure Zinc Chloride

A number of previous workers have investigated the vapour pressure of pure zinc chloride by both absolute[149a,150,192] and relative[149a,164,193] techniques. Small discrepancies between the two result from dimerization. As accurate values for relative zinc chloride vapour pressures are essential for activity measurements, a separate study has been made over a wide range of temperatures. Values are given in table 4-1 and have been plotted with other workers' transpiration values in figure 4-1.

Least squares analysis on these results gave the following vapour pressure equation:

$$\log_{10} P_{ZnCl_2} = 9.545 - \frac{6613.4}{T} \qquad \text{(IV-1)}$$

The heat of vaporisation is 30.3 kcal/mole. Keneshea and Cubicciotti[149a] give values for heats of vaporisation of 31 kcal/mole for the monomer and 22 kcal/mole for the dimer. Assuming 6% dimerisation, the transpiration heat of vaporisation calculated from their data is 30.4 kcal/mole; the agreement is favourable.

The data points exhibit a slight curvature due to slight changes in the heat of vaporisation over the temperature range studied (180°C); the effect is related to differences in heat capacities between liquid and vapour. To produce a more accurate equation, the Σ plot method as given by Lewis and Randall[194] was used. A value of -10 cal/deg.mole given by Brewer[134] was used for the difference in heat capacity between vapour and liquid.

TABLE 4-1

Vapour Pressure of Pure Zinc Chloride

Temperature (^{o}K)	Pressure (mm.)
723.9	2.209
734.3	3.560
754.7	6.245
781.1	12.32
793.9	17.10
803.2	21.39
813.0	26.42
827.7	37.26
827.5	37.14
843.2	50.60
843.5	49.36
858.6	70.31
863.0	75.02
872.8	92.43
877.8	101.2
886.1	116.4
895.1	136.6
899.1	153.0

FIGURE 4-1

VAPOUR PRESSURE OF PURE $ZnCl_2$

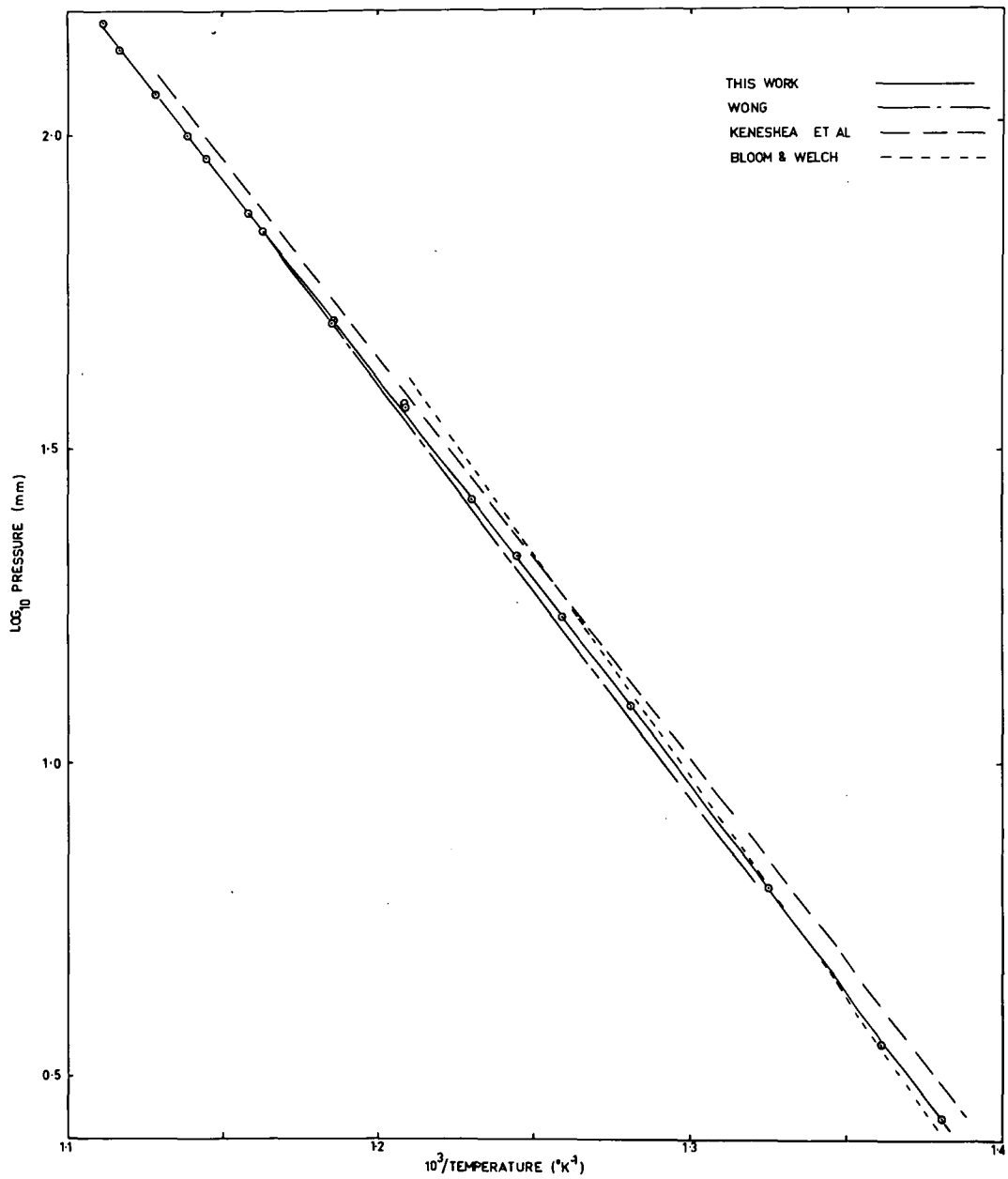

$$\Sigma = \Delta H_0/T + I = R \ln P + \Delta C_p \ln T \qquad \text{(IV-2)}$$

where ΔH_0 is the heat of vaporisation at 0^oK and I is a constant. In practice Σ was calculated for each point from the data, then least squared against 1/T as independent variable to determine ΔH_0 and I. The final derived equation is

$$\log_{10} P = \frac{-8247 \pm 17}{T} - 5.033 \log_{10} T + 26.213 \pm 0.006$$

and $$\Delta H_0 = 37{,}738 \pm 86 \text{ cals.} \qquad \text{(IV-3)}$$

4.3 Binary Mixtures

4.3.1. $Na-Zn-SO_4-Cl$ Binary Combinations

In the study of reciprocal salt mixtures it is necessary to know both the free energy change involved in the exchange reaction and the activity coefficients in the four binaries which can be made from the ions in the ternary system. For the $Na-Zn-SO_4-Cl$ system these binaries are: $NaCl-Na_2SO_4$, $ZnCl_2-ZnSO_4$, $ZnCl_2-NaCl$, $ZnSO_4-Na_2SO_4$. Calculation of ΔG^o is given in Appendix B.

Flood et al[196] have carried out a cryoscopic study on the system $NaCl-Na_2SO_4$ and have found that it forms an ideal solution. Calculations on both branches of the liquidus give RT ln $\gamma = 0$.

(IV-4)

A phase diagram is available for the system $ZnCl_2-ZnSO_4$;[197] however, because of solid solution this could not be used to evaluate accurate activity coefficients. Activities in this system were determined by transpiration vapour pressures, in the same way as for the ternary systems. As it is an anion mixture, deviations from ideality are not expected to be great. High liquidus temperatures restricted measurements to the range $0.62 < N_{ZnCl_2} < 1$. Three measurements were made as shown in table 4-2.

Values of RT ln $\gamma/(X'_{SO_4})^2$ became more accurate with increasing X'_{SO_4}, the equivalent ion fraction of SO_4^{2-} in the melt. Only the last two values were used, weight averaged and fitted to the equation for the system:

$$RT \ln \gamma_{ZnCl_2} = 440 \ (X'_{SO_4})^2 \qquad \text{(IV-5)}$$

TABLE 4-2

Activities of $ZnCl_2$ in the System $ZnCl_2$-$ZnSO_4$

Composition (mole % $ZnCl_2$)	Temperature (°K)	Activity $ZnCl_2$	γ $ZnCl_2$	RT ln $\gamma/(X'_{SO_4})^2$
0.900	832.3	0.906	1.007	1105
0.762	829.2	0.777	1.020	579
0.630	832.3	0.649	1.032	381

In later work it was desired to have an equation for the integral excess free energy of mixing, per equivalent of total salt, $\Delta G^E_{(equiv)}$ for the process of mixing X'_{SO_4} equivalents of $ZnSO_4$ with X'_{Cl} equivalents of $ZnCl_2$:

$$X'_{SO_4}\ ZnSO_4 + X'_{Cl}\ ZnCl_2 = Zn\left\{SO_4(X'_{SO_4}).Cl(X'_{Cl})\right\} \quad \text{(IV-6)}$$

where the term on the right indicates a solution in which the equivalent ion fraction of Zn is 1 and those of SO_4 and Cl are X'_{SO_4} and X'_{Cl} respectively. The terminology has been taken from Meschel and Kleppa.[198] To relate the integral quantity, ΔG^E to the activity coefficient equation for $ZnCl_2$-$ZnSO_4$ determined experimentally, the method given by Lumsden[199] has been used.

Firstly, regular solution behaviour is assumed, so that $\Delta G^E = \Delta H^E$. Using Lumsden's method, it is assumed that the energy ΔG^E of mixing an arbitrary n'_1 equivalents of $ZnSO_4$ and n'_2 equivalents of $ZnCl_2$ is given by:

$$\Delta G^E = b\frac{n'_1\, n'_2}{n'_1 + n'_2} \quad \text{(IV-7)}$$

where b is a constant, equivalent to the λ_{ij} terms used in 4.4.3.

If n_1, n_2 are the number of moles of $ZnSO_4$ and $ZnCl_2$ respectively, then $n'_1 = 2n_1$; $n'_2 = 2n_2$

$$\Delta G^E = 2b \frac{n_1 n_2}{n_1 + n_2} \qquad \text{(IV-8)}$$

Differentiating with respect to n_2

$$\Delta \bar{G}^E_{ZnCl_2(mole)} = RT \ln \gamma_{ZnCl_2} = 2b \frac{n_1^2}{(n_1 + n_2)^2} \qquad \text{(IV-9)}$$

If now $n'_1 = X'_{SO_4}$; $n'_2 = X'_{Cl}$

$$\Delta \bar{G}^E_{ZnCl_2(mole)} = 2b(X'_{SO_4})^2 \qquad \text{(IV-10)}$$

Returning to the integral equation, if $n'_1 = X'_{SO_4}$, $n'_2 = X'_{Cl}$, then

$$\Delta G^E_{(equiv)} = b\, X'_{SO_4}\, X'_{Cl} \qquad \text{(IV-11)}$$

Therefore 2b = 440 (see IV - 9, 10, 11) and:

$$\Delta G^E_{Zn(Cl\text{-}SO_4)(equiv)} = 220\, X'_{SO_4}\, X'_{Cl} \qquad \text{(IV-12)}$$

The system $ZnCl_2$-NaCl has been studied by a number of methods. The most accurate set of results appear to be those of Dijkhuis and Ketelaar,[200] who used the following cell at 600°C:

$$W|Zn \;\Big|\; \begin{matrix} ZnCl_2(1\text{-}N) \\ NaCl(N) \end{matrix} \;\Big|\; \begin{matrix} CdCl_2 \\ NaCl \end{matrix} \;\Big|\; \begin{matrix} ZnCl_2(0.865) \\ NaCl(0.135) \end{matrix} \;\Big|\; Zn|W$$

Integral excess free energies were given

$$\Delta G^E_{(mole)} = (-4{,}370\text{-}5{,}540\ N)\ N(1\text{-}N)\ \text{cals.} \qquad \text{(IV-13)}$$

The authors give an average partial molar enthalpy of mixing for $ZnCl_2$:

$$\Delta \bar{H}_{ZnCl_2(mole)} = -9{,}940(X'_{Na})^2 \qquad \text{(IV-14)}$$

Although this system is not strictly regular, as a first approximation the following equation will be used for integral excess equivalent free energies

$$\Delta G^{E}_{(Na\text{-}Zn)Cl(equiv)} = -4{,}970(X'_{Na})^{2} \qquad \text{(IV-15)}$$

The system $ZnSO_4$-Na_2SO_4 has not received any thermodynamic treatment as yet; moreover, owing to high fusion temperatures and the limited thermal stability of $ZnSO_4$, activities could not be accurately determined by any of the usual methods. There has been no extensive treatment of charge unsymmetrical systems in which the anion is divalent. Nevertheless, from a knowledge of the principles involved and the trends established in other systems, it is possible to set reasonable upper and lower bounds. Assumed activity coefficient parameters for this system are in part dependent upon data from the ternary system. Fortunately, this is not the most important binary as $ZnCl_2$-NaCl has the greatest effect on the ternary system.

Usually the most important factor effecting heats of mixing is the coulombic term which is related to the distance parameter

$$\delta = \frac{d_1 - d_2}{d_1 d_2} \qquad \text{(IV-16)}$$

where d_1 = cation-anion distance of the divalent ion

d_2 = cation-anion distance of the monovalent ion.

These will be evaluated for the systems $ZnSO_4$-Na_2SO_4, $ZnCl_2$-NaCl. Crystal radii[76] are used for Na^+ (0.96 Å), Zn^{2+} (0.74 Å),

Cl^- (1.81 Å) and Kapustinskii's[201] thermochemical radius for SO_4^{2-} (2.30 Å).

$$\delta_{(Zn-Na)SO_4} = -0.022 \ (Å)^{-1}$$

$$\delta_{(Zn-Na)Cl} = -0.0311 \ (Å)^{-1} \qquad \text{(IV-17)}$$

The size parameters are approximately equal for both systems; for singly charged ions this would tend to indicate equal exothermic, coulombic contributions to the heats of mixing. From Lumsden's[44] point of view, the larger, doubly charged SO_4^{2-} ion is likely to be more polarised upon mixing by the small Zn^{2+} ion, than is the Cl^- ion; for this reason one would expect more exothermic heats of mixing and negative deviations from ideality in the (SO_4) than the (Cl) binary. Melnichak and Kleppa[60] have found with the alkali halides that corrected heats of mixing become more exothermic as the halide ion becomes more polarisable.

Non-ionic contributions to the bonding in pure salts tend to make heats of mixing less exothermic.[11] Considerable covalent bonding has been postulated for pure zinc chloride. Tentatively considering the higher melting point of $ZnSO_4$,[120] it is unlikely that this salt is bonded as covalently as $ZnCl_2$. Therefore, assuming that mixing in both binary solutions is random, it would seem that negative deviations from ideality would be greater in the sulphate system.

Recently, Braunstein et al[202] have correlated interaction parameters for alkaline earth halide-alkali halide binary mixtures,

using the Davis type expression:[64]

$$\lim_{N_{AX_2} \to 0} \Delta\bar{G}^{E}_{MX}/N^{2}_{AX_2} = a\delta + b \qquad \text{(IV-18)}$$

An upper limit to the interaction parameter for $(Zn\text{-}Na)SO_4$ may be estimated from the graphs given. For the expression:

$$\Delta G^{E}_{(Zn\text{-}Na)SO_4(equiv)} = b\, X'_{Cl}\, X'_{SO_4} \qquad \text{(IV-19)}$$

reasonable estimated upper and lower bounds for b are:

$$-10{,}000 \leq b \leq -4{,}970.$$

4.3.2. K-Pb-SO_4-Cl Binary Combinations

The binary mixtures of interest here are:

$PbCl_2$-KCl, KCl-K_2SO_4, $PbCl_2$-$PbSO_4$, $PbSO_4$-$PbCl_2$.

Lumsden has carried out a critical evaluation of thermodynamic data in the $PbCl_2$-KCl system; he gives the equation:[203]

$$RT \ln \gamma_{PbCl_2} = -10{,}800\ (X'_K)^2 \qquad \text{(IV-20)}$$

The vapour pressure data of Barton[170] and the e.m.f. data of Markov et al[204] fit the equation well. Therefore for this system:

$$\Delta G^{E}_{(Pb\text{-}K)Cl(equiv)} = -5400\ X'_{Pb}\, X'_{K} \qquad \text{(IV-21)}$$

In a similar manner, Lumsden[205] has classified the KCl-K_2SO_4 system and:

$$\Delta G^{E}_{K(Cl\text{-}SO_4)(equiv)} = 200\ X'_{Cl}\, X'_{K} \qquad \text{(IV-22)}$$

No data was available for the $PbCl_2$-$PbSO_4$ system. As deviations from ideality will be small, the equation used for the similar $Zn(Cl\text{-}SO_4)$ system has been used.

$$\Delta G^{E}_{Pb(Cl\text{-}SO_4)(equiv)} = 220\ X'_{Cl}\, X'_{SO_4} \qquad \text{(IV-23)}$$

No information was available for the $PbSO_4$-K_2SO_4 system. Size parameters, calculated as before are given:[76]

$$Pb^{2+} : 1.20\ (\text{Å}),\ K^{+} : 1.33\ (\text{Å}).$$

$$\delta_{(Pb\text{-}K)SO_4} = -0.0102\ (\text{Å})^{-1}$$

$$\delta_{(Pb\text{-}K)Cl} = -0.0140\ (\text{Å})^{-1} \qquad \text{(IV-24)}$$

The value of δ is significantly less negative for the sulphate binary mixture; $\delta_{(Pb\text{-}K)SO_4}$ is also significantly less negative than the corresponding $\delta_{(Zn\text{-}K)SO_4}$ value. Heats of mixing in the $PbSO_4$-K_2SO_4 system are therefore likely to be less negative than $ZnSO_4$-Na_2SO_4. Furthermore, in the (Zn-Na) systems, heats of mixing were assumed to be more exothermic in the sulphate than in the chloride binary, chiefly because of the large degree of covalent bonding in pure $ZnCl_2$. As $PbCl_2$ does not have a network structure, its bonding is likely to be less covalent than that in molten $ZnCl_2$. Therefore, it seems reasonable to assume that heats of mixing in the $(Pb\text{-}K)SO_4$ are no greater than those in the (Pb-K)Cl binary and are likely to be somewhat smaller. Again assuming regular solution behaviour, integral excess free energies are given:

$$\Delta G^{E}_{(Pb\text{-}K)SO_4(equiv)} = b\ X'_{Pb}\ X'_{K} \qquad \text{(IV-25)}$$

where $-5{,}400 \leq b < 0$.

4.3.3. Na-Pb-SO_4-Cl Binary Combinations

Binary mixtures are: $PbCl_2$-NaCl, NaCl-Na_2SO_4, $PbCl_2$-$PbSO_4$, $PbSO_4$-Na_2SO_4.

Lumsden[206] has tabulated data for the $PbCl_2$-NaCl binary system:

$$RT \ln \gamma_{PbCl_2} = -1800 \ (X'_{Na})^2 \qquad \text{(IV-26)}$$

so that

$$\Delta G^E_{(Pb\text{-}Na)Cl(equiv)} = -900 \ X'_{Pb} \ X'_{Na} \qquad \text{(IV-27)}$$

It was found earlier that NaCl-Na_2SO_4 is ideal, and that $PbSO_4$-$PbCl_2$ may be classified:

$$\Delta G^E_{Pb(SO_4\text{-}Cl)(equiv)} = 220 \ X'_{SO_4} \ X'_{Cl} \qquad \text{(IV-28)}$$

In the (Pb-Na) sulphate and chloride mixtures, size parameters have again been calculated

$$\delta_{(Pb\text{-}Na)SO_4} = +0.021 \ (\text{Å})^{-1}$$

$$\delta_{(Pb\text{-}Na)Cl} = +0.029 \ (\text{Å})^{-1} \qquad \text{(IV-29)}$$

These positive values would indicate that heats of mixing are likely to be small. For the same reasons that were given in considering (Pb-K) binary systems, the interaction parameter for $(Pb\text{-}Na)SO_4$ binary is likely to be less negative than that for the (Pb-Na)Cl binary. Therefore the system has been classified:

$$\Delta G^E_{(Pb\text{-}Na)SO_4(equiv)} = -500 \ X'_{Pb} \ X'_{Na} \qquad \text{(IV-30)}$$

4.4. Na-Zn-SO_4-Cl Reciprocal System

4.4.1. Activity Results

(A) Introduction

In the systems $ZnCl_2$-Na_2SO_4 and $ZnSO_4$-NaCl, a number of activity determinations were made at different temperatures for approximately the same composition; six different sets of results at different compositions were studied in each system in this way. Within any one set of results, compositions varied slightly (> 0.4 mole%) from that found for measurement at one temperature to the next. These composition variations had only a minor effect upon the temperature dependence of activity. In order to make a suitable correction, a least squares analysis was first performed for log P vs $\frac{1}{T}$. At six average temperatures throughout the range, activities were determined from the least squares vapour pressures for each composition and these activities plotted against composition. Activities in any one set of results were selected from these curves so that they were all based upon the same composition, the average for that set. Vapour pressures were calculated from these activities and again least squared against $\frac{1}{T}$. At any temperature, the difference between the first least squared pressure and the second were small (>1.5%) so that no further corrections were made. In some regions of the $ZnSO_4$-NaCl system, the dependence of activity on composition was quite small and where this occurred, corrections for composition variations were negligible.

In a very few cases, the effect of dissociation of zinc chloride dimer was significant and small corrections were made (2%-3%). Allowance was made for the partially compensating effect of $NaZnCl_3(g)$ formation. Only at lower temperatures was the effect of dimer dissociation important.

(B) Experimental Data

The data for these systems is given in tables 4-3 and 4-4, and figures 4-2 and 4-3. The final least squares equations are given in table 4-5.

Using activities calculated from these least squares equations, a comparison is made in tables 4-6, 4-7, and figures 4-4, 4-5, between experimental activities and those predicted by the Temkin and F.F.G. solid solution methods.

It is significant that in both systems, the activity of zinc chloride changes from being greater than Temkin to being less than Temkin over the composition range. Moreover, an appreciable dependence of activity upon temperature is noted, which itself varies with composition, shown in figures 4-6, 4-7.

(C) Partial Molar Quantities

To understand this behaviour, first the free energy per equivalent, ΔG^{o}(equiv), of the exchange reaction:

$$ZnCl_2 + Na_2SO_4 = 2NaCl + ZnSO_4$$

is considered. This has been calculated in appendix A. It varies from +1575 cals at $863^{o}K$ to +1795 cals at $773^{o}K$. The positive sign indicates a tendency for $ZnCl_2$ and Na_2SO_4 to exhibit positive

TABLE 4-3

Activities of $ZnCl_2$ in the System $ZnCl_2$-Na_2SO_4 (773-888°K)

Composition Mole fn $ZnCl_2$	Temperature °K	P_{ZnCl_2} mm.	$P^o_{ZnCl_2}$ mm.	Activity
0.9012	775.0	8.696	10.76	0.808
0.8990	812.9	20.50	26.54	0.772
0.8996	852.2	46.89	61.48	0.763
0.8980	887.7	91.47	122.1	0.749
0.7687	773.9	5.543	10.49	0.528
0.7679	803.6	10.82	21.50	0.503
0.7677	833.3	20.28	41.60	0.488
0.7668	863.1	35.42	76.44	0.463
0.7667	887.8	53.96	122.3	0.441
0.6250	773.9	2.120	10.49	0.202
0.6231	803.2	4.183	21.27	0.197
0.6244	833.2	7.789	41.44	0.188
0.6224	863.4	13.88	76.91	0.180
0.6221	887.4	21.31	121.5	0.175
0.5118	773.1	0.714	10.26	0.0696
0.5113	805.1	1.511	22.23	0.0680
0.5112	834.0	2.802	42.18	0.0664
0.5107	863.5	5.011	77.12	0.0650
0.5109	887.9	7.894	122.5	0.0644
0.4091	862.7	1.793	76.62	0.0234
0.4090	883.8	2.651	113.2	0.0234
0.4089	908.4	4.187	175.9	0.0238
0.3804	834.0	0.714	42.18	0.0157
0.3805	863.6	1.335	77.25	0.0173
0.3804	889.1	2.227	125.3	0.0178

FIGURE 4-2

VAPOUR PRESSURE $ZnCl_2$ IN $ZnCl_2$-Na_2SO_4 MELTS 770-890°K

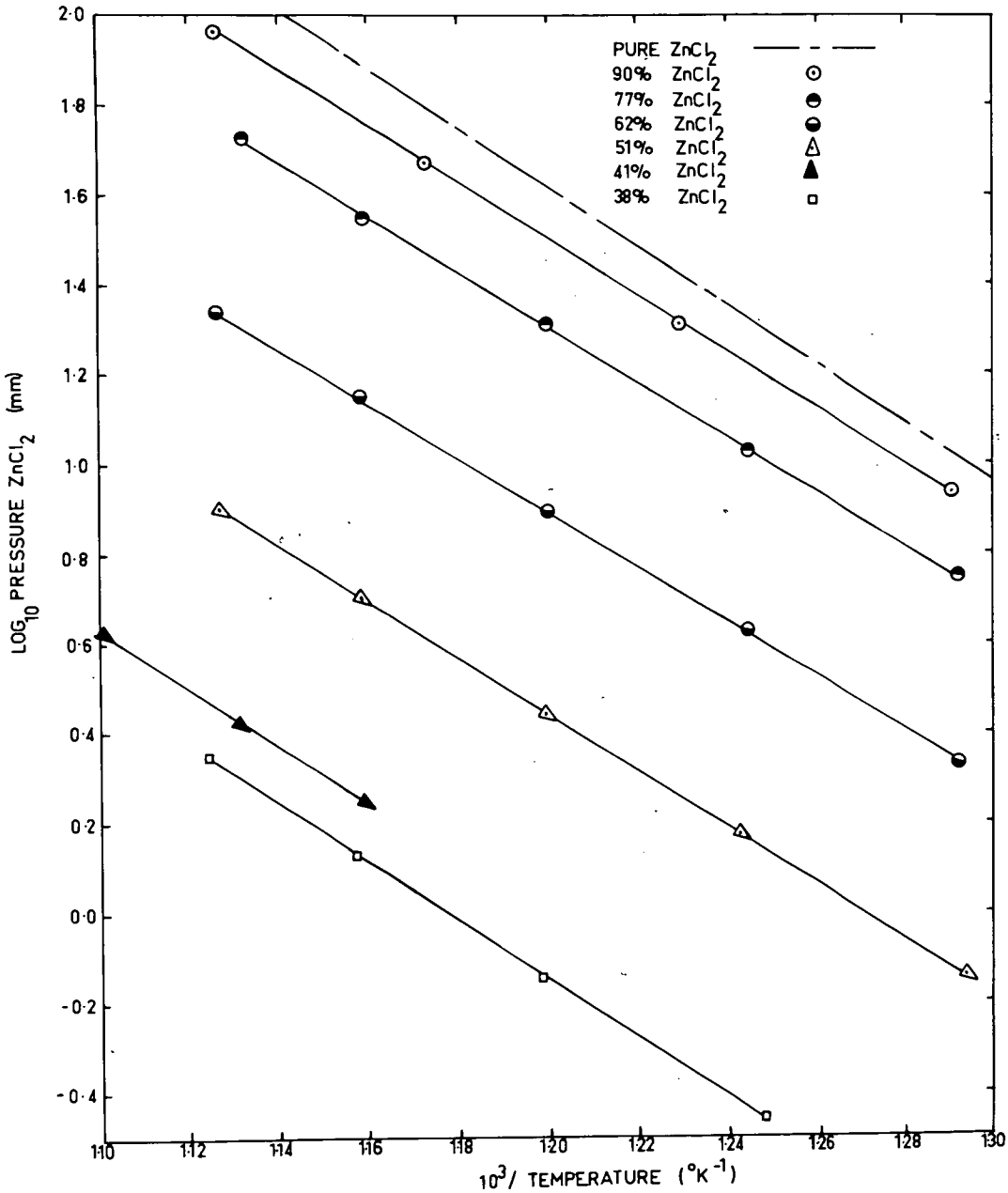

TABLE 4-4

Activities of $ZnCl_2$ in the System $ZnSO_4$-NaCl (803-903°K)

Composition Mole fn $ZnSO_4$	Temperature °K	P_{ZnCl_2} mm.	$P^o_{ZnCl_2}$ mm.	Activity
0.1917	865.1	0.546	79.60	0.0069
0.1915	888.6	0.892	124.1	0.0072
0.1914	902.3	1.158	159.1	0.0073
0.2687	803.9	0.505	21.61	0.0234
0.2679	835.5	1.048	43.50	0.0241
0.2683	862.8	1.869	76.03	0.0246
0.2684	903.2	4.125	161.6	0.0255
0.3490	833.2	2.930	41.44	0.0707
0.3483	862.2	5.246	75.21	0.0698
0.3482	903.8	11.09	163.5	0.0678
0.4284	864.7	9.405	78.40	0.120
0.5104	805.7	3.928	22.53	0.174
0.5103	835.0	6.736	43.09	0.156
0.5094	865.2	12.29	79.74	0.154
0.5084	903.6	23.27	162.8	0.143
0.5235	803.5	3.690	21.46	0.172
0.5235	833.9	6.656	42.11	0.158
0.5237	864.4	11.78	78.49	0.150
0.5234	901.4	22.17	156.7	0.142
0.6278	834.6	6.241	42.68	0.146
0.6276	864.0	10.83	77.88	0.139
0.6281	903.4	20.08	163.4	0.124

FIGURE 4-3

VAPOUR PRESSURE $ZnCl_2$ IN $ZnSO_4$ -NaCl MELTS 803-903°K

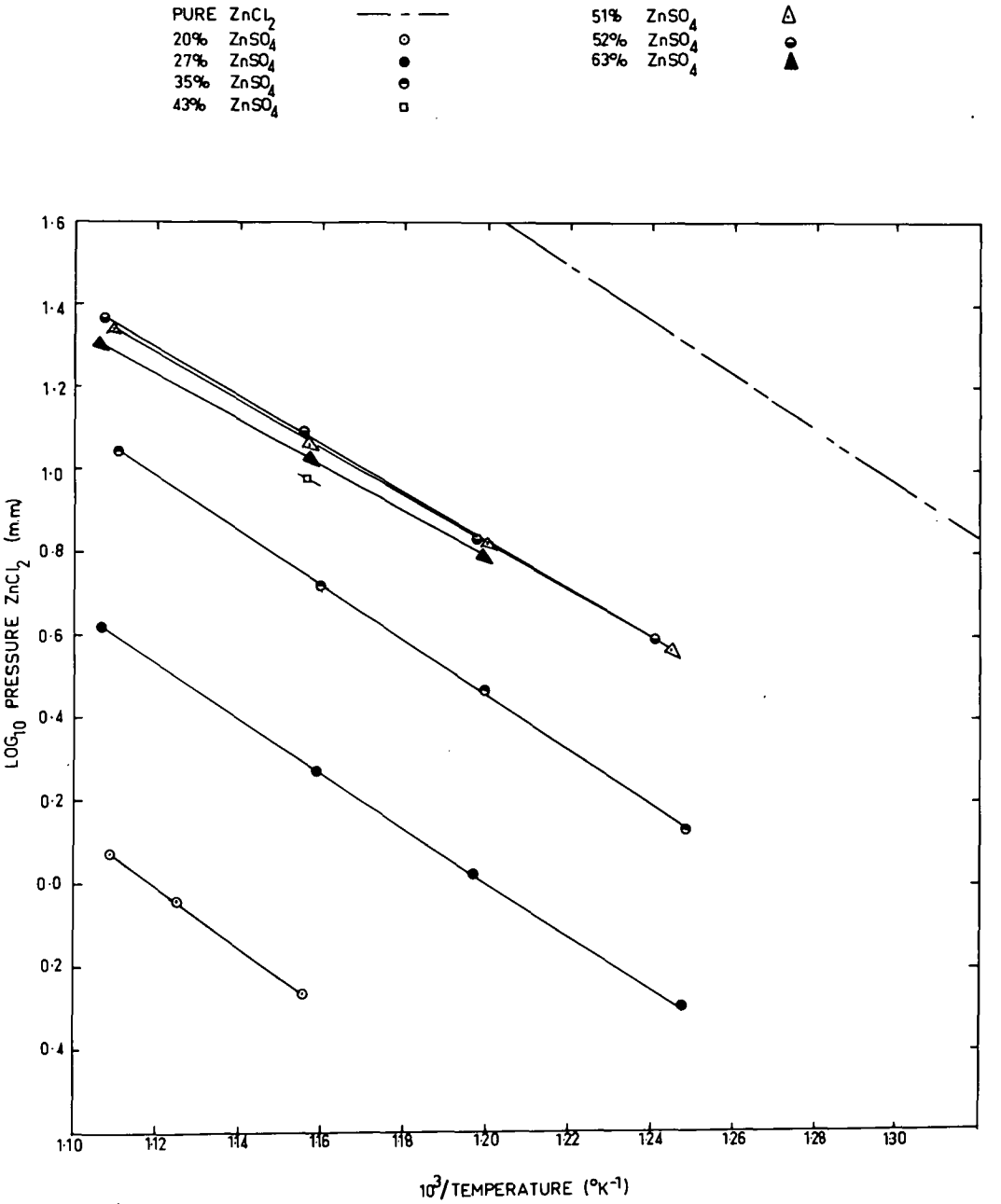

TABLE 4-5

Least Squares Vapour Pressure in $Na-Zn-SO_4-Cl$

(1) $ZnCl_2-Na_2SO_4$ $\log_{10} P_{ZnCl_2} = A - B/T$

Composition Mole fn $ZnCl_2$	A	B
0.8995	9.0152	6,260.0
0.7675	8.5089	6,008.1
0.6229	8.1854	6,081.1
0.5112	7.9172	6,231.6
0.3804	7.9558	6,762.2

(2) $ZnSO_4-NaCl$ $\log_{10} P_{ZnCl_2} = A - B/T$

Composition Mole fn $ZnSO_4$	A	B
0.1915	7.4868	6,698.7
0.2683	7.9971	6,665.9
0.3487	7.8603	6,158.8
0.5096	7.7743	5,789.5
0.5236	7.7428	5,771.7
0.6278	7.4455	5,546.3

TABLE 4-6

Comparison of Least Squares Experimental Activities With Theoretical Values in the System $ZnCl_2$-Na_2SO_4

Composition mole fraction $ZnCl_2$	Temperature (^oK)	Activity $ZnCl_2$	Temkin	F.F.G. (S.S.)
	773.0	0.806		
	803.0	0.782		
0.8995	833.0	0.766	0.733	0.728
	863.0	0.756		
	888.0	0.752		
	773.0	0.531		
	803.0	0.502		
0.7675	833.0	0.479	0.471	0.452
	863.0	0.462		
	888.0	0.450		
	773.0	0.207		
	803.0	0.195		
0.6229	833.0	0.186	0.266	0.242
	863.0	0.180		
	888.0	0.177		
	773.0	0.0715		
	803.0	0.0682		
0.5112	833.0	0.0661	0.157	0.134
	863.0	0.0651		
	888.0	0.0647		
0.4091	863.0	0.0234	0.0872	0.0684
	888.0	0.0235		
	833.0	0.0167		
0.3804	863.0	0.0173	0.0712	0.0555
	888.0	0.0178		

FIGURE 4-4

ACTIVITY ISOTHERMS OF $ZnCl_2$ IN $ZnCl_2$-Na_2SO_4

773 °K – 888 °K

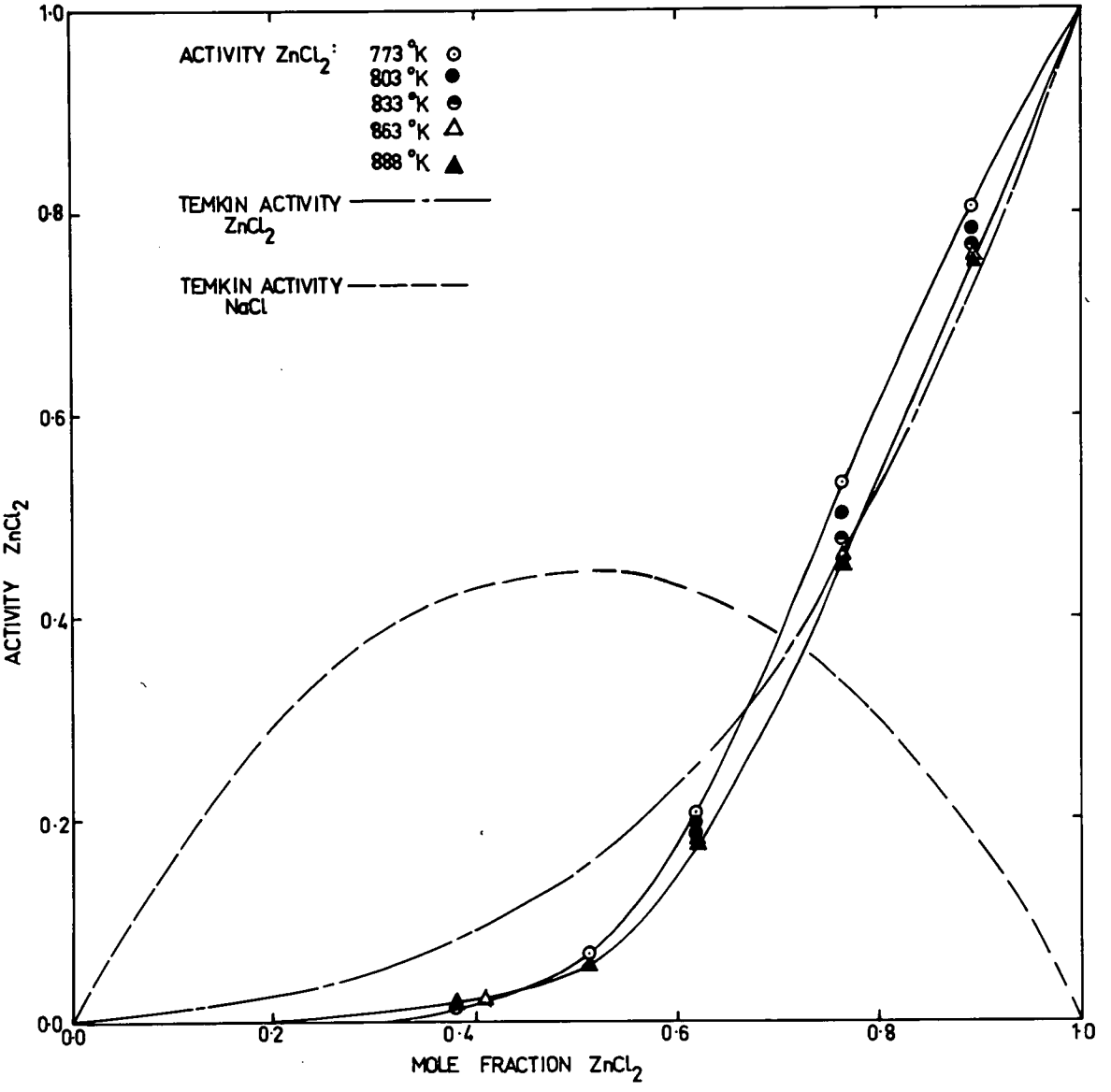

FIGURE 4-5

ACTIVITY ISOTHERMS $ZnSO_4$ - NaCl

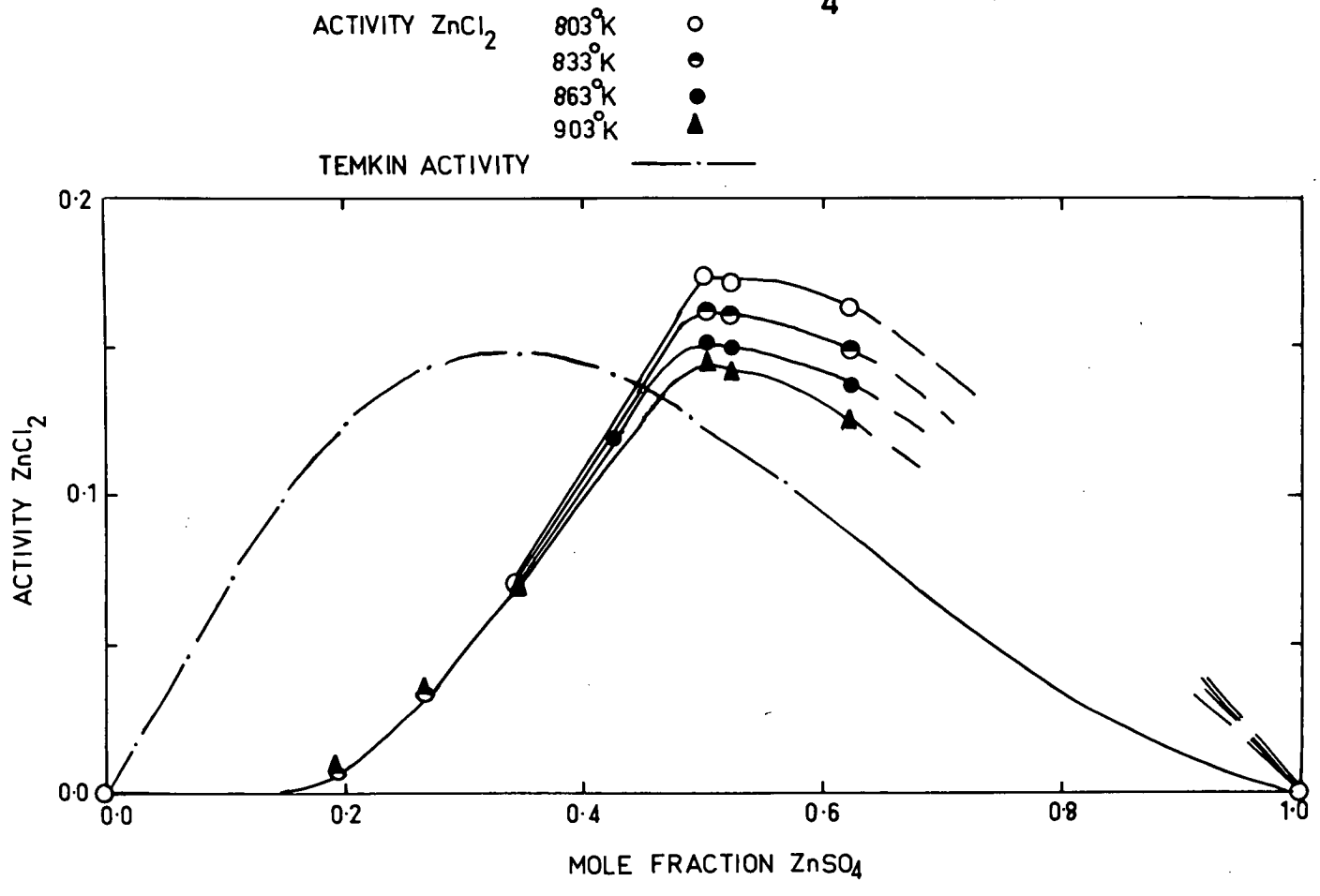

TABLE 4-7

Comparison of Least Squares Experimental Activities With Theoretical Values in the System $ZnSO_4$-NaCl

Composition mole fraction $ZnSO_4$	Temperature (^oK)	Activity $ZnCl_2$	Temkin	F.F.G. (S.S.)
	833.0	0.00675		
0.1915	863.0	0.00695	0.125	0.148
	903.0	0.00727		
	803.0	0.0234		
0.2683	833.0	0.0239	0.144	0.141
	863.0	0.0246		
	903.0	0.0256		
	833.0	0.0700		
0.3487	863.0	0.0700	0.148	0.120
	903.0	0.0700		
0.4284	865.0	0.1200	0.143	0.096
	803.0	0.173		
0.5096	833.0	0.162	0.123	0.071
	863.0	0.152		
	903.0	0.143		
	803.0	0.171		
0.5236	833.0	0.160	0.119	0.067
	863.0	0.150		
	903.0	0.141		
	803.0	0.163		
0.6278	833.0	0.148	0.087	0.040
	863.0	0.137		
	903.0	0.125		

FIGURE 4-6

TEMPERATURE DEPENDENCE OF $ZnCl_2$ ACTIVITY

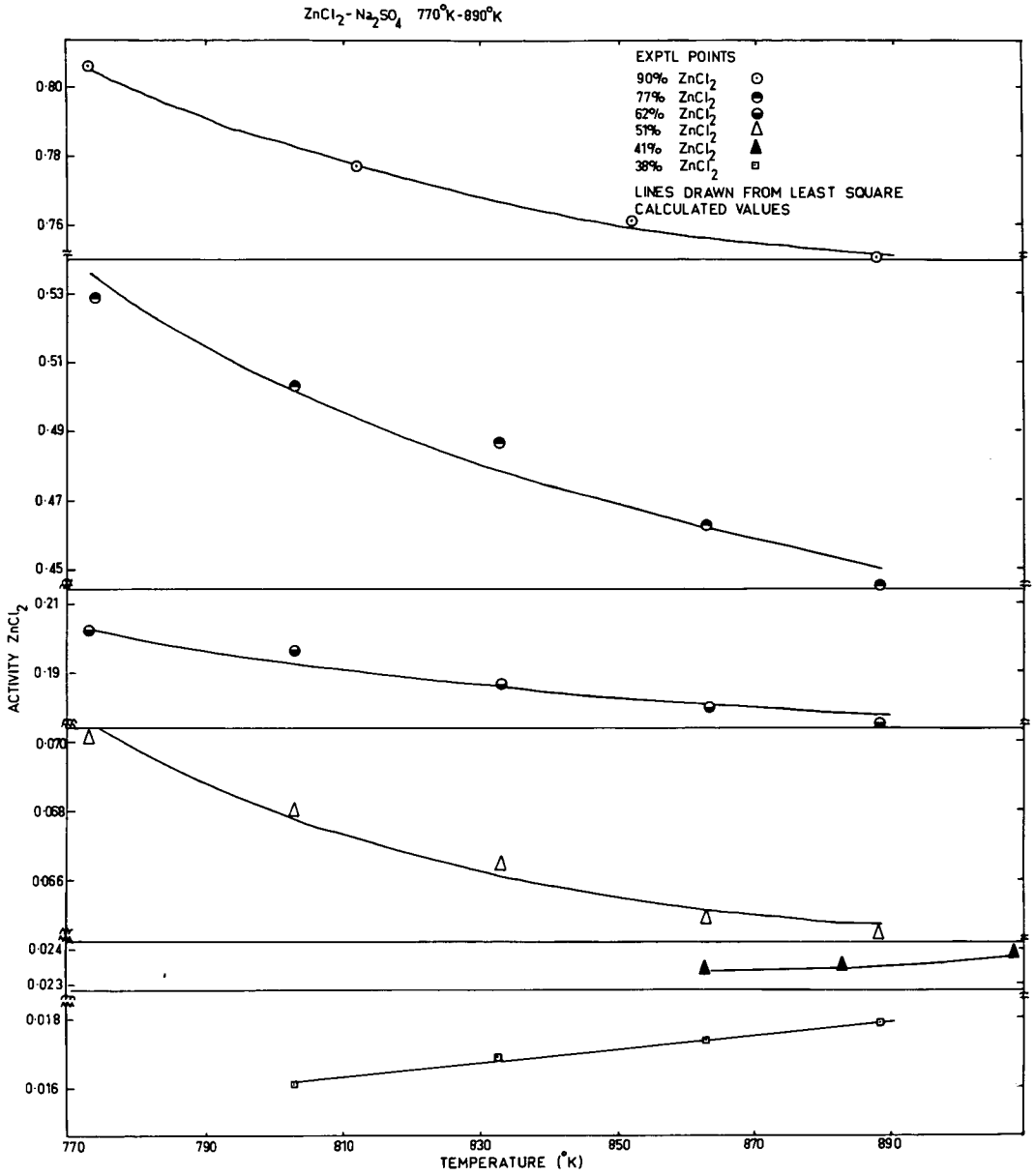

FIGURE 4-7

TEMPERATURE DEPENDENCE OF $ZnCl_2$ ACTIVITY

$ZnSO_4$ - NaCl 803-903 °K

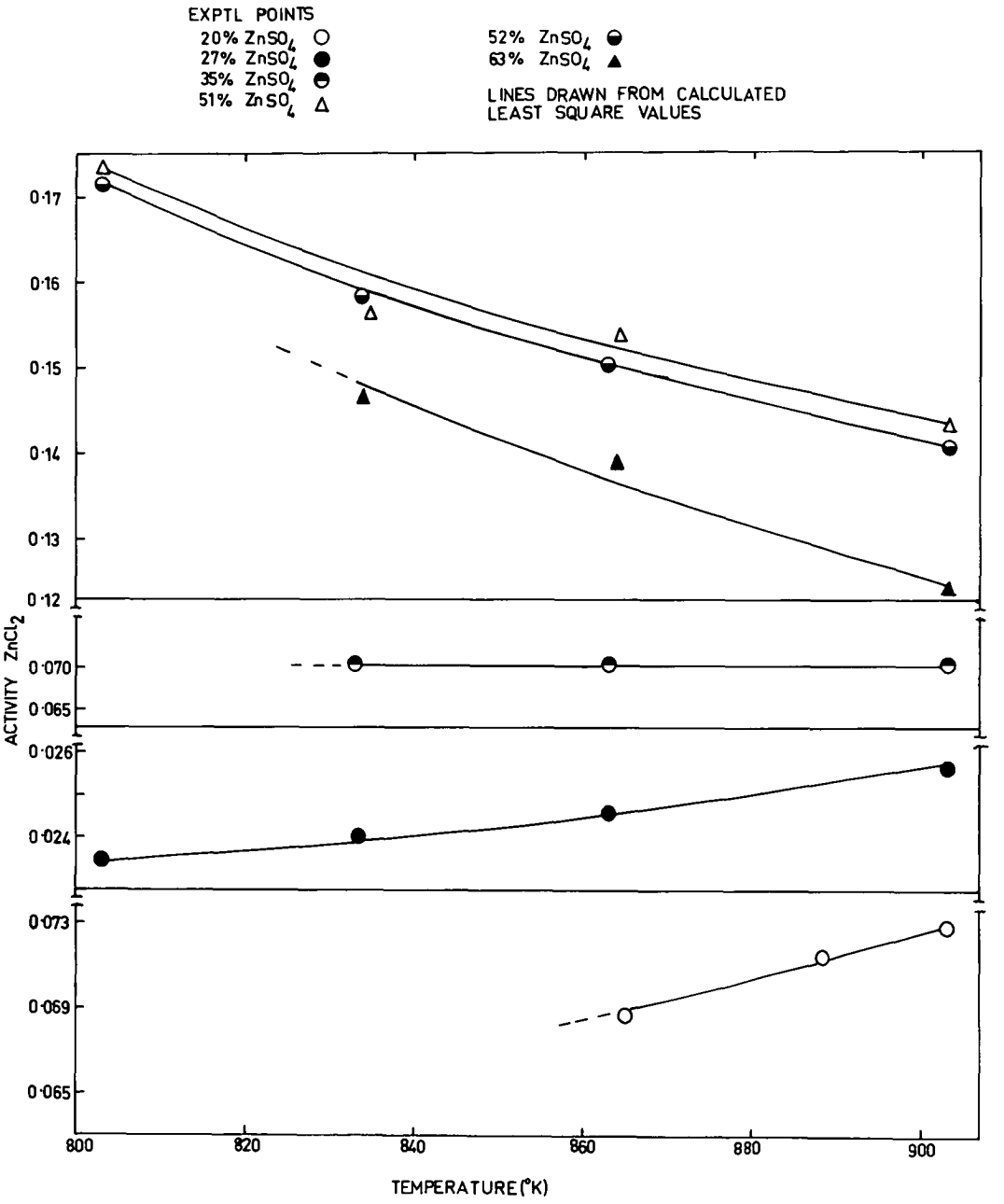

deviations from ideality, the negative temperature coefficient of ΔG^{o} would indicate a tendency towards lower $ZnCl_2$ activities with increasing temperatures.

Secondly, partial molar quantities for $ZnCl_2$ have been calculated using the following equations:

$$\Delta\bar{G}_{ZnCl_2} = RT \ln a_{ZnCl_2} \qquad \text{(IV-31)}$$

$$\Delta\bar{H}_{ZnCl_2} = -RT^2 \frac{\partial \ln a_{ZnCl_2}}{\partial T} \qquad \text{(IV-32)}$$

$$\Delta\bar{S}_{ZnCl_2} = (\Delta\bar{H}_{ZnCl_2} - \Delta\bar{G}_{ZnCl_2})/T \qquad \text{(IV-33)}$$

In practice the integrated forms were used:

$$\Delta\bar{G} = R(\ln a_2 + \ln a_1)/2 \qquad \text{(IV-34)}$$

$$\Delta\bar{H} = -RT_1T_2(\ln a_2 - \ln a_1)/(T_2 - T_1) \qquad \text{(IV-35)}$$

where a_2, a_1 are the activities of $ZnCl_2$ at temperatures T_2 and T_1 respectively. If the ideal activity is taken to be that of the Temkin model, excess partial molar quantities are given by the equations:

$$\Delta\bar{G}^{E}_{ZnCl_2} = \Delta\bar{G}_{ZnCl_2} - RT \ln(X_{Zn}X^{2}_{Cl}) \qquad \text{(IV-36)}$$

$$\Delta\bar{H}^{E}_{ZnCl_2} = \Delta\bar{H}_{ZnCl_2}$$

$$\Delta\bar{S}^{E}_{ZnCl_2} = (\Delta\bar{H}^{E}_{ZnCl_2} - \Delta\bar{G}^{E}_{ZnCl_2})/T \qquad \text{(IV-37)}$$

These partial molar quantities are given in figures 4-8, 4-9, 4-10. It is realised that partial molar enthalpies calculated from the temperature dependence of an equilibrium

FIGURE 4-8

PARTIAL MOLAR QUANTITIES $ZnCl_2$

$ZnCl_2$-Na_2SO_4 830°K

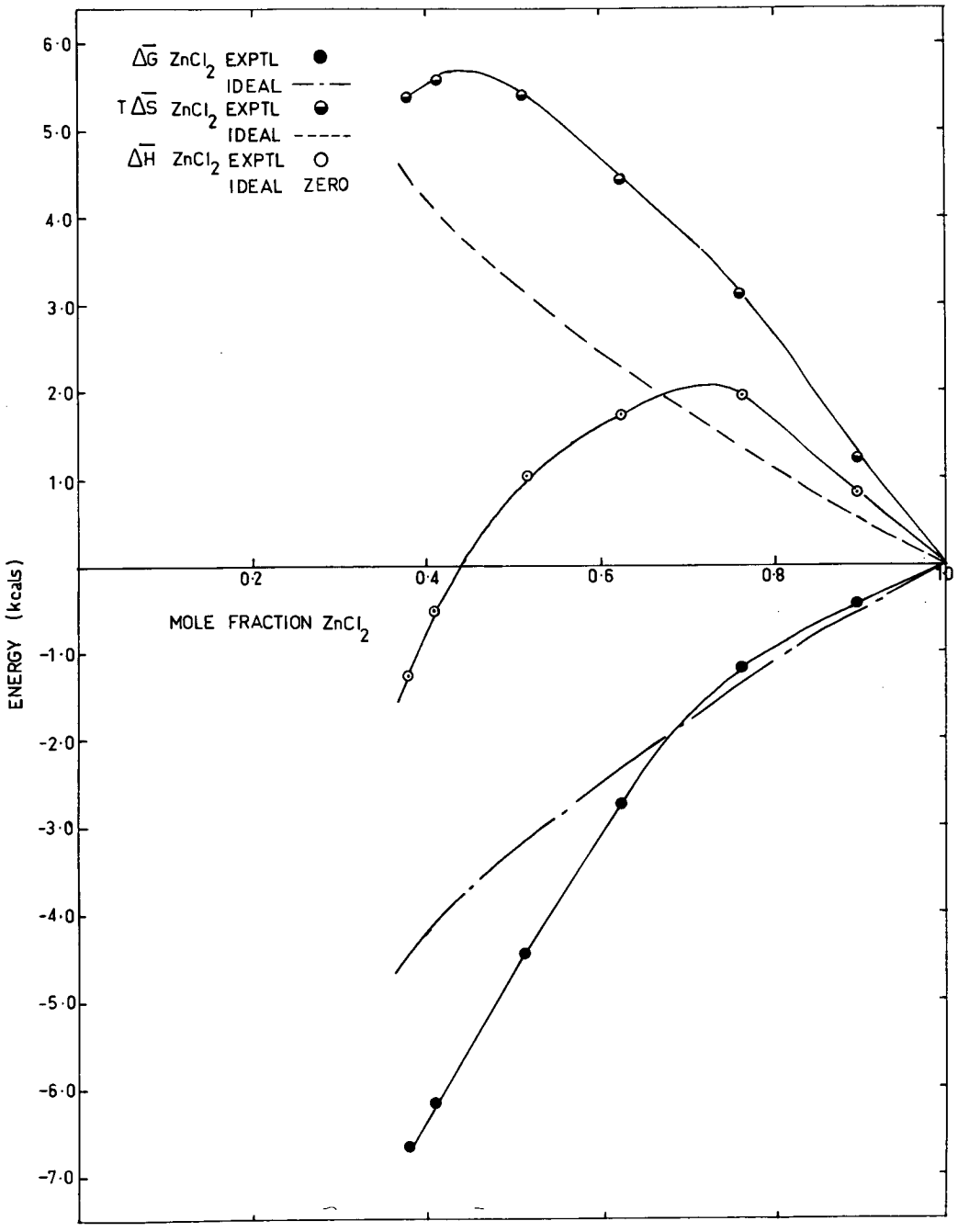

FIGURE 4-9

PARTIAL MOLAR QUANTITIES $ZnCl_2$

$ZnSO_4$ - NaCl 850°K

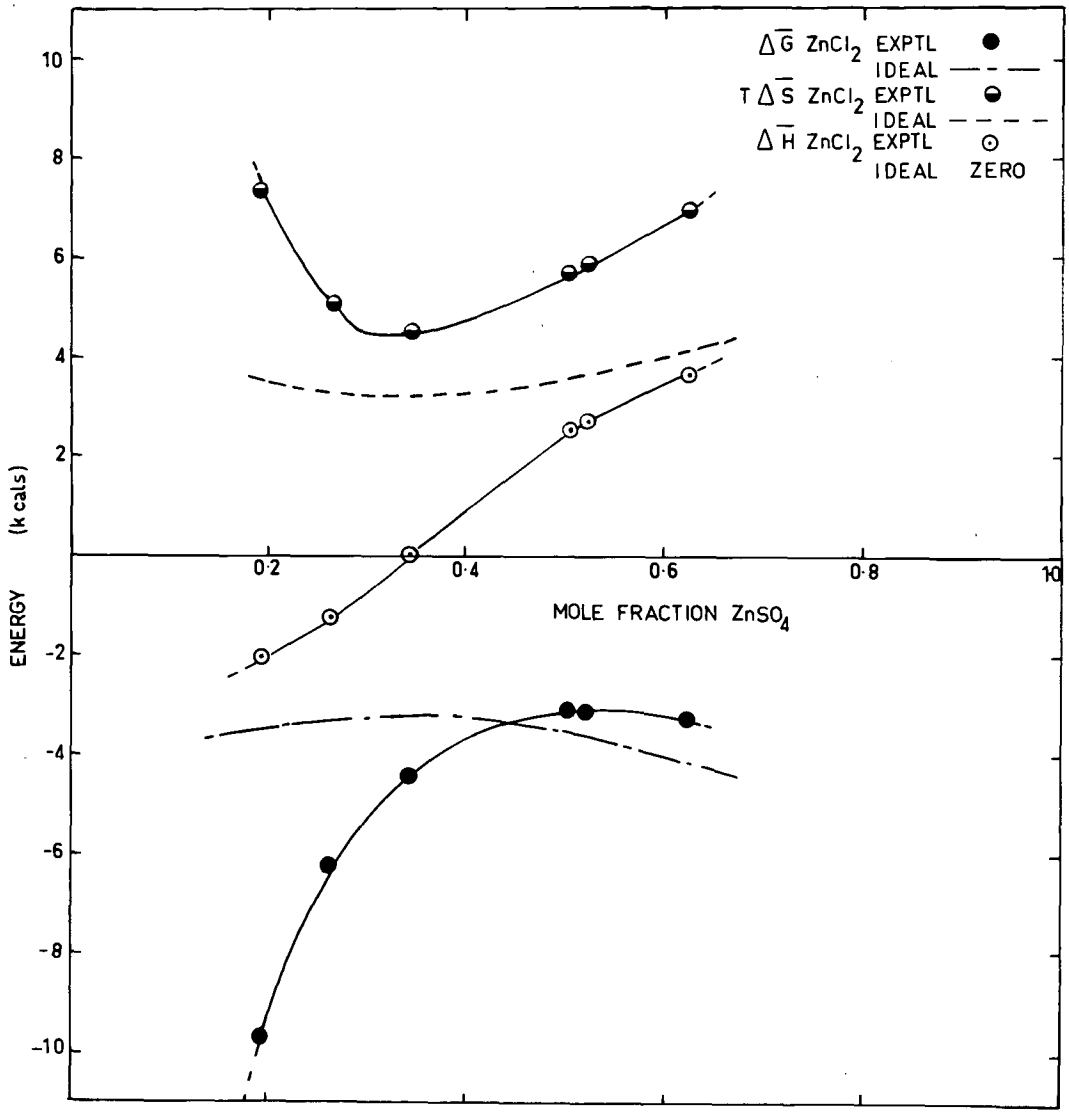

FIGURE 4-10

EXCESS PARTIAL MOLAR QUANTITIES

$Zn\text{-}Na\text{-}Cl\text{-}SO_4$

$\bar{\Delta G}^E_{ZnCl_2}$ ●

$\bar{\Delta H}^E_{ZnCl_2}$ ⊙

$T\bar{\Delta S}^E_{ZnCl_2}$ ◒

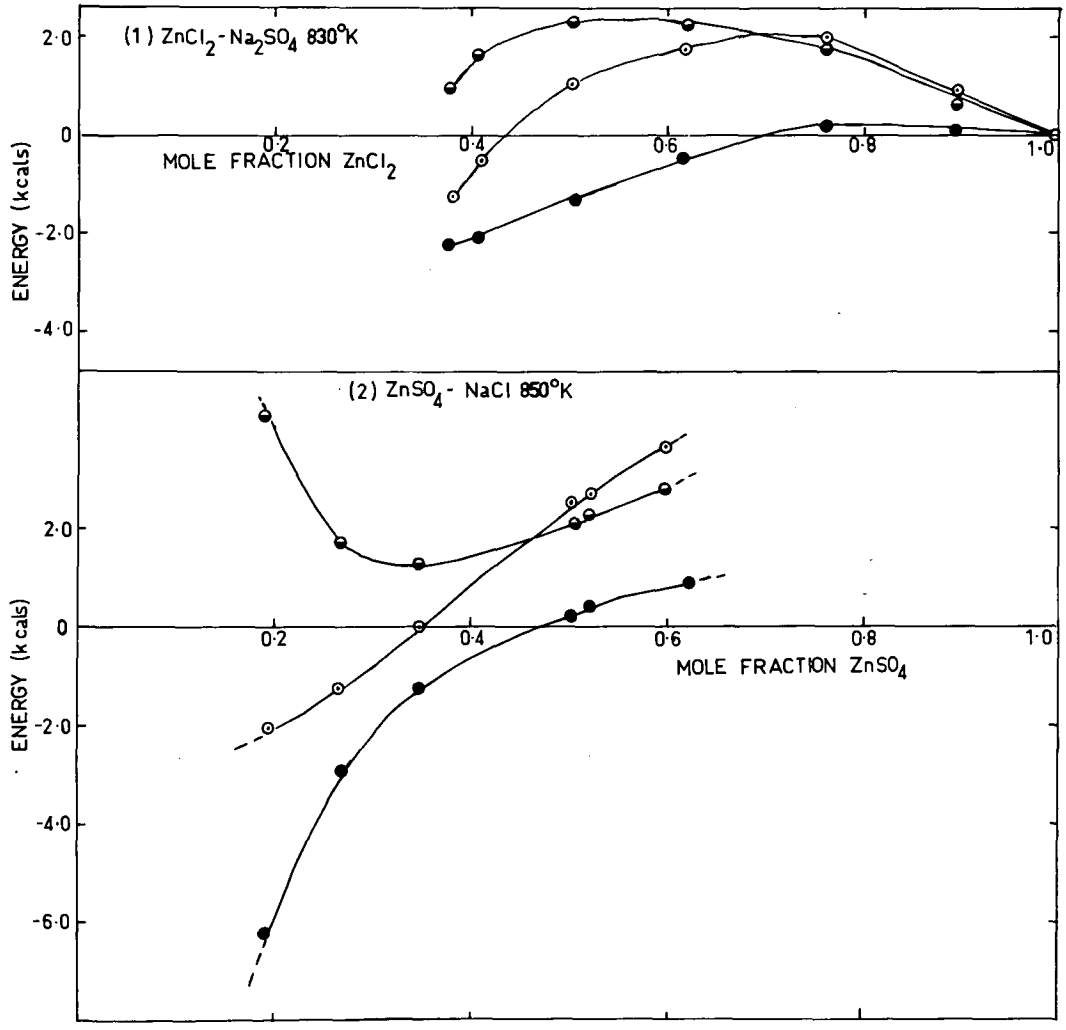

FIGURE 4-11

EXCESS PARTIAL MOLAR QUANTITIES

$ZnCl_2$ - NaCl (823°K)

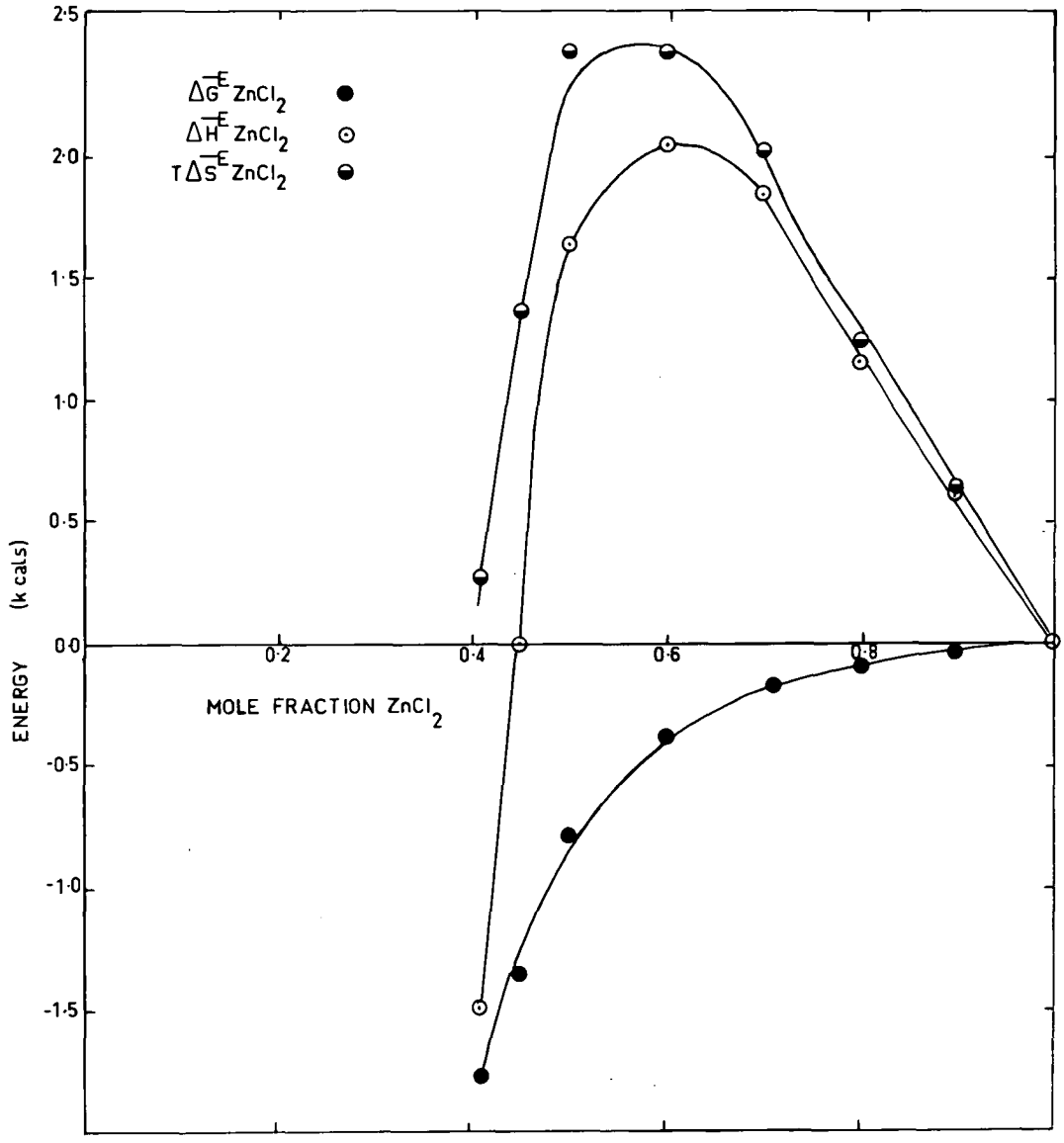

are somewhat prone to errors. In this case they have been made as reliable as possible by correcting for small composition changes and for dimer dissociation. Although the absolute values of $\Delta\bar{H}$ are probably accurate only to one kcal/mole, the overall trends with composition would be meaningful. It is generally agreed that values of $\Delta\bar{G}^E$ calculated from such data are reliable[165,120] within random error. Supporting the validity of calculated values of $\Delta\bar{H}$ is the fact that $\Delta\bar{H}_{ZnCl_2}$ and $\Delta\bar{G}_{ZnCl_2}$ both follow the same general trend with composition. In the similar $PbCl_2$-MCl systems, McCarty and Kleppa [65] have observed the same behaviour. In that study, calorimetrically determined values of $\Delta\bar{H}$ were combined with values of $\Delta\bar{G}^E$, determined from activity data.

In both quasi-binary systems, at those compositions where activities are greater than ideal, $\Delta\bar{H}_{ZnCl_2}$ is positive. The metathetical equilibrium would at least partly contribute to this behaviour. As activities become less than ideal, $\Delta\bar{H}_{ZnCl_2}$ becomes smaller and eventually negative. Binary and possibly ternary type interactions would be bringing about this different type of behaviour. The interactions present in the $ZnCl_2$-NaCl binary are those likely to have the greatest effect on $\Delta\bar{H}_{ZnCl_2}$ in the ternary system. $ZnCl_2$ activities in this binary are known to vary with temperature.[91] Excess partial molar quantities for $ZnCl_2$ in $ZnCl_2$-NaCl have been calculated from the data of Bloom et al[91] and are given in figure 4-11. Dijkhuis and Ketelaar[200] made measurements only at 600°C.

Comparison of figures 4-10 and 4-11 reveals a similarity between the partial molar properties of the $ZnCl_2$-Na_2SO_4 and $ZnCl_2$-NaCl systems. It would appear that the binary interactions influence the behaviour of the ternary system to a large extent. It must be pointed out however that the earlier activity results of Lantratov and Alabyshev[74] by e.m.f. measurement would indicate that $\Delta\bar{H}_{ZnCl_2}$ is negative at all concentrations in the $ZnCl_2$-NaCl system. The more recent vapour pressure results would probably be more accurate. In the Russian work solubilities of metallic zinc and chlorine gas in the melt affect results. Solubilities would vary with temperature introducing an error of unknown magnitude into the temperature dependence of the activity.

Further evidence supporting the change in sign of $\Delta\bar{H}_{ZnCl_2}$ from positive to negative, is the change in sign with composition in average molar volumes in the $ZnCl_2$-NaCl system. The results of Markov et al[96] indicate that ΔV^E is negative at high $ZnCl_2$ concentrations and becomes greater upon further addition of NaCl. The actual change in sign occurs at about 0.5 mole fraction at 600°C. Therefore, it seems reasonable that the change of sign $\Delta\bar{H}_{ZnCl_2}$ with composition is meaningful and is indicative of structural changes in the melt.

It is likely that positive values of $\Delta\bar{H}_{ZnCl_2}$ in both the ternary and binary systems are due to a breaking down of a partial covalent network, present in pure $ZnCl_2$, by ions in the mixture. Kleppa et al have found that partial covalent bonding in pure

Ag^{52} or Tl^{53} salts gives rise to positive contributions to the heats of mixing with alkali salts. The positive $\Delta\bar{H}_{ZnCl_2}$ would tend to make $\Delta\bar{G}_{ZnCl_2}$ also positive. Consequently, the greater than ideal $ZnCl_2$ activities at some concentrations in the ternary system would be due both to this binary type effect and also to the metathetical equilibrium mentioned earlier.

A second influence must be operating to explain negative values of $\Delta\bar{H}_{ZnCl_2}$ and low $ZnCl_2$ activities at other compositions. Again first considering the $ZnCl_2$-NaCl binary, complex ion formation has been postulated to explain its thermodynamic and transport properties. Kleppa et al have shown that complex ion formation in ACl_2-MCl (A = Pb,[65] Mg,[66] Ni[68]) systems is accompanied by strongly exothermic heats of mixing. The results of Lantratov et al[74] further indicate that complex ion formation in ACl_2-MCl (A = Pb, Cd, Zn) binaries results in low ACl_2 activities. Therefore, complex ion formation is the most probable reason for low $ZnCl_2$ activities in the reciprocal as well as in the binary system. The positive values of ΔV^E in $ZnCl_2$-NaCl at high NaCl concentrations[96] are in agreement with the argument for complex ion formation; Lantratov et al[74] and Bloom et al[207] have shown that complex ion formation is accompanied by positive deviations from ideality in volumes of mixing.

Figure 4-4 illustrates the Temkin activity of NaCl in the $ZnCl_2$-Na_2SO_4 system. When the theoretical activity of NaCl is approximately equal to that of $ZnCl_2$, activities sharply fall off

and $\Delta\bar{H}_{ZnCl_2}$ exhibits a maximum before becoming less positive with increasing Na_2SO_4 concentration. The complexing effect gradually becomes important in the ternary system, eventually predominating over the effect of covalent bonding in $ZnCl_2$. Activities in the $ZnSO_4$-NaCl system are in agreement with these conclusions. Where high NaCl concentrations occur, large negative deviations from ideality in the activity and also negative values of $\Delta\bar{H}_{ZnCl_2}$ are found. As NaCl composition decreases, there is a tendency toward high $ZnCl_2$ activities and positive values of $\Delta\bar{H}_{ZnCl_2}$. It is significant that the F.F.G. (S.S.) model best fits the data at high NaCl concentrations. This could indicate a greater degree of order exists in the melt at these concentrations.

Interactions present in the $ZnSO_4$-Na_2SO_4 binary will also be present in the reciprocal system. These are likely to make a negative contribution to $\Delta\bar{H}_{ZnCl_2}$. Ternary excess interactions are also likely to be present; these will be discussed shortly.

4.4.3. Activity Models

(A) Introduction

Neither the Temkin nor F.F.G. solid solution models fit the activity data well. More advanced models will therefore be treated. Concentrations used in this work are too high for use of the quasi-lattice models put forward by Blander[112] and Førland.[14]

(1) F.F.G. Regular Solution Model

Application is quite straightforward. The form of equation

is:

$$RT \ln \gamma_{ZnCl_2} = \Delta G^{o}_{(mole)} X'_{SO_4} \cdot X'_{Cl} \qquad \text{(IV-38)}$$

Earlier it was shown that $\Delta G^{o}_{(mole)} = 2\Delta G^{o}_{(equiv)}$ so that:

$$a_{ZnCl_2} = X_{Zn} X^{2}_{Cl} \exp(2\Delta G^{o}_{(equiv)}/RT \cdot X'_{Na} X'_{SO_4}) \qquad \text{(IV-39)}$$

(2) Conformal Ionic Solution Method

Blander's derivation of the activity coefficient from the integral excess free energy applies to charge symmetrical systems; see equation (11-49). For systems studied in this work, slight modification is necessary.[208*] In treating charge unsymmetrical systems, the method used by Meschel and Kleppa[198] is employed: all standard energies are based upon one equivalent of salt and concentrations are expressed as equivalent ion fractions. Using their notation, the process of mixing X'_D equivalents of BD, X'_A equivalents of AC and $(X'_B - X'_D)$ equivalents of [BC] to form a reciprocal salt mixture is written:

$$X'_D [BD] + X'_A [AC] + (X'_B - X'_D) [BC] = [A](X'_A) \cdot [B](X'_B) \cdot [C](X'_C) \cdot [D](X'_D) \qquad \text{(IV-40)}$$

where [BD] represents one equivalent of salt BD and the term on the right indicates a solution in which equivalent ion fractions

---

*The author would like to express thanks to Dr. Milton Blander for helpful communications concerning the derivation of the activity coefficient equation from the C.I.S. integral form.

of ions A,B,C,D are X'_A, X'_B, X'_D, X'_D.

$$\Delta G^E_{(equiv)} = X'_A X'_D \Delta G^o_{(equiv)} + X'_D \Delta G^E_{12(equiv)} + X'_D \Delta G^E_{34(equiv)}$$

$$+ X'_A \Delta G^E_{13(equiv)} + X'_B \Delta G^E_{24(equiv)} + X'_A X'_B X'_C X'_D \Lambda \qquad \text{(IV-41)}$$

Meschel and Kleppa[198] would set $\Lambda = -(\Delta G^o_{(equiv)})^2/2ZRT$. (Their form is somewhat different in that it is based upon excess enthalpies rather than free energies; they do, however, use $\Delta H^o_{(equiv)}$ in the ternary excess term).

In this case let Na = A, Zn = B, SO_4 = C, Cl = D, then the binary mixtures are 12 = $NaCl-ZnCl_2$, 13 = $NaCl-Na_2SO_4$, 34 = $Na_2SO_4-ZnSO_4$, 24 = $ZnCl_2-ZnSO_4$. Values of $\Delta G^E_{ij(equiv)}$ for these binaries have been expressed previously (4.3.), e.g.

$$\Delta G^E_{12(equiv)} = \lambda_{12} X'_{Zn} X'_{Na}$$

Here Blander's[115] notation, with λ_{ij} in place of b, is used. Now:

$$\Delta G^E_{(equiv)} = X'_{Na} X'_{Cl} \Delta G^o_{(equiv)} + X'_{Cl} X'_{Na} X'_{Zn} \lambda_{12}$$

$$+ X'_{SO_4} X'_{Na} X'_{Zn} \lambda_{34} + X'_{Na} X'_{SO_4} X'_{Cl} \lambda_{13}$$

$$+ X'_{Zn} X'_{SO_4} X'_{Cl} \lambda_{24} + X'_{Na} X'_{Zn} X'_{SO_4} X'_{Cl} \Lambda \qquad \text{(IV-42)}$$

The C.I.S. equation may now be differentiated for an arbitrary number of equivalents of salt with respect to the number of equivalents of $ZnCl_2$ to obtain $\Delta \bar{G}^E_{ZnCl_2(equiv)}$.

Activity coefficients may be determined from

$$RT \ln \gamma_{ZnCl_2} = 2 \Delta \bar{G}^{E}_{ZnCl_2(equiv)} \qquad \text{(IV-43)}$$

If Q is an arbitrary total number of equivalents of all salts, then:

$$\Delta G^{E}_{ZnCl_2(equiv)} = \frac{\partial Q \Delta G^{E}_{(equiv)}}{\partial (n'_{ZnCl_2})} = \frac{\partial Q \Delta G^{E}_{(equiv)}}{\partial (n'_{Zn})} + \frac{\partial Q \Delta G^{E}_{(equiv)}}{\partial (n'_{Cl})}$$

(IV-44)

The differentiation is the same as that made by Blander except that X has been replaced by X'. Therefore, the differentiated equation takes the same form:

$$\begin{aligned}\Delta \bar{G}^{E}_{ZnCl_2(equiv)} = {} & X'_{Na} X'_{SO_4} \Delta G^{o}_{(equiv)} + X'_{Na} X'_{SO_4} (X'_{SO_4} - X'_{Cl})^{\lambda}_{13} \\ & + X'_{SO_4} (X'_{Na} X'_{Cl} + X'_{Zn} X'_{SO_4})^{\lambda}_{24} \\ & + X'_{Na} (X'_{Na} X'_{Cl} + X'_{Zn} X'_{SO_4})^{\lambda}_{12} \\ & + X'_{Na} X'_{SO_4} (X'_{Na} - X'_{Zn})^{\lambda}_{34} \\ & + X'_{Na} X'_{SO_4} (X'_{Na} X'_{Zn} + X'_{Zn} X'_{SO_4} - X'_{Zn} X'_{Cl})^{\Lambda}\end{aligned}$$

(IV-45)

$RT \ln \gamma_{ZnCl_2} = 2 \Delta \bar{G}^{E}_{ZnCl_2(equiv)}$.

If the binary and ternary excess terms are neglected, this equation reduces to the F.F.G. form. If the ternary excess term alone is neglected, the form used by Blander[115,116] to represent the F.F.G. + Førland model is obtained.

In the systems of interest, simplification is possible. In the system $ZnCl_2$-Na_2SO_4:

$$X'_{Zn} = X'_{Cl} = 1 - X'_{Na} = 1 - X'_{SO_4}, \text{ so that:}$$

$$RT \ln \gamma_{ZnCl_2} = 2(X'_{Na})^2 \Big[\Delta G^o_{(equiv)} + \lambda_{13} + \lambda_{34} + 2X'_{Zn} (\lambda_{24} + \lambda_{12} - \lambda_{13} - \lambda_{34}) + X'_{Zn} (3 X'_{Na} - 1)\Lambda \Big] \qquad \text{(IV-46)}$$

In the other system $ZnSO_4$-NaCl:

$$X'_{Zn} = X'_{SO_4} = 1 - X'_{Na} = 1 - X_{Cl}$$

$$RT \ln \gamma_{ZnCl_2} = 2 \Big[X'_{Zn} X'_{Na} \Delta G^o_{(equiv)} + (X'_{Na})^2 (X'_{Na} \lambda_{12} + X'_{Zn} (\lambda_{24} + \lambda_{34} - \lambda_{13})) + (X'_{Zn})^2 (X'_{Zn} \lambda_{24} + X'_{Na} (\lambda_{13} + \lambda_{12} - \lambda_{34})) + ((X'_{Na})^3 X'_{Zn} + X'_{Na} (X'_{Zn})^3 - (X'_{Na})^2 (X'_{Zn})^2) \Lambda \Big]$$

(IV-47)

Values for the various parameters have been found, (4.3.1.):

$\Delta G^o_{(equiv)} = + 1575$ cals, (863^oK)

$\lambda_{12,(Na-Zn)Cl} = - 4{,}970$ cals

$\lambda_{13,Na(Cl-SO_4)} = 0$ cals

$\lambda_{24,Zn(Cl-SO_4)} = + 220$ cals

$\lambda_{34,(Zn-Na)SO_4} = - 10{,}000 \leq \lambda_{34} \leq - 5000$ cals.

A value of 6 has been used for Z.[115] In these systems where the exchange free energy is small and the binary terms are large, the entire non random mixing term has only a minor effect on the results. Values of Z between 4 and 6 have almost the same effect on calculated activities. Moreover, as this term is small, both the C.I.S. and F.F.G.+Førland equations virtually give the same results.

(B) $\underline{ZnCl_2\text{-}Na_2SO_4}$

Values of RT ln γ_{ZnCl_2} have been evaluated for F.F.G., F.F.G.+Førland and C.I.S. equations at 863°K. These have been plotted against $(X'_{Na})^2$ in fig. 4-12 and given in table 4-8. Various values of λ_{34} have been used to determine the effect of this parameter. The experimental curve for RT ln γ_{ZnCl_2} at 863°K has also been plotted.

At the point $X'_{Zn} = X'_{Na} = 0.5$, the C.I.S. equation reduces to:

$$RT \ln \gamma_{ZnCl_2} = 0.5 (\Delta G^{o}_{(equiv)} + \lambda_{24} + \lambda_{12} + X'_{Zn} (3X'_{Na} - 1)\Lambda) \qquad \text{(IV-48)}$$

As the doubtful λ_{34} binary term does not appear in this expression, the ternary excess energy may be calculated at this point and compared with experiment.

Comparison of Ternary Excess Energies, $\underline{ZnCl_2\text{-}Na_2SO_4}$, (863°K)

Experimental RT ln γ_{ZnCl_2}	C.I.S. RT ln γ - 3° excess	Experimental 3° excess	C.I.S. 3° excess
-1430	-1588	+158	-15

TABLE 4-8

Comparison of Experimental and Theoretical Values of RT ln λ_{ZnCl_2} in the System $ZnCl_2$-Na_2SO_4, (863°K)

X'_{Zn}	$(X'_{Na})^2$	RT ln λ_{ZnCl_2} (cals)						
		Exptl.	F.F.G.	F.F.G. + Førland $\lambda_{34} = -7,500$	C.I.S. λ_{34}			
					0	-4,970	-7,500	-10,000
0.9	0.01	45	32	-20	-136	-57	-18	19
0.8	0.04	110	126	-127	-450	-220	-126	0
0.7	0.09	-260	284	-374	-906	-542	-372	-186
0.6	0.16	-840	504	-804	-1315	-992	-844	-671
0.5	0.25	-1570	788	-1588	-1602	-1602	-1602	-1602
0.4	0.36	-2300	1134	-2682	-825	-2334	-2708	-2995

FIGURE 4-12

RT ln γ_{ZnCl_2} in $ZnCl_2$-Na_2SO_4, 863°K

Legend

- - - - - - - - - -	Experimental	
————————	C.I.S. with	
		λ_{34}(cals)
	1	0
	2	-4,970
	3	-7,500
	4	-10,000
———— — ————	5	F.F.G.

FIGURE 4-12

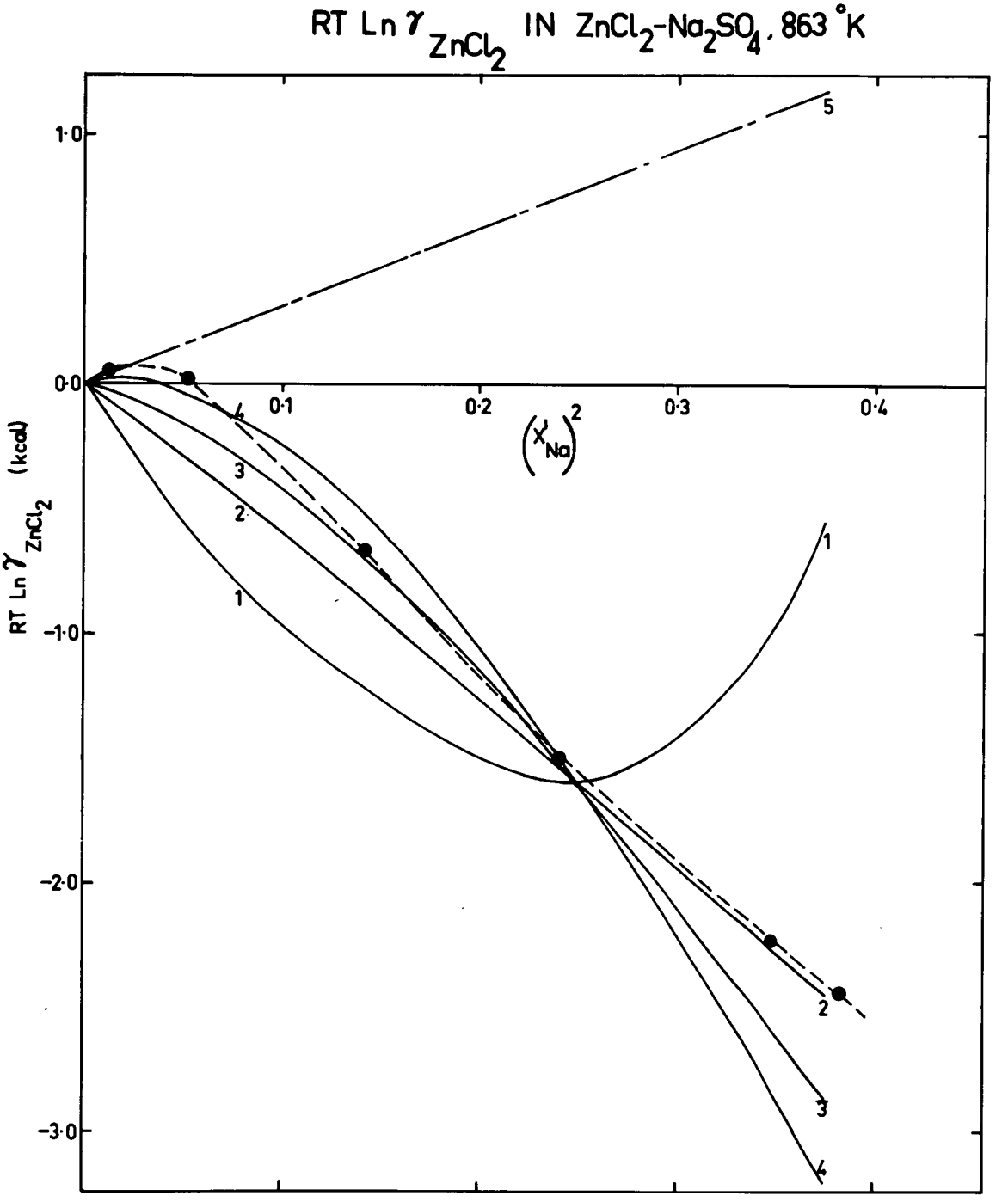
RT Ln γ_{ZnCl_2} IN $ZnCl_2$-Na_2SO_4, 863 °K
RT Ln γ_{ZnCl_2} (kcal)
$(X'_{Na})^2$
1·0
0·0
-1·0
-2·0
-3·0
0·1
0·2
0·3
0·4
1
2
3
4
5

Considering the accumulated scatter in the tabulated data used to calculate the exchange free energies, it is concluded that experimental and C.I.S. ternary excess energies are not in disagreement. When values of RT ln γ_{ZnCl_2} are calculated from the C.I.S. equation using various values for $\lambda_{34,(Na-Zn)SO_4}$, it becomes apparent that a value in the middle of the estimated range, λ_{34} = -7,500 cals, gives the best representation of the data. In fact, values of this parameter from -5000 to -10,000 cals all fit the data well over a large concentration range. It is possible that λ_{34} varies with composition, becoming less negative as X'_{Na} increases. Holm[106] has observed an appreciable asymmetry of heats of mixing in the Li_2SO_4-Na_2SO_4 system with concentration. If similar energetic asymmetry occurs in the $ZnSO_4$-Na_2SO_4 binary, the actual C.I.S. fit would be much better.

As the ternary excess terms are relatively small, values for the F.F.G.+Førland equations are very close to the C.I.S. values and have not been plotted. At high $ZnCl_2$ concentrations, the ternary excess term has the correct sign giving the C.I.S. equation a slightly better fit. The F.F.G. regular solution equation, which does not take binary terms into account, gives a reasonable fit only for dilute solutions of Na_2SO_4 in $ZnCl_2$; at higher concentrations, the F.F.G. equation predicts the wrong direction of change of RT ln γ_{ZnCl_2} with composition and gives it the wrong sign.

(C) $\underline{ZnSO_4\text{-}NaCl}$

Values of RT ln γ_{ZnCl_2} have been calculated for the C.I.S. and F.F.G. equations at 863°K, and compared with experimental results in table 4-9 and in fig. 4-13. As results for the F.F.G.+Førland equation are virtually the same as those for the C.I.S. equation, they have not been given.

At the $X'_{Na} = X'_{Zn} = 0.5$ point, a simpler form is obtained:

$$RT \ln \gamma_{ZnCl_2} = 0.5(\Delta G^{o}_{(equiv)} + \lambda_{12} + \lambda_{24}) + 0.125\Lambda \qquad \text{(IV-49)}$$

Once again, comparison of experimental and C.I.S. ternary excess energies is possible:

Comparison of Ternary Excess Energies $\underline{ZnSO_4\text{-}NaCl}$, (863°K)

Experimental	C.I.S. RT ln γ - 3° excess	Experimental 3° excess	C.I.S. 3° excess
-1630	-1588	-42	-15

In this case quite good agreement is obtained.

For the C.I.S. equation using λ_{34} = -7,500 cals, a reasonable fit to the experimental data is obtained. At high NaCl concentrations, the fit becomes less satisfactory; here, however, results are being compared on a logarithmic scale; calculated activities would fit experimental activities much more closely. The C.I.S. equation successfully predicts an almost linear relationship between RT ln γ_{ZnCl_2} and $(X'_{Na})^2$ over a considerable concentration range. The F.F.G. equation again is obviously insufficient in this system where binary interactions predominate.

TABLE 4-9

Comparison of Experimental and Theoretical Values of RT ln γ_{ZnCl_2} in the System $ZnSO_4$-NaCl, (863°K)

X'_{Zn}	$(X'_{Na})^2$	RT ln γ_{ZnCl_2} (cals)				
		Exptl.	F.F.G.	C.I.S. γ_{34}		
				-7,500	-4,970	-10,000
0.9	0.01	+880	284	+872	+508	+1368
0.8	0.04	+760	504	+830	+346	+1310
0.7	0.09	+450	662	+370	-52	+788
0.6	0.16	-300	756	-454	-696	+220
0.5	0.25	-1630	788	-1602	-1602	-1602
0.4	0.36	-3480	756	-2980	-2732	-3220
0.3	0.49	-5450	662	-4540	-4102	-4958

FIGURE 4-13

RT ln γ_{ZnCl_2} in $ZnSO_4$-NaCl, 863°K

Legend

- - - - - - - - - -	Experimental
————————	C.I.S. with λ_{34}(cals)
1	-4,970
2	-7,500
3	-10,000
——— - ———4	F.F.G.

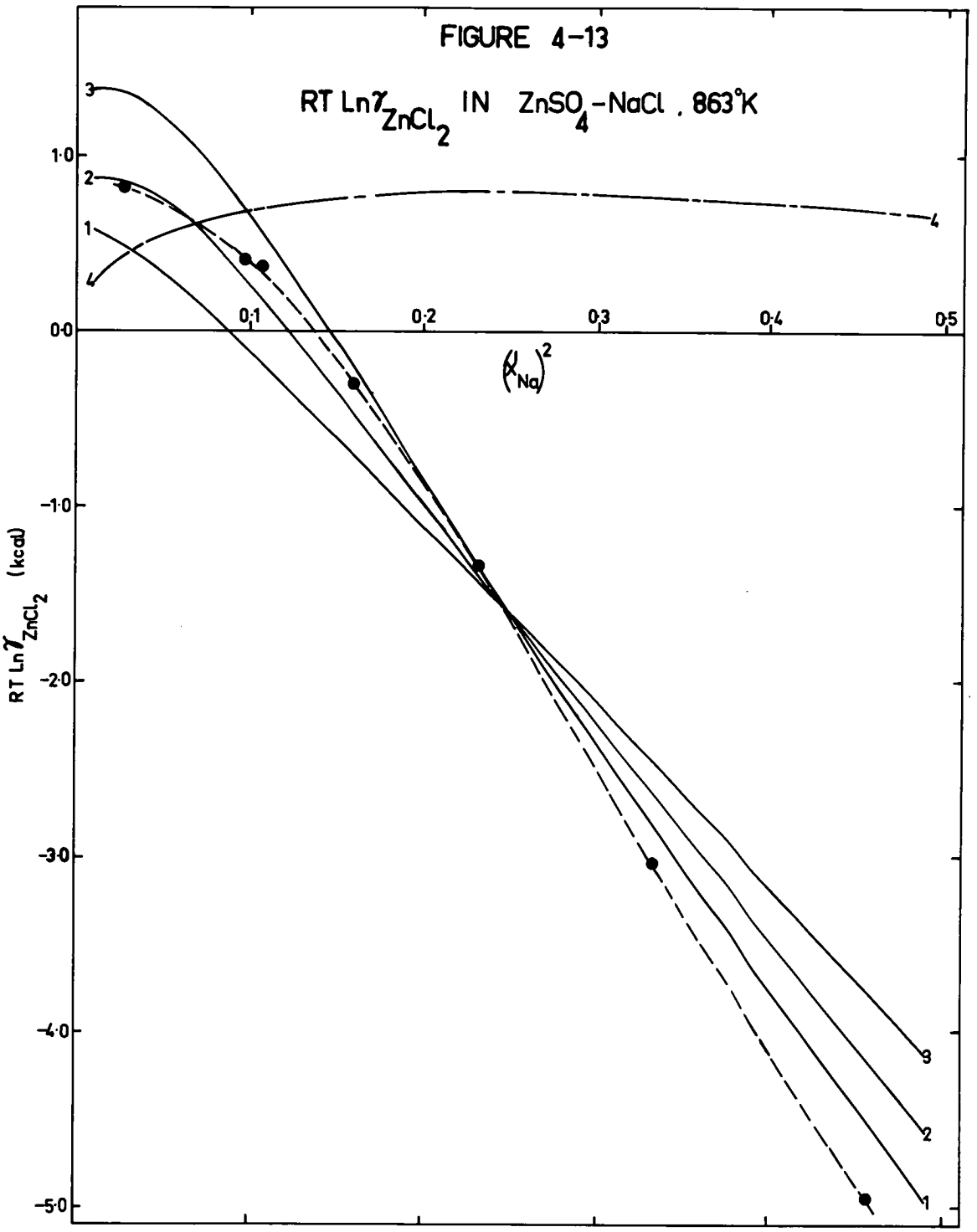
FIGURE 4-13
RT Lnγ_{ZnCl_2} IN $ZnSO_4$-NaCl . 863°K
1·0
0·0
-1·0
-2·0
-3·0
-4·0
-5·0
0·1
0·2
0·3
0·4
0·5
$(\alpha_{Na})^2$
RT Lnγ_{ZnCl_2} (kcal)
1
2
3
4

The most likely reason for the poorer fit with the C.I.S. equation at high NaCl concentrations is the deviation from regular solution behaviour in the $ZnCl_2$-NaCl binary. The results of Dijkhuis and Ketelaar[200] indicate $\Delta G^E_m/N_{NaCl}N_{ZnCl_2}$ becomes more negative as N_{NaCl} increases. In the $ZnSO_4$-NaCl system, if $\lambda_{12,(Na-Zn)Cl}$ becomes more negative with greater NaCl concentration, a better fit would be obtained. In this work an average value was used for λ_{12}; as data for one of the other binary solutions was not available, use of a composition dependent λ_{12} parameter in the integral free energy equation could not be justified.

One may conclude that excess equivalent free energies in the Na_2SO_4-$ZnSO_4$ system are roughly given by the equation

$$\Delta G^E_{(equiv)} = -7{,}500\ X'_{Na}\ X'_{Zn} \qquad \text{(IV-50)}$$

This is an example of the use of data from a ternary system to gain knowledge about an experimentally inaccessible binary system.

(D) Effect of temperature

Temperature effects zinc chloride activities both in the ternary system and in the $ZnCl_2$-NaCl binary. As a further test of the conformal ionic solution theory a simple calculation of temperature dependence was made, assuming the exchange free energy and $\lambda_{12,(Na-Zn)Cl}$ varied with temperature. The data of Bloom et al[91] indicate that zinc chloride activities decrease with increasing temperature over most of the composition range. A reasonable average difference in λ_{12} between 773°K and 863°K of +800 cals best fitted their data in the concentration range of interest.

Values for λ_{12} of -4,200 cals and -4,500 cals at 773°K and 803°K were used.

For the system $ZnCl_2$-Na_2SO_4 values of RT ln γ_{ZnCl_2} at 773°K have been calculated using the C.I.S. equation and plotted in fig. 4-14. A comparison of ternary excess energies is possible at the point where $X'_{Zn} = 0.5$.

Comparison of Ternary Excess Energies $ZnCl_2$-Na_2SO_4, (773°K)

Experimental RT ln γ_{ZnCl_2}	C.I.S. RT ln γ - 3° excess	Experimental 3° excess	C.I.S. 3° excess
-1260	-1092	-168	-22

Using a value of λ_{34} of -7,500 cals, a relatively good fit to the experimental data was achieved. The variation with temperature of RT ln γ_{ZnCl_2} is adequately predicted by the C.I.S. equation.

For the $ZnSO_4$-NaCl system, values of RT ln γ_{ZnCl_2} at 803°K have been plotted in fig. 4-15. Comparing ternary excess energies at $X'_{Zn} = 0.5$:

Comparison of Ternary Excess Energies $ZnSO_4$-NaCl, (803°K)

Experimental RT ln γ_{ZnCl_2}	C.I.S. RT ln γ - 3° excess	Experimental 3° excess	C.I.S. 3° excess
-1460	-1300	-160	-20

Using a value of λ_{34} of -7,500 cals, the C.I.S. equation fits the data as well at this temperature as it did at the higher temperature. Once again the variation with temperature of RT ln γ has been adequately predicted.

FIGURE 4-14

RT ln γ_{ZnCl_2} in $ZnCl_2$-Na_2SO_4, 773°K, 863°K

Legend

- - - - - - - - - - Experimental

1 773°K

2 863°K

———————— C.I.S. with λ_{34} = -7,500 (cals)

3 773°K

4 863°K

———— - - ————5 Bloom and Welch, 863°K

FIGURE 4-14

RT Ln γ_{ZnCl_2} IN $ZnCl_2$-Na_2SO_4

773°K , 863°K

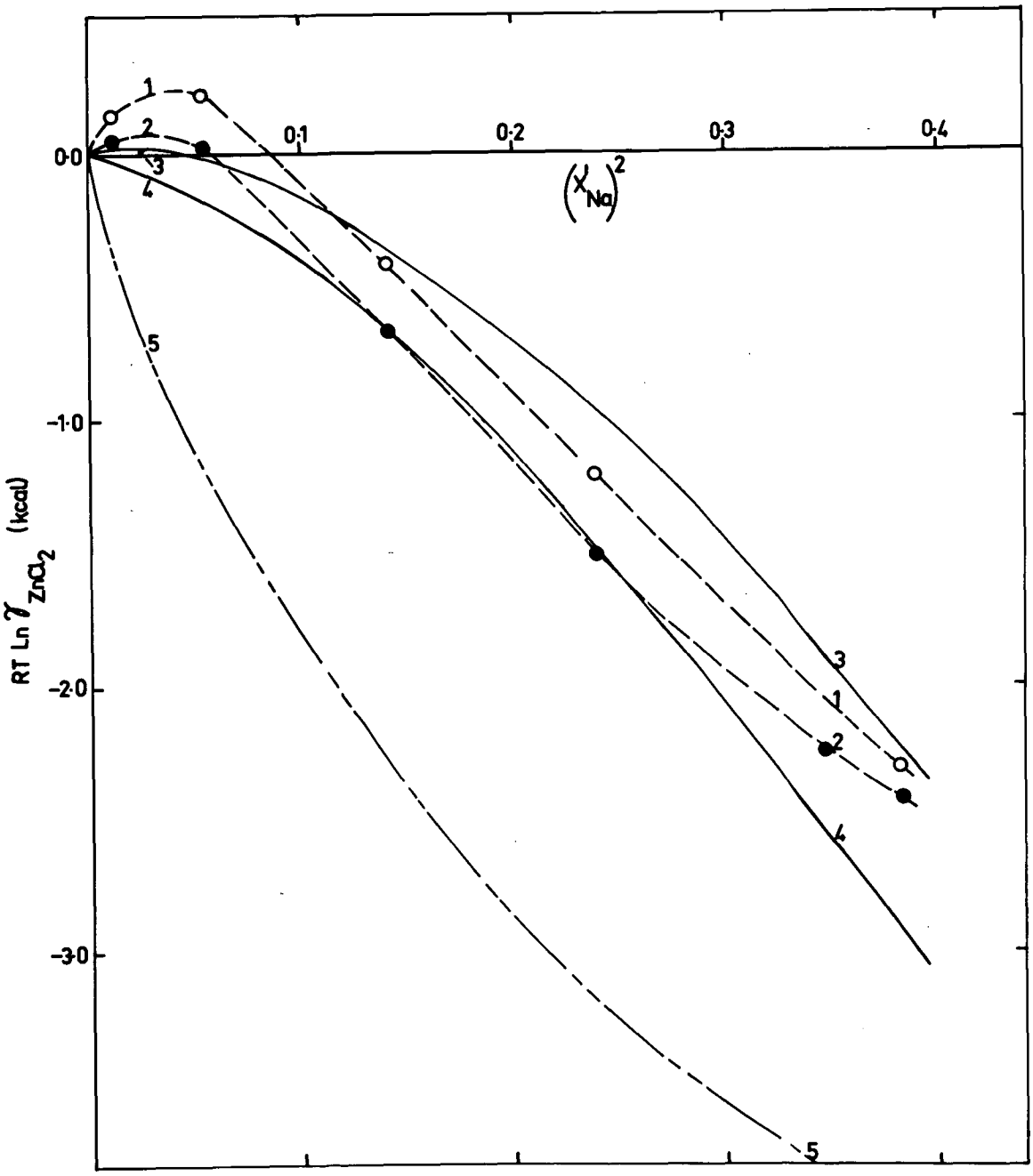

FIGURE 4-15

$RT \ln \gamma_{ZnCl_2}$ in $ZnSO_4$-NaCl, 803°K, 863°K

Legend

- - - - - - - - - -	Experimental
1	803°K
2	863°K
———————	C.I.S. with λ_{34} = -7,500 (cals)
3	803°K
4	863°K
——— - - ———5	Bloom and Welch, 863°K

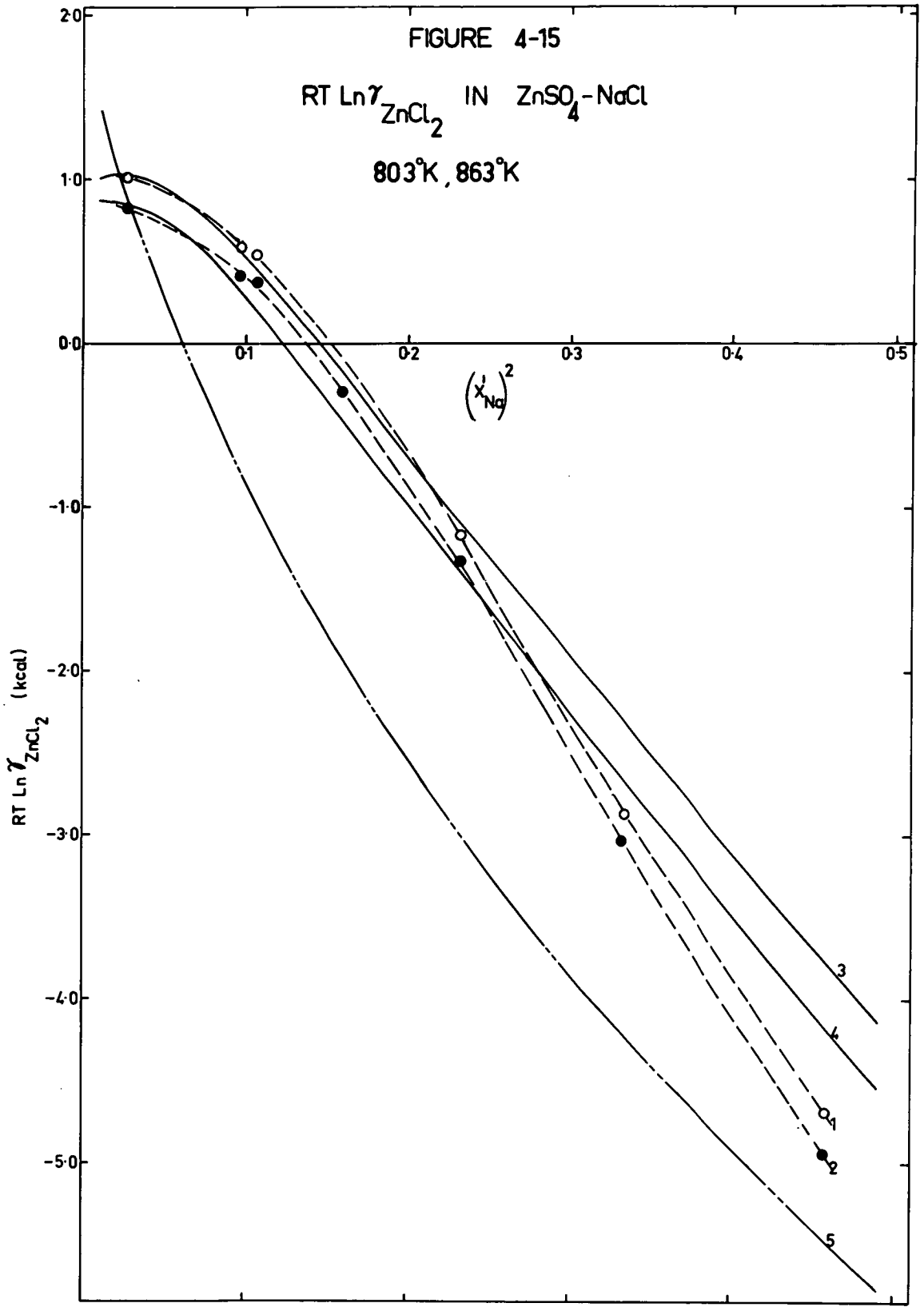
FIGURE 4-15
RT Ln γ_{ZnCl_2} IN $ZnSO_4$-NaCl
803°K, 863°K
RT Ln γ_{ZnCl_2} (kcal)
$(X'_{Na})^2$
2·0
1·0
0·0
-1·0
-2·0
-3·0
-4·0
-5·0
0·1
0·2
0·3
0·4
0·5
1
2
3
4
5

Activities have been calculated from the C.I.S. activity coefficients at two temperatures in both $ZnCl_2$-Na_2SO_4 and $ZnSO_4$-NaCl systems. These are compared with experimental activities in tables 4-10, 4-11 and figures 4-16, 4-17. Usually, quite good agreement between experimental and C.I.S. activities are observed.

(E) Bloom and Welch Method

In reciprocal salt studies, most effort has been directed towards the prediction of ternary behaviour from a knowledge of pure salts and binary mixtures. Bloom and Welch,[20,209] on the other hand, have produced a simple method of extrapolating limited data on a reciprocal mixture over the entire range of compositions; moreover, rough information on binary behaviour is made available.

In the method two binary terms are introduced into the simple F.F.G. equation. Cations are assumed to mix with cations according to the regular solution formula and without regard to anion composition; anions mix in a similar fashion with anions.

In the system Na-Pb-SO_4-Cl the activity of $PbCl_2$ is given by:

$$a_{PbCl_2} = X_{Pb}\, X_{Cl}^2\, \gamma_{Pb}\, \gamma_{Cl}^2 \exp\left(\Delta G^{o}_{(mole)}\, X'_{Na}\, X'_{SO_4}/RT\right) \qquad \text{(IV-51)}$$

where: $RT \ln \gamma_{Pb} = b' X_{Na}^2$; $RT \ln \gamma_{Cl} = 2b' X_{SO_4}^2$ (IV-52)

b,b' are regular solution constants. It will be noted here that Bloom and Welch have used ion fractions rather than equivalent ion fractions in the binary terms. In the system $PbSO_4$-NaCl:[20]

TABLE 4-10

Comparison of Experimental and Calculated C.I.S. Activities in the System $ZnCl_2$-Na_2SO_4, (773°K), (863°K)

Composition mole fn $ZnCl_2$	Activity of $ZnCl_2$				
	773°K		863°K		
	Exptl.	C.I.S.	Exptl.	C.I.S.	Temkin
0.9	0.806	0.740	0.756	0.725	0.733
0.8	0.603	0.527	0.533	0.490	0.527
0.7	0.386	0.335	0.343	0.295	0.366
0.6	0.176	0.176	0.147	0.147	0.241
0.5	0.067	0.074	0.060	0.058	0.148
0.4	0.022	0.022	0.023	0.169	0.082

FIGURE 4-16

Activities of $ZnCl_2$ in $ZnCl_2$-Na_2SO_4, 773°K, 863°K

Legend

- - - - - - - - - -	Experimental
1	773°K
2	863°K
————————	Calculated from C.I.S. activity coefficients
3	773°K
4	863°K

FIGURE 4-16

ACTIVITIES OF $ZnCl_2$ IN $ZnCl_2$-Na_2SO_4

773°K, 863°K

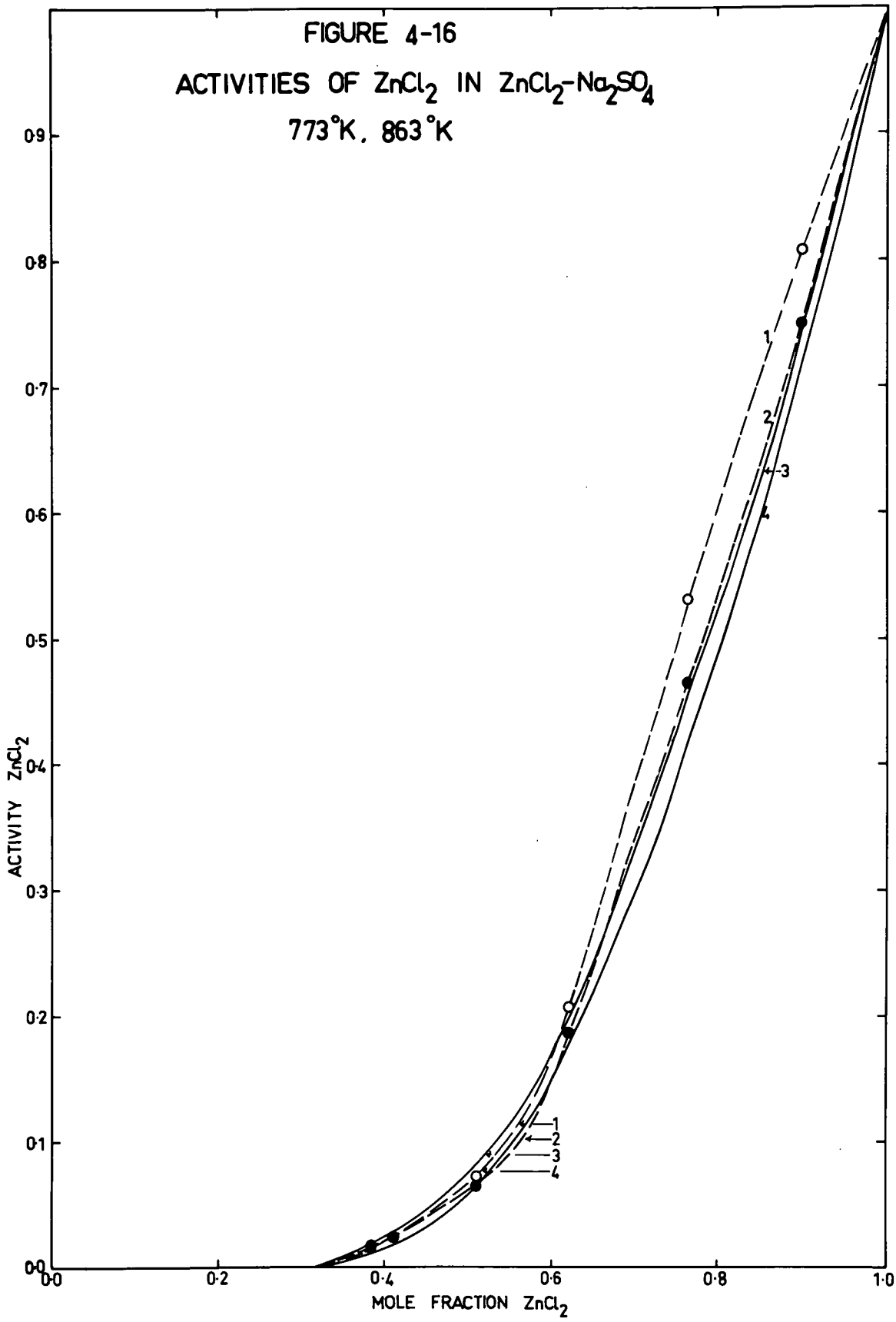

TABLE 4-11

Comparison of Experimental and Calculated C.I.S. Activities in the System $ZnSO_4$-NaCl, (803°K), (863°K)

Composition mole fn $ZnSO_4$	Activity of $ZnCl_2$				
	803°K		863°K		
	Exptl.	C.I.S.	Exptl.	C.I.S.	Temkin
0.20	0.008	0.013	0.010	0.011	0.128
0.25	0.018	0.027	0.019	0.025	0.141
0.30	0.040	0.050	0.050	0.043	0.147
0.35	0.082	0.086	0.076	0.066	0.148
0.40	0.122	0.110	0.108	0.092	0.144
0.45	0.152	0.142	0.145	0.117	0.136
0.50	0.172	0.162	0.161	0.137	0.125
0.55	0.167	0.167	0.158	0.144	0.114
0.60	0.165	0.166	0.151	0.142	0.096
0.65	0.159	0.162	0.132	0.136	0.080

FIGURE 4-17

Activities of $ZnCl_2$ in $ZnSO_4$-NaCl, 803°K, 863°K

Legend

- - - - - - - - - -	Experimental
1	803°K
2	863°K
————————	Calculated from C.I.S. activity coefficients
3	803°K
4	863°K

FIGURE 4-17

ACTIVITY $ZnCl_2$ IN $ZnSO_4$-NaCl

803 °K, 863 °K

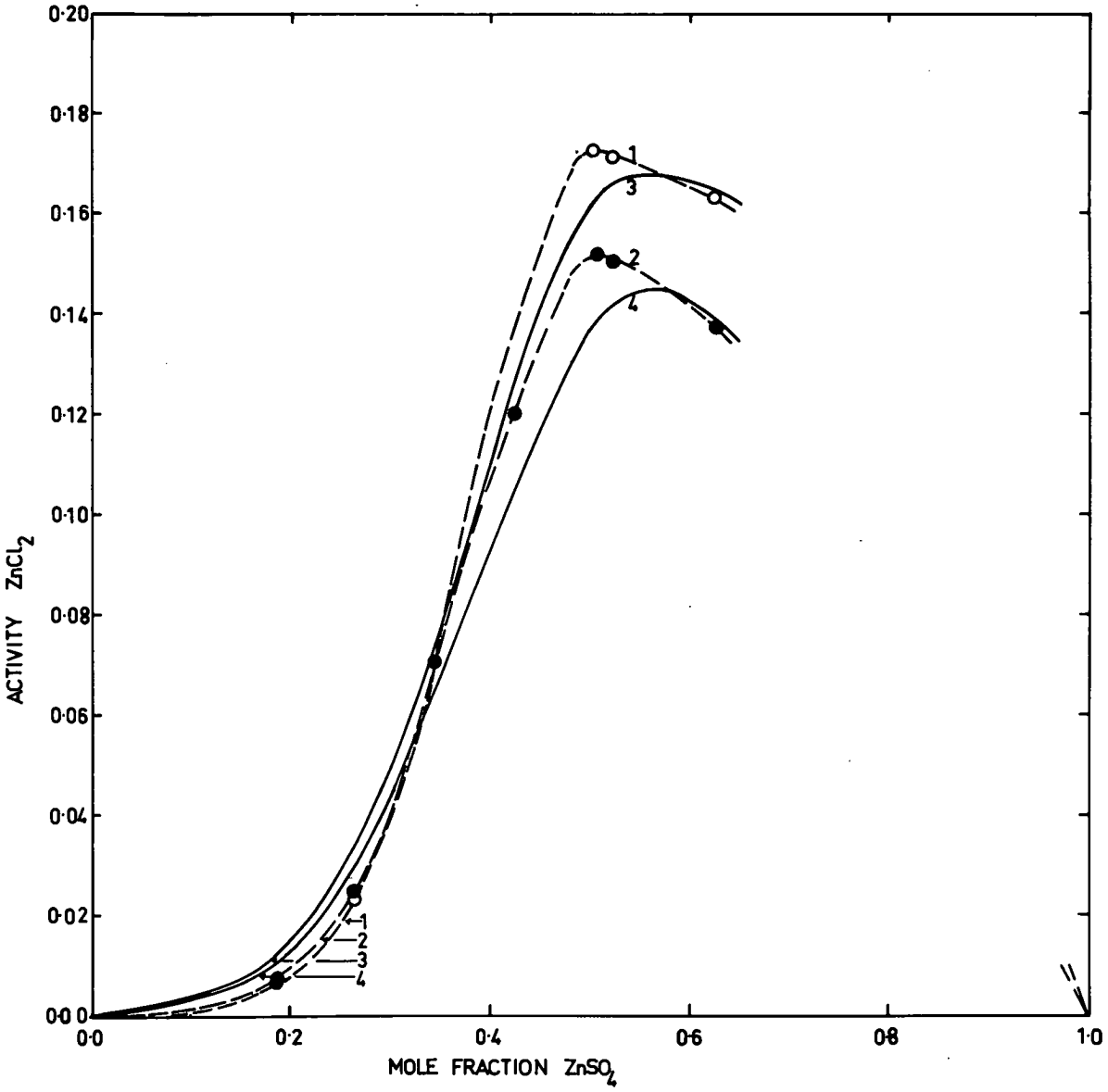

$$RT \ln \gamma_{PbCl_2} = X'_{Na} X'_{SO_4} \Delta G^{o}_{(mole)} + b X^2_{Na} + 2b' X^2_{SO_4} \quad \text{(IV-53)}$$

Where $X_{Na} = 1$, $X'_{Na} = 1$, $X_{SO_4} = 0$, $X_{SO_4} = 0$;
therefore:

$$RT \ln \gamma_{PbCl_2} = b \quad \text{(IV-54)}$$

Where $X_{Na} = 0$, $X'_{Na} = 0$, $X'_{SO_4} = 1$, $X_{SO_4} = 1$;
therefore:

$$RT \ln \gamma_{PbCl_2} = 2b' \quad \text{(IV-55)}$$

The constants b,b' were found from the intercepts on the appropriate axes of a plot of RT ln γ_{PbCl_2} against X_{Na}.

This method has been applied to the data for the system $ZnSO_4$-NaCl in fig. 4-18. The constants were found to be: b = -9,600 cals, 2b' = 2,150 cals.

Activity coefficients calculated by this method for both systems studied have been plotted in figs. 4-14, 4-15. This method is clearly superior to the F.F.G. approach in that it predicts the correct sign of RT ln γ; values are normally within an order of magnitude of the true values. For many metallurgical applications, corrosion problems for example, such a rough fit would be sufficient. Nevertheless the fit is much poorer than that found for the C.I.S. equation; it is better in the $ZnSO_4$-NaCl system and at the extremes of concentration ranges, from where the interaction constants were determined.

Bloom and Welch were able to achieve good agreement with

FIGURE 4-18

EVALUATION OF CONSTANTS FOR THE BLOOM & WELCH EQUATION FOR $ZnSO_4$ - NaCL (863°K)

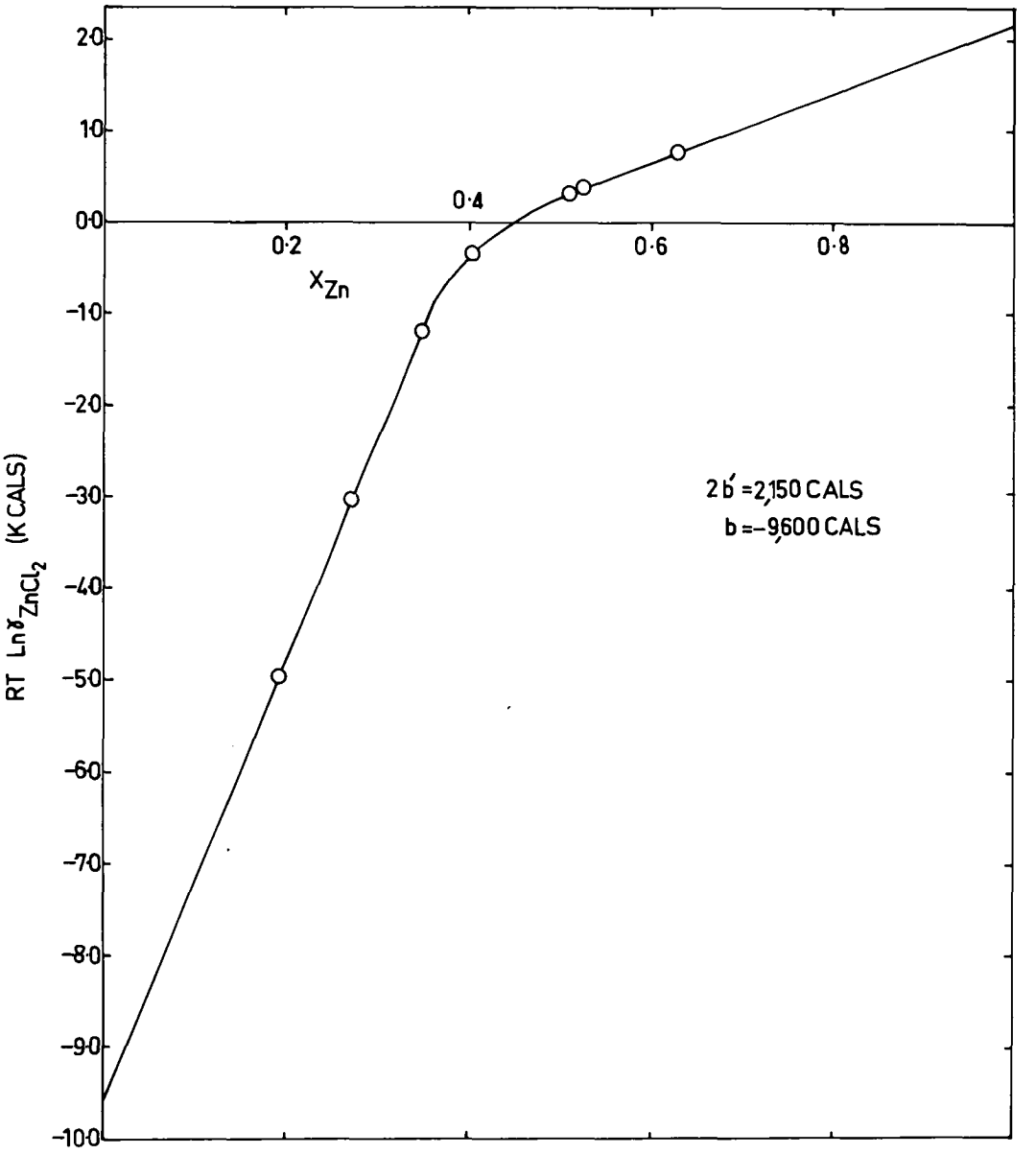

experiment in the systems Pb-Na-Cl-SO_4[20] and Pb-Na-Cl-Br.[209] In both cases, binary interactions are quite small and even the F.F.G. equation gave fairly reasonable results. Hence this method appears best suited to systems which do not deviate too greatly from F.F.G. behaviour. The assumption that cation interactions are unaffected by anion composition, in general, is a poor one.[60] A further disadvantage is that activity measurements are necessary, at least in part, on the ternary system. This approach is useful in one regard. In many systems the information necessary for use of the C.I.S. equation is lacking; a few ternary measurements, followed by a suitable curve fitting procedure may often prove to be the best way of characterising a complicated system.

4.5. $PbCl_2$-K_2SO_4 Reciprocal Salt System

A second sulphate-chloride system was studied for a comparison with the earlier system and as a further test of the C.I.S. equation. Relative sizes of ions in this case are significantly different than in the previous case. The high liquidus temperatures in the K-Zn-Cl-SO_4 system[197] did not permit vapour pressure studies over a reasonable composition range. The lower volatility of $PbCl_2$ permitted activity measurements at higher temperatures with $PbCl_2$-K_2SO_4 and consequently a greater composition range was possible. Furthermore, study of this system allows close comparison with the corresponding Na-Pb-Cl-SO_4 system investigated by Bloom and Welch.[20] In that system activities were all greater than ideal.

Unlike the previous system, significant amounts of vapour phase compounds were transpired with $PbCl_2$. Bloom and Hastie have made vapour pressure[71] and mass spectrometric[31] investigations of the $PbCl_2$-KCl system and found only one complex, $KPbCl_3$, in the vapour. Corrections were made to observed vapour pressures of $PbCl_2$ by subtracting the amount of $KPbCl_3$ from the total amount of $PbCl_2$ transpired. This quantity varied with composition and, as would be expected, exhibited a maximum at about 0.5 mole fraction. At this maximum, $KPbCl_3$ constituted about 9% of the total $PbCl_2$ transpired. In the system $PbCl_2$-KCl (930°K), Bloom and Hastie[71] found somewhat similar quantities of this compound in the vapour. Deviations from ideality in this system were found to be much greater than the corrections applied to activities.

Six determinations of $PbCl_2$ activity at 1012°K and different compositions were made. The results are given in table 4-12. Activities of $PbCl_2$ in this system are less than ideal at all compositions. To determine the effect of temperature, a set of three measurements were made over a range of 100°C on a mixture of 66 mole % $PbCl_2$. The following partial molar quantities have been determined for $PbCl_2$:

$\Delta\bar{H}$ = 1020 cals/mole

$T\Delta\bar{S}$ = 3800 cals/mole, $\Delta\bar{S}$ = 3.76 cals/mole deg.

$\Delta\bar{G}$ = -2800 cals/mole

$T\Delta\bar{S}^E$ = 1586 cals/mole, $\Delta\bar{S}^E$ = 1.57 cals/mole deg.

$\Delta\bar{G}^E$ = -566 cals/mole

It was found that $\Delta\bar{H}_{PbCl_2}$ is slightly positive, much less so than in the corresponding zinc-sodium reciprocal mixture at this composition. Any endothermic mixing cannot arise from interactions present in the $PbCl_2$-KCl binary: Barton,[170] and Markov et al,[204] have found negative values of $\Delta\bar{H}_{PbCl_2}$ from activity measurements at various temperatures. McCarty and Kleppa[265] have carried out a calorimetric study on the $PbCl_2$-KCl system and found $\Delta\bar{H}_{PbCl_2}$ negative at all compositions. Therefore, other interactions present in the ternary system would be responsible for the positive value of $\Delta\bar{H}_{PbCl_2}$. The sign and magnitude of $\Delta\bar{S}^E_{PbCl_2}$ are of the same order as that determined by McCarty and Kleppa[65] in the KCl-$PbCl_2$ binary, +0.6 cal/mole deg. at 0.5 mole fraction.

TABLE 4-12

Experimental Activities in the System $PbCl_2$-K_2SO_4

Composition mole fn $PbCl_2$	Temperature ^oK	P_{PbCl_2} (mm.) $KPbCl_3$ corrected	$P^o_{PbCl_2}$ (mm.)	%$KPbCl_3$ in vapour	Activity $PbCl_2$	Temkin Activity
0.880	1011.5	31.84	49.20	2.1	0.647	0.689
0.758	1011.7	19.15	49.35	3.8	0.390	0.390
0.660	1012.0	11.62	49.55	6.3	0.236	0.236
0.660	963.5	5.21	21.43	6.0	0.243	0.236
0.660	1053.8	22.02	95.06	6.8	0.232	0.236
0.590	1011.8	7.468	49.39	7.0	0.151	0.151
0.520	1011.6	4.813	49.26	9.6	0.098	0.098
0.340	1011.8	1.352	49.37	9.0	0.027	0.027

Activity coefficients have been calculated for this system and plotted as RT ln γ_{PbCl_2} against $(X'_K)^2$ in fig. 4-19; also see table 4-13. Predicted values are also plotted for the F.F.G. and C.I.S. equations for which the necessary data is:

$$\Delta G^{o}_{(equiv)} = +3416 \text{ cals}$$

$$\lambda_{12,(Pb\text{-}Na)Cl} = -5400 \text{ cals}$$

$$\lambda_{13,K(Cl\text{-}SO_4)} = 200 \text{ cals}$$

$$\lambda_{24,Pb(Cl\text{-}SO_4)} = 220 \text{ cals}$$

$$\lambda_{34,(Na\text{-}Pb)SO_4} = -5400 \leq \lambda_{34} < 0 \text{ cals}$$

Again, ternary excess energies are quite small and the F.F.G.+ Førland equation is almost identical to the C.I.S. equation. At the $X'_{Pb} = 0.5$ point, a comparison of ternary excess energies has been made:

Comparison of Ternary Excess Energies $PbCl_2$-K_2SO_4, (1012°K)

Experimental RT ln γ_{PbCl_2}	C.I.S. RT ln γ - 3° excess	Experimental 3° excess	C.I.S. 3° excess
-1080	-882	-198	-59

Experimental and C.I.S. ternary excess energies may be said to be in agreement; the difference may be ascribed mostly to accumulated scatter in the tabulated data used in the exchange free energy calculation. When the calculated C.I.S. values are plotted for the entire composition range, quite good agreement with experiment is obtained. Once again the F.F.G. equation gives a poor picture of this system. Activities of $PbCl_2$ have been calculated from C.I.S. activity coefficients and compared with experiment in table 4-14 and in fig. 4-20. ($\lambda_{34} = -4000$ cals)

TABLE 4-13

Comparison of Experimental and Theoretical Values of RT ln γ_{PbCl_2} in the System $PbCl_2$-K_2SO_4, (1012°K)

X'_{Pb}	$(X'_K)^2$	RT ln γ_{PbCl_2} (cals)					
		Exptl.	F.F.G.	F.F.G. + Førland λ_{34} = -4,000	C.I.S. λ_{34} = 0	C.I.S. λ_{34} = -4,000	C.I.S. λ_{34} = -5,000
0.9	0.01	-50	68	-57	-115	-51	-30
0.8	0.04	-220	273	-207	-387	-195	-130
0.7	0.09	-480	615	-421	-699	-411	-315
0.6	0.16	-800	1093	-652	-927	-671	-590
0.5	0.25	-1080	1708	-882	-941	-941	-941
0.4	0.36	-1240	2460	-1071	-607	-1183	-1396
0.3	0.49	-1350	3348	-1184	+223	-1346	-1905

FIGURE 4--19

$RT \ln \gamma_{PbCl_2}$ in $PbCl_2$-Na_2SO_4, 1012°K

Legend

- - - - - - - - -	Experimental
———————	C.I.S. with λ_{34}(cals)
1	0
2	-4,000
3	-5,400
——— — ———4	F.F.G.

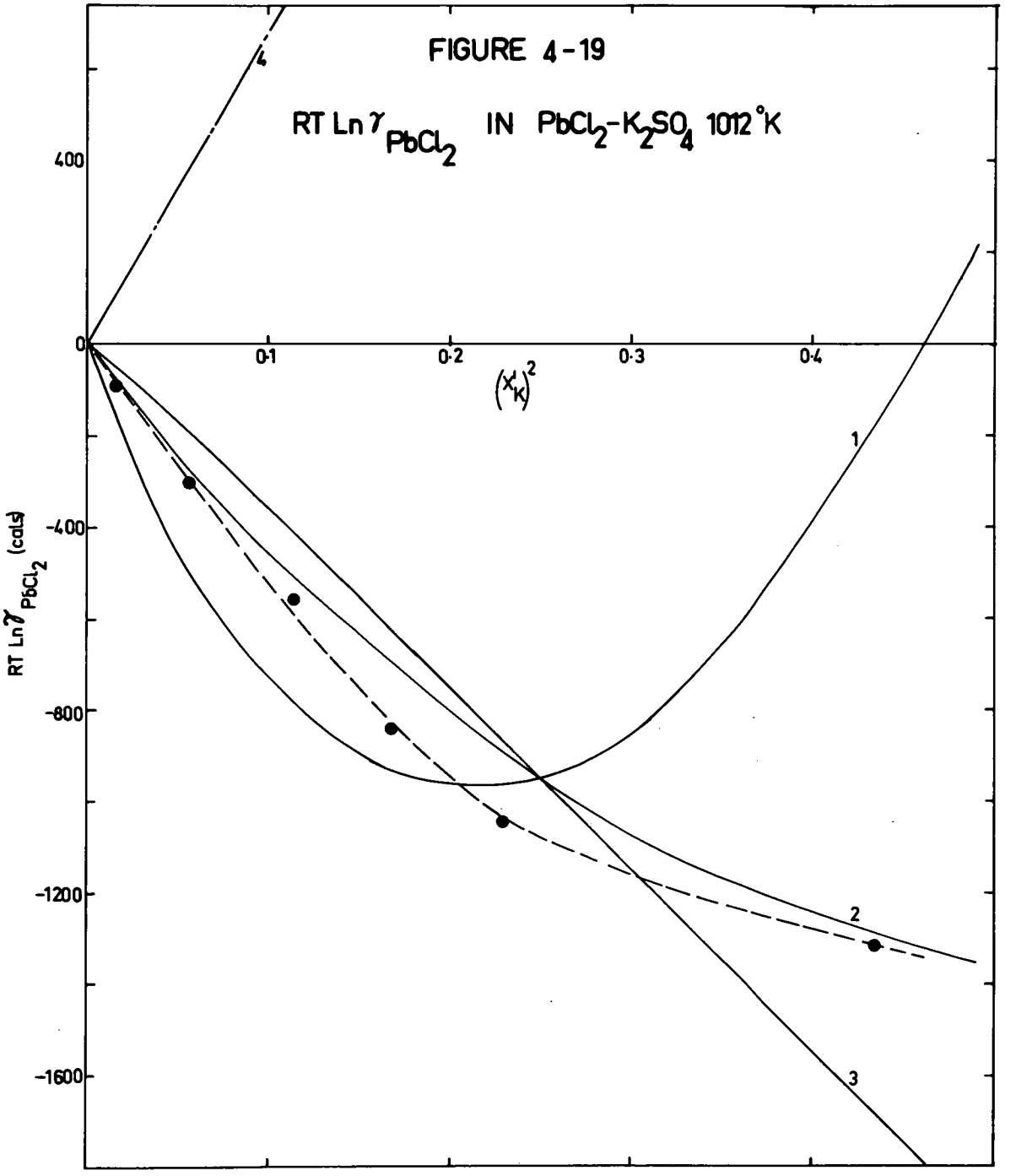
FIGURE 4-19
RT Ln γ PbCl2 IN PbCl2-K2SO4 1012°K
400
0
-400
-800
-1200
-1600
0·1
0·2
0·3
0·4
(X'K)2
RT Ln γ PbCl2 (cals)
1
2
3
4

TABLE 4-14

Comparison of Experimental and Calculated C.I.S. Activities in the System $PbCl_2$-K_2SO_4, (1012°K)

Composition	Activity of $PbCl_2$		
mole fn $PbCl_2$	Exptl.	C.I.S.	Temkin
0.9	0.670	0.715	0.733
0.8	0.435	0.507	0.527
0.7	0.280	0.298	0.366
0.6	0.160	0.173	0.241
0.5	0.086	0.093	0.148
0.4	0.043	0.045	0.082
0.3	0.019	0.019	0.038

FIGURE 4-20

ACTIVITIES OF $PbCl_2$ IN $PbCl_2$-K_2SO_4. 1012°K

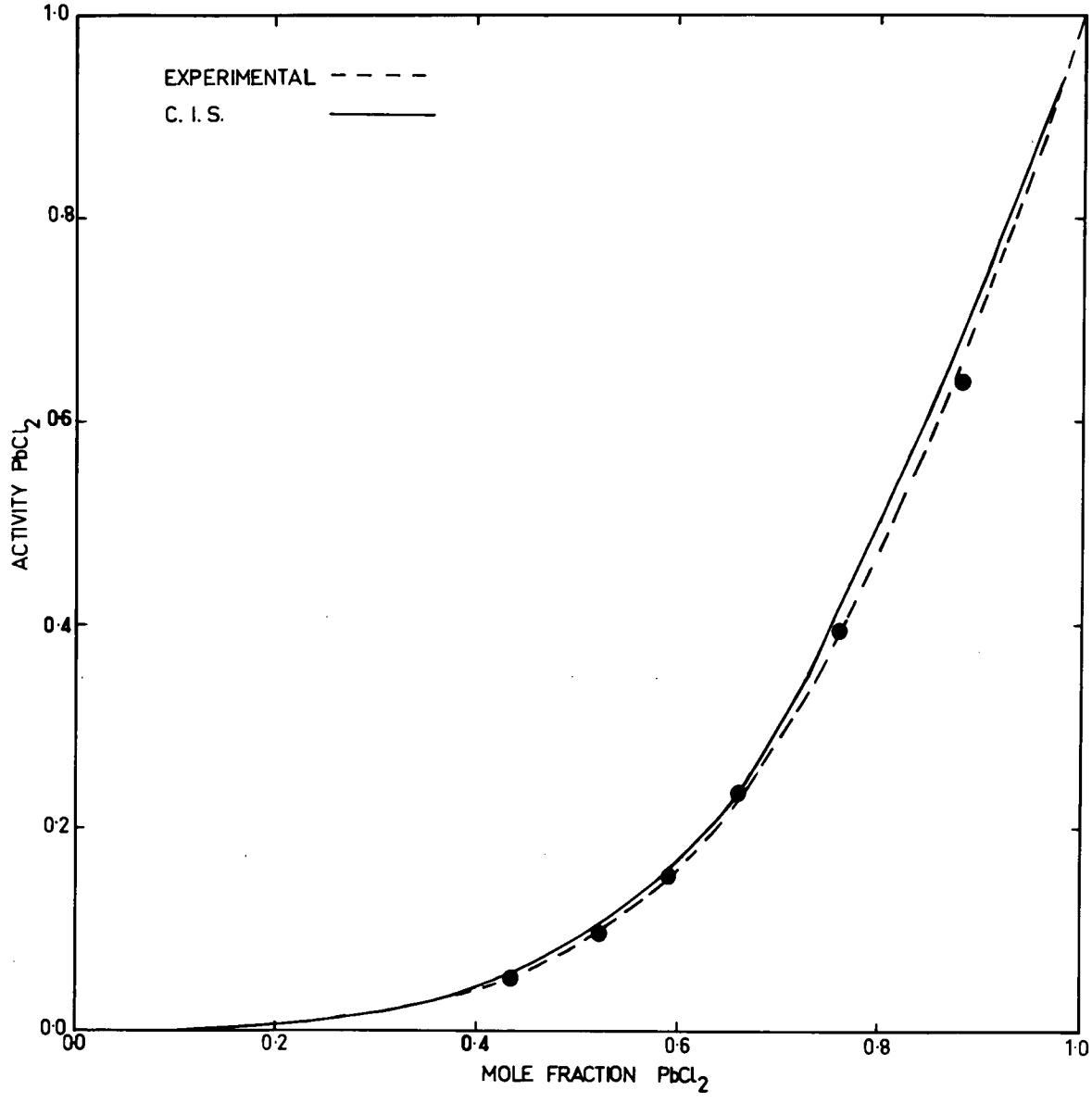

4.6. $PbCl_2$-Na_2SO_4 Reciprocal Salt System

It is interesting to compare these results with those obtained by Bloom and Welch for the $PbCl_2$-Na_2SO_4 system. Binary[20,21] interactions are relatively small in this reciprocal and the exchange free energy predominates. Hence, ternary excess energies become more significant. Unlike the previous systems, measured activities are greater than ideal.

The necessary information used is:

$$\Delta G^{o}_{(equiv)} = +3542 \text{ cals}$$

$$\lambda_{12,(Na\text{-}Pb)Cl} = -900 \text{ cals}$$

$$\lambda_{13,Na(Cl\text{-}SO_4)} = 0 \text{ cals}$$

$$\lambda_{24,Pb(Cl\text{-}SO_4)} = +220 \text{ cals}$$

$$\lambda_{34,(Na\text{-}Pb)SO_4} = -500 \text{ cals}$$

At the $X'_{Na} = 0.5$ point comparison of ternary excess energies is possible.

Comparison of Ternary Excess Energies $PbCl_2$-Na_2SO_4, (1000°K)

Experimental RT ln γ_{PbCl_2}	C.I.S. RT ln γ - 3° excess	Experimental 3° excess	C.I.S. 3° excess
1330	1431	-101	-66

The agreement is reasonable. Calculated values of RT ln γ_{PbCl_2} are compared with experimental results in table 4-15 and figure 4-21. In this system where activity coefficients are greater than one, the C.I.S. equation again best fits the data. The "S" shape in the experimental curve is not as marked in the C.I.S. curve. As any "S" shape in the C.I.S. curve is largely a result

TABLE 4-15

Comparison of Experimental and Theoretical Values of RT ln γ_{PbCl_2} in the System $PbCl_2$-Na_2SO_4, (1000°K.)

(Experimental activities taken from Welch)

X'_{Pb}	$(X'_{Na})^2$	RT ln γ_{PbCl_2} (cals)				
		Exptl.	F.F.G.	F.F.G. + Førland	C.I.S. $\Lambda = \frac{(\Delta G^o_{equiv})^2}{2ZRT}$	C.I.S. $\Lambda = \frac{(\Delta G^o_{mole})^2}{2ZRT}$
0.9	0.01	160	71	54	61	81
0.8	0.04	450	283	220	232	272
0.7	0.09	705	638	502	509	529
0.6	0.16	996	1133	872	852	791
0.5	0.25	1300	1771	1431	1365	1168
0.4	0.36	1700	2550	2087	1965	1601
0.3	0.49	2392	3471	2875	2705	2203
0.2	0.64	3360	4534	3802	3612	3046

FIGURE 4-21

$RT\,Ln\,\gamma_{PbCl_2}$ IN $PbCl_2$–Na_2SO_4, 1000°K

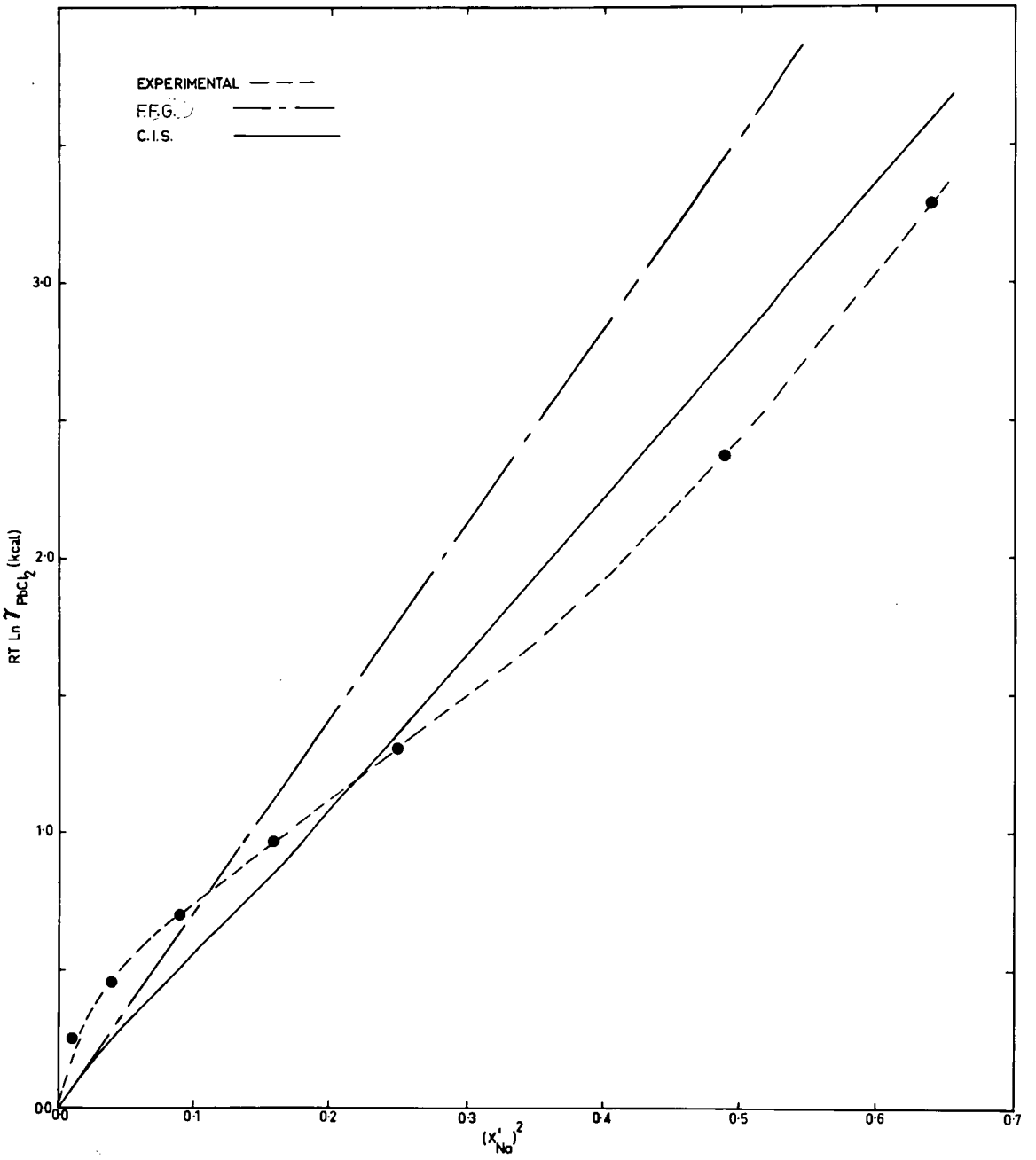

of the ternary excess energy term;[115] this could indicate that a larger value of Λ should be used. In table 4-15, values of RT ln γ_{PbCl_2} have also been calculated using the molar rather than the equivalent exchange free energy in equation (IV-41), i.e.

$$\Lambda = - \frac{(\Delta G^{o}_{mole})^2}{2ZRT} \qquad \text{(IV-56)}$$

The effect is to increase contribution of the ternary excess term to RT ln γ_{PbCl_2}. In table 4-15 it is evident that use of either molar or equivalent exchange free energies results in an equally good fit to the data. C.I.S. activities have been calculated, using equation (IV-41) rather than (IV-56) for Λ, and compared with experiment in figure 4-22. In table 4-16, C.I.S. activities are given using both equations for Λ. The two sets of results seem to fit the data equally well. Activities given by Welch,[21] using the Bloom and Welch equation are also given. His calculated values best fit the experimental data. However, it must be remembered that with the method, binary interaction parameters have been determined from the actual reciprocal system. Moreover, the system studied is quite a simple one.

TABLE 4-16

Comparison of Experimental and Calculated C.I.S. Activities in the System $PbCl_2$-Na_2SO_4 at 1000°K

(Experimental data taken from Welch[21])

Composition	Activity of $PbCl_2$				
mole fn $PbCl_2$	Exptl.	Bloom and Welch[21]	C.I.S. $\Lambda = -\frac{(\Delta G^{o}_{equiv})^2}{2ZRT}$	C.I.S. $\Lambda = -\frac{(\Delta G^{o}_{mole})^2}{2ZRT}$	Temkin
0.9	0.830	0.803	0.756	0.764	0.733
0.8	0.668		0.591	0.604	0.527
0.7	0.522	0.495	0.473	0.478	0.366
0.6	0.392		0.370	0.359	0.241
0.5	0.285	0.285	0.294	0.266	0.148
0.4	0.198		0.220	0.183	0.082
0.3	0.125	0.125	0.146	0.114	0.038
0.2	0.067		0.076	0.057	0.012

FIGURE 4-22

ACTIVITIES OF $PbCl_2$ IN $PbCl_2$-Na_2SO_4 1000°K

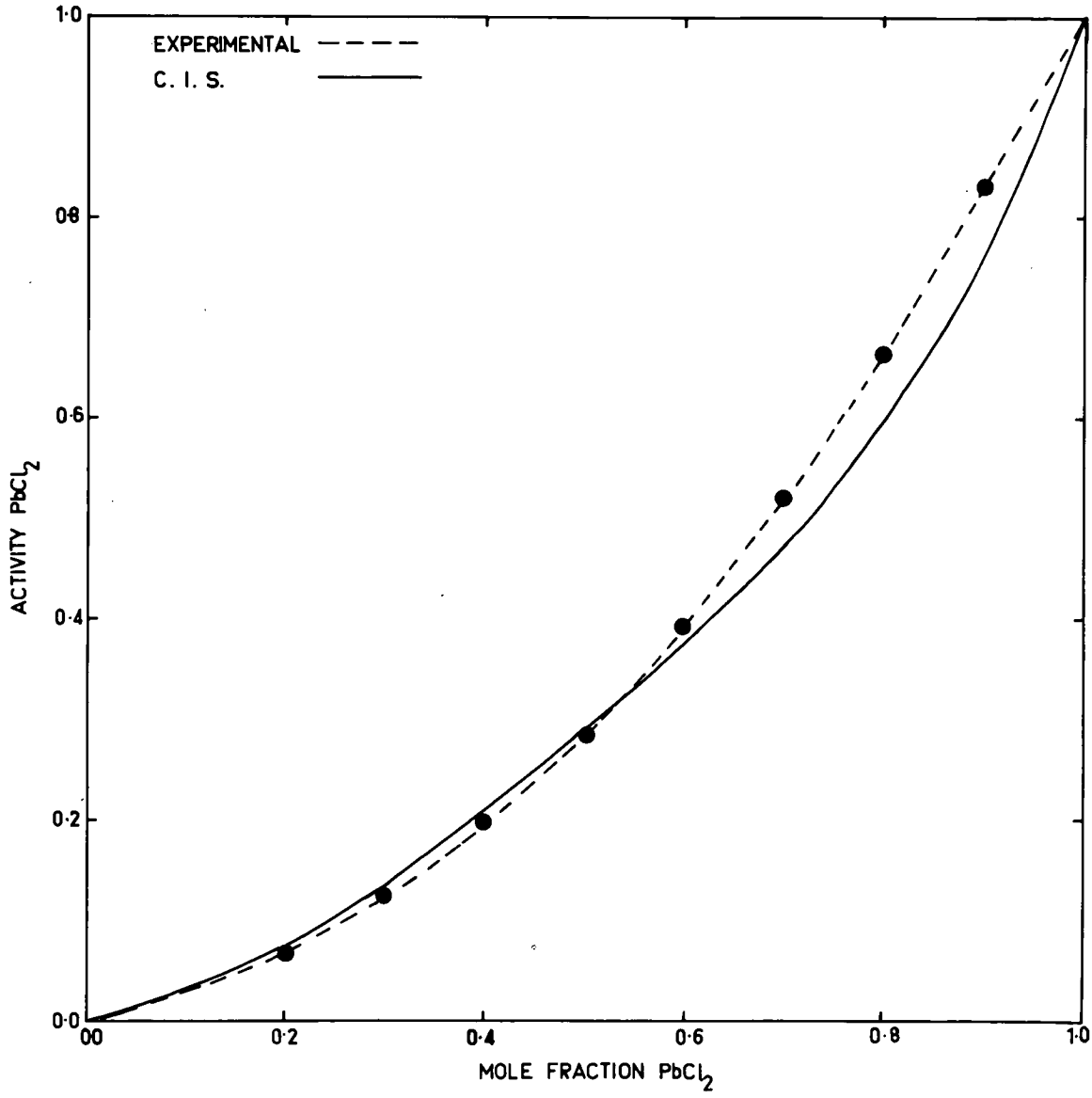

4.7. Discussion

4.7.1. Ternary Excess Energies

It is interesting to compare the results observed here with trends in ternary excess heats of mixing obtained by Kleppa and coworkers[210-213,198] in a number of reciprocal salt systems. Using a thermodynamic unmixing cycle, Toguri and Kleppa[210] obtained an expression for heats of mixing in a ternary system made by AC, BD, AD.

$$\Delta H^{E}_{(equiv)} = X'_B X'_C \Delta H^{o}_{(equiv)} + X'_A \Delta H_{A(C-D)(equiv)}$$

$$+ X'_B \Delta H_{B(C-D)(equiv)} + X'_C \Delta H_{(A-B)C(equiv)}$$

$$+ X'_D \Delta H_{(A-B)D} + \Delta H^{E}_{XS(equiv)} \qquad \text{(IV-57)}$$

The last term is the ternary excess enthalpy. Where univalent salts are considered, X'_i reduces to X_i. This equation then differs from Blander's C.I.S. expression[114,210] for reciprocal heats of mixing, only in that Blander's predicts that ΔH^{E}_{XS} is given by: $X_A X_B X_C X_D (\Delta H^{o})^2/ZRT$.

In charge symmetrical mixtures of similar size ions, ΔH^{o} and ΔH^{E}_{XS} are usually small. In systems such as Na-K-Cl-Br,[210] ternary excess energies were well predicted by Blander's equation. However, in systems of larger ΔH^{o},[212] Blander's equation was not followed and a closer fit was obtained with an expression derived from the quasi-chemical theory:[45]

$$\frac{(X_A X_D + Y)\ (X_B X_C + Y)}{(X_A X_C - Y)\ (X_B X_D - Y)} = \exp\left(\frac{\Delta H^{o}}{ZRT}\right)$$

$$\Delta H^{E}_{XS} = Y \Delta H^{o} \qquad \text{(IV-58)}$$

where Y is the quasi-chemical non-randomness parameter defined previously in equation (11-38). In the systems studied in this work, $\Delta H^{o}_{(equiv)}$ and $\Delta G^{o}_{(equiv)}$ were less than ZRT. Therefore on this account, it is not surprising that Blander's expression fits observed ternary excess energies.

In systems with large differences in ionic sizes,[211,213] e.g. Li-Cs-Cl-Br, ΔH^{E}_{XS} was found to depend upon relative ion sizes rather than on ΔH^{o}. A linear relationship was found between deviations in $\Delta H^{E}_{XS}/Y$ and a reciprocal salt size parameter.

$$\delta_r = (d_1-d_4)\ (d_1-d_3)\ (d_1+d_2)/d_1d_2d_3d_4 \qquad \text{(IV-58)}$$

For the system studied in the work, δ_r values have been calculated using $d_1 = d_{M^+} - Cl^-$; $d_2 = d_{A^{2+}} - SO_4^{2-}$,

$d_3 = d_{M^+} - SO_4^{2-}$, $d_4 = d_{A^{2+}} - Cl^-$

δ_r (Zn-Na-Cl-SO_4) = -9.6×10^{-3} $(\text{Å})^{-1}$

δ_r (Pb-K-Cl-SO_4) = -3.5×10^{-3} $(\text{Å})^{-1}$

δ_r (Pb-Na-Cl-SO_4) = $+8.42 \times 10^{-3}$ $(\text{Å})^{-1}$

These values of δ_r are relatively large on the scale given by Kleppa et al.[212,213] However, differences in ion sizes did not seem to make noticeable contributions to ternary excess free energies.

In charge unsymmetrical systems Cd-Ag-Cl-NO_3, Cd-Tl-Cl-NO_3, Meschel and Kleppa[198] observed two types of behaviour. In the first system the exchange enthalpy predominates over the binary terms; ternary excess enthalpies are in agreement with quasi-

chemical theory predictions. In the second system, the exchange enthalpy is quite small and one of the binaries (Cd-Tl)Cl is associated with quite large negative enthalpies of mixing with a tendency towards complex ion formation. Experimental values of $\Delta H^{E}_{XS}/Y$ are much more negative than predicted, becoming less negative with increasing values of X'_{Cd}. This behaviour is ascribed to perturbation of the strongly interacting binary by the ternary medium. This "medium effect" which reflects the stability of groupings $CdCl_4^{2-}$ is highly sensitive to the ratio of X'_{Cl} to X'_{Cd}.

A similar "medium" effect may be present in the Na-Zn-Cl-SO_4 system studied here. The negative deviations from the C.I.S. equations, at high NaCl concentrations in the $ZnSO_4$-NaCl system, may well be due to ternary, rather than binary interactions. In this region, the ratio X'_{Cl}/X'_{Zn} is quite high; gradual formation of complex ions may well bring about a composition dependent contribution to the ternary excess energy.

4.7.2. Conclusions on Salt Roasting

Activities of $ZnCl_2$ in the $ZnSO_4$-NaCl system were largely less than ideal, despite the fact that the exchange free energy favours $ZnCl_2$ formation. These results tend to oppose the argument that salt roasting proceeds via a liquid phase $ZnSO_4$-NaCl exchange reaction. It was found in preliminary studies that $ZnCl_2$ could be volatilised most readily from mixtures of NaCl and oxidised ZnS at temperatures between 900-950°C. Results of Kellogg[214,215]

indicate that while some sulphate should form at these temperatures, ZnO formation becomes more important as temperatures increase; above 1000°C ZnO is the principle oxidation product. The presence of a liquid phase is likely to effect ZnS oxidation somewhat; however, at the relatively low temperature of 810°C, formation of $ZnO.2ZnSO_4$ rather than $ZnSO_4$ appeared to be predominant.

At temperatures in the range 900-1000°C, it seems reasonable that exchange reactions are likely between liquid NaCl and solid ZnO or $ZnO.2ZnSO_4$; the low solubility of ZnO in molten NaCl[58] is likely to inhibit a liquid-liquid exchange reaction. Besides $ZnCl_2$, Na_2O dissolved in the melt is a likely product. Na_2O would presumably tend to take up gaseous SO_2 or SO_3 to form Na_2SO_4. Some oxidation to $ZnSO_4$, followed by dissolution in the melt is likely. Liquid phase interactions between $ZnCl_2$ and Na_2SO_4 would impede the process, reducing the volatility of $ZnCl_2$.

Salt roasting of PbS is more likely to involve oxidation to sulphate followed by liquid-liquid exchange to form $PbCl_2$. When oxidised in the temperature range of interest, PbS mostly forms lead sulphate and a series of lead oxide sulphates, rather than PbO.[216] Reciprocal $PbCl_2$-Na_2SO_4 interactions will favour $PbCl_2$ formation. Experimentally, it was found that $PbCl_2$ could be volatilised from the ore at lower temperatures than $ZnCl_2$.

In conclusion, it would appear that salt roasting of ZnS is likely to involve liquid NaCl-solid ZnO reactions. $ZnCl_2$-Na_2SO_4 reciprocal interactions will be of secondary importance, reducing $ZnCl_2$ volatility.

5. Vapour Phase Studies

5.1. Mass Spectrometry Results

5.1.1. Initial Investigations

The mass spectrometric investigation was carried out firstly to investigate the vapour phase equilibria involved in salt roasting zinc ores. At the same time, it served as a useful check on the vapour composition determined during transpiration experiments. This study is among the first to use commercial quadrupole mass spectrometers for the investigation of high temperature mixed salt vapours. In his study Hastie[155,189] used a specially adapted quadrupole mass spectrometer.

In order to investigate the usefulness of commercial quadrupole instruments for salt vapour studies and to develop suitable techniques, systems were first chosen where trends indicated extensive vapour phase complexing should take place. A series of cation mixtures of the type $PbBr_2$-MBr (M = Na, K, Rb, Cs) and one anion mixture $CdCl_2$-$CdBr_2$, were investigated in this way.

(A) Pure $PbBr_2$

Using 45 ev and 400 μA ionizing conditions, intensities of ions observed for this salt decreased in the order $PbBr^+$, Pb^+, $PbBr_2$ (about 10:4:3); Br^+ was also observed. No ions corresponding to dimer species were observed. The temperature dependence of ion currents has been plotted in fig. 5-1. Least square slopes of $\ln I^+T$ vs $\frac{1}{T}$ yield the following heats of vaporisation:

TABLE 5-1

Ion Current As a Function of Temperature for Pure $PbBr_2$

Temp (^oK)	$10^3/T$ $(^oK)^{-1}$	$IT(PbBr_2^+)$	$IT(PbBr^+)$	$IT(Pb^+)$
		(arbitrary units)		
663.5	1.507	1.261	5.242	1.957
691.5	1.446	2.766	11.62	3.942
716.0	1.396	6.588	28.80	8.234
734.5	1.361	11.20	50.50	15.42

FIGURE 5-1

ION INTENSITIES $PbBr_2$

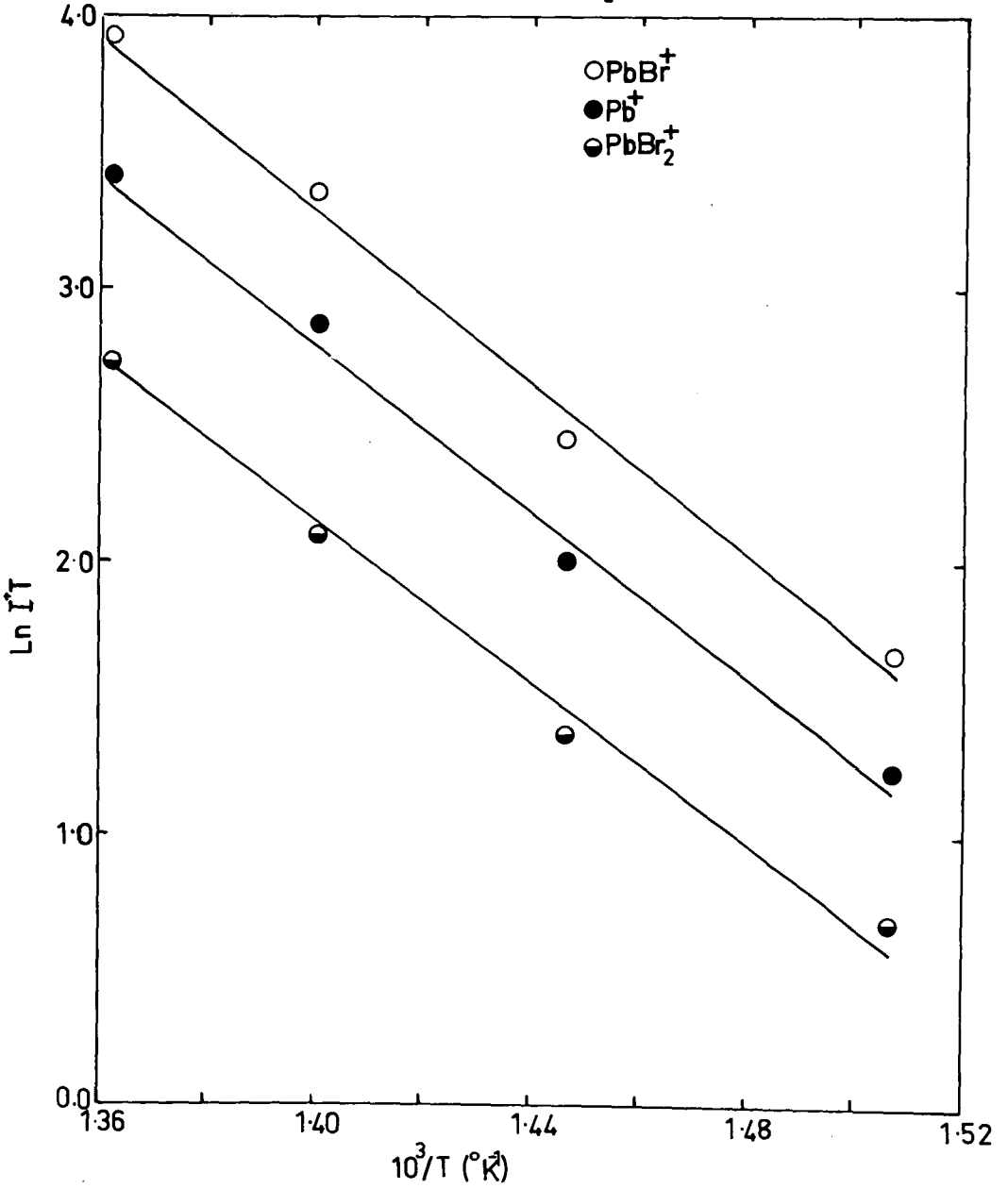

$PbBr_2^+$: 30.2 ± 2.0 kcal/mole

$PbBr^+$: 31.3 ± 2.0 kcal/mole

Pb^+ : 28.0 ± 2.0 kcal/mole

As the temperature dependence of the three ions is the same within experimental error, it is concluded that they all have a common precursor, $PbBr_2$. The value for the heat of vaporisation of $PbBr_2$ is in agreement with that given by Bloom and Hastie[220] of 31.0 kcal/mole.

(B) $PbBr_2$-MBr Mixtures

As expected, quite significant amounts of complex species $MPbBr_3$ were observed above mixtures of $PbBr_2$-MBr, (usually 50 mole %). From NaBr to CsBr, increasingly higher temperatures were necessary to first observe mass spectra of complex species. Ions observed, besides those found with pure lead bromide, were $MPbBr_2^+$, M^+, MBr_2^+, and at higher temperatures lesser amounts of $MPbBr_3^+$ and $MPbBr^+$. Ratios of $I(PbBr^+)$: $I(MPbBr^+)$ were of the order of 20 :1. M^+ was more intense than MBr^+ by a factor of about 100. Ions corresponding to $(MBr)_2$ species were present only at higher temperatures and intensities were weak.

Most species were found as clusters of peaks, owing to different combinations of isotopes of constituent atoms. The assignment of ion peaks of complex species was verified by comparing peak ratios with theoretical values calculated from isotope abundances. From analogy to findings with $PbCl_2$-MCl mixtures,[181] it was assumed that $MPbBr_3^+$, $MPbBr_2^+$, $MPbBr^+$ all had the common precursor $MPbBr_3$ and that all M^+,

MBr^+ were derived from MBr.

Heats of vaporisation for individual species, calculated from the slope of ln I^+T vs $\frac{1}{T}$, frequently differed from published values for pure salts. Changes in melt composition, as the more volatile species vaporised away, may well account for discrepancies in heats of vaporisation. All evidence points to the fact that apart from association reactions, salt vapours at low pressures obey the ideal gas laws. Therefore any composition changes, including those taken during fusion, would effect the relative amounts of monomer species but not the equilibrium constant for the formation of complexes, K_p.

Despite some random error, plots of ln K_r vs $\frac{1}{T}$, where

$$K_r = \frac{IT\ (MPbBr_2^+)}{IT\ (M^+).IT\ (PbBr^+)} \qquad (v\text{-}1)$$

were linear. This would indicate that vapour-liquid equilibrium had been achieved and that a representative sample of salt vapour had entered the ionizer. In the calculation of equilibrium ratios, it was assumed that all M^+ was derived from MBr monomer. In this way, a greater temperature range could be studied in some cases, as M^+ could be observed at a lower temperature than MBr^+. Plots of ln $IT(M^+)$ and ln $IT(MBr^+)$ vs $\frac{1}{T}$ were parallel. The intensity of M^+ was usually much greater than those of $MPbBr_3$ or $(MBr)_2$ peaks. Considering the work of Hastie,[181,155] it is concluded that all M^+ is derived from MBr^+. Therefore, heats of complex formation determined from the temperature dependence of K_r will be valid.

In calculating K_r the current of the most intense peak in an ion cluster was used. These may be summarised as follows:

Ion	m/e (amu)	Major Contributing Species	Precursor
$PbBr^+$	287	$Pb^{208}Br^{79}$, ($Pb^{206}Br^{81}$)	$PbBr_2$
$NaPbBr_2^+$	391	$Na^{23}Pb^{208}Br^{79}Br^{81}$	$NaPbBr_3$
$KPbBr_2^+$	407	$K^{39}Pb^{208}Br^{79}Br^{81}$	$KPbBr_3$
$RbPbBr_2^+$	453	$Rb^{85}Pb^{208}Br^{79}Br^{81}$	$RbPbBr_3$
		($Rb^{87}Pb^{208}Br^{79}Br^{79}$)	
$CsPbBr_2^+$	501	$Cs^{133}Pb^{208}Br^{79}Br^{81}$	$CsPbBr_3$

Heats of formation were derived from least squares analysis of $\ln K_r$ vs $\frac{1}{T}$; algebraic summation of apparent heats of vaporisation yielded the same results for the same set of data. Results are given in tables 5-2 to 5-5 and figs. 5-2, 5-3.

Despite the scatter in the data points, least squares analysis revealed that calculated heats of formation fitted the data to within kcal/mole. Hastie[126] has recently stated that the maximum accuracy which can be expected for heats of formation is ±2 kcal/mole. In the corresponding chloride complex equilibria, Bloom and Hastie quoted the accuracy of second law heats of formation to 6 kcal/mole. Only one of these systems has been done before; Hastie[217] has given a second law value of - 38.0 ± 3.0 kcal/mole for the heat of formation of $KPbBr_3$.

TABLE 5-2

Ion Current As a Function of Temperature For 50 Mole % $PbBr_2$-NaBr

Temp °K	$10^3/T$ $(^oK)^{-1}$	$IT(Na^+)$	$IT(PbBr_2^+)$	$I^-(NaPbBr_2^+)$	$K_r \times 10^5$
		(arbitrary units)			
760	1.316	98.80	600.4	34.96	58.94
776	1.289	186.2	716.2	52.38	39.28
785	1.274	246.5	1,021.0	75.99	32.44
796	1.256	367.5	1,309.0	103.8	21.72
810	1.235	466.9	2,025.0	131.0	13.95
850	1.177	1,122.0	5,865.0	261.8	3.978

$NaCl^+$ was not recorded because of partial overlap with a weak Pb^{2+} peak.

$$\Delta H_f \ NaPbBr_3 = -38.9 \pm 2.0 \text{ kcal/mole.}$$

TABLE 5-3

Ion Current As a Function of Temperature For 50 Mole % $PbBr_2$-KBr

Temp (^oK)	$10^3/T$ $(^oK)^{-1}$	$IT(K^+)$	$IT(KBr^+)$	$IT(PbBr^+)$	$IT(KPbBr_2^+)$	$K_r \times 10^5$
		(arbitrary units)				
788	1.269	33.29	-	46.88	2.088	134.4
799	1.252	64.50	-	67.12	2.956	68.89
808	1.238	82.40	-	77.97	3.798	59.10
818	1.223	106.4	-	86.91	3.971	43.37
828	1.208	121.7	1.000	94.39	4.306	37.83
838	1.193	163.4	1.170	113.4	4.525	27.21
849	1.178	225.8	1.420	127.3	5.230	18.27
862	1.160	339.6	2.043	191.8	6.138	9.432

$$\Delta H_f \ KPbBr_3 = -43.2 \pm 4.0 \text{ kcal/mole}$$

FIGURE 5-2

K_r as a Function of Temperature

For $PbBr_2$-MBr, (M = Na, K)

Legend

● $PbBr_2$-NaBr

○ $PbBr_2$-KBr

FIGURE 5-2

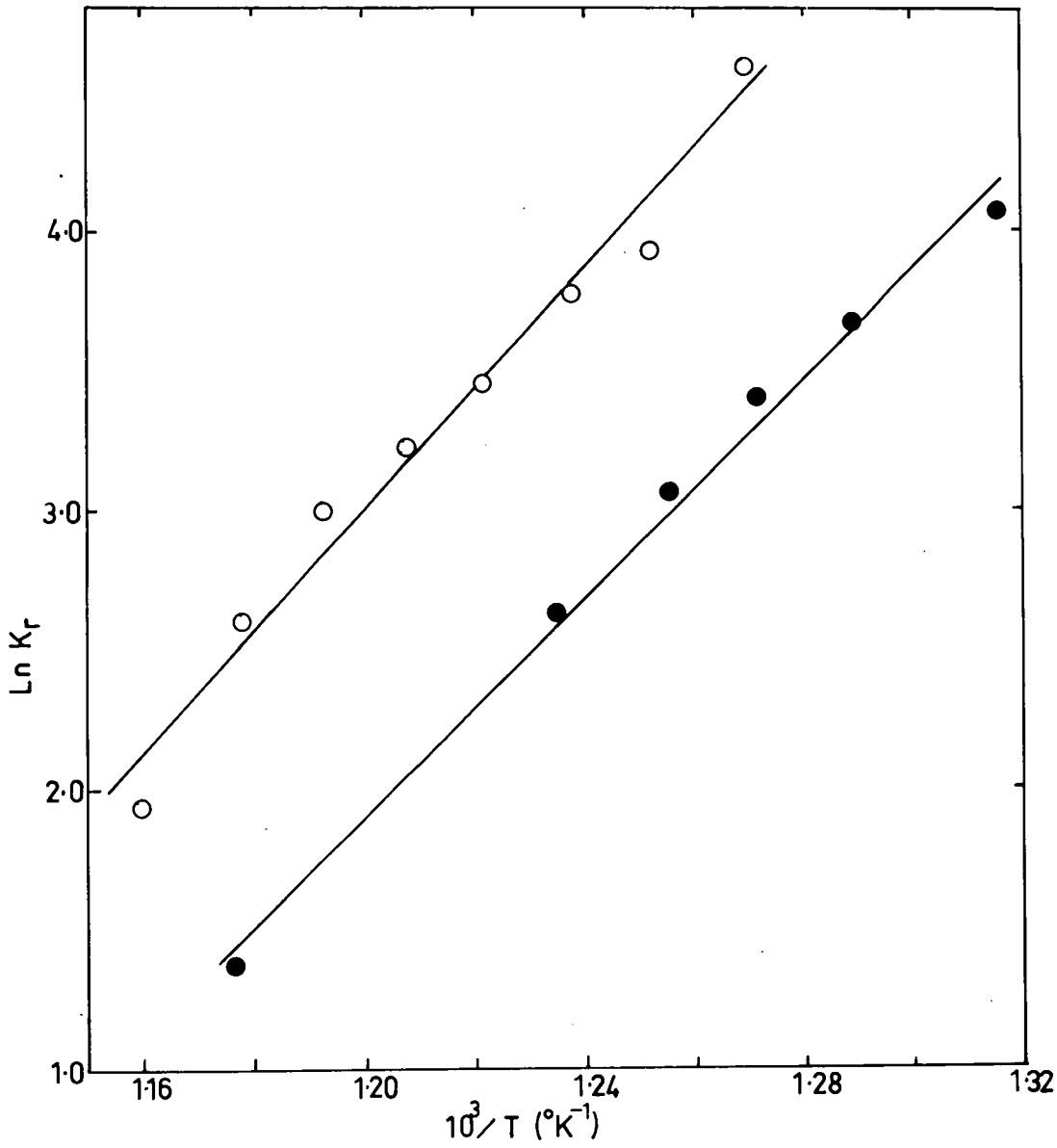

TABLE 5-4

Ion Current As a Function of Temperature For 50 Mole % $PbBr_2$-RbBr

Temp (^oK)	$10^3/T$ $(^oK)^{-1}$	$IT(Rb^+)$	$IT(RbBr^+)$	$IT(PbBr^+)$	$IT(RbPbBr_2^+)$	$K_r \times 10^4$
		(arbitrary units)				
780	1.282	5.226	0.0749	93.60	7.098	145.1
794	1.259	9.369	0.145	115.1	12.23	113.4
815	1.227	18.50	0.273	149.1	26.08	95.55
824	1.214	25.87	0.326	185.4	28.84	60.13
833	1.201	30.82	0.412	249.1	31.15	40.57
844	1.85	39.67	0.566	329.2	36.33	27.53
855	1.170	46.17	0.637	384.8	37.45	21.08
873	1.146	73.33	0.889	497.6	41.73	11.44
891	1.122	95.60	1.250	570.0	41.88	7.686

ΔH_f $RbPbBr_3$ = 41.3 ± 2.0 kcal/mole.

TABLE 5-5

Ion Current As a Function of Temperature For $PbBr_2$-CsBr

(1)60 mole % $PbBr_2$

Temp (°K)	$10^3/T$ $(°K)^{-1}$	$IT(Cs^+)$	$IT(CsBr^+)$	$IT(PbBr^+)$	$IT(CsPbBr_2^+)$	$K_r \times 10^6$
		(arbitrary units)				
812	1.232	266.3	6.171	122.6	3.573	1094.0
820	1.220	304.2	9.020	173.0	5.904	1122.0
829	1.206	464.2	10.36	190.7	6.300	711.7
848	1.180	699.9	13.99	267.1	7.869	439.8
864	1.157	985.0	20.30	414.7	10.54	258.8
873	1.146	1142.0	23.57	436.5	11.86	248.8
886	1.129	1533.0	31.90	584.8	11.96	133.4

$\Delta H_f CsPbBr_3$ = 40.8 ± 2 kcal/mole

(2)50 mole % $PbBr_2$

794	1.259	294.0	-	62.65	1.270	68.95
805	1.242	355.8	-	67.62	1.691	70.28
823	1.215	679.0	-	168.7	3.045	26.58
836	1.196	873.6	-	209.0	4.932	26.99
862	1.160	1513.0	-	364.6	7.930	13.83
876	1.142	2165.0	-	556.5	8.619	7.154

$\Delta H_f CsPbBr_3$ = 37.8 ± 4.0 kcal/mole

FIGURE 5-3

K_r as a Function of Temperature

For $PbBr_2$-MBr, (M = Rb, Cs)

Legend

○ $PbBr_2$-RbBr

● $PbBr_2$-CsBr, (50 mole% $PbBr_2$)

◒ $PbBr_2$-CsBr, (60 mole% $PbBr_2$)

FIGURE 5-3

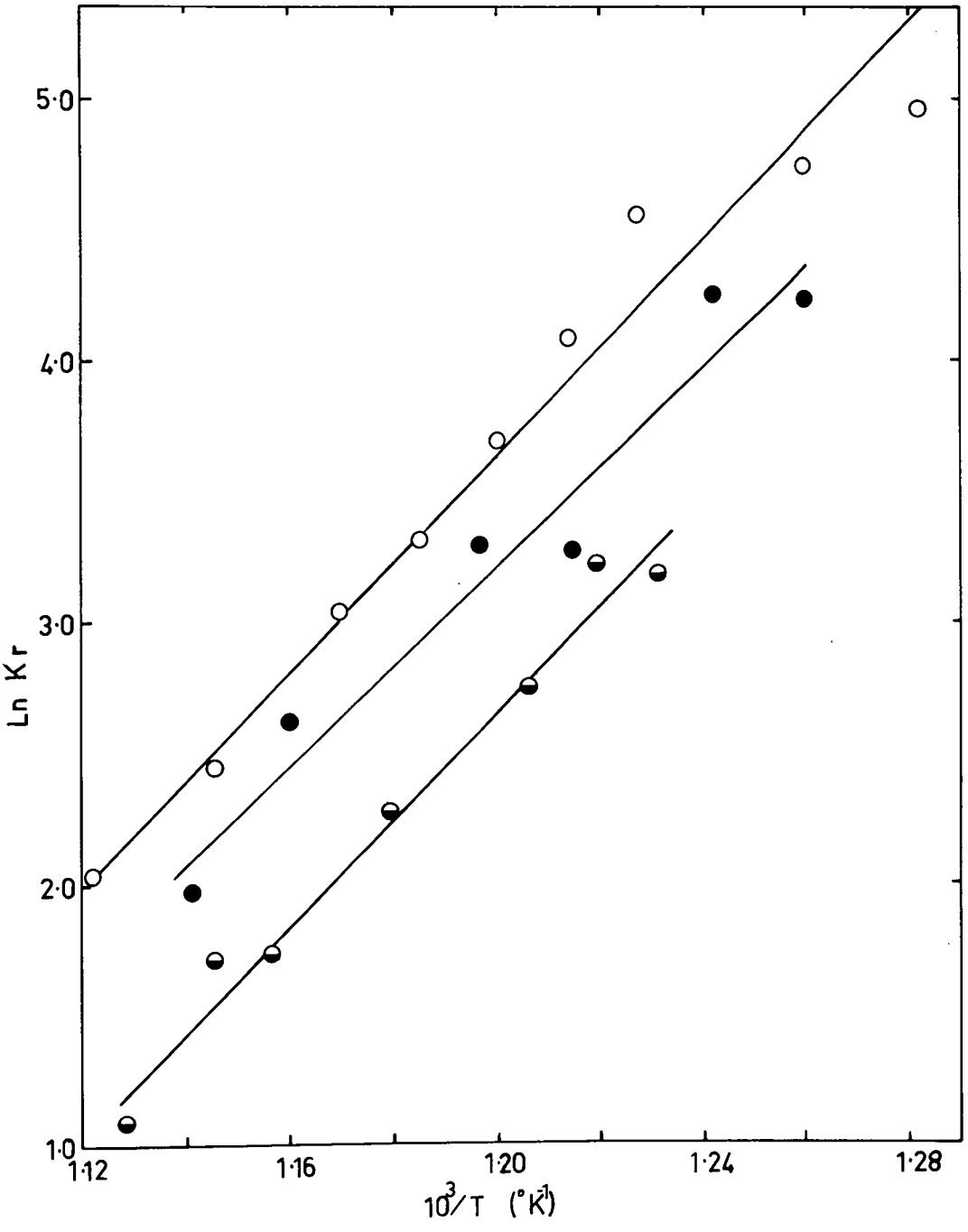

For a related set of systems like this, little significance should be placed upon small variations in K_r from system to system. These values vary as much upon mass discrimination as upon properties of the system.

(C) $\underline{CdCl_2\text{-}CdBr_2}$

Greiner and Jellinek[218] have studied the molten system $CdCl_2$-$CdBr_2$ using a transpiration vapour pressure technique. High apparent activities of $CdCl_2$ indicated possible vapour phase complexing which they ascribed to $CdCl_2.CdBr_2$ formation. However, in the comparable chromium II systems,[219] and lead[220], CrClBr and PbClBr are present and it is likely that a similar cadmium complex is formed. A mass spectrometric investigation has been carried out to determine vapour phase species. Unlike previous systems, the components in this experiment were solid throughout the entire range of temperatures used.

Ions were observed in the following order of decreasing intensity : $CdBr_2^+ > CdClBr^+ > CdBr^+ > CdCl_2^+ > CdCl^+ > Cd^+$, (about 140:60:40:5:4:1 at 750°K). The assignment of peaks to ions was verified by comparing peak ratios. The following ion-precursor relationships are assumed to apply : $CdClBr^+ \}CdClBr$, $CdBr_2^+ \}CdBr_2$, $CdCl_2^+ \}CdCl_2$; Cd^+, $CdCl^+$, $CdBr^+$ could presumably be derived from more than one parent ion. At the temperatures used, no peaks corresponding to any other complex species or to dimers were found.

The heat of formation of CdClBr was determined from the temperature dependence of ion currents in the range 720-771°K;

table 5-6, fig. 5-5. The most intense peak in an ion cluster was considered i.e.:

Ion	m/e (amu)	Major Contributing Species	Precursor
$CdBr_2^+$	274	$Cd^{114}Br^{79}Br^{81}(Cd^{112}Br^{81}Br^{81})$	$CdBr_2$
$CdClBr^+$	228	$Cd^{114}Cl^{35}Br^{79}(Cd^{112}Cl^{35}Br^{81})$	CdClBr
$CdCl_2$	184	$Cl^{114}Cl^{35}Cl^{35}(Cd^{112}Cl^{35}Cl^{37})$	$CdCl_2$

In this experiment reasonable heats of sublimation of $CdBr_2$ and $CdCl_2$ were obtained:

Vapour Species	ΔH_{sub}(kcal/mole)	
	Experimental	Value at m.p.[120]
$CdBr_2$	32.0 ± 2.0	33.5 ± 2.0
$CdCl_2$	41.2 ± 4.0	38.9 ± 2.0
CdClBr	37.0 ± 3.5	-

In this experiment compositions would be more uniform than in earlier work, because vapour losses of $CdCl_2$ and $CdBr_2$ would be similar. This tends to confirm the belief that in PbBr-MBr systems, changes in composition were responsible for the errors in calculated heats of vaporisation. The heat of formation of two moles of CdClBr is given:

$$\Delta H_f(CdClBr) = 2\Delta H_{sub}(CdClBr) - \Delta H_{sub}(CdCl_2) - \Delta H_{sub}(CdBr_2)$$
$$= 0.8 \text{ kcal/2moles.}$$

Least squares analysis of the dependence of $\ln K_r$ upon $\frac{1}{T}$ where

$$K_r = \frac{(IT(CdClBr^+))^2}{IT(CdCl_2^+).\ IT(CdBr_2^+)} \qquad (v\text{-}2)$$

yielded the same value. This figure may be compared with values of ΔH_f of 0 kcal/mole for CrClBr[219] and 1 kcal/mole for PbClBr.[220]

(D) Conclusions To Preliminary Study

From these preliminary studies it was found that a representative sample of salt vapour was reaching the ionizer; vapour-liquid equilibrium and Knudsen flow conditions were being achieved. No sign of second order ion-molecule reactions was evident. Therefore, having developed a suitable technique, it is now feasible to examine the $ZnCl_2$ mixtures of interest.

5.1.2. $ZnCl_2$-MCl Mixtures

With pure $ZnCl_2$ ions observed in order of decreasing intensity at 670°K were $ZnCl_2^+ > Zn^+ > ZnCl^+ > Zn_2Cl_3^+$ (200 - 90 - 40 - 1) Small signals corresponding to doubly charged ions, e.g. $ZnCl^{++}$ were observed in some runs. From analogy with the corresponding lead systems, the following ion-precursor relationships are assumed to apply:

$$ZnCl_2^+,\ ZnCl^+,\ Zn^+\} ZnCl_2;\quad Zn_2Cl_3^+\} Zn_2Cl_4.$$

Relative amounts of dimer and monomer, and ratios of various fragments found are in agreement with the previous qualitative mass spectrometric studies on zinc chloride by Keneshea and Cubicciotti,[149a] and Rice and Gregory.[150]

Mass spectra of vapours above $ZnCl_2$-MCl mixtures, (40 mole % $ZnCl_2$,

TABLE 5-6

Ion Currents as a Function of Temperature in the System $CdCl_2$-$CdBr_2$

Temp (°K)	$10^3/T$ $(°K)^{-1}$	IT($CdBr_2^+$)	IT($CdCl_2^+$)	IT($CdClBr^+$)	K_r x 10
		(arbitrary units)			
721	1.387	42.18	6.994	13.34	6.032
731	1.368	59.94	13.52	22.30	6.136
738	1.355	75.28	19.19	29.89	6.184
750	1.333	103.5	28.75	44.63	6.752
759	1.318	123.3	34.76	51.61	6.215
771	1.297	190.4	49.04	76.18	6.213

$\Delta H_f CdClBr = 0.4 \pm 2.0$ kcal/mole

FIGURE 5-4

Ion Intensities as a Function

of Temperature For $CdCl_2$-$CdBr_2$

Legend

● : $CdBr_2^+$

◒ : $CdClBr^+$

○ : $CdCl_2^+$

◓ : K_r

FIGURE 5-4

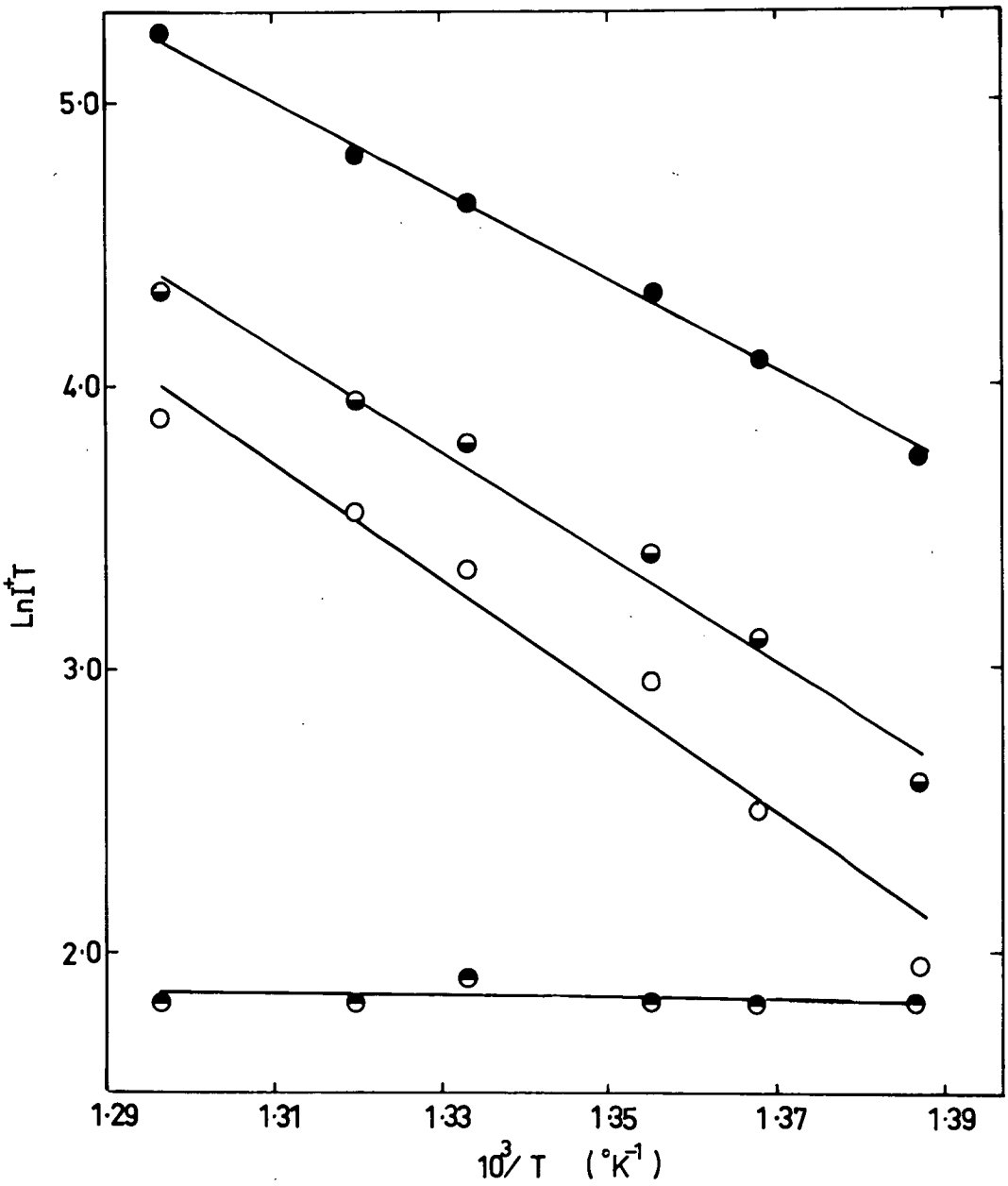

M = Na, K, Rb, Cs) at 820°K all contained ions found with zinc chloride, as well as peaks corresponding to $MZnCl_2^+$. It is assumed that these ions have $MZnCl_3$ as precursors. Parent ions, e.g. $NaZnCl_3$, were observed in some cases. Ratios of $I(ZnCl_2^+):I(M^+):I(MZnCl_2^+)$ were of the order of 1,000: 200 - 100 :1. No other complex species were detected, even when quite high monomer pressures were obtained by raising the cell temperature to 900°K.

These results are in agreement with the transpiration results of Rice and Gregory [154] who found less than 1% $NaZnCl_3$ above $ZnCl_2$ - NaCl mixtures. They also confirm earlier findings in this work, that only a small degree of complex formation occurs in this system. The earlier assumptions made during the transpiration study, concerning vapour phase composition, have been confirmed. Moreover, it has been established that from the metallurgical point of view, the degree of NaCl transpired as $NaZnCl_3$ during salt roasting of zinc ores would be quite small.

Attempts to carry out quantitative measurements on these systems were not successful : the intensities of $MZnCl_2^+$ were too small to permit measurement over a reasonable temperature range while maintaining Knudsen conditions. Increasing sensitivity at the expense of resolution was not sufficient to obtain satisfactory results. An attempt was made to compensate for different volatilities of $ZnCl_2$ and NaCl by generating $ZnCl_2$ indirectly at 1000°K by the reaction:

$$ZnO + 2NaCl = ZnCl_2 + Na_2O.$$

Although approximately equal partial pressures of $ZnCl_2$ and NaCl were obtained, very little complex was observed above this system. It is apparent that the degree of complexing above $ZnCl_2$-MCl mixtures is very much less than that found above PbX_2-MX.

5.1.3. $CdCl_2$-MCl Mixtures

To complement the study on $ZnCl_2$, mixtures of $CdCl_2$-MCl were examined. Many of the properties of liquid phase mixtures of $ZnCl_2$ and $CdCl_2$ with MCl are similar and it was thought interesting to compare vapour phase equilibria. Furthermore, the work of Bloom and Welch[20] on $CdSO_4$-NaCl reciprocal salt mixtures reveals that salt roasting of CdS ores is a possibility; vapour phase species should be known.

With mixtures of $CdCl_2$-CsCl, $CdCl_2$-RbCl, the following ions were observed in order of decreasing intensity:

$$CdCl_2^+ > CdCl^+ > Cd^+ > MCdCl_2^+ > MCdCl^+ > Cd_2Cl_3^+ > Cd_2Cl_2^+$$

The ratios of $CdCl_2^+$ to $MCdCl_2^+$ were of the order of the 10,000:1. The position of Cd^+ on the scale was very much affected by resolution settings. The following ion-precursor relationships are assumed:

$CdCl_2^+$, $CdCl^+$, Cd^+ } $CdCl_2$; $MCdCl_2^+$, $MCdCl^+$ } $MCdCl_3$

$Cd_2Cl_3^+$, $Cd_2Cl_2^+$ } $(CdCl_2)_2$

No ions corresponding to higher complexes were observed. These results indicating the formation of $RbCdCl_3$ and $CsCdCl_3$ are in agreement with those of Bloom and Hastie[31]. Formation of the dimer

$(CdCl_2)_2$ was observed at the temperatures used in these experiments. In earlier work at lower temperatures, this species was not observed. The quite small relative intensity of $Cd_2Cl_3^+$ is in agreement with the work of Keneshea and Cubicciotti,[149b] who found only a small degree of dimerization in saturated $CdCl_2$ vapour. Difficulty was experienced with the KCl and NaCl mixtures with $CdCl_2$. Quite weak peaks corresponding to $KCdCl_2^+$ indicated possible formation of $KCdCl_3$; identification cannot be said to be positive. In NaCl mixtures, no peaks corresponding to complex species were observed; this would indicate that, any vapour phase complexes present in this system would have a very low partial pressures in the saturated vapour. It is concluded that the degree of complex formation above $CdCl_2$-MCl melts is quite small.

5.2. Discussion of Mass Spectrometry Results

5.2.1. Introduction

Mass spectrometry results will now be compared in the light of trends known to exist in other systems. An estimation of possible vapour phase structures will be made. Where possible, experimental results and theoretical predictions will be compared.

The most striking feature of the results is the much lower stability of $MZnCl_3$ and $MCdCl_3$ than $MPbX_3$. A much greater degree of complexing was observed in PbX_2–MX vapour mixtures, even when qualitative allowance was made for the effects of differing cell pressures and of mass discrimination. Enthalpies of formation of $MZnCl_3$, $MCdCl_3$, $MPbCl_3$ are comparable and therefore differences in stability are due to more negative entropies of formation of $MZnCl_3$ and $MCdCl_3$.

5.2.2. Comparison of Systems

For a comparison, heats and entropies of complex formation, where available, have been tabulated; ΔH_f for alkali halide dimers are also given. Bromide vapours usually form with a more negative entropy change of about 1 e.u. over values for chlorides;[221,222] entropies of formation of $MPbBr_3$ have therefore been estimated from published values[161] for $MPbCl_3$, determined from vapour pressure measurements.[71] Heats of formation and the degree of complex formation do not vary greatly with the alkali metal atom (M) within any one set of systems. It would seem that structures of complexes within any one set are quite similar and the choice of M merely modifies the basic structure.

TABLE 5-7

Heats and Entropies of Formation

(1) $MPBX_3$

M	$-\Delta H_f$ ($MPbBr_3$) kcal/mole	$-\Delta S_f$ ($MPbBr_3$) e.u.	$-\Delta H_f$ ($MPbCl_3$) kcal/mole		$-\Delta S_f$ ($MPbCl_3$) e.u.
	2nd law		2nd law	3rd law	
Na	38.9	20.0	38.0	36.5	21.0
K	43.2	19.6	41.0	39.5	20.6
Rb	41.3	19.3	33.5	41.0	20.3
Cs	39.8	19.0	35.0	38.0	20.0

(2) MAX_3	$-\Delta H_f$ (kcal/mole)
$NaZnCl_3$ [154]	42.0
$KZnCl_3$ [148]	39.5
$CsCdCl_3$ [155]	45.0
$NaSnF_3$ [223]	60.0
$NaSnCl_3$ [159]	48.0

(3) Dimers

M	$-\Delta H_f$ $(MCl)_2$ 1000°K kcal/mole	$-\Delta H_f$ $(MBr)_2$ 1000°K kcal/mole	
		Bauer and Porter [119]	Murgulescu et al [224]
Na	48.0	45.5	-
K	43.0	41.0	-
Rb	40.0	39.0	36.6
Cs	37.0	36.0	40.4
$(ZnCl_2)_2$	40.1		

For the results available, entropies within any one set appear to be fairly constant, as distinct from the estimated large variation in ΔS_f between sets, for example $MPbCl_3$ and $MZnCl_3$. Therefore within any one set of systems, heats of formation may as a first approximation be tentatively taken as a measure of vapour complex stability.

To aid any comparison of thermodynamic properties and as a starting point in estimation of structures, one may first consider the liquid phase. It is considered that complex ions, e.g. $ZnCl_4^{2-}$, contain a discrete charge and are in part covalently bonded. By analogy, vapour phase complexes could consist of essentially electrostatically bonded M^{a+} and AX_3^{a-} ($a \leq 1$).

In PbX_2-MX liquid mixtures, complex ion stability increases as M varies from Na to Cs.[65, 74, 207] In the vapours above those mixtures however, heats of formation of $MPbX_3$ ($-\Delta H_f$) appear to be greatest for $KPbX_3$ and $RbPbX_3$. Both the Na and Cs complexes seem to have lower stability. It would seem that there are two opposing influences on the formation of these vapour complexes.

In the melt, smaller M^+ ions tend to destabilise complex ions by weakening A-X bonds. A similar process may be occurring in the vapour, where the effect will probably become more important as A-X becomes more covalent. Occupying a position close to an X atom, one can envisage M^{a+} draining charge away from the covalent bond onto the X atom. A second explanation for the decrease in stability of $NaPbX_3$ over $KPbX_3$, is the possible weak Pb^{2+}-M^+ covalent bond

postulated by Hastie;[155] overlap would presumably be favoured by a large M^+ so that the bond strength would fall off from Cs to Na.

The opposing influence may be a packing phenomenon where the larger Cs^{a+} is least easily accommodated within the $MPbX_3$ molecule. Packing effects would not be crucial in the liquid mixtures, as these consist of imperfect ion lattices rather than discrete molecules.[1]

One may postulate that in the lead systems these two influences occur resulting in largest $(-\Delta H_f)$ for K and Rb complexes. In the zinc systems, $KZnCl_3$ appears to have a smaller $(-\Delta H_f)$ than $NaZnCl_3$.[154,148] This could indicate that the "packing" effect predominates and $RbZnCl_3$, $CsZnCl_3$ should have progressively smaller values of $(-\Delta H_f)$. If this is indeed true, it is likely that there is more ionic bonding in zinc than in lead complexes.

Alkali halide dimers are known to have essentially ionic bonding;[119,126] both heats and free energies of formation become more negative in the series from Na to Cs. This is most probably due to an increase in strength of M^+-X^- in the bond as the charge density on M^+ increases. Packing effects are also likely to favour the smaller ion. Replacement of chlorine by bromine atoms reduces dimer stability; strong M^+-X^- ionic bonds would be favoured by smaller anions.

In $MPbX_3$, replacement of chlorine by bromine increases $(-\Delta H_f)$. The situation is analogous to that in the melt where complex ions

increase in stability as halide atoms become more polarisable.[77,78] In the vapour, the Pb-Br bond is probably more covalent than Pb-Cl in $MPbX_3$ as the larger Br atom would permit greater overlap. However, the greater value of $(-\Delta H_f)$ $NaSnF_3$ over $NaSnCl_3$ is in opposition to this trend. A likely explanation is that Sn^{2+}-F^- bonding is almost entirely electrostatic in nature; the high charge density on F^- produces so strong an ionic bond that loss of covalency is more than compensated for. Pauling's figures[225] indicate an electronegativity difference of 2.20 between F and Sn; this is similar to that found for the ionic alkali chlorides.

(C) Structures of MAX_3

From the discussion given above, MAX_3 is most likely composed of M^{a+}-AX_3^{a-}, in which the degree of covalency in A-X bonding varies from system to system and has some effect on vapour complex stability. In the melts, it is believed that $ZnCl_4^{2-}$ and $PbCl_4^{2-}$ probably have distorted tetrahedral structures and $ZnCl_3^-$ and $PbCl_3^-$ are pyramidal.[88,226] For vapour phase complexes there are two likely structures, both involving M-X-A bridging bonds; these are given in figure 5-5.

In the bipyramidal structure, all M-X bond lengths are equal; X-A-X angles are likely to vary from 90^o to the tetrahedral angle of 109^o28^1. For lead complexes, Hastie[126,155] has pointed out that the first structure is more likely, as the lone pair of non bonding s electrons will take up the fourth tetrahedral position

FIGURE 5-5

LIKELY STRUCTURES OF MAX_3

1. BIPYRAMIDAL

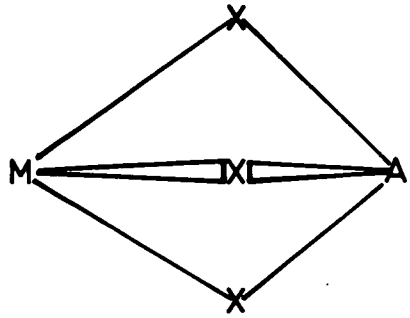

2. PLANAR

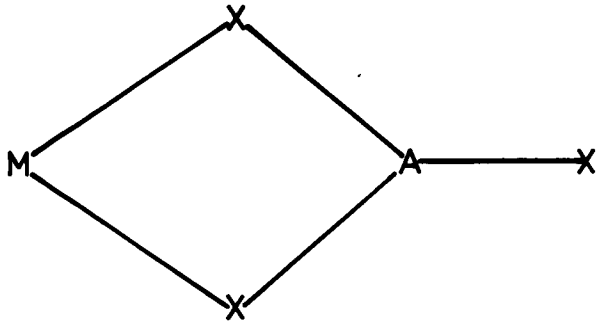

$(ZnCl_2)$

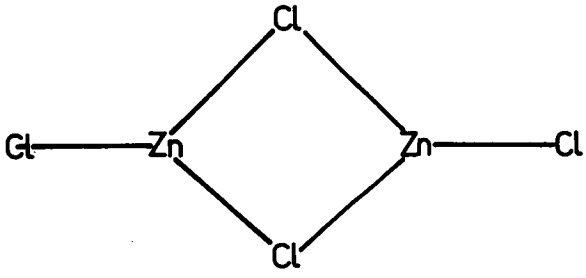

$NaAlF_4$

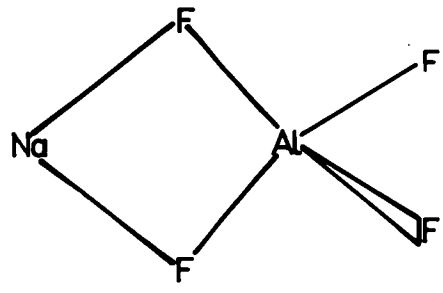

to Pb. The second structure is a possibility for $MZnCl_3$ and $MCdCl_3$ because of its similarity to the proposed dimer structure.[144] From X-ray measurements, Spiridonov and Erokhin[227] have assigned a type (2) structure to $NaAlF_4$, this having two terminal Al-F bonds in a plane at right angles to that of the ring.

The most useful way of determining the most likely structure is an LCAO-Molecular Orbital approach. Classical ionic model methods,[228,229] based upon lattice energy calculations for an ionic crystal, have been successfully applied to alkali halide dimerization. They cannot be used however to estimate degrees of covalency in A-X bonding.

LCAO theory assumes that, in the neighbourhood of a nucleus,[230] a molecular orbital will resemble the atomic orbital of that nucleus in the isolated atom. The molecular orbital is written as a linear combination of atomic orbitals. For an electron in the Kth M.O.

$$\psi_K = \sum_j a_j \phi_j \qquad \text{(v-3)}$$

where ψ_K is the Kth M.O.

ϕ_j is the jth A.O.

a_j is the coefficient or eigen vector of the jth atomic orbital.

The aim of the calculation is to determine the coefficients a_{Kj} and orbital energies, or eigen values E_K.

If there are n atomic orbitals, n secular equations in the n

coefficients are obtained:

$$\sum_j a_j (H_{ij} - ES_{ij}) = 0 \qquad \text{(v-4)}$$

H_{ij} represent bond integrals, the energy of interaction of two atomic orbitals ϕ_i, ϕ_j; S_{ij} represents the overlap integral. The n sets of coefficients are obtained as solutions to the secular equations.

Molecular orbital methods differ in their selection of atomic orbitals ϕ_i, ϕ_j and their Hamiltonian operators H_{ii}, H_{ij}. Extended Huckel methods have proved to be useful in the prediction of high temperature structures.[160] The form most commonly used is that given in a computer program devised by Hoffman.[231]

Input requirements are given below:

(1) A cartesian atomic coordinate system in Angstrom units containing all atoms.

(2) Slater type atomic orbitals for each atom; exponents for these atomic orbitals may be calculated using Slater's rules or published values for the exponents may be used.

(3) Hamiltonian operators. H_{ii} or coulomb integrals are chosen as negative values of valence state ionization energies. Off diagonal H_{ij} terms have been found to be best approximated by the Ballhausen and Gray equation:[232]

$$H_{ij} = KS_{ij} (H_{ii} H_{jj})^{\frac{1}{2}} \qquad \text{(v-5)}$$

Hoffman[231-235] has recommended a value of -1.75 for K; this value has proved to be the most satisfactory in the calculation of structures of high temperature species.[160] Calculated bonding energies however are usually found to be too large using this value.

(4) The number of electrons to be fed into the molecular orbitals, beginning with the most bonding.

For a given set of input parameters, the computing procedure given in appendix B is carried out. Most likely structures were determined using a trial and error procedure i.e. computations were carried out using various input structural parameters and that structure with the most negative total Molecular Orbital energy selected. Absolute values of bond energies are generally not likely to be very reliable; nevertheless, trends in energy variation will be meaningful.

Apart from relative bond energies, other information is obtainable from the Molecular Orbital calculation:

1. Population analyses and charge distributions throughout the molecule. Hence the degree of covalent bonding may be estimated.

2. Ionization potentials, chosen as the orbital energy of that occupied molecular orbital with the lowest energy.

3. The computation may be repeated with one electron less; thereby charge distributions in the singly ionized molecule may be obtained.

It must be kept in mind that these calculations are approximate, especially with atoms beyond the third row in the periodic table. The results obtained must be treated with caution and as far as possible compared with experimental results.

5.3. Molecular Orbital Calculations.

The Molecular Orbital (M.O.) calculations were quite complex and involved considerable computer time. Limited computer availability imposed a restriction upon the total number of calculations which could be performed. Therefore a certain amount of interpolation will be necessary in the deduction of the most likely structures. Calculations were first performed on relatively simple molecules of known structure. Exponents to the Slater orbitals were chosen as the optimised values given by Clementi and Raimondi.[236,237] Coulomb integrals were taken as V.S.I.E.'s of the free atom, obtained from Moore's atomic energy level tables;[238] these may also be obtained from plots given by De Vault.[239]

5.3.1. Triatomic Molecules

(A) $ZnCl_2$

It was stated earlier (2.2.1), that this molecule is linear. X-ray measurements[29] give the Zn-Cl bond length as 2.05 Å. The filled Zn(3d) and Zn(4P) atomic orbitals have been included to determine whether these take any part in bonding.

atomic orbitals:						
Zn	: $3d^{10}$	$4s^2$	$4p^0$	Cl:	$3s^2$	$3p^5$
V.S.I.E. (ev)	: -17.33	-9.39	-4.90	:	-24.55	-12.95
Slater Exponent	: 4.626	1.491	1.491	:	2.356	2.039

Results: (1) Bond Energy: The difference in energy between the total molecular orbital (M.O.) energy and the total energy of all

atomic orbitals which were initially occupied is the total bond energy of the molecule. For $ZnCl_2$ the calculated bond energy is -230 kcal/mole. This value may be compared with the experimental value of -157 kcal/mole given by Brewer et al.[134] The calculated M.O. energy is usually somewhat dependent[155] upon the value of K used in the Ballhausen and Gray equation, (V-5). Using K = -1.75, it is usually found that bonding energies are too large, due to an incomplete cancellation of electron-electron repulsion energies. Correcting for K = -1, the bond energy becomes -230/1.75 = -132 kcal/mole. It would be expected that the true figure would lie between these two calculated values.[241]

(2) Charge Patterns: The charge patterns for the molecule indicate that a significant amount of covalent bonding is taking place:

atom		charge(q)	Δq
Zn	:	+ 1.85	(+0.02)
Cl	:	- 0.92	(+0.49)

Ionization potential = 12.91 ev

The figures in brackets indicate the charge that is lost from that atom upon single ionization. The calculation would indicate that the Zn-Cl bond has about 92% ionic character. Inspection of the eigen vectors and Mulliken overlap populations reveals that the covalent overlap is essentially between Zn(4s) and Cl(3p) orbitals. The Zn(3d) orbitals take only a minor part in covalent bond formation; a small degree of occupation of the Zn(4p) orbitals

occurs as evidenced by significant Zn(4p)-Cl(3s) overlap. The calculated value of ionization potential, 12.9 ev, may be compared with an experimental value of 11.7 ev given by Kiser et al.[240] The agreement is good, as it is usually found that calculated I.P.'s are up to 2 ev too high.[241] Upon ionization, almost all of the charge is derived from the chlorine atoms, specifically from their 3p orbitals.

(B) $CdCl_2$

X-ray measurements indicate a Cd-Cl bond length of 2.21 Å in $CdCl_2$.

Atomic orbitals			
Cd	$4d^{10}$	$5s^2$	$5p^0$
V.S.I.E. (ev)	-19.93	-8.99	-4.89
Slater Exponents	3.969	1.638	1.638

Results: Bond Energy: The bond energy calculated from the total M.O. energy is -232 kcal/mole. Correcting for K = -1, a value of -132 kcal/mole is obtained which may be compared with an experimental figure[134] of -135 kcal/mole.

Charge Pattern	q	Δq
Zn	1.884	(0.004)
Cl	-0.442	(0.498)
I.P. (ev)	12.92	

The degree of ionic bonding in $CdCl_2$ is somewhat greater than in $ZnCl_2$. The calculated I.P. is in good agreement with that given by Hastie[155] of 11.2 ev. Upon ionization, charge is mostly

lost from the Cl(3p) orbitals.

(C) $PbBr_2$

Pb-Br bond lengths are known[29] to be 2.60 Å in this molecule. The bond angle is not as accurately known and the value given by Brewer et al[134] of 95° has been used.

atomic orbitals:

	Pb			Br		
	$5d^{10}$	$6s^2$	$6p^2$	$4s^2$	$4p^5$	
V.S.I.E. (ev)	-22.30	-15.30	-7.40	-23.71	-11.61	
Slater Exponents	4.630	2.350	2.065	4.638	2.257	

Results: Bond Energy: Calculating bond energies as before, a value of -154 kcal/mole is obtained which reduces to -88 kcal/mole when divided by 1.75. These values may be compared with an experimental value[134] of -126 kcal/mole.

Charge Patterns. In this molecule, a substantial degree of covalent bonding occurs. The charge pattern found is compared with Hastie's[155] figures for $PbCl_2$.

$PbBr_2$			$PbCl_2$		
Pb	1.00	(0.60)	Pb	1.85	(0.79)
Br	-0.50	(0.20)	Cl	-0.92	(0.105)
I.P. (ev)	9.48			12.02	

The observed increase in covalency in the Pb-X bond, upon exchanging a chlorine for a bromine atom, is in agreement with earlier discussion. The results indicate that covalent bonding essentially involves Pb(6s) and Br(4p) overlap with a smaller amount

of Pb(6s)-Br(4p) overlap.

When single ionization of $PbBr_2$ occurs, most of the charge is lost from the Pb(6s) orbitals and only a small amount from the Br(4p) orbitals. It is interesting now to examine experimental ratios of parent to fragmented ions in the light of M.O. results. Parent ion stability was found to decrease in the series:

$$ZnCl_2^+ \approx CdCl_2^+ > PbBr_2^+ > MCl^+ \approx MBr^+$$

Hastie[155] has pointed out that ionization of KCl involves loss of charge from the chlorine ions to leave K^+-Cl. This species will readily fragment, as it is bound together only by a weak covalent bond. Upon single ionization of $PbBr_2$ or $ZnCl_2$, there remains a considerable amount of A-X ionic and covalent bonding; therefore $PbBr_2^+$ and $ZnCl_2^+$ would be more stable than MX^+. Bond energies indicate that Zn-Cl bonds are stronger than Pb-Br bonds. Therefore it is to be expected that $ZnCl_2^+$ would be more stable than $PbBr_2^+$.

5.2.2. Dimers

To further investigate the M.O. method, some calculations were performed on $(ZnCl_2)_2$ and $(CdCl_2)_2$. The most likely basic structure has already been given in fig. 2-2. As no X-ray measurements have been carried out on these structures, estimates of structural parameters must be used.

(A) $ZnCl_2$

Loewenschuss et al[144] have suggested that the ring angle is 90^o. Dimerization may bring about either an increase or a decrease in the

Zn-Cl bond lengths. Alkali halide dimerization involves a lengthening of M-X bonds.[119] Alternatively, if the degree of covalent bonding in the dimer is greater than that in the monomer, bond lengths could decrease. The terminal Zn-Cl bonds are likely to be shorter than the bridging bonds. With Al_2Cl_6 vapour molecules,[29] the Al-Cl terminal bonds are about 10% shorter than the bridge bonds. Two calculations have been carried out, each with different Zn-Cl bond lengths. Atomic orbital input structural parameters were the same as before.

			Structure A.	Structure B.
Bond lengths (Å)	Zn-Cl (bridge)	:	2.05	2.25
	Zn-Cl (terminal)	:	1.85	2.05
	Cl-Cl (bridge)	:	2.90	3.18
M.O. energy (ev)		:	-861.39	-860.24
charges	Zn	:	1.97 (0.010)	+1.82 (0.00)
	Cl (bridge)	:	-0.94 (0.490)	-0.87 (0.497)
	Cl (terminal)	:	-1.03 (0.000)	-0.95 (0.000)
I.P. (ev)		:	12.71	12.85

The results indicate that structure A is the more stable. It is surprising that the bridge Cl-Cl interatomic distance for this structure is a good deal smaller than twice the crystal ionic radius of Cl^- (i.e. < 3.60 Å). The interatomic distance is however a good deal greater than twice the chlorine covalent radius (i.e. > 2.00).

Comparing charge distributions with those of the monomer, an increase in the degree of ionic bonding is apparent. The terminal Zn-Cl bonds are more ionic in nature than the bridging Zn-Cl bonds. Upon ionization, almost all of the lost charge is derived from the 3p orbitals of the bridging Cl atoms.

It is interesting to compare theoretical and experimental heats of dimerization. The calculated energy is given by:

$$\Delta E_D\ (ZnCl_2)_2 = \text{M.O. energy (dimer)} - 2\ \text{M.O. energy (monomer)}$$
$$= -43.1\ \text{kcal/mole.}$$

This figure agrees with the experimental enthalpy of dimerization -40.1 kcal/mole, given by Keneshea and Cubicciotti.[149a]

(B) $(\underline{CdCl_2})_2$

Lengths of 2.21 Å and 2.44 Å were used for Cd-Cl terminal and bridging bonds respectively. A ring angle of 90° has been assumed. The results are as follows.

Bond length Cl - Cl (Å)		: 3.12	
M.O. Energy (ev)		: -870.57	
Charges	Cd	: 1.870	(0.010)
	Cl bridge	: -0.925	(0.490)
	Cl terminal	: -0.925	(0.000)
I.P. (ev)		: 12.2	

The charges on the chlorine atoms are about the same as those found for $(ZnCl_2)_2$. By analogy with the previous example, the bridge Cl-Cl distance is likely to be shorter than was first

assumed. Estimated distances are: Cl-Cl, 3.13 Å; Cd-Cl (bridge) 2.21 Å ; Cd-Cl (terminal), 2.12 Å.

Molecular Orbital results for these relatively simple molecules appear to be in substantial agreement with experiment. Therefore the method may be applied with some confidence to the complex vapour species of interest.

5.2.3. $\underline{MAX_3}$

Limitations on available computing time restricted the number of calculations which could be performed. As the basic structure is not likely to change with the selection of the alkali atom, calculations were carried out only for the potassium complexes. In this way, comparison with Hastie's[155] results for $KPbCl_3$ is possible. To determine most likely structures, calculations were made using different values of structural parameters; both the bipyramidal and planar terminal bonded configurations were examined. Calculations on the $KPbBr_3$ molecule are somewhat more straightforward than the others, and it is considered first.

(A) $\underline{KPbBr_3}$.

(1) Bipyramidal Structure. Specification of the Pb-Br and K-Br bond lengths and the Br-Pb-Br bond angle defines the coordinates of the molecule. It is likely that the Pb-Br bond length will be about the same and that in $PbBr_2$, 2.60 Å. The K-Br bond distance is likely to lie between that found in the KBr monomer, 2.62 Å, and that of its dimer, 3.08 Å; values between

2.91 - 3.00 Å are reasonable. The Br-Pb-Br bond angle is likely to vary from 90° to the tetrahedral angle of 109°.

Other bonds lengths should also be considered. In $KPbCl_3$, Hastie[155] found that the Cl-Cl distance was less than twice the crystal ionic radius of Cl^-. Therefore, the Br-Br distance in $KPbBr_3$ is likely to be smaller than twice the Br^- ionic radius (i.e. < 3.92 Å) and certainly greater than twice the Br covalent radius (i.e. > 2.28 Å). The K-Pb bond length should be greater than the sums of ionic radii i.e. 2.54 Å.

Four M.O. calculations were carried out as follows:

			Structure			
			A	B	C	D
Bond Lengths (Å)	Pb-Br	:	2.60	2.60	2.60	2.60
	K-Br	:	3.00	3.00	3.00	2.91
	Br-Br	:	4.24	4.02	3.68	4.01
	K-Pb	:	2.62	3.09	3.63	2.94
Br-Pb-Br angle		:	109	101	90	101
M.O. Energy (ev)		:	-751.59	-752.53	-752.94	-752.48
Charges	Pb	:	0.726 (0.658)	0.731 (0.650)	0.809 (0.625)	0.740 (0.640)
	K	:	1.120 (0.012)	1.094 (0.012)	1.073 (0.012)	1.107 (0.011)
	Cl	:	-0.613 (0.110)	-0.609 (0.013)	-0.627 (0.120)	-0.615 (0.113)
I.P. (ev)		:	8.28	8.82	9.33	8.82

Although the differences in M.O. energies are not very great, structure C, with a bond angle of 90°, appears to be the most stable.

In $KPbCl_3$, the bond lengths given by Hastie[155] correspond to a Cl-Pb-Cl angle of 92°. The charge distribution determined for that molecule was: Pb : 1.75, K : 1.00, Cl : -1.875.

2. Planar Structure. Turning now to the planar configuration, one calculation was performed as follows:

Bond Lengths (Å)	Pb-Br (bridge)	:	2.60
	Pb-Br (terminal)	:	2.50
	Br-Br (bridge)	:	3.63
	Pb-K	:	4.21
Ring angle		:	90°
M.O. Energy (ev)		:	-751.0
Charges	Pb	:	2.522 (0.373)
	K	:	0.812 (0.111)
	Br (bridge)	:	-1.107 (0.156)
	Br (terminal)	:	-1.120 (0.204)
I.P. (ev)		:	4.82

The M.O. energies suggest that the bipyramidal structure is the most likely. Furthermore, the low I.P. of the planar structure is improbable; the calculated value for the bipyramidal structure seems more reasonable. The experimental[155] I.P. for $KPbCl_3$ is 9.3 ev.

Considering the charge distribution of the bipyramidal structure, the molecule may be thought to consist of electrostatically bonded K^+-$PbBr_3^-$.

The Pb-Br bonds are somewhat more covalent in the complex than in $PbBr_2$. The K-Br distance appears to have little effect on total M.O. energy; this supports the earlier argument that the function of M is merely to modify a common $MPbBr_3$ structure. Inspection of eigen vectors and Mulliken overlap populations indicates a very small degree of overlap between K and Pb, principally via s orbitals. M-Pb covalent bonding could increase with increasing size of M. It is doubtful however whether relative strengths of M-Pb covalent bonds predominantly effect heats of formation of complexes.

(B) $KZnCl_3$ and $KCdCl_3$

As the results for these two molecules complement each other, the two are considered together.

(1) Bipyramidal Configurations. Likely size ranges for structural parameters have again been determined. The A-Cl distances will probably be close to those in the ACl_2 monomers. The K-Cl distance is likely to lie between 2.77-2.87 Å. As the A-Cl distances are relatively short, Cl-Cl interatomic distances are likely to become important. These are likely to lie in the range 2.00 - 3.46 Å, and will be dependent very much on the Cl-A-Cl bond angle. The Zn-K, Cd-K distances should be greater than their ionic radii sums of 2.07 and 2.21 Å respectively.

A number of calculations were carried out for $KZnCl_3$ as follows:

		Structure				
Bond Distances		A	B	C	D	E
Zn-Cl	:	2.05	2.05	2.05	2.00	2.05
K-Cl	:	2.87	2.87	2.87	2.87	2.77
Cl-Cl	:	3.36	3.16	2.90	3.08	3.16
Zn-K	:	2.83	3.16	3.63	3.16	3.02
Cl-Zn-Cl angle	:	109	101	90	101	101
M.O. Energy (ev)	:	-706.78	-706.29	-705.17	-706.22	-706.21
Charges. Zn	:	1.871 (0.014)	1.892 (0.011)	1.920 (0.007)	1.940 (0.012)	1.900 (0.120)
K	:	1.072 (0.000)	1.068 (0.000)	1.062 (0.000)	1.067 (0.000)	1.068 (0.000)
Cl	:	-0.981 (0.329)	-0.987 (0.329)	-0.994 (0.331)	-1.002 (0.329)	-0.990 (0.330)
I.P. (ev)	:	12.57	12.41	14.04	12.31	12.42

The figures in brackets are again the amount of charge lost upon single ionization.

The most stable structure is A, with a Cl-Zn-Cl angle of 109^{o}; in this structure the Cl-Cl bond length is a maximum. It is noted that in the most stable $(ZnCl_2)_2$ structure, the Cl-Cl distance was somewhat smaller than that found here for structure A.

One M.O. calculation was carried out on $KCdCl_3$.

Bond Distances ($\mathring{A}$)	Cd-Cl	:	2.21
	K-Cl	:	2.87
	Cl-Cl	:	3.42
	Cd-K	:	3.09
Cl-Zn-Cl Angle		:	101

M.O. Energy (ev)	:	-711.67
Charge Distribution		
Zn	:	1.900 (0.028)
K	:	1.067 (0.000)
Cl	:	-0.989 (0.324)
I.P. (ev)	:	12.51

With the longer Cd-Cl bond in this system, Cl-Cl repulsion is not likely to be as critical as it seemed to be in the $KZnCl_3$ molecule. In this structure, the Cl-Cl bond length is 3.42 Å; in the A structure of $KZnCl_3$ it is 3.36 Å. Therefore an increase in the Cl-Cd-Cl angle is not likely to add significantly to the total M.O. energy.

(2) Planar Structures. One calculation each was performed on $KZnCl_3$ and $KCdCl_3$.

Bond Distances (Å)		$KZnCl_3$		$KCdCl_3$
A-Cl (bridge)	:	2.12	:	2.21
A-Cl (terminal)	:	1.95	:	2.11
K-Cl (bridge)	:	2.87	:	2.87
Cl-Cl (bridge)	:	3.00	:	3.12
A-K	:	3.95	:	3.97
Ring Angle	:	90°	:	90°
M.O. Energy (ev)	:	-706.54	:	-711.76
Charge Distribution				
A	:	1.910 (0.007)	:	1.952 (0.023)

K	:	1.038	(0.000)	: 1.036	(0.000)
Cl (bridge)	:	-0.985	(0.496)	: -0.999	(0.488)
Cl (terminal)	:	-0.977	(0.001)	: -0.999	(0.002)
I.P. (ev)	:	12.27		: 12.31	

In the case of $KZnCl_3$, increasing the Cl-Zn-Cl angle from 90^o resulted in greater M.O. energy. It is likely then that increasing Cl-A-Cl angles in the planar structures is likely to increase the M.O. energy by about -0.3 to -0.4 ev. It seems likely that the planar structures are marginally more stable. However it must be remembered that these Extended Hückel (E.H.) calculations are very approximate and small differences in calculated energies may not be meaningful. Although a greater number of calculations is likely to clarify the situation somewhat, it is doubtful whether a definite conclusion could be reached by M.O. methods alone.

From other considerations, the planar structures appear to be the most likely. As they have a greater degree of asymmetry their entropies of formation are likely to be less negative than those of the bipyramidal structures; this would tend to make their free energies of formation more negative. From the point of view of "mixed dimer" formation:

$$(ACl_2)_2 + (MCl)_2 = 2\ MACl_3$$

the planar structures could be formed from $(ACl_2)_2$ with less bond rearrangement than could the first structure.

A structure of this second type has been experimentally determined for $NaAlF_4$.[227] From these considerations, planar structures for Zn and Pb complexes seem reasonable. The influence of the 6s electrons is the most likely reason why $KPbBr_3$ has a bipyramidal structure. Most likely structural parameters for $KZnCl_3$ and $KCdCl_3$ are:

Bond Distances (Å)	$KZnCl_3$	$KCdCl_3$
A-Cl (bridge)	2.05	2.21
A-Cl (terminal)	2.00	2.11
K-Cl (bridge)	1.87	2.87
Cl-Cl (bridge)	3.36	3.41
A-K	3.41	3.71
Cl-A-Cl angle	109°	101°

$KZnCl_3$ (and also $KCdCl_3$) may be considered to consist of K^+-ACl_3^-. The Zn-Cl bonds appear to be essentially ionic in nature, much more so than those in $ZnCl_2$. It is recalled that Pb-Br bonds become more covalent upon complex formation. The apparent insensitivity of the M.O. energy of $KZnCl_3$ to the K-Cl distance would tend to indicate that the effect of the alkali ion on complex stability would again be small.

Ionization of $KZnCl_3$ involves loss of charge from the bridging chlorine atoms. The greater number of Cl^- attached to any one Zn^{2+} would probably render individual Zn-Cl bonds weaker in $KZnCl_3$ than in $ZnCl_2$. This fact, together with the smaller degree of covalent bonding in $KZnCl_3$, would explain the observed

low stability of $KZnCl_3^+$.

5.2.4. Stability of Complexes

Experimentally it was found that $MZnCl_3$ (and $MCdCl_3$) were much less stable than $KPbBr_3$; this fact is believed to be due to a more negative entropy of formation of $KZnCl_3$ from the monomers. Having deduced likely structures, it is interesting to investigate this behaviour.

Hastie[126] has recently examined complex formation from the point of view of "mixed dimer" formation:

$$(MX)_2 + (AX_2)_2 = 2\ MAX_3$$

In a large number of cases, ΔH for this reaction would be close to zero; the driving force for complex ion formation would be the small positive entropy change accompanying the reaction, about 2 cals/mole deg.,resulting from a decrease in symmetry.
It is noted that the enthalpy change for the reaction:

$$CdCl_2 + CdBr_2 = 2\ CdClBr$$

was found to be positive if anything, and the driving force would be associated with a decrease in symmetry.

The formation of $KPbBr_3$ and $KZnCl_3$ is represented in figure 5.6. Although not a "mixed dimer" reaction, formation of $KPbBr_3$ does not involve a great deal of bond rearrangement, as $PbBr_2$ is already bent. However the formation of bent Cl-Zn-Cl bridging bonds involves considerable bond rearrangement and presumably negative entropy change.

FIGURE 5-6

FORMATION OF MAX_3

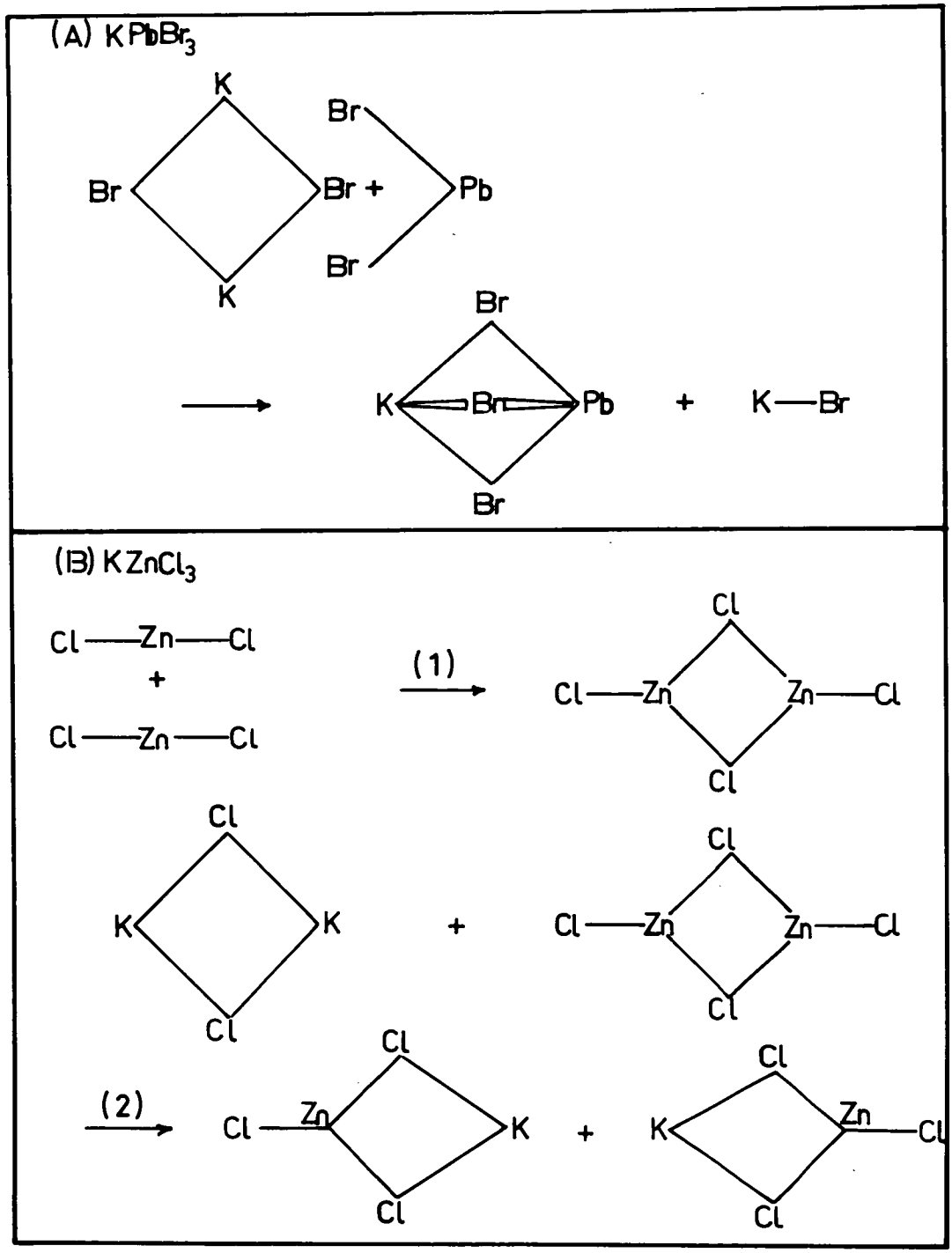

It may be concluded that where monomers are linear, the degree of complex formation is likely to be dependent upon the amounts of dimers present in the vapour phase. If A-Cl bonds are more stable than M-Cl bonds, ΔH for the mixed dimer reaction will be negative, increasing the degree of complex formation. When A-Cl bonds are very stable, formation of higher complexes: M_2ACl_4, MA_2Cl_5, or $(MACl_3)_2$ is possible.

6. Summary and Conclusions

An example of a complex system of metallurgical interest has been taken to determine the usefulness of theory in the prediction of its thermodynamic properties.

Activities in the system Zn-Na-Cl-SO_4 were found to be quite different from ideality. Simple theories such as the Temkin and F.F.G. regular solution models were not successful in predicting activities. The Conformal Ionic Solution Theory however did fit the data quite reasonably. The C.I.S. equation also fitted data for the $PbCl_2$-K_2SO_4, $PbCl_2$-Na_2SO_4 systems. This emphasises the need to incorporate binary interaction and non random mixing terms in activity equations for fused reciprocal salt mixtures.

An investigation of partial molar quantities in the Zn-Na-Cl-SO_4 system revealed that non-ideality in the system is probably caused firstly,by the breakdown of a network structure in pure $ZnCl_2$ and secondly,by complex ion formation between $ZnCl_2$ and NaCl. Interactions present in the $ZnCl_2$-NaCl system very much influence the ternary system.

The low activities of $ZnCl_2$ in $ZnSO_4$-NaCl would tend to oppose the argument that liquid phase exchange between $ZnSO_4$ and NaCl is the primary mechanism for salt roasting of oxidised ZnS. Exchange reactions between molten NaCl and solid ZnO seem more likely. Reciprocal $ZnCl_2$-Na_2SO_4 interactions are likely to lower $ZnCl_2$ partial pressures.

Investigations of vapour phase equilibria likely to be

encountered in salt roasting type reactions revealed the presence of vapour complexes of the type MAX_3 and AClBr. It seems that complexing in the vapour phase is the rule rather than the exception. Fortunately, the amount of $NaZnCl_3$ above molten $ZnCl_2$-NaCl mixtures was found to be quite small.

Experience with a commercial quadrupole mass spectrometer revealed that it is quite suitable for the investigation of high temperature vapour phase equilibria. However a considerable amount of additional apparatus is needed for Knudsen cell work. To measure appearance potentials, a more suitable ionizer would have to be constructed. Quantitative studies on mixtures of components of very different volatilities could probably be carried out using a double Knudsen cell technique.[247]

Likely structures for the vapour phase compounds investigated have been found using Molecular Orbital techniques. These consist essentially of electrostatically bound M^+-AX_3^-. $MPbBr_3$ probably has a bipyramidal structure with three M-Br-Pb bridges; the Pb-Br bonds are significantly covalent. Results are not as conclusive for $MZnCl_3$ (and $MCdCl_3$) but a planar, terminal A-Cl bonded, structure is more likely. The Zn-Cl, Cd-Cl bonds are essentially electrostatic in nature.

Experimental trends have been related to proposed dimer structures. When ACl_2 forms a dimer, complex formation is best regarded as "mixed dimer" formation:

$$(MCl)_2 + (ACl_2)_2 = 2MACl_3$$

The degree of complex formation is likely to depend very much on the degree of dimerization in pure ACl_2 vapour. Formation of $KPbBr_3$ can also be regarded as involving alkali halide dimers.

The degree of $MPbBr_3$ formation is greater than that of $MZnCl_3$ owing to the latter's more negative entropy of formation. This is probably related to the need to form bent Zn-Cl-Zn bonds from the linear $ZnCl_2$ molecule. The effect of M on complex stability is not very great. If AX_3^- is essentially electrostatically bound, the Na complex is likely to be the most stable as the smaller Na^+ is better packed. As A-X bonding becomes more covalent, the disruptive effect of smaller M^+ ions on covalent bonding becomes important.

REFERENCES

1. Bloom, H., "The Chemistry of Molten Salts", (Benjamin: New York, (1967)).
2. Blander, M., (Ed.), "Molten Salt Chemistry", (Interscience: New York, (1964)).
3. Sundheim, B.R., (Ed.), "Fused Salts", (McGraw-Hill, Inc., (1964)).
4. Mamantov, G., (Ed.), "Molten Salts", (Marcel Dekker: New York, (1969)).
5. Margrave, J.L., (Ed.), "The Characterization of High-Temperature Vapors", (John Wiley: New York, (1967)).
6. Gittus, J.H., "Uranium", (Butterworths: London (1963)), p. 124.
7. McQuillan, A.D., McQuillan, M.K., "Titanium", (Butterworths: London, (1956)), p. 29.
8. Muan, A., Osborn, E.F., "Phase Equilibria Among Oxides in Steelmaking:, (Addison-Wesley: Reading, (1965)), p. 165.
9. Grjotheim, K., Krohn, C., Thonstad, J., Revs. Pure and Appl. Chem., 18, 219, (1968).
10. Frish, M.A., Greenbaum, M.A., Farber, M., J. Phys. Chem., 69, 3001, (1965).
11. Kleppa, O.J., Ann. Revs. Phys. Chem., 16, 187, (1965).
12. Blander, M., "Thermodynamic Properties of Solutions", ref. 2, p. 127.
13. Blander, M., "Some Fundamental Concepts", ref. 4, p.1.

14. Førland, T., "Thermodynamic Properties of Fused Salt Systems", ref. 3, p.63.

15. Lumsden, J., "Thermodynamics of Molten Salt Mixtures", (Academic Press: New York, (1966)).

16. Liddell, D.M., "Handbook of Non-Ferrous Metallurgy, Recovery of the Metals", (McGraw-Hill, Inc.: New York, 1945)).

17. Gerlach, J.K., Pawlek, F.E., Trans. Met. Soc. AIME, 239, 1557, (1967).

18. Donaldson, J.G., Kershner, K.K., U.S. Bureau of Mines. R.I., 6310, (1963).

19. Ref. 1, p. 155.

20. Bloom, H., Welch, B.J., Disc. Faraday Soc., 32, 115, (1961).

21. Welch, B.J., Ph.D. Thesis, Univ. N.Z., (1960).

22. Stillinger, F.H., "Equilibrium Theory of Pure Fused Salts", ref. 2. p.1.

23. Bloom, H., Bockris, J.O'M., "Structural Aspects of Ionic Liquids", ref. 3., p.1.

24. Ref. 1., p.76.

25. Levy, H.A., Danford, M.D., "Diffraction Studies of the Structure of Molten Salts", ref. 2., p.109.

26. Angell, C.A., J. Chem. Phys., 46, 4673, (1967).

27. Cohen, M.A., Turnbull, D., ibid., 31, 1164, (1959).

28. Miller, R.C. Kusch, P., ibid., 25, 860, (1956).

29. Grimley, R.T., "Mass Spectrometry", ref. 5, p. 195.

30. Kellogg, H.H., Trans. Met. Soc. AIME, 236, 602, (1966).

31. Bloom, H., Hastie, J.W., Aust. J. Chem., 19, 1003, (1966).

32. Reiss, H., Mayer, S.W. Katz, J.L., J. Chem. Phys., 35 820, (1961).

33. Temkin, M., Acta. Physicochim., URSS, 20, 411, (1945).

34. Haase, R., J. Phys. Chem., 73, 1160, (1969).

35. Flood, H., Førland, T., Grjotheim, K., Z. Anorg. Allgem. Chem., 296, 369, (1954).

36. Førland, T., Norg. Tek. Vitenskapsakad., Ser. 2, No. 4, (1957).

37. Førland, T., J. Phys. Chem., 59, 152, (1955).

38. Ref. 14, p. 124.

39. Hildebrand, J.H., Salstrom, E.J., J. Am. Chem. Soc., 54, 4257, (1932).

40. Ref. 15, p. 32.

41. Kleppa, O.J., J. Phys. Chem., 64, 1937, (1960).

42. Kleppa, O.J., Hersh, L.S., J. Chem. Phys., 34, 351, (1961).

43. Blander, M., J. Chem. Phys., 34, 697, (1961).

44. Lumsden, J., Disc. Faraday Soc., 32, 138, (1961).

45. Guggenheim, E.A., "Mixtures, (Oxford Univ. Press: London, (1952)).

46. Hildebrand, J.H., Scott, R.L., "Solubility of Non Electrolytes", (Reinhold: New York, (1950)).

47. Katz, J.L., Powers, B.F., Kleppa, O.J., J. Chem. Phys., 35, 765, (1961).

48. Powers, B.F., Katz, J.L., Kleppa, O.J., J. Phys. Chem., 66, 103, (1962).

49. Reiss, H., Katz, J.L., Kleppa, O.J., J. Chem. Phys., 36, 144, (1962).

50. Blander, M., ibid., 37, 172, (1962).

51. Davis, H.T., McDonald, J., ibid, 48, 1644, (1968).

52. Kleppa, O.J., Clarke, R.B., Hersh, L.S., ibid, 35, 175, (1961).

53. Kleppa, O.J., Hersh, L.S., ibid, 36, 544, (1962).

54. Blander, M., ibid, 36, 1092, (1962).

55. Davis, H.T., Rice, S.A., ibid, 41, 14, (1964).

56. Hersh, L.S., Kleppa, O.J., ibid, 42, 1309, (1965).

57. Ref. 15, p. 68.

58. Janz, G.J., "Molten Salts Handbook", (Academic Press: New York, (1967)), pp. 97-264.

59. Holm, J.L., Kleppa, O.J., J. Chem. Phys., 49, 2425, (1968).

60. Melnichak, M.E., Kleppa, O.J., ibid, 52, 1790, (1970).

61. Kleppa, O.J., Hersh, L.S., Toguri, J.M., Acta. Chem. Scand., 17 2681, (1963).

62. Kleppa, O.J., Meschel, S.V., J. Phys. Chem., 67, 668, (1963).

63. Kleppa, O.J., Meschel, S.V., ibid, 67, 2750, (1963).

64. Davis, H.T., J. Chem. Phys. 41, 2761, (1964).

65. McCarty, F.G., Kleppa, O.J., J. Phys. Chem., 68, 3846, (1964).

66. Kleppa, O.J., McCarty, F.G., ibid., 70, 1249, (1966).

67. Holm, J.L., Kleppa, O.J., Inorg. Chem., 8, 207, (1969).

68. Papatheodorou, G.N., Kleppa, O.J., J. Inorg. Nucl. Chem., 32, 889, (1970).

69. Luks, K.D., Davis, H.T., Ind. Eng. Chem. Fund., 6, 194, (1967).

70. Flood, H., Urnes, S., Z. Elektrochem., 59, 834, (1955).

71. Bloom, H., Hastie, J.W., J. Phys. Chem., 72, 2361, (1968).

72. Braunstein, J., ibid, 73, 754, (1969).

73. Ref. 15, p. 248.

74. Lantratov, M.F., Alabyshev, A.F., Zh. Prikl. Khim., 27, 722, (1954).

75. Ref. 1, p. 65, Ref. 23.

76. Handbook of Chemistry and Physics, 48th ed., (Chemical Rubber Publ. Co., Ohio, (1968)), p. F-143.

77. Lantratov, M.F., Shevlyakova, T.N., Zh. Neorg. Khim., 6, 192, (1961). [Russ. J. Inorg. Chem., 6, 95, (1961)].

78. Lantratov, M.F., Shevlyakova, T.N., Zh. Neorg. Khim., 4, 1153, (1959). [Russ. J. Inorg. Chem., 4, 1153, (1959)].

79. Mackenzie, J.D., Murphy, W.K., J. Chem. Phys., 33, 366, (1960).

80. Bues, W., Z. Anorg. Allgem. Chem., 279, 104, (1955).

81. Crook, E.H., Ph.D. Thesis, Univ. Pennsylvania, (1960), p. 460.

82. Gruber, G.J., Litovitz, T.A., J. Chem. Phys., 40, 13, (1964).

83. Bockris, J.O'M., Richards, S.R., Nanis, L., J. Phys. Chem., 69, 1627, (1965).

84. Brehler, B., Z. Krist., 115, 375, (1961).

85. Bredig, M.A., Van Artsdalen, E.R., J. Chem. Phys., 24, 478, (1956).

86. Irish, D.E., Young, T.F., ibid., 43, 1765, (1965).

87. Moyer, J.R., Evans, J.C., Lo, G.Y.S., J. Electrochem. Soc., 113, 158, (1966).

88. Ellis, R.B., ibid., 113, 485, 1966.

89. Wilmhurst, J.K., J. Chem. Phys., 39, 1779, 1963.

90. Ref. 58, p. 359.

91. Bloom, H., Spurling, T.H., Wong, J., Aust. J. Chem., 23, 501, (1970).

92. Markov, B.F., Volkov, S.V., Ukr. Khim. Zh. 30, 341, (1964).

93. Markov, B.F., Volkov, S.V., ibid., 30, 545, (1964).

94. Markov, B.F., Volkov, S.V., ibid., 30, 906, (1964).

95. Volkov, S.V., Lazorenko, R.A., ibid., 34, 528, (1968).

96. Markov, B.F., Volkov, S.V., ibid., 29, 945, (1963).

97. Weeks, I.A., Ph.D. Thesis, Univ. Tas., (1969).

98. Burrows, B.W., Hills, G.J., J. Inst. Fuel, 168, (1966).

99. Burrows, B.W., Hills, G.J., Electrochim. Acta., 15, 445, (1970).

100. Gul'din, I.T., Buzhinskaya, A.V., Soviet Electrochemistry, 1, 634, (1965).

101. Welch, B.J., private communication.

102. Zanzycki, J., Disc. Faraday. Soc., 32, 38, (1961).

103. Walrafen, G.E., J. Chem. Phys., 43, 479, (1965).

104. Ref. 15, p. 272.

105. Øye, H.A., Thesis, Tech. Univ. Norway, (1963).

106. Holm, J., Acta. Chem. Scand., 24, 709, (1970).

107. Ricci, J.E., ref. 2., p. 326.

108. Flood, H., Førland, T., Grjotheim, K., Z. Anorg. Allgem. Chem., 276, 289, (1954).

109. Blander, M., Luchsinger, E.B., J. Am. Chem. Soc., 86, 319, (1964).

110. Grjotheim, K., Krohn, C., Toguri, J.M., Trans. Faraday Soc., 57, 1949, (1961).

111. Brynestad, J., Grjotheim, K., Krohn, C., Rev. Roum. Chim., 9, 163, (1964).

112. Blander, M., Braunstein, J., Ann. N.Y., Acad. Sci., 79, 838, (1960).

113. Blander, M., J. Chem. Phys., 34, 432, (1961).

114. Blander, M., Yosim, S.J., ibid., 39, 2610, (1963).

115. Blander, M., Topol, L.E., Electrochim. Acta., 10, 1161, (1965).

116. Blander, M., Topol, L.E., Inorg. Chem., 5, 1641, (1966).

117. Blander, M., Chem. Geol., 3, 33, (1968).

118. Hagemark, K., J. Phys. Chem., 72, 2316, (1968).

119. Bauer, S.H., Porter, R.F., ref. 2., p. 607.

120. Kubaschewski, O., Evans, E.L.L., Alcock, C.B., "Metallurgical Thermochemistry", 4th ed., (Pergamon: Oxford (1967), p. 303ff.

121. Berkowitz, J., Chupka, W.A., J. Chem. Phys., 29, 653, (1958).

122. Novikov, G.I., Gavryuchenkov, F.G., Russ. Chem. Rev., 3, 156, (1967).

123. Bauer, S.H., Diner, R.M., Porter, R.F., J. Chem. Phys., 29, 991, (1958).

124. Akishin, P.A., Rambidi, N.G., Spiridonov, V.P., ref. 5., p. 300.

125. Bauer, S.H., Ino, T., Porter, R.F., J. Chem. Phys., 33, 685, (1960).

126. Hastie, J.W., "Thermodynamics Studies - by Mass Spectrometry - of Molten Mixed Halide Systems", in "Advances in Molten Salt Chemistry", Braunstein, J., Mamantov, G., Smith, G.P. (Eds.), (Plenum Press: New York, (1970)).

127. Snelson, A., J. Phys. Chem., 73, 1919, (1969).

128. Keneshea, F.J., Cubicciotti, D., ibid., 69, 3910, (1965).

129. Cubicciotti, D., High Temp. Sci., 2, 65, 1970.

130. Schoonmaker, R.C., Porter, R.F., J. Chem. Phys., (a) 29, 1070, (1958); ibid., (b) 30, 283, (1959); (c) J. Phys. Chem., 62, 486, (1958).

131. Milne, T.A., Klein, H.M., J. Chem. Phys., 33, 1628, (1960).

132. Blander, M., J. Chem. Phys., 41, 170, 1964.

133. Guion, J., Hengstenberg, D., Blander, M., J. Phys. Chem., 72, 4620, (1968).

134. Brewer, L., Somayajulu, G.R., Brackett, E., Chem. Rev., 63, 111, (1963).

135. Berkowitz, J., Marquart, J.R., J. Chem. Phys., 37, 1853, (1962).

136. Schrier, E.E., Clark, H.M., J. Phys. Chem., 67, 1259, (1963).

137. Büchler, A., Stauffer, J.L., Klemperer, W., J. Amer. Chem. Soc., 86, 4544, (1964).

138. Hastie, J.W., Hauge, R.H., Margrave, J.L., "Matrix Isolation Spectroscopy", to appear in "Spectroscopy in Inorganic Chemistry", J. Ferraro (Ed.), (Academic Press: New York, 1970).

139. Hastie, J.W., Hauge, R.H., Margrave, J.L., Ann. Rev. Phys. Chem., 21, 475, (1970).

140. Hildenbrand, D.L., J. Chem. Phys., 52, 5751, (1970).

141. Zmbov, K.F., Chem. Phys. Letters, 4, 191, (1969).

142. Klemperer, W., J. Chem. Phys., 25, 1066, 1956.

143. Büchler, A., Klemperer, W., Emslie, A.G., ibid., 36, 2499, (1962).

144. Loewenschuss, A., Ron, A., Schnepp, O., ibid., 49, 272, (1968).

145. Cubicciotti, D., Eding, H., J. Chem. Phys., 40, 978, (1964).

146. Büchler, A., Stauffer, J.L., Klemperer, W., ibid., 40, 3471, (1964).

147. Akishin, P.A., Spiridonov, V.P., Kristallografiya, 2, 475, (1957).

148. Moss, H.I., Ph.D. Thesis, Univ. Indiana, (1960).

149. Keneshea, F.J., Cubicciotti, D., (a) J. Chem. Phys., 40, 191, (1964), (b) ibid, 40, 1778, (1964).

150. Rice, D.W., Gregory, N.W., J. Phys. Chem., 72, 3361, (1968).

151. Thompson, K.R., Carlson, K.D., J. Chem. Phys., 49, 4379, (1968).

152. Kerridge, D.H., J. Chem. Soc., A., 217, 1178, (1963).

153. Corbett, J.D., Lynde, R.A., Inorg. Chem., 6, 2199, (1967).

154. Rice, D.W., Gregory, N.W., J. Phys. Chem., 72, 4524, (1968).

155. Hastie, J.W., Ph.D. Thesis, Univ. Tas., (1966).

156. Porter, R.F., Zeller, E.E., J. Chem. Phys., 33, 858, (1960).

157. Sidorov, L.N., Kolosov, E.N., Russ. J. Phys. Chem., 42, 1382, (1968).

158. Zmbov, K.F., Hastie, J.W., Hauge, R., Margrave. J.L., Inorg. Chem. 7, 608, (1968).

159. Karpenko, N.V., Novikov, G.I., Russ. J. Inorg. Chem., 12, 1556, (1967).

160. Hastie, J.W., Margrave, J.L., J. Phys. Chem., 73, 1105, (1969).

161. Bloom, H., Hastie, J.W., ibid., 72, 2706, (1968).

162. Honig, R.E., J. Chem. Phys., 22, 126, (1954).

163. Bloom, H., Barton, J.L., Richards, N.E., Soc. Chem. Ind., 439, (1956).

164. Wong, J., Thesis, Univ. Tas., (1965).

165. Buesman, C., ORNL. Rep. 2323, (1957).

166. Ref. 12, p. 182.

167. N.B.S. Circ. 561, (1955); N.B.S. Circ. 590, (1958), (U.S. Dept. Commerce; Washington, D.C.).

168. Ref. 76, p. E-29, P. D-110;

169. Merten, V., Bell, W.E., "The Transpiration Method", Ref. 5, p. 91.

170. Barton, J.L., Ph.D. Thesis, Univ. N.Z. (1956).

171. Vogel, A.I., "A Textbook of Quantitative Analysis", (Longmans" third ed., (1966)).

172. Ostroff, A.G., Sanderson, R.T., J. Inorg. Nucl. Chem., 9, 45, (1959).

173. Stern, K.H., Weise, E.L., Nat. Stand. Ref. Data Ser., Nat. Bur. Stand. (U.S.) NSRDS-NBS, 7, (1966), (Natl. Bur. Std., Washington, D.C.).

174. Coughlin, J.P., J. Amer. Chem. Soc., 77, 868, (1955).

175. Reed, R.I., (Ed.), "Mass Spectrometry (Academic Press: New York (1965)).

176. McDowell, C.A., (Ed.), "Mass Spectrometry", (McGraw-Hill, Inc: New York, (1963)).

177. Carlson, D.K., "The Knudsen Effusion Method", ref. 5, p. 115.

178. Porter, R.F., Bidinosti, D.R., Watterson, K.F., J. Chem. Phys., 36, 2104, (1962).

179. Hastie, J.W., Bloom, H., Morrison, J.D., ibid., 47, 1580, (1967).

180. Berkowitz, J., Walter, T.A., ibid., 49, 1184, (1968).

181. Bloom, H., Hastie, J.W., ibid., 49, 2230, (1968).

183. Friedman, L., J. Chem. Phys., 23, 477, (1955).

184. Paul, W., Reinhard, H.P., Proc. Intern. Symposium Isotope Separation Amsterdam, 1957 (Pub. 1958), p. 640; Paul, W., Reinhard, H.P., U. von Zahn, Z. Physik, 152, 143, (1958).

185. Kiser, R.W., "Introduction to Mass Spectrometry and its Applications", (Prentice-Hall: 1965) pp. 114, 89, 191, 166.

186. Instrument Manuel, E.A.I. Quad 360, (1970), (E.A.I. Electronic Associaties Pty. Ltd., Palo Alto, California, U.S.A.).

187. Marchand, P., Paquet, C., Marmet, P., Rev. Sci, Instrum., 37, 1702, (1966).

188. Beynon, J.H., "Mass Spectrometry and its Applications to Organic Chemistry", (Elsevier, 1960)p. 206.

189. Hastie, J.W., Swingler, D.L., High Temp. Sci., 1, 46, (1969).

190. Farber, M., Darnell, H.J., J. Phys. Chem., 59, 156, (1955).

191. Ref. 76, vol. 43, p. 2275.

192. Bloom, H., Bockris, J.O'M., Richards, N.E., Taylor, R., J. Amer. Chem. Soc., 80, 2044, (1958).

193. Bloom, H., Welch, B.J., J. Phys. Chem., 62, 1594, (1958).

194. Lewis, G.N., Randall, M., "Thermodynamics", revised by Pitzer, K.S., Brewer, L., (McGraw-Hill Inc: New York, (1961)).

195. Brewer, L., Somayajulu, G.R., Brackett, E., Chem. Revs., 63, 111, (1963).

196. Flood, H., Förland, T., Nesland, A., Acta. Chem. Scand., 5, 1193, 1951.

197. Levin, E.M., Robbins, C.R., McMurdie, H.F., "Phase Diagrams for Ceramists", (The American Ceramic Society: Ohio, (1964)).

198. Meschel, S.V., Kleppa, O.J., J. Chem. Phys., 46, 1853, (1967).

199. Ref. 15, p. 184.

200. Dijkhuis, C.G.M., Ketelaar, J.A.A., Electrochim. Acta., 12, 795, (1967).

201. Kapustinskii, A.F., Quart. Revs., 10, 283, (1956).

202. Braunstein, J., in press.

203. Ref. 15, p. 193.

204. Markov, B.F., Delimarskii, Yu. K., Panchenko, I.D., Zh. Fiz. Khim., 28, 1987, (1954).

205. Ref. 15, p. 274.

206. ibid., p. 195.

207. Bloom, H., Boyd, P.W.D., Laver, J.L., Wong, J., Aust. J. Chem., 19, 1591, (1966).

208. Blander, M., private communication.

209. Bloom, H., Welch, B.J., Trans. Faraday Soc., 59, 410, (1963).

210. Kleppa, O.J., Toguri, J.M., "Selected Topics in High Temperature Chemistry", (Universitetsforlaget: Oslo (1966)), p. 15.

211. Meschel, S.V., Kleppa, O.J., J. Phys. Chem., 68, 3840, (1964).

212. Meschel, S.V., Kleppa, O.J., J.C.P., 43, 4160, (1965).

213. Meschel, S.V., Toguri, J.M., Kleppa, O.J., ibid., 45, 3075, (1966).

214. Kellogg, H.H., Trans. Met. Soc. AIME 230, 1622, (1964).

215. Ingraham, T.R., Kellogg, H.H., ibid., 227, 1419, (1963).

216. Kellogg, H.H., Basu, S.K., Trans. Met. Soc. AIME. 218, 70, (1960).

217. Bloom, H., Hastie, J.W., Aust. J. Chem., 21, 583, (1968).

218. Greiner, B., Jellinek, K., Z. Phys. Chem., 165, 97, (1933).

219. Schoonmaker, R.C., Friedman, A.H., Porter, R.F., J. Chem. Phys., 31, 1586, 1959.

220. Bloom, H., Hastie, J.W., J. Phys. Chem., 71, 2360, (1967).

221. "JANAF Thermochemical Tables". (Ed. Stull, D.R.,) (Dow Chemical Company: Midland Mich., U.S.A., (1964).

222. Novikov, G.E., Kuz'menko, A.L., Vest. leningr. gas. Univ., 19(16), Ser. Fiz. i.Khim., 3, 165, (1966); also Chem. Abstr., 62, 1317b, 3431f, (1965).

223. Hastie, J.W., Zmbov, R.F., Margrave, J.L., J. Inorg. Nucl. Chem., 30, 729, (1968).

224. Murgulescu, I.G., Topor, L., Rev. Roum. Chem., 13, 1109, (1968).

225. Pauling, L., "The Nature of the Chemical Bond", Pauling, L., (Connell, Univ. Press: New York, 3rd ed., (1960), pp. 92-99.

226. Balasubrahmanyam, K., Nanis, L., J. Chem. Phys., 40, 2657, (1964).

227. Spiridonov, V.P., Erokhin, E.V., Russ. J. Inorg. Chem., 14, 332, (1969).

228. Rittner, E.S., J. Chem. Phys., 19, 1030, 1951.

229. Milne, T.A., Cubicciotti, D., ibid., 29, 846, (1958).

230. Ballhausen, C.J., Gray, H.B., "Molecular Orbital Theory", (Benjamin: New York, (1964).

231. Hoffmann, R., J. Chem. Phys., 39, 1397, (1963).

232. Lohr, L.L., Lippscomb, W.N., J. Chem. Phys., 38, 1607, (1963).

233. Hoffmann, R., Lippscomb, W.N., ibid., 36, 2179, (1962).

234. Hoffmann, R., Lippscomb, W.N., ibid., 40, 2474, (1964).

235. Hoffmann, R., ibid., 40, 2474, (1964).

236. Clementi, E., Raimondi, D.L., J. Chem. Phys., 38, 2686, (1963).

237. Clementi, E., Raimondi, D.L., Reinhardt, W.P., ibid., 47, 1300, (1967).

238. Moore, C.E., N.B.S. Circ. 467, (U.S. Dept. Commerce, Natt. Bur. Std: Washington D.C., 1949, 1952, 1958).

239. De Vault, D., J. Chem. Ed., 21, 575, (1944).

240. Kiser, R.W., Dillard, J.G., Duggar, D.L., Advan. Chem. Ser., 72, 153, (1968).

241. Morrison, J.D., private communication.

242. Grimley, R.T., Joyce, T.E., J. Phys. Chem., 73, 2047, (1969).

Appendix A.

Calculation of Exchange Free Energies.

The molar exchange free energy of the reaction:

$$ZnCl_2(l) + Na_2SO_4(l) = 2NaCl(l) + ZnSO_4(l)$$

was calculated using the standard thermodynamic formula:

$$\Delta G^{o}_{(T)} = \Delta H^{o}_{(T)} - T\Delta S^{o}_{(T)}.$$

The calculation was carried out over three temperature ranges as follows:

range (1): 298 - 514 (^{o}K).

A solid state transition for Na_2SO_4 occurs at 514^{o}K.

range (2): 514 - T(f) (^{o}K)

T(f) is the average fusion temperature of the mixture.

range (3): T(f) - T (^{o}K)

T is the temperature of the liquid mixture under consideration.

In each of these ranges differences of heat capacities have been calculated:

$$\Delta C_p(i) = 2C_p(i)\ (NaCl) + C_p(i)\ (ZnSO_4) - C_p(i)\ (Na_2SO_4) - C_p(i)\ (ZnCl_2)$$

where i is the ith temperature range, $\Delta H_{T(r)}$, $\Delta S_{T(r)}$ are the enthalpy and entropy respectively for the solid state transition in Na_2SO_4 at 514 (^{o}K); $\Delta H_{fus}(A)$, $\Delta S_{fus}(A)$ are the enthalpy and entropy of fusion of bracketed salt (A).

Molar enthalpies and entropies were calculated as follows:

$$\Delta H_T^o = \Delta H_{298}^o + \int_{298}^{514} \Delta C_p(1)dT + \Delta H_{T(r)} + \int_{514}^{T(f)} \Delta C_p(2)dT$$

$$+ 2\Delta H_{fus}(NaCl) + \Delta H_{fus}(ZnSO_4) - \Delta H_{fus}(Na_2SO_4) - \Delta H_{fus}(ZnCl_2)$$

$$+ \int_{T(f)}^{T} \Delta C_p(3)dT.$$

$$\Delta S_T^o = \Delta S_{298}^o + \int_{298}^{514} \frac{\Delta C_p(1)dT}{T} + \Delta S_{T(r)} + \int_{514}^{T(f)} \frac{\Delta C_p(2)T}{T}$$

$$+ 2\Delta S_{fus}(NaCl) + \Delta S_{fus}(ZnSO_4) - \Delta S_{fus}(Na_2SO_4) - \Delta S_{fus}(ZnCl_2)$$

$$+ \int_{T(f)}^{T} \frac{C_p(3)dT}{T}$$

The necessary data was obtained from tables given by Kubaschewski, Evans and Alcock.[1] The heat capacity of $ZnSO_4(l)$ was not available and was estimated firstly from an approximate equation for liquids,[1] $C_p(l) = 8$ cal/g. atom. If this rule applies for molten sulphates, $C_p(Na_2SO_4)(l)$ should be 56 cal/mole. deg., (actually 47.2). A value of 48 x 47.2/56 = 40.4 cal/mole. deg., was used for $C_p(ZnSO_4)(l)$. It was found that contribution for ΔH_T and ΔS_T from the third temperature range was relatively small and this approximation would have little effect on the accuracy of the calculated free energy.

Heats f fusion and melting points for the pure salts were all available[1] except for $ZnSO_4$. The heat of fusion of $ZnSO_4$ was estimated from published phase diagrams for the systems Li_2SO_4-$ZnSO_4$

and $ZnSO_4$-$ZnCl_2$[2]. At high $ZnSO_4$, no solid solution occurs in these phase diagrams. Assuming ideal behaviour, $a(ZnSO_4) = N(ZnSO_4)$ and

$$\ln N = -\frac{\Delta H_{fus}(ZnSO_4)}{R}\left(\frac{1}{T(f)} - \frac{1}{T(m)}\right)$$

where T(m) is the melting point of the pure salt .

The heat of fusion was found from the slope of $\ln N_{ZnSO_4}$ vs $\frac{1}{T(f)}$; although the plots for neither system were true straight lines, values determined from the two most reasonable slopes were in good agreement.

System	$\Delta H_{fus}(ZnSO_4)$ (kcal/mole)
$LiSO_4$ - $ZnSO_4$	5.30
$ZnSO_4$ - $ZnCl_2$	4.80

Activities would become more ideal with increasing $ZnSO_4$ concentrations. Therefore more weight was given to the first figure as a wider composition range was available in that system. A value of 5.2 (kcal/mole) was used. The melting point was taken as 1003(^oK) from the Zn-Na-Cl-SO_4 reciprocal phase diagram[3]. The error introduced into the exchange free energy by using an approximate $\Delta H_{fus}(ZnSO_4)$ would be of the order of ± 0.4 kcal/mole.

Free energies of fusion are zero at the melting of the pure compound, but take finite values at other temperatures. Heats and entropies of fusion of each of the four salts at the average fusion temperature T(f) were calculated using the formulae:

$$\Delta H_{fus,T(f)} = \Delta H_{fus,T(m)} + \int_{T(m)}^{T(f)} \Delta C_p dT$$

$$\Delta S_{fus,T(f)} = \Delta S_{fus,T(m)} + \int_{T(m)}^{T(f)} \frac{\Delta C_p dT}{T}$$

$$\Delta C_p = C_p(l) - C_p(s)$$

$$\Delta S_{fus,T(m)} = \frac{\Delta H_{fus,T(m)}}{T(m)}$$

Exchange free energies per equivalent of salt were calculated:

$$\Delta G^o_{(equiv)} = \frac{\Delta G^o_{(mole)}}{2}$$

From an examination of the diagonals of the Zn-Na-SO_4-Cl reciprocal phase diagram[3], an average fusion temperature of 623°K was chosen as best fitting this system. $\Delta G^o_{(equiv)}$ was calculated to be +1795, +1720 and +1575 cals/equivalent at temperature of 773°K, 803°K and 863°K respectively. Assumed fusion temperature had only a very small effect on $\Delta G^o_{(equiv)}$. At 863°K for example, if an average fusion temperature of 773°K is assumed $\Delta G^o_{(equiv)}$ was calculated to be +1536 cals/equivalent. Therefore the effect of assumed fusion temperature is quite small and can be neglected.

Exchange free energies were calculated in the same manner for the $PbCl_2$-K_2SO_4 system assuming an average fusion temperature of 773°K. For

$$PbCl_2 + K_2SO_4 = PbSO_4 + 2KCl$$

the exchange free energy at 1012°K was +3416 cals/equivalent. In

his calculation of exchange free energies for the system

$$PbCl_2 + Na_2SO_4 = PbSO_4 + 2NaCl$$

Welch[4] did not take fusion into account. Taking an average fusion point of 773°K, the corrected exchange free energy is +3542 cals/equivalent at 1000°K.

References.

1. Kubaschewski, O., Evans, E.Ll., Alcock, C.B., "Metallurgical Thermochemistry", 4th ed., (Pergamon : Oxford (1967)), P.303ff.

2. Timmermans, J., "The Physico-chemical constants of Binary Systems in Concentrated Solutions", vol. 3, (Interscience Pub. Inc : New York (1960)), pp.189,291.

3. Levin, E.M., Robbins, C.R., McMurdie, H.F., "Phase Diagrams for Ceramists", (The American Ceramic Society : Ohio (1964)).

4. Welch, B.J., Ph.D Thesis, Univ. N.Z. (1960).

Appendix B.

Computation Procedure in the Extended Hückel Program.

A typical set of computer print out is given in fig.B1-7. The computation procedure is as follows[1].

(1) The input parameters are printed and the matrix of interatomic distances is calculated.

(2) The total overlap matrix is computed. Values of S_{ii} are 1 along the diagonals of the matrix. Values of S_{ij} vary from 0 to 1 and may be negative. Significantly positive S_{ij} values indicate overlap and possible formation of bonding orbitals.

(3) The total Hamiltonian matrix is then calculated from the overlap matrix using the Ballhausen-Gray approximation[2]. Large negative values of H_{ij} indicate stable bonding orbitals.

(4) The secular equations are solved to yield n eigen values or molecular orbital energies. Orbitals are printed in order of increasing stability, or most negative energy. Those of least stability are possibly antibonding orbitals.

(5) Eigen vectors a_{ij} are obtained by substituting the eigen values into the determinant of the secular equations. The actual values indicate electron density at atom j in the ith M.O.

(6) Mulliken overlap populations are performed for any specified number of electrons; two electrons are fed into each molecular orbital beginning with the most bonding until all electrons are used up. The reduced overlap population atom by atom is also computed: if two atoms have positive total overlap populations they

are bonded; if negative, they are anti-bonded. Orbital charges are then calculated and the overall charges on each atom found. It is possible to repeat the Mulliken overlap population calculation with one (or a greater number) less electrons. From the resultant charges on the atoms, the loss of charge from each atom upon ionization may be found.

References.

1. Morrison, J.D., private communication.

2. Lohr, L.L., Lippscomb, W.N., J. Chem. Phys., 38, 2686, (1963).

FIGURES B-1 to B-7

Computer Print Out For Molecular

Orbital Calculations on $ZnCl_2$

ZINC CHLORIDE A
THE ORBITALS ARE NUMBERED AS FOLLOW

ORBITAL	ATOM	N	L	M	SIGMA	X	Y	Z	EXP ALPHA
1	1	3	2	0	0	0.000000	0.000000	0.000000	4.626-17.33
2	1	3	2	1	0	0.000000	0.000000	0.000000	4.626-17.33
3	1	3	2	2	0	0.000000	0.000000	0.000000	4.626-17.33
4	1	3	2	1	1	0.000000	0.000000	0.000000	4.626-17.33
5	1	3	2	2	1	0.000000	0.000000	0.000000	4.626-17.33
6	1	4	0	0	0	0.000000	0.000000	0.000000	1.491 -0.39
7	1	4	1	0	0	0.000000	0.000000	0.000000	1.491 -4.90
8	1	4	1	1	0	0.000000	0.000000	0.000000	1.491 -4.90
9	1	4	1	1	1	0.000000	0.000000	0.000000	1.491 -4.90
10	2	3	0	0	0	0.000000	2.050000	0.000000	2.356-24.55
11	2	3	1	0	0	0.000000	2.050000	0.000000	2.039-12.95
12	2	3	1	1	0	0.000000	2.050000	0.000000	2.039-12.95
13	2	3	1	1	1	0.000000	2.050000	0.000000	2.039-12.95
14	3	3	0	0	0	0.000000	-2.050000	0.000000	2.356-24.55
15	3	3	1	0	0	0.000000	-2.050000	0.000000	2.039-12.95
16	3	3	1	1	0	0.000000	-2.050000	0.000000	2.039-12.95
17	3	3	1	1	1	0.000000	-2.050000	0.000000	2.039-12.95

H(I,J)=K*S(I,J)*SQRTF(H(I,I)*H(J,J)) WITH K= -1.75

DISTANCE MATRIX

FIGURE B1

	1	2	3
1	0.0000	2.0500	2.0500
2	2.0500	0.0000	4.1000
3	2.0500	4.1000	0.0000

TOTAL OVERLAP MATRIX

	1	2	3	4	5	6	7	8	9	10	11	12	13	14	15
1	1.0000	0.0000	0.0000	0.0000	0.0000	0.0000	0.0000	0.0000	0.0000	-0.0065	0.0000	-0.0080	0.0135	-0.0065	0.0000
2	0.0000	1.0000	0.0000	0.0000	0.0000	0.0000	0.0000	0.0000	0.0000	0.0000	0.0000	0.0000	0.0000	0.0000	0.0000
3	0.0000	0.0000	1.0000	0.0000	0.0000	0.0000	0.0000	0.0000	0.0000	-0.0113	0.0000	0.0046	0.0234	-0.0113	0.0000
4	0.0000	0.0000	0.0000	1.0000	0.0000	0.0000	0.0000	0.0000	0.0000	0.0000	0.0093	0.0000	0.0000	0.0000	-0.0093
5	0.0000	0.0000	0.0000	0.0000	1.0000	0.0000	0.0000	0.0000	0.0000	0.0000	0.0000	0.0000	0.0000	0.0000	0.0000
6	0.0000	0.0000	0.0000	0.0000	0.0000	1.0000	0.0000	0.0000	0.0000	0.2985	0.0000	0.0000	-0.2477	0.2985	0.0000
7	0.0000	0.0000	0.0000	0.0000	0.0000	0.0000	1.0000	0.0000	0.0000	0.0000	0.1939	0.0000	0.0000	0.0000	0.1939
8	0.0000	0.0000	0.0000	0.0000	0.0000	0.0000	0.0000	1.0000	0.0000	0.0000	0.0000	0.1939	0.0000	0.0000	0.0000
9	0.0000	0.0000	0.0000	0.0000	0.0000	0.0000	0.0000	0.0000	1.0000	0.4427	0.0000	0.0000	-0.3081	-0.4427	0.0000
10	-0.0065	0.0000	-0.0113	0.0000	0.0000	0.2985	0.0000	0.0000	0.4427	1.0000	0.0000	0.0000	0.0000	0.0004	0.0000
11	0.0000	0.0000	0.0000	0.0093	0.0000	0.0000	0.1939	0.0000	0.0000	0.0000	1.0000	0.0000	0.0000	0.0000	0.0000
12	-0.0080	0.0000	0.0046	0.0000	0.0000	0.0000	0.0000	0.1939	0.0000	0.0000	0.0000	1.0000	0.0000	0.0000	0.0000
13	0.0135	0.0000	0.0234	0.0000	0.0000	-0.2477	0.0000	0.0000	-0.3081	0.0000	0.0000	0.0000	1.0000	-0.0017	0.0000
14	-0.0065	0.0000	-0.0113	0.0000	0.0000	0.2985	0.0000	0.0000	-0.4427	0.0004	0.0000	0.0000	-0.0017	1.0000	0.0000
15	0.0000	0.0000	0.0000	-0.0093	0.0000	0.0000	0.1939	0.0000	0.0000	0.0000	0.0005	0.0000	0.0000	0.0000	1.0000
16	0.0080	0.0000	-0.0046	0.0000	0.0000	0.0000	0.0000	0.1939	0.0000	0.0000	0.0000	0.0005	0.0000	0.0000	0.0000
17	-0.0135	0.0000	-0.0234	0.0000	0.0000	0.2477	0.0000	0.0000	-0.3081	0.0017	0.0000	0.0000	-0.0054	0.0000	0.0000

	16	17
1	0.0080	-0.0135
2	0.0000	0.0000
3	-0.0046	-0.0234
4	0.0000	0.0000
5	0.0000	0.0000
6	0.0000	0.2477
7	0.0000	0.0000
8	0.1939	0.0000
9	0.0000	-0.3081
10	0.0000	0.0017
11	0.0000	0.0000
12	0.0005	0.0000
13	0.0000	-0.0054
14	0.0000	0.0000
15	0.0000	0.0000
16	1.0000	0.0000
17	0.0000	1.0000

TOTAL H MATRIX

-17.330000	0.000000	0.000000	0.000000	0.000000	0.000000	0.000000	0.000000
0.000000	0.234736	0.000000	0.219732	-0.353845	0.234736	0.000000	-0.210732
0.353845							
0.000000	-17.330000	0.000000	0.000000	0.000000	0.000000	0.000000	0.000000
0.000000	0.000000	0.000000	0.000000	0.000000	0.000000	0.000000	0.000000
0.000000							
0.000000	0.000000	-17.330000	0.000000	0.000000	0.000000	0.000000	0.000000
0.000000	0.406575	0.000000	-0.121666	-0.612878	0.406575	0.000000	0.121666
0.612878							
0.000000	0.000000	0.000000	-17.330000	0.000000	0.000000	0.000000	0.000000
0.000000	0.000000	-0.243332	0.000000	0.000000	0.000000	0.243332	0.000000
0.000000							
0.000000	0.000000	0.000000	0.000000	-17.330000	0.000000	0.000000	0.000000
0.000000	0.000000	0.000000	0.000000	0.000000	0.000000	0.000000	0.000000
0.000000							
0.000000	0.000000	0.000000	0.000000	0.000000	-9.390000	0.000000	0.000000
0.000000	-7.932211	0.000000	0.000000	4.780352	-7.932211	0.000000	0.000000
-4.780352							
0.000000	0.000000	0.000000	0.000000	0.000000	0.000000	-4.900000	0.000000
0.000000	0.000000	-2.702621	0.000000	0.000000	0.000000	-2.702621	0.000000
0.000000							
0.000000	0.000000	0.000000	0.000000	0.000000	0.000000	0.000000	-4.900000
0.000000	0.000000	0.000000	-2.702621	0.000000	0.000000	0.000000	-2.702621
0.000000							
0.000000	0.000000	0.000000	0.000000	0.000000	0.000000	0.000000	0.000000
-4.900000	-8.497939	0.000000	0.000000	4.295625	8.497939	0.000000	0.000000
4.295625							
0.234736	0.000000	0.406575	0.000000	0.000000	-7.932211	0.000000	0.000000
-8.497939	-24.550000	0.000000	0.000000	0.000000	-0.018494	0.000000	0.000000
-0.054486							
0.000000	0.000000	0.000000	-0.243332	0.000000	0.000000	-2.702621	0.000000
0.000000	0.000000	-12.950000	0.000000	0.000000	0.000000	-0.011558	0.000000
0.000000							
0.210732	0.000000	-0.121666	0.000000	0.000000	0.000000	0.000000	-2.702621
0.000000	0.000000	0.000000	-12.950000	0.000000	0.000000	0.000000	-0.011558
0.000000							
-0.353845	0.000000	-0.612878	0.000000	0.000000	4.780352	0.000000	0.000000
4.295625	0.000000	0.000000	0.000000	-12.950000	0.054486	0.000000	0.000000
0.121301							
0.234736	0.000000	0.406575	0.000000	0.000000	-7.932211	0.000000	0.000000
8.497939	-0.018494	0.000000	0.000000	0.054486	-24.550000	0.000000	0.000000
0.000000							

0.000000	0.000000	0.000000	0.243332	0.000000	0.000000	-2.702621	0.000000
0.000000	0.000000	-0.011558	0.000000	0.000000	0.000000	-12.950000	0.000000
0.000000							
-0.210732	0.000000	0.121666	0.000000	0.000000	0.000000	0.000000	-2.702621
0.000000	0.000000	0.000000	-0.011558	0.000000	0.000000	0.000000	-12.950000
0.000000							
0.353845	0.000000	0.612878	0.000000	0.000000	-4.780352	0.000000	0.000000
4.295625	-0.054486	0.000000	0.000000	0.121301	0.000000	0.000000	0.000000
-12.950000							

NR= 150

NR= 99

EIGEN VALUES

E(1)=	9.040554	0
E(2)=	-1.034269	0
E(3)=	-4.076661	0
E(4)=	-4.076661	0
E(5)=	-12.919953	2
E(6)=	-12.938123	2
E(7)=	-12.938123	2
E(8)=	-12.963834	2
E(9)=	-12.963834	2
E(10)=	-13.534195	2
E(11)=	-17.330000	2
E(12)=	-17.330000	2
E(13)=	-17.333100	2
E(14)=	-17.333100	2
E(15)=	-17.341455	2
E(16)=	-24.609726	2
E(17)=	-25.344622	2

SUM= -429.76013502 EV = -9914.56631494 KCAL

FIGURE B2

EIGENVECTORS

	1	2	3	4	5	6	7	8	9	10	11	12	13	14	15
1	*0.0000	0.0289	0.0000	-0.0000	-0.0000	-0.0344	0.0000	0.0000	-0.0000	-0.0492	0.0000	0.0000	0.0000	0.8654	0.4971
2	0.0000	0.0000	0.0000	0.0000	0.0000	0.0000	0.0000	0.0000	0.0000	0.0000	0.0000	1.0000	0.0000	0.0000	0.0000
3	0.0000	0.0501	0.0000	-0.0000	-0.0000	0.0198	0.0000	0.0000	0.0000	-0.0852	0.0000	0.0000	0.0000	-0.4996	0.8611
4	0.0000	0.0000	-0.0000	0.0000	0.0000	0.0000	0.0397	-0.0000	0.0000	0.0000	0.0000	0.0000	-0.9993	0.0000	0.0000
5	0.0000	0.0000	0.0000	0.0000	0.0000	0.0000	0.0000	0.0000	0.0000	0.0000	1.0000	0.0000	0.0000	0.0000	0.0000
6	0.0000	-1.1656	0.0000	-0.0000	-0.0000	0.0000	0.0000	0.0000	0.0000	-0.2593	0.0000	0.0000	0.0000	0.0000	0.0134
7	0.0000	0.0000	-1.0393	0.0000	0.0000	0.0000	0.0000	0.0329	0.0000	0.0000	0.0000	0.0000	0.0000	0.0000	0.0000
8	*0.0000	0.0000	0.0000	-1.0393	-0.0000	0.0000	0.0000	0.0000	-0.0329	-0.0000	0.0000	0.0000	0.0000	0.0000	-0.0000
9	*1.5316	0.0000	0.0000	-0.0000	-0.0478	-0.0000	0.0000	0.0000	-0.0000	0.0000	0.0000	0.0000	0.0000	-0.0000	-0.0000
10	0.5714	0.3777	0.0000	0.0000	0.0095	-0.0000	0.0000	0.0000	0.0000	0.0906	0.0000	0.0000	0.0000	0.0000	0.0887
11	0.0000	0.0000	0.2237	0.0000	0.0000	0.0000	-0.7071	0.7002	0.0000	0.0000	0.0000	0.0000	-0.0188	0.0000	0.0000
12	*0.0000	-0.0000	0.0000	0.2237	0.0000	-0.7071	0.0000	0.0000	-0.7002	-0.0000	0.0000	0.0000	0.0000	-0.0188	0.0000
13	*0.4989	-0.4399	0.0000	-0.0000	0.6937	-0.0000	0.0000	0.0000	-0.0000	0.6233	0.0000	0.0000	0.0000	0.0000	0.0529
14	*0.5714	0.3777	0.0000	0.0000	-0.0095	-0.0000	0.0000	0.0000	-0.0000	0.0906	0.0000	0.0000	0.0000	0.0000	0.0887
15	0.0000	0.0000	0.2237	0.0000	0.0000	0.0000	0.7071	0.7002	0.0000	0.0000	0.0000	0.0000	0.0188	0.0000	0.0000
16	0.0000	-0.0000	0.0000	0.2237	-0.0000	0.7071	0.0000	0.0000	-0.7002	0.0000	0.0000	0.0000	0.0000	0.0188	-0.0000
17	*0.4989	0.4399	0.0000	0.0000	0.6937	0.0000	0.0000	0.0000	0.0000	-0.6233	0.0000	0.0000	0.0000	-0.0000	-0.0529

	16	17
1	*0.0141	-0.0000
2	0.0000	0.0000
3	*0.0245	0.0000
4	0.0000	0.0000
5	0.0000	0.0000
6	0.0539	0.0000
7	0.0000	0.0000
8	*0.0000	-0.0000
9	*0.0000	0.2371
10	0.6895	-0.8040
11	0.0000	0.0000
12	*0.0000	-0.0000
13	0.0053	0.0666
14	0.6895	0.8040
15	0.0000	0.0000
16	0.0000	-0.0000
17	*0.0053	0.0666

FIGURE B3

2222222222220000

MULLIKEN OVERLAP POPULATIONS FOR 26 ELECTRONS

	1	2	3	4	5	6	7	8	9	10	11	12	13	14	15
1	3.9996	0.0000	0.0000	0.0000	0.0000	0.0000	0.0000	0.0000	0.0000	-0.0000	0.0000	-0.0003	-0.0002	-0.0000	0.0000
2	0.0000	4.0000	0.0000	0.0000	0.0000	0.0000	0.0000	0.0000	0.0000	0.0000	0.0000	0.0000	0.0000	0.0000	0.0000
3	0.0000	0.0000	3.9974	0.0000	0.0008	0.0000	0.0000	0.0000	0.0000	-0.0000	0.0000	-0.0001	-0.0007	-0.0000	0.0000
4	0.0000	0.0000	0.0000	4.0007	0.0000	0.0000	0.0000	0.0000	0.0000	0.0000	-0.0003	0.0000	0.0000	0.0000	-0.0003
5	0.0000	0.0000	0.0000	0.0000	4.0000	0.0000	0.0000	0.0000	0.0000	0.0000	0.0000	0.0000	0.0000	0.0000	0.0000
6	0.0000	0.0000	0.0000	0.0000	0.0000	0.2812	0.0000	0.0000	0.0000	0.0168	0.0000	0.0000	0.1591	0.0168	0.0000
7	0.0000	0.0000	0.0000	0.0000	0.0000	0.0000	0.0043	0.0000	0.0000	0.0000	0.0179	0.0000	0.0000	0.0000	0.0179
8	0.0000	0.0000	0.0000	0.0000	0.0000	0.0000	0.0000	0.0043	0.0000	0.0000	0.0000	0.0179	0.0000	0.0000	0.0000
9	0.0000	0.0000	0.0000	0.0000	0.0000	0.0000	0.0000	0.0000	0.2340	-0.3384	0.0000	0.0000	0.0214	-0.3384	0.0000
10	-0.0000	0.0000	-0.0000	0.0000	0.0000	0.0168	0.0000	0.0000	-0.3384	4.5239	0.0000	0.0000	0.0000	-0.0003	0.0000
11	0.0000	0.0000	0.0000	-0.0003	0.0000	0.0000	0.0179	0.0000	0.0000	0.0000	3.9625	0.0000	0.0000	0.0000	-0.0000
12	-0.0003	0.0000	-0.0001	0.0000	0.0000	0.0000	0.0000	0.0179	0.0000	0.0000	0.0000	3.9625	0.0000	0.0000	0.0000
13	-0.0002	0.0000	-0.0007	0.0000	0.0000	0.1591	0.0000	0.0000	0.0214	0.0000	0.0000	0.0000	3.5082	-0.0008	0.0000
14	-0.0000	0.0000	-0.0000	0.0000	0.0000	0.0168	0.0000	0.0000	-0.3384	-0.0003	0.0000	0.0000	-0.0008	4.5239	0.0000
15	0.0000	0.0000	0.0000	-0.0003	0.0000	0.0000	0.0179	0.0000	0.0000	0.0000	-0.0000	0.0000	0.0000	0.0000	3.9625
16	-0.0003	0.0000	-0.0001	0.0000	0.0000	0.0000	0.0000	0.0179	0.0000	0.0000	0.0000	-0.0000	0.0000	0.0000	0.0000
17	-0.0002	0.0000	-0.0007	0.0000	0.0000	0.1591	0.0000	0.0000	0.0214	-0.0008	0.0000	0.0000	-0.0020	0.0000	0.0000

	16	17
1	-0.0003	-0.0002
2	0.0000	0.0000
3	-0.0001	-0.0007
4	0.0000	0.0000
5	0.0000	0.0000
6	0.0000	0.1591
7	0.0000	0.0000
8	0.0179	0.0000
9	0.0000	0.0214
10	0.0000	-0.0008
11	0.0000	0.0000
12	-0.0000	0.0000
13	0.0000	-0.0020
14	0.0000	0.0000
15	0.0000	0.0000
16	3.9625	0.0000
17	0.0000	3.5082

FIGURE B4

REDUCED OVERLAP POPULATION MATRIX ATOM BY ATOM

	1	2	3
1	20.5216	-0.1070	-0.1070
2	-0.1070	15.9571	-0.0039
3	-0.1070	-0.0039	15.9571

CHARGE MATRIX FOR MO'S WITH TWO ELECTRONS ON EACH

	1	2	3	4	5	6	7	8	9	10	11	12	13	14	15
1	0.0000	0.0007	0.0000	0.0000	0.0000	0.0016	0.0000	0.0000	0.0000	0.0033	0.0000	0.0000	0.0000	1.4984	0.4953
2	0.0000	0.0000	0.0000	0.0000	0.0000	0.0000	0.0000	0.0000	0.0000	0.0000	0.0000	2.0000	0.0000	0.0000	0.0800
3	0.0000	0.0021	0.0000	0.0000	0.0000	0.0005	0.0000	0.0000	-0.0000	0.0099	0.0000	0.0000	0.0000	0.4995	1.4860
4	0.0000	0.0000	0.0000	0.0000	0.0008	0.0000	0.0021	0.0000	0.0000	0.0000	0.0000	0.0000	1.9979	0.0000	0.0800
5	0.0000	0.0000	0.0000	0.0000	0.0000	0.0000	0.0000	0.0000	0.0000	0.0000	2.0000	0.0000	0.0000	0.0000	0.0800
6	0.0000	1.6834	0.0000	0.0000	0.0008	0.0000	0.0000	0.0000	0.0000	0.2665	0.0000	0.0000	0.0000	0.0000	0.0801
7	0.0000	0.0000	1.9800	0.0000	0.0000	0.0000	0.0000	0.0200	0.0000	0.0000	0.0000	0.0000	0.0000	0.0000	0.0800
8	0.0000	0.0000	0.0000	1.9800	0.0008	0.0000	0.0000	0.0000	0.0200	0.0000	0.0000	0.0000	0.0000	-0.0000	0.0800
9	2.2000	0.0000	0.0000	0.0000	0.0446	0.0000	0.0000	0.0000	-0.0000	0.0000	0.0000	0.0000	0.0000	0.0000	0.0800
10	-0.1232	0.0226	0.0000	-0.0000	-0.0002	0.0000	0.0000	0.0000	0.0000	0.0024	0.0000	0.0000	0.0000	0.0000	0.0811
11	0.0000	0.0000	0.0100	0.0000	0.0008	0.0000	0.9989	0.9900	0.0000	0.0000	0.0000	0.0000	0.0011	0.0000	0.0800
12	0.0000	0.0000	0.0000	0.0100	-0.0008	0.9989	0.0000	0.0000	0.9900	0.0000	0.0000	0.0000	0.0000	0.0011	0.0800
13	0.0232	0.1343	0.0000	-0.0000	0.9779	0.0000	0.0000	0.0000	0.0000	0.8577	0.0000	0.0000	0.0000	0.0000	0.0881
14	-0.1232	0.0226	0.0000	0.0000	-0.0002	0.0000	0.0000	0.0000	0.0000	0.0024	0.0000	0.0000	0.0000	0.0000	0.0811
15	0.0000	0.0000	0.0100	0.0000	0.0008	0.0000	0.9989	0.9900	0.0000	0.0000	0.0000	0.0000	0.0011	0.0000	0.0800
16	-0.0000	0.0000	0.0000	0.0100	0.0008	0.9989	0.0000	0.0000	0.9900	0.0000	0.0000	0.0000	0.0000	0.0011	0.0800
17	0.0232	0.1343	0.0000	0.0000	0.9779	0.0000	0.0000	0.0000	0.0000	0.8577	0.0000	0.0000	0.0000	0.0000	0.0881

	16	17
1	0.0006	0.0000
2	0.0000	0.0000
3	0.0019	0.0000
4	0.0000	0.0000
5	0.0000	0.0000
6	0.0500	0.0000
7	0.0000	0.0000
8	0.0000	0.0000
9	-0.0000	-0.2447
10	0.9738	1.1234
11	0.0000	0.0000
12	0.0000	0.0000
13	-0.0001	-0.0011
14	0.9738	1.1234
15	0.0000	0.0000
16	0.0000	0.0000
17	-0.0001	-0.0011

FIGURE B5

ORBITAL CHARGES

1	1.999298
2	2.000000
3	1.997895
4	2.000000
5	2.000000
6	0.316575
7	0.020013
8	0.020013
9	-0.200027
10	2.100621
11	1.989994
12	1.989994
13	1.842509
14	2.100621
15	1.989994
16	1.989994
17	1.842509

NET CHARGES

1	1.846234
2	-0.923117
3	-0.923117

TOTAL CHARGE= -0.000000

70/10/277

2222222222210000

MULLIKEN OVERLAP POPULATIONS FOR 25 ELECTRONS

	1	2	3	4	5	6	7	8	9	10	11	12	13	14	15
1	3.9996	0.0000	0.0000	0.0000	0.0000	0.0000	0.0000	0.0000	0.0000	-0.0000	0.0000	-0.0003	-0.0002	-0.0000	0.0000
2	0.0000	4.0000	0.0000	0.0000	0.0000	0.0000	0.0000	0.0000	0.0000	0.0000	0.0000	0.0000	0.0000	0.0000	0.0000
3	0.0000	0.0000	3.9974	0.0000	0.0000	0.0000	0.0000	0.0000	0.0000	-0.0000	0.0000	-0.0001	-0.0007	-0.0000	0.0000
4	0.0000	0.0000	0.0000	4.0007	0.0008	0.0000	0.0000	0.0000	0.0000	0.0000	-0.0003	0.0000	0.0000	0.0000	-0.0003
5	0.0000	0.0000	0.0000	0.0000	4.0008	0.0000	0.0000	0.0000	0.0000	0.0000	0.0000	0.0000	0.0000	0.0000	0.0000
6	0.0000	0.0000	0.0000	0.0000	0.0008	0.2812	0.0000	0.0000	0.0000	0.0168	0.0000	0.0000	0.1591	0.0168	0.0000
7	0.0000	0.0000	0.0000	0.0000	0.0008	0.0000	0.0043	0.0000	0.0000	0.0000	0.0179	0.0000	0.0000	0.0000	0.0179
8	0.0000	0.0000	0.0000	0.0000	0.0008	0.0000	0.0000	0.0043	0.0000	0.0000	0.0000	0.0179	0.0000	0.0000	0.0000
9	0.0000	0.0000	0.0000	0.0000	0.0008	0.0000	0.0000	0.0000	0.2294	-0.3380	0.0000	0.0000	0.0010	-0.3380	0.0000
10	-0.0000	0.0000	-0.0000	0.0000	0.0000	0.0168	0.0000	0.0000	-0.3380	4.5237	0.0000	0.0000	0.0000	-0.0003	0.0000
11	0.0000	0.0000	0.0000	-0.0003	0.0000	0.0000	0.0179	0.0000	0.0000	0.0000	3.9625	0.0000	0.0000	0.0000	-0.0000
12	-0.0003	0.0000	-0.0001	0.0000	0.0000	0.0000	0.0000	0.0179	0.0000	0.0000	0.0000	3.9625	0.0000	0.0000	0.0000
13	-0.0002	0.0000	-0.0007	0.0000	0.0000	0.1591	0.0000	0.0000	0.0010	0.0000	0.0000	0.0000	2.5456	-0.0008	0.0000
14	-0.0000	0.0000	-0.0000	0.0000	0.0000	0.0168	0.0000	0.0000	-0.3380	-0.0003	0.0000	0.0000	-0.0008	4.5237	0.0000
15	0.0000	0.0000	0.0000	-0.0003	0.0000	0.0000	0.0179	0.0000	0.0000	0.0000	-0.0000	0.0000	0.0000	0.0000	3.9625
16	-0.0003	0.0000	-0.0001	0.0000	0.0000	0.0000	0.0000	0.0179	0.0000	0.0000	0.0000	-0.0000	0.0000	0.0000	0.0000
17	-0.0002	0.0000	-0.0007	0.0000	0.0000	0.1591	0.0000	0.0000	0.0010	-0.0008	0.0000	0.0000	0.0031	0.0000	0.0000

	16	17
1	-0.0003	-0.0002
2	0.0000	0.0000
3	-0.0001	-0.0007
4	0.0000	0.0000
5	0.0000	0.0000
6	0.0000	0.1591
7	0.0000	0.0000
8	0.0179	0.0000
9	0.0000	0.0010
10	0.0000	-0.0008
11	0.0000	0.0000
12	-0.0000	0.0000
13	0.0000	0.0031
14	0.0000	0.0000
15	0.0000	0.0000
16	3.9625	0.0000
17	0.0000	2.5456

FIGURE B6

REDUCED OVERLAP POPULATION MATRIX ATOM BY ATOM

	1	2	3
1	20.5170	-0.1271	-0.1271
2	-0.1271	14.9944	0.0012
3	-0.1271	0.0012	14.9944

CHARGE MATRIX FOR MO'S WITH TWO ELECTRONS ON EACH

	1	2	3	4	5	6	7	8	9	10	11	12	13	14	15
1	0.0000	0.0007	0.0000	0.0000	0.0000	0.0016	0.0000	0.0000	0.0000	0.0033	0.0000	0.0000	0.0000	1.4984	0.4953
2	0.0000	0.0000	0.0000	0.0000	0.0008	0.0000	0.0000	0.0000	0.0000	0.0000	0.0000	2.0000	0.0000	0.0000	0.0000
3	0.0000	0.0021	0.0000	0.0000	0.0008	0.0005	0.0000	0.0000	-0.0000	0.0099	0.0000	0.0000	0.0000	0.4995	1.4860
4	0.0000	0.0000	0.0000	0.0000	0.0000	0.0000	0.0021	0.0000	0.0000	0.0000	0.0000	0.0000	1.9979	0.0000	0.0000
5	0.0000	0.0000	0.0000	0.0000	0.0000	0.0000	0.0000	0.0000	0.0000	0.0000	2.0000	0.0000	0.0000	0.0000	0.0000
6	0.0000	1.6834	0.0000	0.0000	0.0008	0.0000	0.0000	0.0000	0.0000	0.2665	0.0000	0.0000	0.0000	0.0000	0.0801
7	0.0000	0.0000	1.9800	0.0000	0.0000	0.0000	0.0000	0.0200	0.0000	0.0000	0.0000	0.0000	0.0000	0.0000	0.0000
8	0.0000	0.0000	0.0000	1.9800	0.0000	0.0000	0.0000	0.0000	0.0200	0.0000	0.0000	0.0000	0.0000	-0.0000	0.0000
9	2.2000	0.0000	0.0000	0.0000	0.0446	0.0000	0.0000	0.0000	-0.0000	0.0000	0.0000	0.0000	0.0000	0.0000	0.0000
10	-0.1232	0.0226	0.0040	-0.0000	-0.0002	0.0000	0.0001	0.0000	0.0000	0.0024	0.0000	0.0000	0.0000	0.0000	0.0011
11	0.0000	0.0000	0.0140	0.0000	0.0000	0.0000	0.9989	0.9900	0.0000	0.0000	0.0000	0.0000	0.0011	0.0000	0.0000
12	0.0000	0.0000	0.0040	0.0100	-0.0000	0.9989	0.0000	0.0000	0.9900	0.0000	0.0000	0.0000	0.0000	0.0011	0.0000
13	0.0232	0.1343	0.0000	-0.0000	0.9779	0.0000	0.0000	0.0000	0.0000	0.8577	0.0000	0.0000	0.0000	0.0000	0.0081
14	-0.1232	0.0226	0.0000	0.0000	-0.0002	0.0000	0.0000	0.0000	0.0000	0.0024	0.0000	0.0000	0.0000	0.0000	0.0811
15	0.0000	0.0000	0.0140	0.0000	0.0008	0.0000	0.9989	0.9900	0.0000	0.0000	0.0000	0.0000	0.0011	0.0000	0.0000
16	-0.0000	0.0000	0.0000	0.0100	0.0008	0.9989	0.0000	0.0000	0.9900	0.0000	0.0000	0.0000	0.0000	0.0011	0.0000
17	0.0232	0.1343	0.0000	0.0000	0.9779	0.0000	0.0000	0.0000	0.0000	0.8577	0.0000	0.0000	0.0000	0.0000	0.0081

	16	17
1	0.0006	0.0000
2	0.0000	0.0000
3	0.0019	0.0000
4	0.0000	0.0000
5	0.0000	0.0000
6	0.0500	0.0000
7	0.0000	0.0000
8	0.0000	0.0000
9	-0.0000	-0.2447
10	0.9738	1.1234
11	0.0000	0.0000
12	0.0000	0.0000
13	-0.0001	-0.0011
14	0.9738	1.1234
15	0.0000	0.0000
16	0.0000	0.0000
17	-0.0001	-0.0011

FIGURE B7

ORBITAL CHARGES

1	1.999208
2	2.000000
3	1.997805
4	2.000000
5	2.000100
6	0.316575
7	0.020013
8	0.020013
9	-0.222345
10	2.100720
11	1.989994
12	1.989994
13	1.353568
14	2.100720
15	1.989994
16	1.989994
17	1.353568

NET CHARGES

1	1.868551
2	-0.434276
3	-0.434276

TOTAL CHARGE= 1.000000

70/10/2741

Auxiliary Publications During the Course of This Work:

1. Anthony, R.G., Welch, B.J., Steele, R.J., "Open Circuit Voltage and Cathode Polarisation of Lithium Chlorine Battery in the Presence of Potassium Chloride", Aust. J. Chem., 21, 789, (1968).

2. Anthony, R.G., Welch, B.J., Stitt, D.M., "The Corrosion of Recrystallized Alumina by Some Fluoride Melts", J. Aust. Ceram. Soc., 4, 51, (1968).